

AN INVESTIGATION OF THE RHEOLOGICAL PROPERTIES OF HIGH  
SOLIDS KRAFT BLACK LIQUORS

By

ABBAS ALI ZAMAN

A DISSERTATION PRESENTED TO THE GRADUATE SCHOOL  
OF THE UNIVERSITY OF FLORIDA IN PARTIAL FULFILLMENT  
OF THE REQUIREMENTS FOR THE DEGREE OF  
DOCTOR OF PHILOSOPHY

UNIVERSITY OF FLORIDA

1993

Copyright 1993  
by  
Abbas Ali Zaman

To my wife, my daughter, and to my parents

## ACKNOWLEDGEMENTS

It would be impossible to specifically thank everyone who has helped me along this way. However, there are people that should be noted for their outstanding contributions:

I extend my sincere gratitude to my research advisor, Dr. A.L. Fricke, for his moral, intellectual and monetary support over my graduate career. The amazing breadth of his knowledge has been very inspiring. I would also like to express my thanks to my supervisory committee members: Dr. C.L. Beatty for his friendship and advice, Dr. C.W. Park for an accurate review of my thesis, Dr. R. Abbaschian and Dr. G. Hoflund for their willingness, invaluable guidance, and encouragement during this study and their participation in the review of this dissertation. Their doors were always open when I needed help or guidance during my stay at the University of Florida.

I gratefully acknowledge the financial support provided by the United States Department of Energy for the project on physical properties of kraft black liquors.

I am indebted to my loving parents, Mohammadreza and Sharbanoo, my loving wife, Masoumeh, my loving daughter, Neda, my relatives and friends for their support and encouragement, which has brought me so far.



No acknowledgement could be complete without mention of the people with whom I work every day. My special thanks go to my colleagues at Dr. Fricke's research group for their cooperation and friendship during my graduate study. Also I would like to acknowledge the help of the faculty members and staff, the friendship and support of the graduate students in the Chemical Engineering Department. These people have been an integral part of my life during the past four years, and their absence will leave a space that will be difficult to fill.

## TABLE OF CONTENTS

ACKNOWLEDGEMENTS .....	iii
LIST OF TABLES .....	viii
LIST OF FIGURES .....	xi
ABSTRACT .....	xxi
CHAPTERS	
1 INTRODUCTION .....	1
2 OVERVIEW AND BACKGROUND .....	6
2.1 Composition of Black Liquor .....	6
2.2 Literature Review on Rheology of Black Liquor .....	8
2.3 Black Liquor Preparation .....	14
2.4 Concentration and Handling of Liquors .....	15
2.5 Definition of Rheology .....	18
2.6 Simple Shear Flow .....	18
2.7 Definition of Newtonian and non-Newtonian Behavior ..	20
3 CONCENTRIC CYLINDER VISCOMETER .....	23
3.1 Introduction .....	23
3.2 Mathematical Analysis .....	23
3.3 Solution of the Difference Equation .....	26
3.4 Alternative Solution .....	32
3.5 Comparison of Methods for Calculating Shear Rate in Coaxial Cylinder Viscometer .....	33
3.6 End Effects and Equivalent Length .....	35
3.7 Analysis of the Experimental Data .....	40
4 CAPILLARY FLOW VISCOMETRY .....	43

4.1	Introduction .....	43
4.2	Theory .....	43
4.3	Creeping Flow Solution for a non-Newtonian Fluid ....	44
4.4	Entry Flow Corrections .....	51
4.5	Wall Slip in Capillary Flow .....	53
4.6	Determination of the Slip Velocity .....	55
4.7	Experimental Setup and Data Analysis .....	57
4.8	Data Analysis .....	59
5	LOW SOLIDS VISCOSITY .....	87
5.1	Introduction .....	87
5.2	Glass Capillary Viscometer .....	87
5.3	Experimental Setup .....	88
5.4	Viscosity-Temperature Relationships .....	90
5.5	Reduced Correlation for Low Solids Viscosity .....	96
5.6	Results and Discussion .....	97
5.7	Conclusions .....	98
6	SHEAR VISCOSITY OF BLACK LIQUORS .....	114
6.1	Introduction .....	114
6.2	High Solids Viscosity .....	116
6.3	Dependence of Viscosity on Shear Rate .....	118
6.4	Reduced Correlations for Shear Viscosity of Black Liquors .....	122
6.5	Relation Between $T_s$ and $T_g$ .....	126
6.6	Analytical Expression for $a_{ST}$ .....	127
6.7	Conclusions .....	129
7	CORRELATIONS FOR NEWTONIAN VISCOSITY OF BLACK LIQUORS .....	178
7.1	Introduction .....	178
7.2	Background .....	178
7.3	Determination of the Newtonian Viscosity .....	179
7.4	Estimation of Zero Shear Rate Viscosities .....	180
7.5	Glass Transition Temperature of Kraft Black Liquors .	182
7.6	Influence of Temperature on Zero Shear Rate Viscosity .....	183
7.7	Results and discussions .....	186
7.8	Comparison with Previous Work .....	187
7.9	Conclusions .....	190

8	VISCOELASTIC PROPERTIES OF HIGH SOLIDS KRAFT BLACK LIQUORS .....	209
8.1	Introduction .....	209
8.2	Small Amplitude Oscillatory Shear Flow .....	210
8.3	The Parallel-Plate Geometry in Oscillatory Shear Flow .....	215
8.4	Slip at the Wall of a Parallel-Plate Rheometer .....	219
8.5	Dynamic Mechanical Testing .....	223
8.6	Results .....	225
8.7	Correlations for Dynamic Viscosity and Storage Modulus .....	227
8.8	Time-Temperature Superposition .....	230
8.9	Relations Between Shear Viscosity and the Magnitude of the Complex Viscosity .....	235
8-10	The Effect of Black Liquor Viscoelasticity on Droplet Formation .....	236
9	SUMMARY, CONCLUSIONS AND RECOMMENDATION .....	290
	REFERENCE LIST .....	299
	BIOGRAPHICAL SKETCH .....	311

## LIST OF TABLES

<u>Table</u>	<u>Page</u>
2-1	Composition of organic and inorganic materials in three different kraft black liquors (slash pine) . . . . . 7
2-2	Pulping conditions, kappa number, lignin concentration and lignin molecular weight for black liquors used in this study . . . . 16
5-1	Coefficients of equation (5-9) for different black liquors . . . . 111
5-2	Coefficients of equation (5-10) for different black liquors . . . . 112
5-3	$B_2$ as in equation (5-10) for different black liquors . . . . . 113
6-1	The power-law model parameters for black liquor ABAFX011,12 . . . . . 171
6-2	The power-law model parameters for black liquor ABAFX013,14 . . . . . 172
6-3	The power-law model parameters for black liquor ABAFX025,26 . . . . . 172
6-4	The power-law model parameters for black liquor ABAFX043,44 . . . . . 173
6-5	The Cross model parameters for different black liquors $\eta=f(\dot{\gamma})$ . . . . . 174
6-6	The Carreau-Yasuda model parameters for different black liquors $\eta=f(\dot{\gamma})$ . . . . . 174
6-7	The Cross model parameters for different black liquors $\eta_r=f(a_T\dot{\gamma})$ . . . . . 175

6-8	The Carreau-Yasuda model parameters for different black liquors $\eta_r = f(a_T \dot{\gamma})$ .....	175
6-9	The Cross model parameters for different black liquors $\eta_r = f(a_S a_T \dot{\gamma})$ .....	176
6-10	The Carreau-Yasuda model parameters for different black liquors $\eta_r = f(a_S a_T \dot{\gamma})$ .....	176
6-11	The Carreau-Yasuda model parameters for different black liquors $\eta_r = f(a_S \dot{\gamma})$ .....	176
6-12	$T_g$ and $T_S$ for different black liquors .....	177
7-1	Comparison between the calculated and measured Newtonian viscosity of different black liquors at different temperatures ..	204
7-2	Constants A, B, and C as given in equation (7-8) for different black liquors at different solids concentrations .....	205
7-3	Constants B and C as in equation (7-8) for different black liquors with A considered as a universal constant .....	206
7-4	Comparison between the calculated and measured zero shear rate viscosity of black liquor ABAFX013,14 .....	207
7-5	Comparison between the calculated and measured zero shear rate viscosity of black liquor ABAFX025,26 .....	208
8-1	The power-law model parameters for dynamic viscosity as a function of frequency for black liquor ABAFX013,14 .....	282
8-2	Cross model parameters for dynamic viscosity as a function of frequency for different black liquors .....	283
8-3	Carreau-Yasuda model parameters for dynamic viscosity as a function of frequency for different black liquors .....	284
8-4	The power-law model parameters for storage modulus as a function of frequency for different black liquors .....	285
8-5	Model parameters as in equation (8-40) for storage modulus as a function of frequency for different black liquors .....	286

8-6	Model parameters for dynamic viscosity as a function of reduced frequency as in equation (8-45) for three black liquors . . . . .	287
8-7	Model parameters for dynamic viscosity as a function of reduced frequency as in equation (8-46) for three black liquors . . . . .	287
8-8	Model parameters for storage modulus as a function of reduced frequency as in equation (8-47) for different black liquors . . .	288
8-9	Model parameters for reduced dynamic viscosity as a function of reduced frequency as in equation (8-49) for black liquors . .	288
8-10	Model parameters for reduced dynamic viscosity as a function of reduced frequency as in equation (8-50) for different black liquors . . . . .	289

## LIST OF FIGURES

<u>Figure</u>	<u>Page</u>
2-1	Steady simple shear flow between two parallel plates ..... 19
3-1	Schematic of a concentric cylinder viscometer ..... 24
3-2	Experimental setup of a pressure cell coaxial cylinder viscometer ..... 39
4-1	Flow through a capillary tube ..... 44
4-2	Experimental setup for a capillary viscometer ..... 52
4-3	Pressure profile along the reservoir and capillary ..... 52
4-4	Pressure drop as a function of $L/D$ for black liquor ABAFX013,14 at 70.05% solids at 55 °C ..... 63
4-5	Pressure drop as a function of $L/D$ for black liquor ABAFX013,14 at 75.05% solids at 40 °C ..... 64
4-6	Pressure drop as a function of $L/D$ for black liquor ABAFX013,14 at 75.05% solids at 55 °C ..... 65
4-7	Pressure drop as a function of $L/D$ for black liquor ABAFX013,14 at 75.05% solids at 70 °C ..... 66
4-8	Pressure drop as a function of $L/D$ for black liquor ABAFX025,26 at 75.7% solids at 40 °C ..... 67
4-9	Pressure drop as a function of $L/D$ for black liquor ABAFX025,26 at 75.7% solids at 55 °C ..... 68
4-10	Pressure drop as a function of $L/D$ for black liquor ABAFX025,26 at 81.05% solids at 40 °C ..... 69



4-11	Pressure drop as a function of L/D for black liquor ABAFX025,26 at 81.05% solids at 55 °C .....	70
4-12	Pressure drop as a function of L/D for black liquor ABAFX043,44 at 72.89% solids at 40 °C .....	71
4-13	Pressure drop as a function of L/D for black liquor ABAFX043,44 at 72.89% solids at 55 °C .....	72
4-14	Pressure drop as a function of L/D for black liquor ABAFX043,44 at 76.28% solids at 40 °C .....	73
4-15	Pressure drop as a function of L/D for black liquor ABAFX043,44 at 76.28% solids at 55 °C .....	74
4-16	Schematic of the extrusion barrel assembly .....	58
4-17	Shear stress as a function of $Q/(\pi R^3)$ for black liquor ABAFX013,14 at 70.05% solids at 40 °C .....	75
4-18	Shear stress as a function of $Q/(\pi R^3)$ for black liquor ABAFX013,14 at 70.05% solids at 55 °C .....	76
4-19	Shear stress as a function of $Q/(\pi R^3)$ for black liquor ABAFX013,14 at 75.05% solids at 40 °C .....	77
4-20	Shear stress as a function of $Q/(\pi R^3)$ for black liquor ABAFX013,14 at 75.05% solids at 55 °C .....	78
4-21	Shear stress as a function of $Q/(\pi R^3)$ for black liquor ABAFX013,14 at 75.05% solids at 70 °C .....	79
4-22	Shear stress as a function of $Q/(\pi R^3)$ for black liquor ABAFX025,26 at 77.7% solids at 40 °C .....	80
4-23	Shear stress as a function of $Q/(\pi R^3)$ for black liquor ABAFX025,26 at 75.7% solids at 55 °C .....	81
4-24	Shear stress as a function of $Q/(\pi R^3)$ for black liquor ABAFX025,26 at 81.05% solids at 40 °C .....	82
4-25	Shear stress as a function of $Q/(\pi R^3)$ for black liquor ABAFX025,26 at 81.05% solids at 55 °C .....	83

4-26	Shear stress as a function of $Q/(\pi R^3)$ for black liquor ABAFX043,44 at 72.89% solids at 40 °C .....	84
4-27	Shear stress as a function of $Q/(\pi R^3)$ for black liquor ABAFX043,44 at 72.89% solids at 40 °C .....	85
4-28	Shear stress as a function of $Q/(\pi R^3)$ for black liquor ABAFX043,44 at 76.28% solids at 40 °C .....	86
5-1	Experimental setup of glass capillary viscometer .....	89
5-2	Kinematic viscosity as a function of temperature for black liquor ABAFX015,16 .....	100
5-3	Kinematic viscosity as a function of temperature for black liquor ABAFX025,26 .....	101
5-4	Kinematic viscosity as a function of temperature for black liquor ABAFX035,36 .....	102
5-5	Kinematic viscosity as a function of temperature for black liquor ABAFX043,44 .....	103
5-6	Kinematic viscosity as a function of temperature for black liquor ABAFX053,54 .....	104
5-7	Reduced kinematic viscosity for black liquor ABAFX015,16 ..	105
5-8	Reduced kinematic viscosity for black liquor ABAFX025,26 ..	106
5-9	Reduced kinematic viscosity for black liquor ABAFX035,36 ..	107
5-10	Reduced kinematic viscosity for black liquor ABAFX043,44 ..	108
5-11	Reduced kinematic viscosity for black liquor ABAFX053,54 ..	109
5-12	$B_2$ as a Function of solids concentrations for different black liquors .....	110
6-1	Viscosity as a function of shear rate for black liquor ABAFX011,12 at 55.84% solids .....	131
6-2	Viscosity as a function of shear rate for black liquor ABAFX011,12 at 63.49% solids .....	132

6-3	Viscosity as a function of shear rate for black liquor ABAFX011,12 at 72.67% solids .....	133
6-4	Viscosity as a function of shear rate for black liquor ABAFX011,12 at 75.36% solids .....	134
6-5	Viscosity as a function of shear rate for black liquor ABAFX011,12 at 84.14% solids .....	135
6-6	Viscosity as a function of shear rate for black liquor ABAFX013,14 at 50.82% solids .....	136
6-7	Viscosity as a function of shear rate for black liquor ABAFX013,14 at 59.08% solids .....	137
6-8	Viscosity as a function of shear rate for black liquor ABAFX011,12 at 67.2% solids .....	138
6-9	Viscosity as a function of shear rate for black liquor ABAFX013,14 at 70.05% solids .....	139
6-10	Viscosity as a function of shear rate for black liquor ABAFX013,14 at 75.05% solids .....	140
6-11	Viscosity as a function of shear rate for black liquor ABAFX025,26 at 53.08% solids .....	141
6-12	Viscosity as a function of shear rate for black liquor ABAFX025,26 at 57.68% solids .....	142
6-13	Viscosity as a function of shear rate for black liquor ABAFX025,26 at 71.98% solids .....	143
6-14	Viscosity as a function of shear rate for black liquor ABAFX025,26 at 75.70% solids .....	144
6-15	Viscosity as a function of shear rate for black liquor ABAFX025,26 at 81.05% solids .....	145
6-16	Viscosity as a function of shear rate for black liquor ABAFX043,44 at 53.12% solids .....	146
6-17	Viscosity as a function of shear rate for black liquor ABAFX043,44 at 58.33% solids .....	147

6-18	Viscosity as a function of shear rate for black liquor ABAFX043,44 at 64.17% solids .....	148
6-19	Viscosity as a function of shear rate for black liquor ABAFX043,44 at 72.89% solids .....	149
6-20	Viscosity as a function of shear rate for black liquor ABAFX043,44 at 76.28% solids .....	150
6-21	Viscosity as a function of shear rate for different black liquors T=70 °C .....	151
6-22	Viscosity as a function of solids concentrations for different black liquors at T=70 °C .....	152
6-23	Reduced plot for viscosity of black liquor ABAFX011,12 at 75.36% solids .....	153
6-24	Reduced plot for viscosity of black liquor ABAFX013,14 at 75.05% solids .....	154
6-25	Reduced plot for viscosity of black liquor ABAFX025,26 at 71.98% solids .....	155
6-26	Reduced plot for viscosity of black liquor ABAFX025,26 at 75.7% solids .....	156
6-27	Reduced plot for viscosity of black liquor ABAFX043,44 at 72.89% solids .....	157
6-28	Reduced plot for viscosity of black liquor ABAFX043,44 at 76.28% solids .....	158
6-29	Reduced plot for viscosity of black liquor ABAFX013,14 ....	159
6-30	Reduced plot for viscosity of black liquor ABAFX025,26 ....	160
6-31	Reduced plot for viscosity of black liquor ABAFX043,44 ....	161
6-32	Reduced plot for viscosity of black liquor ABAFX011,12 ....	162
6-33	Reduced plot for viscosity of black liquor ABAFX013,14 ....	163
6-34	Reduced plot for viscosity of black liquor ABAFX025,26 ....	164

6-35	Reduced plot for viscosity of black liquor ABAFX043,44 . . . .	165
6-36	Shift factor for black liquor ABAFX011,12 at different solids concentrations . . . . .	166
6-37	Shift factor for black liquor ABAFX013,14 at different solids concentrations . . . . .	167
6-38	Shift factor for black liquor ABAFX025,26 at different solids concentrations . . . . .	168
6-39	Shift factor for black liquor ABAFX043,44 at different solids concentrations . . . . .	169
6-40	Composite plot for shift factor of different black liquors . . . .	170
7-1	Glass transition temperature as a function of solids concentrations for different black liquors . . . . .	192
7-2	Effect of temperature on zero shear rate viscosity of black liquor ABAFX011,12 . . . . .	193
7-3	Effect of temperature on zero shear rate viscosity of black liquor ABAFX013,14 . . . . .	194
7-4	Effect of temperature on zero shear rate viscosity of black liquor ABAFX025,26 . . . . .	195
7-5	Effect of temperature on zero shear rate viscosity of black liquor ABAFX043,44 . . . . .	196
7-6	B as in equation (7-8) for different black liquors with A considered as a universal constant . . . . .	197
7-7	C as in equation (7-8) for different black liquors with A considered as a universal constant . . . . .	198
7-8	Reduced plot of zero shear rate viscosity for black liquor ABAFX011,12 . . . . .	199
7-9	Reduced plot of zero shear rate viscosity for black liquor ABAFX013,14 . . . . .	200

7-10	Reduced plot of zero shear rate viscosity for black liquor ABAFX025,26 .....	201
7-11	Reduced plot of zero shear rate viscosity for black liquor ABAFX043,44 .....	202
7-12	Reduced plot of zero shear rate viscosity for different black liquors .....	203
8-1	Small amplitude oscillatory shear flow between two parallel plates .....	211
8-2	The parallel plate system .....	216
8-3	Dynamic viscosity as a function of frequency for black liquor ABAFX013,14 at 67.2% solids .....	238
8-4	Dynamic viscosity as a function of frequency for black liquor ABAFX013,14 at 70.05% solids .....	239
8-5	Dynamic viscosity as a function of frequency for black liquor ABAFX013,14 at 75.05% solids .....	240
8-6	Dynamic viscosity as a function of frequency for black liquor ABAFX025,26 at 71.98% solids .....	241
8-7	Dynamic viscosity as a function of frequency for black liquor ABAFX025,26 at 75.7% solids .....	242
8-8	Dynamic viscosity as a function of frequency for black liquor ABAFX025,26 at 81.05% solids .....	243
8-9	Dynamic viscosity as a function of frequency for black liquor ABAFX043,44 at 65.4% solids .....	244
8-10	Dynamic viscosity as a function of frequency for black liquor ABAFX043,44 at 72.89% solids .....	245
8-11	Dynamic viscosity as a function of frequency for black liquor ABAFX043,44 at 76.28% solids .....	246
8-12	Storage modulus as a function of frequency for black liquor ABAFX013,14 at 67.2% solids .....	247

8-13	Storage modulus as a function of frequency for black liquor ABAFX013,14 at 70.05% solids .....	248
8-14	Storage modulus as a function of frequency for black liquor ABAFX013,14 at 75.05% solids .....	249
8-15	Storage modulus as a function of frequency for black liquor ABAFX025,26 at 71.98% solids .....	250
8-16	Storage modulus as a function of frequency for black liquor ABAFX025,26 at 75.7% solids .....	251
8-17	Storage modulus as a function of frequency for black liquor ABAFX025,26 at 81.05% solids .....	252
8-18	Storage modulus as a function of frequency for black liquor ABAFX043,44 at 65.4% solids .....	253
8-19	Storage modulus as a function of frequency for black liquor ABAFX043,44 at 72.89% solids .....	254
8-20	Storage modulus as a function of frequency for black liquor ABAFX043,44 at 76.28% solids .....	255
8-21	Reduced dynamic viscosity for black liquor ABAFX013,14 at 67.2% solids .....	256
8-22	Reduced dynamic viscosity for black liquor ABAFX013,14 at 70.05% solids .....	257
8-23	Reduced dynamic viscosity for black liquor ABAFX013,14 at 76.05% solids .....	258
8-24	Reduced dynamic viscosity for black liquor ABAFX025,26 at 71.98% solids .....	259
8-25	Reduced dynamic viscosity for black liquor ABAFX025,26 at 75.7% solids .....	260
8-26	Reduced dynamic viscosity for black liquor ABAFX025,26 at 81.05% solids .....	261
8-27	Reduced dynamic viscosity for black liquor ABAFX043,44 at 65.4% solids .....	262

8-28	Reduced dynamic viscosity for black liquor ABAFX043,44 at 72.89% solids .....	263
8-29	Reduced dynamic viscosity for black liquor ABAFX043,44 at 76.28% solids .....	264
8-30	Reduced storage modulus for black liquor ABAFX013,14 at 67.2% solids .....	265
8-31	Reduced storage modulus for black liquor ABAFX013,14 at 70.05% solids .....	266
8-32	Reduced storage modulus for black liquor ABAFX013,14 at 76.05% solids .....	267
8-33	Reduced storage modulus for black liquor ABAFX025,26 at 71.98% solids .....	268
8-34	Reduced storage modulus for black liquor ABAFX025,26 at 75.7% solids .....	269
8-35	Reduced storage modulus for black liquor ABAFX025,26 at 81.05% solids .....	270
8-36	Reduced storage modulus for black liquor ABAFX043,44 at 65.4% solids .....	271
8-37	Reduced storage modulus for black liquor ABAFX043,44 at 72.89% solids .....	272
8-38	Reduced storage modulus for black liquor ABAFX043,44 at 76.28% solids .....	273
8-39	Reduced dynamic viscosity for black liquor ABAFX013,14 ...	274
8-40	Reduced dynamic viscosity for black liquor ABAFX025,26 ...	275
8-41	Reduced dynamic viscosity for black liquor ABAFX043,44 ...	276
8-42	Complex and shear viscosity of black liquor ABAFX013,14 at 70.05% solids .....	277
8-43	Complex and shear viscosity of black liquor ABAFX013,14 at 76.05% solids .....	278



8-44	Complex and shear viscosity of black liquor ABAFX025,26 at 81.05% solids .....	279
8-45	Complex and shear viscosity of black liquor ABAFX043,44 at 72.89% solids .....	280
8-46	Complex and shear viscosity of black liquor ABAFX013,14 at 76.28% solids .....	281

Abstract of Dissertation Presented to the Graduate School  
of the University of Florida in Partial Fulfillment of the  
Requirements for the Degree of Doctor of Philosophy

AN INVESTIGATION OF THE RHEOLOGICAL PROPERTIES OF HIGH  
SOLIDS KRAFT BLACK LIQUORS

By

Abbas Ali Zaman

August 1993

Chairperson: Arthur L. Fricke  
Major Department: Chemical Engineering

The rheological properties of several softwood kraft black liquors from a two level, four variable factorially designed pulping experiment were determined for solids concentrations from 10% to 85%, temperatures from 25 °C to 140 °C, and shear rates up to 10,000 sec<sup>-1</sup>. Glass capillary methods were used to determine the kinematic viscosities of the liquors at low solids concentrations. Relationships between kinematic viscosity and temperature can be expressed by using either free volume theory and an average value for the freezing point of the liquors or absolute rate theory. A reduced variables method for dilute polymer solutions was used to correlate the viscosity with the combined effects of temperature and solids concentration.

The viscosity of the liquors at high solids concentrations (≥50%) were determined using Instron capillary, Haake coaxial cylinder and Parallel plate

rheometers. It was shown that the slip velocity at the wall of the capillary is insignificant and that a two capillary method can be used to determine the viscosity of the samples. At high solids, black liquor can exhibit non-Newtonian behavior and in general, the liquors behave as pseudoplastic fluids. The exact level of viscosity at any given condition is dependent upon the solids composition, which will vary from liquor to liquor. The flow behavior of the liquors was described using Cross and Carreau-Yasuda models. Superposition principles developed for concentrated polymer solutions were applied to obtain reduced correlations for viscosity behavior of the liquors. A generalized WLF type shift factor was obtained for the liquors used in this study and can be used to obtain a reduced plot of viscosity behavior of other black liquors.

Methods of measurement and estimation of zero shear rate viscosities from viscosity-shear rate data are described and compared. The combination of the absolute reaction rates and free volume concepts were used to express the relationship between the Newtonian viscosity and temperature. An empirical method is suggested to correlate the Newtonian viscosities to temperature and solids concentration.

The linear viscoelastic functions of black liquor, the dynamic viscosity and storage modulus are affected by temperature, solids concentrations, solids composition and frequency. At sufficiently low shear rates and frequencies, shear viscosity and the magnitude of the complex viscosity are close to each other. These data were used to estimate the viscoelasticity of black liquors near normal firing

conditions and it was found that black liquors, even at very high solids concentrations (~81%), will not have problems in droplet formation due to the viscoelasticity of the fluid at temperatures above 120 °C.

## CHAPTER 1 INTRODUCTION

In the kraft pulping process, large amounts of relatively expensive cooking chemicals are used to separate cellulose fibers from fibrous raw material through a series of chemical reactions at elevated temperatures. In kraft pulping, wood is chemically delignified using a solution of sodium hydroxide and sodium sulfide. The products of delignification are cellulose fibers and black liquor. Black liquor contains inorganic salts, extracted light organic compounds, carbohydrate derivatives and organic constituents in the form of polymeric lignin.

The recovery and recycling of the cooking chemicals contained in black liquor are economically and environmentally essential which has resulted in the development of an advanced and complex technology for the recovery of inorganic chemicals that is combined with energy recovery that supplies most of the energy requirements for pulping and paper making.

The kraft recovery process requires that kraft black liquors be concentrated from 12-15% solids to about 65% solids or more by multiple effect evaporators and high solids concentrators. The concentrated black liquor is fed to a recovery furnace where the organic materials are burned and inorganics fall to the bottom of the furnace where sulfur compounds are reduced. The resulting sodium salts are

dissolved in water, causticized with lime, and then clarified and recycled to the pulping process.

In order to make the recovery process more energy-efficient, there is a continuous trend towards firing black liquor at higher solids concentrations in the recovery furnace. At present, the water remaining in the liquor after concentration in evaporators and concentrators is evaporated in the furnace at a steam economy of less than 1/1 (1 pound of water is evaporated for 1 pound of steam consumed), while evaporators operate at a steam economy of 4/1. If the solids content for firing were increased from 65% to 80% before combustion at a steam economy of 4/1, the energy savings would be about  $760 \times 10^9$  J/day for a typical 1000 ton/day mill (Fricke 1987). In addition to energy savings by firing at higher concentrations, the efficiency and capacity of the furnace would be increased and safety of the operation would be improved. Also, sulfur emissions would be reduced substantially.

Knowledge of black liquor physical properties, especially rheological properties, over a wide range of temperature, concentration and shear rate is essential for improvement in design and operation of kraft recovery systems such as evaporators, concentrators and recovery furnaces. Not only do rheological properties affect evaporator and concentrator operation and power requirements for fluid transport, but they affect droplet formation, and drying and swelling characteristics in the furnace.

The strong dependence of rheological properties of black liquor on temperature, solids concentration and shear rate has been well-established in the

past. However, our present knowledge of the rheological properties of black liquor, especially at high concentrations, is incomplete due to the complex behavior of the liquors and variation of the rheological properties over a very wide range depending upon temperature, solids content, cooking conditions and type of wood species. Quantitative models for correlating these effects have not been developed prior to this work.

The data for rheological properties of black liquor should be developed in a manner similar to that successfully used of other commercially important systems such as polymers, crude oils and other petroleum fractions. Fundamentally based correlations should be developed to predict rheological properties at process conditions from the knowledge of black liquor composition and cooking conditions. No such methods and generalized correlations currently have been reported in the literature for black liquor. At present the only successful method that has been developed is to treat black liquor as a polymer solution, but the published correlations are based upon data from only a few black liquors.

The primary purpose of this research was to study the rheological properties of softwood black liquors especially at high solids concentrations, using a series of well-characterized liquors, pulped under carefully controlled conditions. Objectives of the work were to

1. Determine the effects of temperature, solids concentrations, solids composition and shear rate on viscosity of softwood kraft black liquors, especially at high solids concentration.

2. Develop fundamentally based quantitative models for viscosity as a function of temperature, solids content and shear rate.
3. Develop universal correlations for viscosity behavior of black liquors at low ( $\leq 50\%$ ) and high ( $\geq 50\%$ ) solids concentrations.
4. Determine the viscoelastic properties of high solids kraft black liquors to develop rheological models and universal correlations for linear viscoelastic functions of black liquor.
5. Estimate the viscoelasticity of black liquor near normal firing conditions.

In this study, rheological data have been taken for a series of well-characterized liquors from experimental cooks made at a wide range of pulping conditions by using different precise instruments especially designed to maintain very accurate temperature control.

The theoretical basis, description of the experimental equipment and description of the data analysis used for two important rheological instruments (a Haake coaxial cylinder viscometer and an Instron capillary rheometer) employed in this work are described in chapters 3 and 4. Viscosity of black liquors at low solids concentrations ( $\leq 50\%$ ), viscosity-temperature relationship and reduced variables method for viscosity as a function of the combined effect of temperature and concentration at low solids are discussed in chapter 5. In chapters 6 and 7, the viscosity of black liquors at high solids concentrations ( $\geq 50\%$ ), the effects of temperature, solids concentration and shear rate on the viscosity of the liquors, and appropriate correlations for defining the viscosity as a function of shear rate and



temperature are discussed. Specific attention has been given to development of reduced variables methods to correlate the viscosity of the liquors which combine the effects of temperature, solids concentrations and shear rate. Finally in chapter 8, a description of the parallel plate rheometer used, the measurement of viscoelastic properties of high solids kraft black liquors, and a description of the generalized correlations for linear viscoelastic functions and viscoelasticity of black liquors near normal firing conditions are described.

## CHAPTER 2 OVERVIEW AND BACKGROUND

### 2.1 Composition of Black Liquor

Black liquor is the by-product of chemical pulping in pulp and paper industry and it is a complex solution of organic and inorganic components in water. The non-volatile constituents consist of lignin, low molecular weight organic components and inorganic salts dissolved in water during the pulping process (e.g, Rydholm 1965 and Fricke 1990). It is widely known that the lignin concentration and its molecular weight, the organic-to-inorganic ratio, and concentration of inorganics in the non-volatiles are affected by the pulping conditions (Fricke 1987, 1990). Table (2-1) shows the analysis of different black liquors which is a representation of the complexity of black liquor.

The organics are about 50% to 75% of the total solids in black liquor, and the remaining solids are inorganics from the spent cooking chemicals in the form of sodium salts, such as sodium sulfate, sodium sulfide, sodium sulfite, and sodium carbonate. Lignin, which is a complex, heterogeneous natural polymer, comprises up to 50% of the organic components in the liquor and consists of phenylpropane monomers containing carboxylic, ether, and hydroxyl groups. More than two thirds of the phenylpropane units in lignin are linked by ether bonds and the rest by carbon-

Table (2-1): Composition of Organic and Inorganic Materials in Three Different Kraft Black Liquors (Slash Pine).

Components, g/g solids	ABAFX011,12	ABAFX025,26	ABAFX043,44
chloride	$2.52 \times 10^{-3}$	$3.10 \times 10^{-3}$	$3.47 \times 10^{-3}$
sulfite	$2.78 \times 10^{-3}$	$3.15 \times 10^{-3}$	$2.94 \times 10^{-3}$
sulfate	$1.42 \times 10^{-2}$	$2.08 \times 10^{-2}$	$2.44 \times 10^{-2}$
oxalate	$6.39 \times 10^{-3}$	$5.18 \times 10^{-3}$	$6.22 \times 10^{-3}$
thiosulfate	$3.28 \times 10^{-2}$	$6.32 \times 10^{-2}$	$4.70 \times 10^{-2}$
carbonate	$2.89 \times 10^{-2}$	$6.56 \times 10^{-2}$	$6.02 \times 10^{-2}$
lactate/glycolate	$6.58 \times 10^{-2}$	$9.41 \times 10^{-2}$	$8.06 \times 10^{-2}$
formate	$6.96 \times 10^{-2}$	$7.77 \times 10^{-2}$	$7.08 \times 10^{-2}$
acetate	$5.19 \times 10^{-2}$	$4.94 \times 10^{-2}$	$5.49 \times 10^{-2}$
lignin	0.35	0.3928	0.4178
calcium	$1.88 \times 10^{-3}$	$1.81 \times 10^{-3}$	$2.22 \times 10^{-3}$
magnesium	$6.73 \times 10^{-4}$	$6.33 \times 10^{-3}$	$7.77 \times 10^{-4}$
potassium	$1.15 \times 10^{-3}$	$6.85 \times 10^{-4}$	$7.17 \times 10^{-4}$
organic-to-inorganic ratio	2.12	2.051	2.227

to-carbon bonds. The weight average molecular weight of lignin in black liquor is relatively high and varies between 10,000 to 40,000 (Sjöström 1981). In wood, lignin is a three dimensional network polymer and its amount in different type of hardwoods and softwoods can vary from 20% to 40% (Casey 1980). It is called a

"cementing" material, since it is concentrated in the thickest layer of the cell wall to provide enough strength to wood to hold the cellulose fibers in place.

## 2.2 Literature Review on Rheology of Black Liquor

A literature review on the rheological properties of black liquor shows that the most important rheological property of black liquor is its viscosity which is not only a function of temperature, concentration and shear rate (at high solids) but also is a function of black liquor composition and the type of the wood species.

Knowledge of black liquor viscosity over a wide range of temperature, concentration, and shear rate is essential for the optimum design and efficient operation of kraft recovery systems, particularly at high solids concentrations.

Many studies have reported viscosity data for black liquors, but relatively few studies have been performed on liquors at high solids concentrations. Morre (1923), Kobe and McCormack (1949), Hunter et al. (1953), Harvin (1955), Han (1957), Melcher (1961), Bodenheimer (1969), Lankenau and Flores (1969), Polyakov et al. (1970), Wight (1985), Zaman and Fricke (1991, 1993) have reported viscosity data for black liquors for concentrations below 50% solids and temperatures up to 100 °C (373.16 K). The most extensive data are reported by Wight (1985), Fricke (1987), and Zaman and Fricke (1993) who have also shown that black liquors behave as Newtonian fluids at concentrations up to 50% solids.

Marton (1971), Ghalke and Veeramani (1977), Oye et al. (1977), Herrick et al. (1979), Kim (1980), Wight et al. (1981), Sandquist (1981, 1983), Stenuf and

Agarwal (1981), Co et al. (1982), Small (1984, 1985), Wight (1985), Kim et al. (1981), Söderhjelm (1986, 1988, 1992), Stevens (1987), Janson and Söderhjelm (1988), Milanova and Dorris (1989) have reported viscosity data for black liquors at high solids concentrations using a variety of types of viscometers designed for studies of polymeric fluids. In these studies, viscosity data are reported at temperatures up to 120 °C (393.16 K) and concentrations up to 75% solids. The most recent extensive data have been reported by Zaman and Fricke (1991) for temperatures up to 140 °C (413.16 K) and concentrations approaching 85% solids. Most of this past work is suspect because black liquors at high solids concentrations behave generally as non-Newtonian fluids, but data have not always been taken to account for this.

Black liquor viscosity is very dependent upon temperature and the viscosity of most black liquors is known to decrease with time when the liquor is held at high temperatures (above 110 °C or 383.16 K) at high solids concentrations (above 65%), as has been shown by Small (1985) and Söderhjelm (1986, 1988). This decrease occurs most probably as a result of degradation of the lignin contained in black liquor (Small 1985). As a result, special equipment and procedures are required to have precise temperature control during measurement to obtain data that are accurate and for which no degradation of lignin has occurred.

At high solids concentrations, black liquor shows non-Newtonian behavior under certain conditions (e.g. Kim 1980, Fricke 1987, Zaman and Fricke 1991). At very low shear rates, the viscosity is a constant and black liquor can be treated as a Newtonian fluid (the value of viscosity at this range is called Newtonian or zero shear

rate viscosity). At higher shear rates, it is a non-Newtonian fluid exhibiting pseudo-plastic (shear thinning) behavior. This could substantially complicate calculation of black liquor flow and spray behavior, unless the temperature is increased enough that the behavior of the liquor changes from a non-Newtonian to a Newtonian flow pattern. Some of the researchers (e.g. Söderhjelm 1986 and 1988, Wennberg 1989) have reported thixotropic behavior for highly viscous hardwood black liquors. The apparent viscosity of these liquors will change from its initial value after some period of steady shearing. This kind of behavior has not been reported for softwood black liquors, which is probably due to the fact that the lignin molecular weight in hardwoods is smaller than that of softwoods (Wennberg 1989). At normal mill conditions, the viscosity of the liquors is low enough that the thixotropic behavior is insignificant.

The viscosity of black liquor is a strong function of the solids concentrations and depends upon temperature, it may change by as much as 2-8 orders of magnitude as the solids content changes from 20% to 80% (e.g. Ghalke and Veeramani 1977, Wennberg 1989, Zaman and Fricke 1991). The increase in viscosity will be more rapid above 50% solids, which can be attributed to the organic components of black liquor. The rapid increase in viscosity around 50% solids is due to the fact that, above this concentration, there is a transition from a water continuous phase to a polymer continuous phase.

It is well known that the viscosity of black liquor is a decreasing function of temperature and depends upon concentration, it may decrease by as much as 2-6

orders of magnitude as the temperature increases from 40 °C (313.16 K) to 140 °C (413.16 K). Over narrow ranges of temperature, the relationship between the Newtonian (zero shear rate) viscosity of black liquors and temperature can be expressed by the application of absolute reaction rates (Arrhenius relationship) (e.g, Wight 1985 and Fricke 1987) and free volume theory (e.g, Wennberg 1985). Over wide ranges of temperature, the shape of the viscosity-temperature curves is nonlinear (e.g, Zaman and Fricke 1991) and either approach fails to express the viscosity temperature relationship adequately. Some empirical correlations can be found in the literature (e.g, Wennberg 1985, Söderhjelm 1986) that have been used to fit experimental data for Newtonian viscosity as a function of temperature; however, these models do not have a theoretical basis.

Of all the organic and inorganic constituents of black liquor, lignin, which composes up to 50% of the organic components, is believed to have the main effect on viscosity. Therefore, black liquor can be treated as a polymer solution and theories developed for polymer solutions should be useful for modeling the viscosity data. There was a big drop in the viscosity of several black liquors when the high molecular fraction of lignin was removed by ultrafiltration from the liquors at the same solids concentrations (Söderhjelm 1986). The effects of lignin concentration and its molecular weight on viscosity have been studied by several investigators. Wight (1985) and Fricke (1987) have shown that the log of the Newtonian viscosity of softwood black liquors at low solids content ( $\leq 50\%$ ) has a linear relationship with  $c\bar{M}_w$ , where  $c$  is the lignin concentration and  $\bar{M}_w$  is the average lignin molecular

weight. No such relationship has been reported in the literature for high solids black liquors. In a more recent work (Söderhjelm 1988), no obvious correlation was found between the viscosity and molecular weight of lignin for several birch black liquors. The presence of xylan in large concentrations as a free polysaccharide or as a carbohydrate-lignin complex was believed to have a strong effect on the viscosity of birch black liquors. However, in addition to lignin molecular weight and its concentration, other organic and inorganic constituents of black liquor may make a significant contribution to the rheological properties of black liquors and the viscosity can be expected to vary significantly among different black liquors compared at the same solids concentrations.

The viscosity data for a liquor below about 50% solids can be reduced to a single curve by the use of  $ST_0/T$  (e.g, Fricke 1987, Zaman and Fricke 1991) or  $S/T$  (Zaman and Fricke 1993) as a reducing function, where  $S$  = solids mass fraction,  $T$  = absolute temperature, and  $T_0$  = an arbitrary reference temperature. This curve can be defined for a liquor by two or, at most, three constants which are dependent upon the solids composition. The constants can be correlated empirically with non-volatile composition and pulping conditions for liquors from one wood species. Therefore, it is clear that the data for liquors of single species must be available before a general correlation can be developed.

The theories developed for polymer solutions have been used to obtain generalized correlations for viscosity of black liquors as a function of solids concentrations, temperature, and shear rate (e.g, Fricke 1987, Zaman and Fricke



1991), but the work was still not complete. A WLF type shift factor based on an arbitrary reference temperature, as suggested by Fricke (1987), to account for the temperature dependence of viscosity in the non-Newtonian region has been used successfully for a number of liquors. Also, an empirical shift factor to account for the effects of solids concentration has been successfully applied to different liquors to express the viscosity of a single liquor as a function of temperature, solids concentration and shear rate (e.g, Zaman and Fricke 1991). However, this empirical approach is not completely satisfactory as a basis for a universal shift factor to account for the effects of temperature and solids concentrations on viscosity in the non-Newtonian region. It is known that for concentrated polymer solutions, the viscosity data can be correlated much better by using the glass transition temperature,  $T_G$ , as the reference temperature. Since  $T_G$  for black liquors is a function of solids concentrations and solids composition (Fricke 1987), a WLF type shift factor based on a reference temperature related to  $T_G$ , could possibly be used to combine the effects of solids concentrations and temperature on viscosity into one correlating factor.

It is known that, the droplet formation and the flow of some of the non-Newtonian fluids through pipes and nozzles are affected by the viscoelasticity of the fluid. Few studies have been performed on the viscoelastic properties of high solids black liquors (Co and Wight 1982, Wight 1985) and the reported data are for only two black liquors. More work has to be done in this area to study the linear viscoelastic functions of different black liquors especially at high solids concentrations

to obtain generalized quantitative correlations that can be used to estimate the viscoelasticity of the liquors near normal firing conditions and to determine the operating conditions where viscoelasticity of the liquors will be insignificant.

### 2.3 Black Liquor Preparation

The black liquors used in this study are from a four variable-two level factorially designed experiment for pulping slash pine conducted in a pilot scale digester at the University of Florida under carefully controlled conditions. Full details of the design and the results of pulping have been given elsewhere (Fricke 1987, Zaman *et al.* 1991). The four pulping variables, which cover a wide range of pulping conditions, are the cooking time, cooking temperature, effective alkali, and sulfidity. The effects of each variable as well as the interaction between variables can be determined on the physical properties of black liquor. In the pulping process, constant wet weights of sized slash pine chips were loaded into the digester. Synthetic white liquors at 85% causticizing efficiency and 93% reduction were prepared from  $\text{Na}_2\text{S}$ ,  $\text{NaOH}$ ,  $\text{Na}_2\text{CO}_3$ , and  $\text{Na}_2\text{SO}_4$  and preheated. The liquor was loaded at a 4/1 liquor-to-wood ratio, and the digester was brought to cooking temperature. After cooking, the liquor was drained, two controlled volumes of wash water were introduced and drained into the liquor, and then chips were given a final wash and removed from the digester.

The liquors used in this study were chosen so that a wide range of behavior might be expected. Liquors ABAFX011,12 and ABAFX025,26 are extremes and

liquor ABAFX043,44 is the center point of the design. Each liquor is a combination of two liquors that were made at the same pulping conditions and combined when the kappa numbers agreed within 10 percent. The pulping conditions for the liquors used in this work along with the kappa number, lignin concentration and lignin weight average molecular weight measured by GPC are shown in Table (2-2). The values for kappa number and lignin concentration are the averages for two pulping experiments and the lignin molecular weights are for the combined liquors.

#### 2.4 Concentration and Handling of Liquors

After liquors were drained out of the digester into a receiver, they were allowed to cool to the ambient temperature and then were pumped through a glass fiber filter to remove the fibers from the liquor. A pilot scale evaporator was used to concentrate the liquors to about 35% to 45% solids and then loaded into five gallon HDPE carboys and stored inside a cold room to prevent the degradation of lignin and oxidation of the black liquor.

For rheological and thermal studies, the black liquors must be concentrated to about 85% solids. For this purpose, a small scale evaporator was constructed which could be used for both concentrating the liquors and studying the vapor-liquid equilibria of black liquors. The details of the design and operating procedure have been given elsewhere (Fricke 1987, Stoy et al. 1992). The evaporator is essentially a five liter still pot with three basic parts. At the bottom section, a two liter stainless steel reaction vessel equipped with a conical glass flange at the top and a stainless

Table (2-2): Pulping Conditions, Kappa Number, Lignin Concentration and Lignin Molecular Weight for Black Liquors Used in This Study.

Cook	Time, hour	T, K	EA	SU	K#	%Lignin	$M_w$ , by GPC
ABAFX011,12	0.6667	438.7	13.0	20.0	107.0	35.00	6411.0
ABAFX013,14	1.3333	450.0	13.0	20.0	40.2	43.46	6618.0
ABAFX015,16	1.3333	438.7	16.0	20.0	61.1	37.98	8687.0
ABAFX025,26	1.3333	450.0	16.0	35.0	18.5	39.28	3910.0
ABAFX035,36	0.667	438.7	13.0	35.0	77.0	37.85	5995.5
ABAFX043,44	1.000	444.3	14.5	27.5	51.1	41.78	9672.0
ABAFX053,54	1.000	444.3	11.5	27.5	42.0	41.69	7154.0

steel block with drainage slots machined in the sides and with a step for the stirrer shaft. At the middle section, a three-liter glass vessel with conical glass flange and at the top section, openings for the stirrer, condenser, pressure transducer, and platinum resistance thermometer.

The heating for the system was provided through an electric heating jacket connected to a variac to control the heating rate. The pressure control system consists of a PID controller, pressure transducer, bleed valve, and a vacuum pump to control the pressure inside the system. A stirrer with two turbine blade impellers, connected to a D.C. motor, was used for mixing. The stirrer speed can be varied from 0-300 rpm and the direction of the speed is reversible.

The liquor was concentrated to the desired solids content while operating at a low pressure (normally 120-215 mm Hg) and a moderately high evaporation rate

(about 8-12 ml per minute). At these conditions, the operating temperature is low enough (usually less than 90 °C) that the lignin degradation does not occur. The weight of the collected condensate in the condensate vessel and cold trap was used to estimate the solids content of the liquor in the evaporator. When the desired concentration was reached, the evaporation rate was reduced to 1-1.5 ml per minute and the still operated at total reflux. Boiling points at this constant concentration were determined as a function of pressure, by establishing steady state at each pressure. Then, the liquor was removed from the evaporator into 250-500 ml HDPE bottles and stored in the cold room for rheological and thermal studies.

Solids content of the concentrated black liquors was determined using a modification of the Tappi method T625cm-85. The liquors were diluted to about 20% or less and a dilution ratio was determined. A glass fiber filter pad was placed in an aluminum pan of about 5 cm in diameter, dried for one hour in a convection oven at 105 °C (378.16 K) and weighed quickly to the nearest 0.1 mg. While the pad and pan were in the balance, approximately 1.5-2 grams of black liquor was dispersed onto the pad and weighed immediately. The pan was then allowed to dry for at least 12 hours in a convection oven at 105 °C (378.16 K) and then was placed in a desiccator to cool to room temperature. The pan was weighed again to obtain the loss in weight and determine the solids content of the diluted liquor. The dilution ratio was then used to determine the solids content of the undiluted black liquor. For every liquor at a specific solids content, the measurements were always done in duplicate. The average was taken if the results were within 1 percent; otherwise the

procedure was repeated. The repeatability of this procedure was found to be  $\pm 0.25\%$  solids.

## 2.5 Definition of Rheology

The original definition of rheology was given by Bingham in 1929 as "rheology is the study of the deformation and flow of matter." It is a very extensive area and beyond the scope of this investigation. The focus of this study is the experimental measurement of the rheological properties of black liquors "rheometry." Rheology is the study of the response of the material to an applied stress or strain to govern the relationship between stress and strain. In rheometry, we must either measure the deformation resulting from a given force (stress) or measure the force required to produce a given deformation. The aspects of rheology can be summarized as

1. Development of a quantitative relationship between stress and strain for a material of interest which is possible by experimental measurements.
2. Development of relationships between the rheological properties and structure, composition of the material, temperature, and pressure. This is a very difficult subject and has not been accomplished except for very simple materials such as Newtonian fluids.

## 2.6 Simple Shear Flow

The type of the flow that is usually used to perform rheological measurements can be approximated by a simple shear flow (viscometric flow) that is easy to

generate experimentally. In this kind of flow, the motion of the fluid is kinematically equivalent to the relative motion of two parallel plates when the fluid is placed between them. The layers of the fluid are moving relative to each other without stretching (Figure 2-1). The velocity field can be defined as (Bird et al. 1987)

$$v_x = \dot{\gamma}_{yx} y, \quad v_y = 0, \quad v_z = 0 \quad (2-1)$$

where  $v_x$ ,  $v_y$  and  $v_z$  are the components of velocity and  $\dot{\gamma}_{yx}$  is the velocity gradient and equal to

$$\dot{\gamma}_{yx} = \frac{dv_x}{dy} \quad (2-2)$$

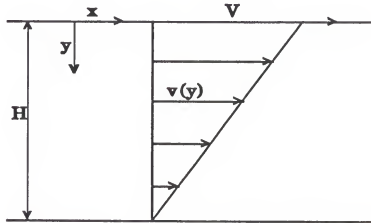


Figure (2-1): Steady Simple Shear Flow Between Two Parallel Plates

The absolute value of  $\dot{\gamma}_{yx}$  is called the shear rate ( $\dot{\gamma}$ ,  $\text{sec}^{-1}$ ) and it can be assumed that when the shear rate has been constant for a long period of time that the stresses in the fluid are time independent. While the fluid layers are moving

relative to one another, stresses (force per unit area, pas) will be generated in the fluid. Two types of stress can be defined for every fluid element, shear stresses act in a direction parallel (tangent) to the layer of the fluid and normal stresses act in a direction perpendicular to the layer. Thus for every element of the fluid, there are nine components of the stress. It is worthwhile to mention that the normal stresses are not rheologically meaningful if the material of interest is incompressible. Only shear stresses and differences between normal stresses have rheological significance. Several simplifying assumptions are usually made in rheological experiments, these are

1. The fluid is incompressible so that the viscosity of the sample is uniform throughout the field of flow in a rheometer.
2. The material is a "continuum" rather than a collection of discrete subunits.
3. The material is isotropic in its rest state so the properties of the sample are independent of the direction.

## 2.7 Definition of Newtonian and non-Newtonian Behavior

The viscosity of a fluid, which is commonly associated with how easily it flows, is a fundamental rheological property and is defined as the ratio of the magnitude of the shear stress to the shear rate in a simple shear flow.

$$\eta = \frac{\tau}{\dot{\gamma}} \quad (2-3)$$

where  $\eta$  (pas-sec) is the viscosity of the fluid and  $\tau$  (pas) is the shear stress. For



some of fluids (e.g, low molecular weight compounds) at a specific temperature (and pressure), the viscosity is constant and independent of shear rate. A material that behaves in this way is called a Newtonian fluid for which the viscosity is a "material constant." It does not depend on the amount of strain nor on the time of shearing. The stress in the fluid falls to zero immediately when the shearing is stopped.

The viscosity of many solid-liquid and liquid-liquid suspensions, emulsions, polymer solutions and polymer melts is shear rate dependent. These material are called "non-Newtonian" fluids. The structure of these materials will change with shear rate and the change in structure results in a change in viscosity. Thus, the viscosity of these fluids is not a "material constant" but a "material function."

If the viscosity decreases as the shear rate is increased, the fluid is said to be shear thinning or "pseudoplastic," and this type of behavior can be observed in most polymer solutions and polymer melts. For shear thinning materials, the general shape of the viscosity-shear rate curve has two distinguishable regions. At very low shear rates, the viscosity is a constant and the value of the viscosity in this range is called the "zero shear rate viscosity." At higher shear rates, shear thinning behavior will be observed. Also, it seems that, at relatively large shear rates, there will be another limiting value for viscosity, referred to as the "second Newtonian region." Most of the time, this region is out of the range of the experimental measurements.

If the viscosity increases as the shear rate is increased, the material is said to be shear thickening or "dilatant." The resistance of this material will be increased as the shear rate is increased. There must be an expansion in the structure of the fluid

to show this kind of behavior. Relatively few materials have been reported to be dilatant. Asphalt shows this behavior below a critical shear rate.

Other phenomena that can be observed in non-Newtonian fluids are viscoplasticity, thixotropic and rheopectic or "time dependent structure" and viscoelasticity. Viscoplastic, or "Bingham," fluids will not flow below a critical shear stress called the "yield stress." Above this stress, the material will deform like a fluid. If the shear rate approaches zero, the shear stress will approach a finite limiting value and the viscosity will approach infinity.

Some non-Newtonian fluids may not respond instantaneously to shearing deformation so that there will be a transient period during which the shear stress will vary with time. In fact, the adjustment in the structure of these materials needs a period of time when the shear rate is changed. However, there will not be any elastic energy storage and their response to an applied stress or strain will be purely viscous. The viscosity of these fluids is a function of shear rate and time. It may decrease with time and be said to be "thixotropic" or increase with time and be said to be "rheopectic."

Most of the polymer solutions and polymer melts are "viscoelastic" fluids and they have a directional memory of past deformation, i.e, if the shearing action is stopped, the shear stress does not return to zero instantaneously. Also, they have the tendency to spring back to their original state after the removal of shear stress, which is called "elastic recoil."

## CHAPTER 3 CONCENTRIC CYLINDER VISCOMETER

### 3.1 Introduction

The concentric cylinder viscometer is generally used for shear viscosity measurements of fluids in flows which approximate a simple shearing motion. A closed system of this type is an appropriate instrument in cases where evaporation is a major problem. Also it is possible to measure the normal stress differences (Broadbent and Lodge 1971, Collyer and Clegg 1988). The basic features of a concentric cylinder viscometer are shown in Figure 3-1. The fluid is contained in the gap between two cylinders. In a "Couette" type viscometer, the outer cylinder of radius  $R_o$  is fixed, while the inner one of radius  $R_i$  rotates at an angular velocity  $\omega$ . The applied torque,  $T$ , which is required to turn the rotating cylinder, or to hold the stationary cylinder in place is measured.

### 3.2 Mathematical Analysis

The basic assumptions for mathematical analysis of a coaxial cylinder viscometer are

1. steady-state laminar flow,
2. incompressible fluid,

3. constant temperature,
4. negligible inertial effects,
5. no-slip boundary conditions,
6. negligible end effects.

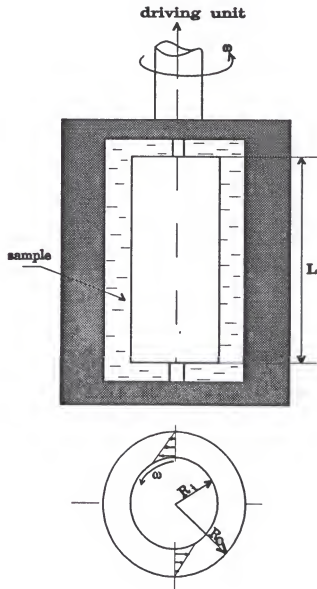


Figure 3-1: Schematic of a Concentric Cylinder Viscometer

With the above assumptions, the equations of continuity and momentum can be solved to yield the fundamental equations for the concentric cylinder viscometer (Bird et al., 1960). We use a cylindrical coordinate system where the inner and outer bounding surfaces of the fluid are at  $r=R_i$  and  $r=R_o$ , respectively. When the fluid inside the gap is in laminar flow, the velocity of the fluid can be assumed to be in the  $\theta$ -direction only (Collyer and Clegg 1988)

$$v = (0, r \Omega(r), 0) \quad (3-1)$$

where  $\Omega$  is the angular velocity of the fluid. The corresponding shear rate is

$$\frac{dv}{dr} = r \frac{d\Omega}{dr} = \frac{d\Omega}{d \log_e r} \quad (3-2)$$

The shear stress,  $\tau$ , is related to the torque as follows

$$\tau = \frac{T}{2 \pi r^2 L} \quad (3-3)$$

where  $L$  is the length of the rotor. At steady state conditions,  $T$  will be constant; therefore, taking the derivative of both sides of equation (3-3) would yield

$$d\tau = -\frac{T dr}{\pi r^3 L} = -2\tau \frac{dr}{r} \quad (3-4)$$

or

$$\frac{d\tau}{\tau} = -2 \frac{dr}{r} \quad (3-5)$$

$$d \log_e \tau = -2 d \log_e r \quad (3-6)$$

The functional relationship between the shear stress and shear rate can be expressed

as (Krieger and Elrod 1953)

$$\dot{\gamma} = \frac{dv}{dr} = g(\tau) \quad (3-7)$$

Combining equations (3-2), (3-5) and (3-7) would yield

$$g(\tau) = \frac{d\Omega}{d\log_e r} = -2 \frac{d\Omega}{d\log_e \tau} \quad (3-8)$$

Equation (3-8) can be integrated, with the following boundary conditions to give

$$\text{at } r=R_i \quad \tau=\tau_i \quad \text{and} \quad \Omega=\omega$$

$$\text{at } r=R_o \quad \tau=\tau_o \quad \text{and} \quad \Omega=0$$

$$\omega = -\frac{1}{2} \int_{\tau_i}^{\tau_o} g(\tau) d\log_e \tau = -\frac{1}{2} \int_{\epsilon^2 \tau_o}^{\tau_o} d\log_e \tau \quad (3-9)$$

where  $\epsilon = R_o/R_i$ .

When equation (3-9) is differentiated with respect to  $\tau_i$ , the following difference equation is obtained (Krieger and Maron 1952, 1954)

$$\frac{d\omega}{d\tau_i} = -\frac{1}{2\tau_i} [g(\tau_o) - g(\tau_i)] \quad (3-10)$$

### 3.3 Solution of the Difference Equation

A function  $h(\tau_i)$  can be defined as (Krieger and Elrod 1953)

$$h(\tau_i) = 2 \frac{d\omega}{d \log_e \tau_i} \quad (3-11)$$

From equation (3-10), we will have

$$h(\tau_i) = g(\tau_i) - g\left(\frac{\tau_i}{e^2}\right) \quad (3-12)$$

and

$$h\left(\frac{\tau_i}{e^2}\right) = g\left(\frac{\tau_i}{e^2}\right) - g\left(\frac{\tau_i}{e^4}\right) \quad (3-13)$$

$$h\left(\frac{\tau_i}{e^4}\right) = g\left(\frac{\tau_i}{e^4}\right) - g\left(\frac{\tau_i}{e^6}\right) \quad (3-14)$$

or finally

$$h\left(\frac{\tau_i}{e^k}\right) = g\left(\frac{\tau_i}{e^k}\right) - g\left(\frac{\tau_i}{e^{k+2}}\right) \quad (3-15)$$

Since  $g(0)=0$  and  $\epsilon = R_o/R_i > 1$ , as  $k \rightarrow \infty$ ,  $e^{(k+2)} \rightarrow \infty$ , then

$$g(\tau_i) = \sum_{k=0}^{\infty} h\left(\frac{\tau_i}{e^{2k}}\right) \quad (3-16)$$

The sum is a slowly convergent one and can be evaluated using the Euler-Maclaurin sum formula (Krieger and Elrod 1953)

$$\begin{aligned} \sum_{k=0}^m g(k) = & \int_0^m g(x) dx + \frac{1}{2} [g(0) + g(m)] + \sum_{n=1}^{\infty} \frac{B_{2n}}{(2n!)} \\ & [g^{2n-1}(m) - g^{2n-1}(0)] + \sum_{i=0}^{m-1} \int_i^{i+1} p_{2i+1}(x-i) g^{2i+1}(x) dx \end{aligned} \quad (3-17)$$

Here  $B_i$  is the  $i$ th Bernouilli number and  $p_i$  the Bernouilli polynomial. This formula

can be applied to the summation in equation (3-16), and then the integral can be evaluated by defining a new variable  $y$  as

$$y = \frac{\tau_i}{e^{2x}} \quad (3-18)$$

Since  $g(\tau_i)$  and its derivatives are zero when  $\tau_i = 0$ , the final expression for shear rate at  $r = R_1$  may be written as

$$\dot{\gamma}(\tau_i) = g(\tau_i) = \frac{\omega}{\log_e e} \left[ 1 + \log_e e \frac{d \log_e \omega}{d \log_e \tau_i} + \frac{(\log_e e)^2}{3 \omega} \frac{d^2 \omega}{d (\log_e \tau_i)^2} - \frac{(\log_e e)^4}{45 \omega} \frac{d^4 \omega}{d (\log_e \tau_i)^4} + \dots \right] \quad (3-19)$$

Krieger and Maron (1954), have shown that equation (3-19) can be expressed as

$$\dot{\gamma}(\tau_i) = \frac{2 \omega}{1 - e^{-2}} \left\{ 1 + \frac{e^2 - 1}{2 e^2} \left( 1 + \frac{2}{3} \log_e e \right) \left( \frac{d \log_e N}{d \log_e \tau_i} - 1 \right) + \frac{e^2 - 1}{6 e^2} \log_e e \left[ \left( \frac{d \log_e N}{d \log_e \tau_i} - 1 \right)^2 + \frac{d \left( \frac{d \log_e N}{d \log_e \tau_i} - 1 \right)}{d (\log_e \tau_i)} \right] + \dots \right\} \quad (3-20)$$

where  $N$  is the rotational speed of the rotor. Equation (3-20) is valid for values of  $e$  greater than 1.1 and can be used for all time independent fluids.

Krieger (1968), expressed the Euler-Maclaurian solution as a series of summable subseries which has the leading term

$$g_1(\tau_i) = \frac{2 \pi \omega}{(1 - e^{-2\pi})} \quad (3-21)$$

where



$$n = \frac{d \log_e \omega}{d \log_e \tau_i} = \frac{d \log_e N}{d \log_e \tau_i} \quad (3-22)$$

then, equation (3-20) may be written as

$$\dot{\gamma}(\tau_i) = \frac{2n\omega}{1 - e^{-2n}} \left[ 1 + \frac{1 - e^{-2n}}{2n \log_e e} \sum_{k=1}^{\infty} \frac{B_{2k}}{(2k!)} \left( \frac{\frac{d^{2k} \omega}{\omega}}{n^{2k}} - 1 \right) (2n \log_e e)^{2k} \right] \quad (3-23)$$

For a Newtonian fluid the relationship between the shear rate and shear stress can be written as

$$\dot{\gamma}(\tau) = g(\tau) = \frac{\tau}{\mu} \quad (3-24)$$

where  $\mu$  is the viscosity of the fluid. Replacing  $g(\tau)$  in equation (3-9) and integrating would yield

$$\omega = -\frac{1}{2} \int_{\tau_i}^{\tau_i} \frac{1}{\tau^3} \frac{1}{\mu} \tau d \log_e \tau = -\frac{1}{2\mu} \int_{\tau_i}^{\tau_i} \frac{1}{\tau^3} d\tau = \frac{1}{2\mu} \tau_i \left[ 1 - \frac{1}{e^2} \right] \quad (3-25)$$

hence,

$$d\omega = \frac{1}{2\mu} \left[ 1 - \frac{1}{e^2} \right] d\tau_i \quad (3-26)$$

$$\frac{d\omega}{\omega} = \frac{d\tau_i}{\tau_i} \quad (3-27)$$

or

$$\frac{d \log_e \omega}{d \log_e \tau_i} = 1 \quad (3-28)$$

Therefore, for a Newtonian fluid, equation (3-20) can be written as

$$\dot{\gamma}(\tau_i) = \frac{2 \omega}{1 - \epsilon^{-2}} = \frac{2 \omega}{1 - (\frac{R_i}{R_o})^2} \quad (3-29)$$

For a fluid that obeys the power-law model, the relationship between the shear rate and the shear stress can be written as

$$\dot{\gamma}(\tau) = g(\tau) = a \tau^b \quad (3-30)$$

where  $b$  is the reciprocal of the power-law index. Equation (3-9) may be written as

$$\omega = -\frac{1}{2} \int_{\tau_i}^{\tau_i} a \tau^b d \log_e \tau = -\frac{a}{2} \int_{\tau_i}^{\tau_i} \tau^{(b-1)} d \tau \quad (3-31)$$

$$\omega = -\frac{a}{2} \frac{1}{b} \left[ \frac{1}{\epsilon^{2b}} - 1 \right] \tau_i^b \quad (3-32)$$

$$d \omega = -\frac{a}{2} \left[ \frac{1}{\epsilon^{2b}} - 1 \right] \tau_i^{(b-1)} d \tau_i \quad (3-33)$$

$$\frac{d\omega}{\omega} = b \frac{d\tau_i}{\tau_i} \quad (3-34)$$

finally

$$\frac{d \log_e \omega}{d \log_e \tau_i} = b \quad (3-35)$$

Therefore, from equation (3-22),  $n = b = \text{constant}$  and for a power-law fluid, equation (3-33) would yield

$$n \omega \frac{d\tau_i}{\tau_i} = -\frac{a}{2} \left[ \frac{1}{e^{2b}} - 1 \right] \tau_i^{(b-1)} d\tau_i \quad (3-36)$$

$$n \omega = \frac{a}{2} [1 - e^{-2b}] \tau_i^b \quad (3-37)$$

hence,

$$\dot{\gamma}(\tau_i) = \frac{2n\omega}{1 - e^{-2n}} = \frac{2n\omega}{1 - \left(\frac{R_o}{R_i}\right)^{-2n}} \quad (3-38)$$

It is clear that equation (3-23) expresses the shear rate in terms of a power-law approximation plus a correction term.

Calderbank and Moo-Yang (1959) have evaluated a further expansion of equation (3-20) They were able to calculate shear rate with an accuracy of better than 1% for values of  $\epsilon$  up to 1.75 using

$$\begin{aligned}
\dot{\gamma}(\tau_i) = & \frac{2\omega}{1-\epsilon^{-2}} \left( 1 + \frac{\epsilon^2-1}{2\epsilon^2} \left( \frac{d\log_e N}{d\log_e \tau_i} - 1 \right) \left[ 1 + \frac{2}{3} \log_e \epsilon + \right. \right. \\
& \frac{\log_e \epsilon}{3} \left( \frac{d\log_e N}{d\log_e \tau_i} - 1 \right) - \frac{(\log_e \epsilon)^3}{45} \left( \frac{d\log_e N}{d\log_e \tau_i} - 1 \right)^3 + \\
& \left. \left. \frac{2(\log_e \epsilon)^5}{945} \left( \frac{d\log_e N}{d\log_e \tau_i} - 1 \right)^5 - \frac{(\log_e \epsilon)^7}{4725} \left( \frac{d\log_e N}{d\log_e \tau_i} - 1 \right)^7 + \dots \right] \right) \quad (3-39)
\end{aligned}$$

### 3.4 Alternative Solution

Code and Raal (1973), by defining a constant power-law departure factor,  $\alpha$ , ( $\alpha = (d\log_e n)/(d\log_e \tau_i)$  and  $n = (d\log_e \omega)/(d\log_e \tau_i)$ ) which they assumed to be constant, proposed an alternative way to sum the series of equation (3-11) and obtained the following relationship:

$$\dot{\gamma}(\tau_i) = 2n\omega \sum_{k=0}^{\infty} \epsilon^{2k\alpha} \exp\left[\frac{n}{\alpha} (\epsilon^{2k\alpha} - 1)\right] \quad (3-40)$$

Code and Raal compared their modified power-law model with the original power-law and with two truncations of the 1953 Krieger-Elrod solution. They found that, for positive values of the power-law departure  $\alpha$ , the truncated Krieger-Elrod series did not adequately represent their modified power-law model.

It should be pointed out that the limiting behavior of the Code-Raal model at low and at high shear rates is very strange (Yang and Krieger 1978):

for $\alpha < 0$	$\lim_{\tau \rightarrow 0} n \rightarrow \infty$	and	$\lim_{\tau \rightarrow \infty} n \rightarrow 0$
for $\alpha > 0$	$\lim_{\tau \rightarrow 0} n \rightarrow 0$	and	$\lim_{\tau \rightarrow \infty} n \rightarrow \infty$

thus, for  $\alpha < 0$ , the viscosity becomes infinity at both limits, while for  $\alpha > 0$ , the viscosity vanishes at both limits.

Yang and Krieger (1978), by defining another modified power-law departure factor  $\beta$ , were able to modify the Code-Raal model as

$$\dot{\gamma}(\tau_1) = 2\omega \sum_{p=0}^{\infty} e^p [1 + (n-1)e^{p\beta}] \exp\left[\frac{(n-1)(e^{p\beta} - 1)}{\beta}\right] \quad (3-41)$$

where

$$\beta = \frac{n\alpha}{(n-1)} \quad (3-42)$$

The limiting behavior of the modified Code-Raal model is

$\beta < 0$	$\lim_{\tau \rightarrow 0} n \rightarrow \infty$	$\lim_{\tau \rightarrow \infty} n \rightarrow 1$
$\beta > 0$	$\lim_{\tau \rightarrow 0} n \rightarrow 1$	$\lim_{\tau \rightarrow \infty} n \rightarrow \infty$

Thus for  $\beta < 0$ , at the low-shear limit, the viscosity is infinity and becomes Newtonian at high shear rates. For  $\beta > 0$ , there is a Newtonian low shear limit, and a vanishing viscosity at high shear.

### 3.5 Comparison of Methods for Calculating Shear Rate in Coaxial Cylinder Viscometer

Yang and Krieger (1978) have compared the accuracies of the most powerful approximate methods which have been derived from Krieger and Elrod series solutions and the Code-Raal model. However, truncation of this series is necessary in practice. There are three alternative truncations worthy of consideration (Yang

and Krieger 1978):

1. Retention of only the first correction:

$$\dot{\gamma}_1(\tau_i) = \frac{2n\omega}{(1 - e^{-2n})} \left[ 1 + \frac{n^{(1)}}{n^2} f_1(t) \right] \quad (3-43)$$

2. Retention of all terms in  $n^{(1)}$ :

$$\dot{\gamma}_2(\tau_i) = \frac{2n\omega}{(1 - e^{-2n})} \left[ 1 + \frac{n^{(1)}}{n^2} f_1(t) + \frac{3}{n^4} (n^{(1)})^2 f_3(t) \right] \quad (3-44)$$

3. Inclusion of the leading term in  $n^{(2)}$ :

$$\dot{\gamma}_3(\tau_i) = \frac{2n\omega}{(1 - e^{-2n})} \left[ 1 + \frac{n^{(1)}}{n^2} f_1(t) + \frac{3}{n^4} (n^{(1)})^2 f_3(t) + \frac{n^{(2)}}{n^3} f_2(t) \right] \quad (3-45)$$

where

$$n = \frac{d \log_e \omega}{d \log_e \tau_i} \quad (3-46)$$

$$n^{(1)} = \frac{dn}{d \log_e \tau_i} \quad (3-47)$$

$$n^{(2)} = \frac{d^2 n}{d(\log_e \tau_i)^2} \quad (3-48)$$

$$t = -2n \log_e e \quad (3-49)$$

$$f_1(t) = t(\exp t - 1)^{-2} \frac{(t \exp t - 2 \exp t + t + 2)}{2} \quad (3-50)$$

$$f_2(t) = t^2(\exp t - 1)^{-3} \frac{(-t \exp 2t + 3 \exp 2t - 4t \exp t - t - 3)}{6} \quad (3-51)$$

$$f_3(t) = t^3(\exp t - 1)^{-4} \frac{t \exp 3t - 4 \exp 3t + 11t \exp 2t - 12 \exp 2t + 11t \exp t + 12 \exp t + t + 4}{24} \quad (3-52)$$

By using Williamson and Bingham plastic models, Yang and Krieger found that Krieger's 1968 method truncated after the first term in  $n^{(2)}$  gives accurate shear rates for both types of non-Newtonian fluids. Exclusion the  $n^{(2)}$  term will reduce the accuracy, but results are still very good, except in the neighborhood of plug flow. In fully developed flow, for fluids exhibiting yield stresses, equation (3-45) has been recommended. The Code-Raal method is comparable in accuracy to the series method including  $n^{(1)}$  terms. Modification of the Code-Raal model gives only small improvement in accuracy of calculating shear rates. For fluids which do not show yield stresses, any of the equations (3-40), (3-41), (3-43) or (3-44) will give accurate results (Yang and Krieger 1978).

### 3.6 End Effects and Equivalent Length

In the coaxial cylinder viscometer, the equations have been derived based on the infinite length of the cylinder (rotor) or no axial variation in the flow pattern.

Since in practice the rotor has finite length, at the ends this can not be the case. End effects may be expressed as the torque due to the cylinder ends or as an increase in the effective cylinder length due to the ends.

End effects can be corrected by substituting an effective length  $L_e$  instead of actual length of the rotor in equation (3-3). Highgate and Whorlow (1969) have studied the end effects in concentric cylinder rheometer. They suggested using Newtonian fluids of known viscosity to determine equivalent length and concluded that there is no completely satisfactory way of eliminating the end effects for non-Newtonian fluids.

When the gap size between the inner and outer cylinder is small and the length of the inner cylinder is not too small, it should be possible to limit the error due to end effects to about 2% considering an equivalent length for the system (Dealy 1982).

The system can be loaded with a standard Newtonian fluid of known viscosity and then the values of the torque,  $T$ , corresponding to different rotational speeds can be noted. Using the values of angular velocity, the shear rate can be calculated from equation (3-29). When the values of shear rate are available, the shear stress at the wall of the rotor can be determined from

$$\tau_r = \mu \dot{\gamma}(\tau_r) \quad (3-53)$$

where  $\mu$  is the viscosity of the standard fluid. Once the shear stress is known, the equivalent length  $L_e$  can be determined from equation (3-3) as



$$L_s = \frac{T}{2\pi R_i^2 \tau_i} \quad (3-54)$$

A Haake RV12 viscometer was used in this investigation. At temperatures higher than 90 °C evaporation is a major problem; therefore, above this range, the data were collected by using a closed pressure cell coaxial cylinder (Figure 3-2). The inner radius of the cell ( $R_o$ ) was 2.4 cm and the radius of the rotor ( $R_i$ ) was 2.29 cm. The pressure cell will operate at pressures up to 40 bars and temperatures up to 300 °C.

At lower temperatures an open cup arrangement was used. The radius of the cell (cup,  $R_o$ ) was 2.1 cm and the radius of the rotor ( $R_i$ ) was 1.84 cm.

The temperature of the system was maintained through the use of an oil bath, circulating silicon oil as the heat transfer fluid through the jacket.

In the pressure cell system a calibrated type J thermocouple, inserted at the middle of the cell, was used to measure the temperature of the sample. The oil bath was equipped with a gear pump circulator which circulates the oil from the bath through the oil jacket of the pressure cell and back into the oil bath. This was designed to maintain precise temperature control; with this arrangement, the temperature of the sample was maintained to within 0.1 °C.

In the open cup arrangement, a calibrated thermometer was used to measure the temperature of the oil in the jacket. The oil bath for this system was equipped with a Haake N-3 circulator which circulated the oil from the bath through the oil jacket of the open cup and back into the bath.

Before loading the system, the effects of friction due to rotation of the rotor must be considered for the pressure cell. The frictional torque can be determined as a function of the rotational speed, and later the resulting black liquor readings can be corrected for friction accordingly. For the open cup system, the zero on the RV12 unit must be checked. This can be done by running the rotor at different constant speeds in air and changing the zero knob until the zero number flashes from 00 to -00 rapidly.

Several Newtonian standard fluids (Cannon) with known viscosity were used at different temperatures and shear rates for equivalent length determination. The equivalent length was found to be  $7.373 \pm 0.34$  cm for open cup and  $18.66 \pm 0.9$  cm for closed cell at a 95% confidence interval.

A portion of the black liquor to be investigated was heated in a constant temperature bath up to 70 °C for the closed cell and up to 40 - 50 °C for the open cup. Then it was loaded into the pressure cell using a loading cylinder designed for this system. The loading cylinder was connected through a high temperature ball valve to the feed port located at the bottom of the cell and then black liquor was loaded by screwing the plunger handle inward and forcing the sample into the cell. During the loading operation, the top valve (overflow valve) must be open. When the cell is full of sample, the liquor will start to come out of this valve, then both valves are closed and the loading cylinder disconnected and cleaned.

Once the liquor is loaded into the system, the flow rate of the oil through the jacket can be increased by increasing the rotational speed of the gear pump to heat

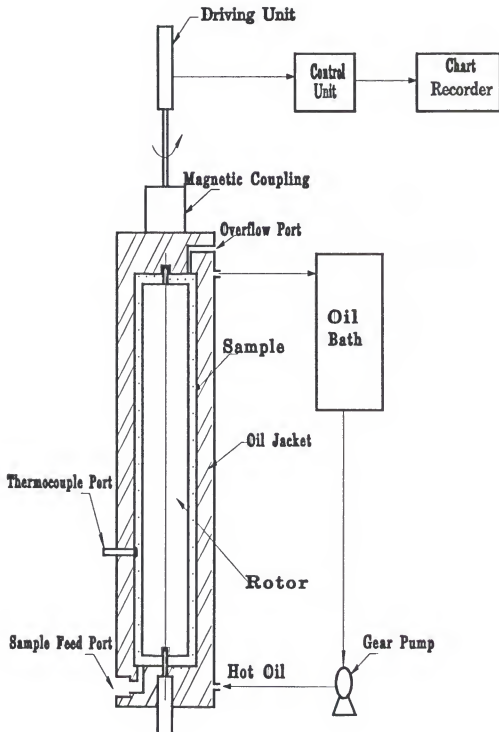


Figure 3-2: Experimental Setup of a Pressure Cell Coaxial Cylinder Viscometer

up the sample to the desired temperature. When the sample is at constant temperature, data collection can be initiated. Loading the open cup system is easier than loading the closed cell. Sufficient amount of the liquor can be poured into the cup and then the cup replaced into the system.

For data collection, the inner cylinder (rotor) is rotated at different constant speeds and the torque which is required to maintain the rotor's motion is transmitted to a torsion bar (through a magnetic coupling and shaft for the pressure cell) in the measuring drive unit which produces an output signal proportional to the amount of deviation. The output signal can be routed to a digital voltmeter or a strip chart recorder (or both).

The measured torque and the corresponding rotational speed were used to calculate the shear stress and the corresponding shear rate at the wall of the rotor.

### 3.7 Analysis of the Experimental Data

The readings corresponding to each rotational speed can be converted to shear stress and shear rate using the following procedure:

1. Calculate the torque at each speed from

$$T = \frac{(y - y_{corr})}{100} HF \quad (3-55)$$

where

y = output of the drive unit, read from the voltmeter or chart recorder when the system is loaded with the sample,

$y_{\text{corr}}$  = the corresponding reading due to friction when the cell is empty,

HF= head factor, N-cm, Two kind of heads (driving units) were used in this work,

a: M150 for low viscosity samples with HF=1.47 N-cm, and b: M500 for higher viscosities with HF=4.9 N-cm.

2. Calculate the shear stress at the wall of the rotor at each rotational speed from

$$\tau_i = \frac{T}{2 \pi R_i^2 L_e} \quad (3-56)$$

3. Plot shear stress,  $\tau_i$ , as a function of rotational speed, N, or angular velocity ( $\omega = 2\pi R_i N$ ) on a log-log scale and determine the slope of the curve,  $n''$ , at each value of  $\tau_i$ , this will be equal to

$$n'' = \frac{d \log_e \tau_i}{d \log_e N} \quad (3-57)$$

In this work linear regression methods were used to find the best correlation between  $\log_e(\tau)$  and  $\log_e(N)$ . For the solid and temperature ranges that were used with these systems, a first order polynomial will fit the experimental data satisfactorily with  $R^2 \geq 0.99$ , therefore,

$$\log_e(\tau_i) = a_1 + b_1 \log_e(N) \quad (3-58)$$

hence,

$$\frac{d \log_e N}{d \log_e \tau_i} = \frac{1}{n''} = \frac{1}{b_1} \quad (3-59)$$

Equation (3-39) truncated after the fourth term (inside the bracket) was used to calculate the shear rate at the wall of the rotor corresponding to each value of shear

stress. When these values are available, the viscosity can be calculated from

$$\eta = \frac{\tau_t}{\dot{\gamma}(\tau_t)} \quad (3-60)$$

## CHAPTER 4 CAPILLARY FLOW VISCOMETRY

### 4.1 Introduction

The capillary viscometer is perhaps the most popular instrument for studying the flow properties of highly concentrated fluids for a variety of shear rates, ranging from  $0.1 \text{ sec}^{-1}$  to  $10^5 \text{ sec}^{-1}$ . By measuring the pressure drop as a function of flow rate in the capillary, it is possible to fit the data to a Newtonian fluid, a power-law fluid or in terms of an apparent viscosity. Many investigators have used this instrument for studying the flow properties of molten polymers (e.g., McLuckie and Rogers 1969, Laun 1983), polymer solutions (e.g., Kraynik and Schowalter 1981), Calcium Carbonate/ Polystyrene Composites (Kelly 1989), black liquors (Kim et al. 1981) and suspensions (Attal 1989).

### 4.2 Theory

If we make a number of sweeping assumptions about the flow in a capillary, the mathematical analysis of the flow will be more convenient. These are

1. fluid velocity is zero at the wall of the capillary (no-slip boundary condition),
2. the flow is laminar, fluid stream lines are parallel to the wall and there is no circumferential motion,

3. the flow is fully developed and viscometric, i.e., does not change with the axial position and time,
4. the flow is isothermal and the fluid is incompressible,
5. hydrostatic pressure is uniform across the radial section of the capillary,
6. entrance and exit effects are ignored.

### 4.3 Creeping Flow Solution for a non-Newtonian Fluid

With the above assumption, one can postulate that

1.  $v_z = v_z(r)$
2.  $v_\theta = v_r = 0$
3.  $P = p + p_h = p + \rho gh$

where  $v_r$ ,  $v_\theta$ , and  $v_z$  are the velocity components.  $p$  can be regarded as the pressure resulting from the fact that the fluid is flowing and  $p_h$  is hydrostatic pressure.

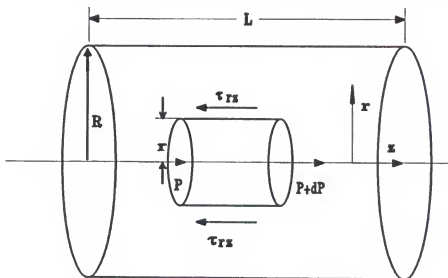


Figure 4-1



The z component of the equation of motion in terms of  $\tau$  for an element shown in Figure 4-1 is (Bird et al. 1987)

$$-\frac{1}{r} \frac{\partial}{\partial r}(r\tau_{rz}) - \frac{\partial P}{\partial z} = 0 \quad (4-1)$$

This may be integrated to give

$$\tau_{rz} = \frac{(P_0 - P_L)r}{2L} + \frac{C_1}{r} \quad (4-2)$$

Since the stress has to be finite at  $r=0$ , the constant  $C_1$  will be equal to zero. At the wall of the capillary equation (4-2) can be written as

$$\tau_w = \frac{R}{2} \frac{(P_0 - P_L)}{L} \quad (4-3)$$

The volumetric flow rate is

$$Q = 2\pi \int_0^R r v_z dr \quad (4-4)$$

Performing integration by parts gives

$$Q = 2\pi \left[ \frac{1}{2} r^2 v_z(r) \right]_0^R - 2\pi \int_0^R \frac{r^2}{2} \frac{dv_z}{dr} dr \quad (4-5)$$

$$Q = \pi R^2 v_s - \pi \int_0^R r^2 \left( \frac{dv_z}{dr} \right) dr \quad (4-6)$$

where  $v_s$  is the slip velocity at the wall of the capillary.

Assuming no-slip at the wall of the capillary, the first term on the right side of equation (4-6) is zero and it becomes

$$Q = -\pi \int_0^R r^2 \left( \frac{dv_z}{dr} \right) dr \quad (4-7)$$

From equations (4-2) and (4-3), we obtain  $r = R(\tau_w/\tau_w)$ , a relationship that can be utilized to change the integration variable in equation (4-7),

$$Q = -\pi \int_0^{\tau_w} \left( R \frac{xu_{rz}}{\tau_w} \right)^2 \left( \frac{dv_z}{dr} \right) \frac{R}{\tau_w} d\tau_w \quad (4-8)$$

or

$$Q = -\int_0^{\tau_w} \frac{\pi R^3}{\tau_w^3} \left( \frac{dv_z}{dr} \right) \tau_w^2 d\tau_w \quad (4-9)$$

Equation (4-9) can be differentiated with respect to  $\tau_w$  by using the "Leibnitz" formula:

$$\frac{d}{d\tau_w} \int_{a(x)}^{b(x)} g(t, x) dt = \int_{a(x)}^{b(x)} \frac{\partial g}{\partial x} dt + [g(b, x) \frac{db}{dx} - g(a, x) \frac{da}{dx}] \quad (4-10)$$

to give

$$\frac{dQ}{d\tau_w} = \int_0^{\tau_w} \frac{3\pi R^3}{\tau_w^4} \left( \frac{dv_z}{dr} \right) \tau_w^2 d\tau_w - \frac{\pi R^3}{\tau_w} \left( \frac{dv_z}{dr} \right) \Big|_{r=R} \quad (4-11)$$

or

$$\frac{dQ}{d\tau_w} = -\frac{3Q}{\tau_w} - \frac{\pi R^3}{\tau_w} \left( \frac{dv_z}{dr} \right) \Big|_{r=R} \quad (4-12)$$

Considering that, the shear rate at the wall of the capillary,  $\dot{\gamma}_w = -(dv_z/dr)|_{r=R}$ , equation (4-12) can be written as

$$\frac{dQ}{d\tau_w} = -\frac{3Q}{\tau_w} + \frac{\pi R^3}{\tau_w} \dot{\gamma}_w \quad (4-13)$$

or

$$\dot{\gamma}_w = \frac{1}{\pi R^3} [3Q + \tau_w \frac{dQ}{d\tau_w}] \quad (4-14)$$

Equation (4-14) can be written as

$$\dot{\gamma}_w = \frac{Q}{\pi R^3} \left[ 3 + \frac{\frac{dQ}{d\tau_w}}{\frac{Q}{\tau_w}} \right] = \frac{Q}{\pi R^3} \left[ 3 + \frac{d \log_e Q}{d \log_e \tau_w} \right] \quad (4-15)$$

If we define  $n' = (d \log_e \tau_w) / (d \log_e Q)$ , then

$$\dot{\gamma}_w = \frac{4Q}{\pi R^3} \left[ \frac{(3n' + 1)}{4n'} \right] \quad (4-16)$$

Equation (4-16) has been associated with the names of Weissenberg (1929), Rabinowitch (1929) and Mooney (1931), while the bracketed term is called the Rabinowitch correction.

For a fluid that obeys the power-law model, the shear stress is related to the shear rate by

$$\tau_{rz} = k \dot{\gamma}^n = k \left( -\frac{dv_z}{dr} \right)^n \quad (4-17)$$

Combining equations (4-17) and (4-2), we can obtain a relationship between the pressure gradient and the velocity gradient:

$$\frac{r}{2} \left( \frac{P_0 - P_L}{L} \right) = k \left( - \frac{dv_z}{dr} \right)^n \quad (4-18)$$

Taking the velocity at the wall to be zero, the velocity profile can be determined by integrating equation (4-18):

$$dv_z = - \left( \frac{1}{2k} \frac{P_0 - P_L}{L} \right)^{\frac{1}{n}} (r)^{\frac{1}{n}} dr \quad (4-19)$$

$$\begin{aligned} v_z &= \frac{R^{(1+\frac{1}{n})}}{(1+\frac{1}{n})} \left( \frac{1}{2k} \frac{P_0 - P_L}{L} \right)^{\frac{1}{n}} \left[ 1 - \left( \frac{r}{R} \right)^{\frac{(1+n)}{n}} \right] = \\ &\quad \left( \frac{R}{1+\frac{1}{n}} \right) \left( \frac{\tau_w}{k} \right)^{\frac{1}{n}} \left[ 1 - \left( \frac{r}{R} \right)^{1+\frac{1}{n}} \right] \end{aligned} \quad (4-20)$$

The shear rate at the wall of the capillary for a power-law fluid will be

$$\dot{\gamma}_w = \left( \frac{\tau_w}{k} \right)^{\frac{1}{n}} \quad (4-21)$$

The volumetric flow rate can be calculated from

$$Q = \int_0^R 2\pi r v_z dr = 2\pi \int_0^R \left( \frac{R}{1+\frac{1}{n}} \right) \left( \frac{\tau_w}{k} \right)^{\frac{1}{n}} \left[ 1 - \left( \frac{r}{R} \right)^{1+\frac{1}{n}} \right] r dr \quad (4-22)$$

or

$$Q = \frac{\pi R^3}{(3 + \frac{1}{n})} (\frac{\tau_w}{k})^{\frac{1}{n}} \quad (4-23)$$

Combining equations (4-21) and (4-23) and replacing Q in equation (4-14), we will conclude that, for a power-law fluid  $(d \log_e \tau_w)/(d \log_e Q) = n = n'$ .

For a Newtonian fluid, the relationship between shear stress and shear rate can be expressed as

$$\tau_{rz} = \mu \dot{\gamma}(r) \quad (4-24)$$

Combining equations (4-24) and (4-2) would yield

$$\dot{\gamma}(r) = \frac{r}{2\mu} (\frac{P_0 - P_L}{L}) \quad (4-25)$$

Shear rate at the wall of the capillary would be equal to

$$\dot{\gamma}_w = \frac{R}{2\mu} (\frac{P_0 - P_L}{L}) \quad (4-26)$$

Combining equations (4-25) and (4-26) and considering that  $\dot{\gamma}(r) = -(dv_z)/(dr)$ , we will have

$$-\frac{dv_z}{dr} = \frac{r}{2\mu} (\frac{P_0 - P_L}{L}) \quad (4-27)$$

or

$$dv_z = - \frac{\left(\frac{P_0 - P_L}{L}\right)}{2\mu} r dr \quad (4-28)$$

The velocity profile can be obtained by integrating both sides of equation (4-28) and assuming no-slip at the wall of the capillary:

$$v_z = \left(\frac{P_0 - P_L}{L}\right) \left(\frac{1}{4\mu}\right) \left[1 - \left(\frac{r}{R}\right)^2\right] \quad (4-29)$$

The average velocity of the fluid in the capillary is equal to

$$\bar{v} = \frac{Q}{\pi R^2} = \frac{\int_0^R 2\pi r v_z dr}{\int_0^R 2\pi r dr} \quad (4-30)$$

or

$$\bar{v} = \left(\frac{P_0 - P_L}{L}\right) \left(\frac{1}{8\mu}\right) \quad (4-31)$$

and the velocity profile will be equal to

$$v_z = 2\bar{v} \left[1 - \left(\frac{r}{R}\right)^2\right] = \frac{2Q}{\pi R^2} \left[1 - \left(\frac{r}{R}\right)^2\right] \quad (4-32)$$

The shear rate at the wall of the capillary will be equal to

$$\dot{\gamma} = - \left(\frac{dv_z}{dr}\right) \Big|_{r=R} = \frac{4Q}{\pi R^3} \quad (4-33)$$

Combining equations (4-14) and (4-28) would give

$$\frac{4Q}{\pi R^3} = \frac{1}{\pi R^3} [3Q + \tau_w \frac{dQ}{d\tau_w}] \quad (4-34)$$

or  $(d\log_e \tau_w)/(d\log_e Q) = n' = 1$  for a Newtonian fluid.

#### 4.4 Entry Flow Corrections

In the fully developed flow region, the assumptions of steady and isothermal flow, constant density, and uniform pressure across the cross section of the capillary result in the conclusion that  $-\partial(P)/\partial(z) = (P_0 - P_L)/L$ . This conclusion is not correct near the capillary entrance. Several investigators (e.g., Bagley 1957, Weissberg 1962, Grant and Dieckman 1965, McLuckie and Rogers 1969, Arai 1970, Han and Charles 1970, Hyun 1974, White and Kondo 1977/1978, White and Baried 1988) have studied and discussed the flow pattern and possible sources of error for flow of polymer melts and viscoelastic fluids through capillaries and dies.

In all of these studies, it is accepted that the pressure drop due to the entry region of the capillary and reservoir is significant and suitable correction has to be made to eliminate the entrance effects.

Figure 4-2 shows the experimental setup of a capillary viscometer and Figure 4-3 represents the pressure drop along the reservoir and capillary. As can be seen, three flow regions can be observed in a capillary viscometer, the entrance, fully developed, and exit regions. In practice it is the difference between the driving pressure in the reservoir and the ambient pressure at the capillary exit that is measured, while the equations for a capillary viscometer have been performed on the

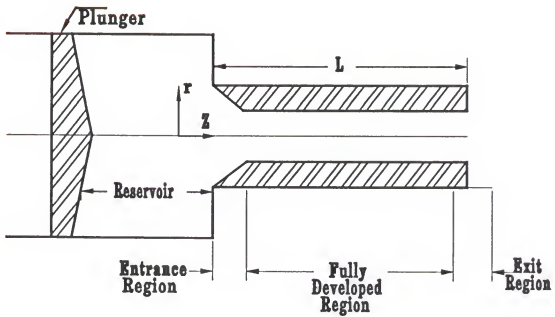


Figure 4-2. Experimental Setup for a Capillary Viscometer

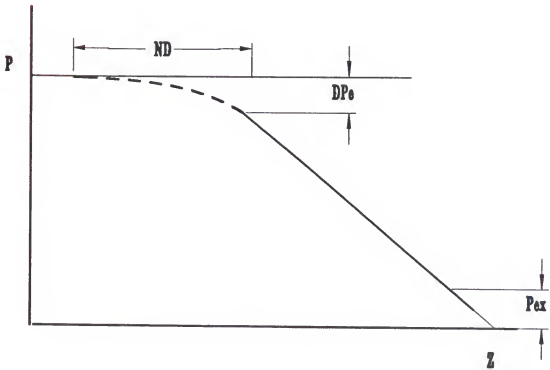


Figure 4-3. Pressure Profile Along the Reservoir and Capillary



basis of the driving pressure in the fully developed region of the capillary. In order to account for pressure drop due to the entry region of the capillary it is usual to make the so-called Bagley (1957) correction. This simply involves making measurements of the pressure drop for different capillaries with the same diameter (different  $L/D$ ) at constant flow rates. Several investigators (e.g., Bagley 1957, Toms 1958, Fredrickson 1964, Kim *et al.* 1981) have shown that a plot of  $\Delta P$  as a function of  $L/D$  at constant flow rate will be a straight line at moderate  $L/D$  values. Bagley assumed that the entry pressure drop is equivalent to an "added length" of capillary given by  $N \times D$ , where  $N$  is the intersection of these lines with the  $L/D$  axis, as shown in Figures (4-4) through (4-15) for different black liquors. Thus, the shear stress at the wall of the capillary can be written as

$$\tau_w = \frac{(P_0 - P_L)D}{4(L + ND)} \quad (4-35)$$

when  $(P_0 - P_L) = 0$ , the negative intercept yields the value of  $N$  which is a function of flow rate.

#### 4.5 Wall Slip in Capillary Flow

The no-slip assumption that was used to derive the equations for capillary flow is based on the assumption that the velocity of the liquid is that of the solid surface at a solid-liquid interface. It is assumed that the liquid will adhere to the wall and the relative velocity with respect to the wall will be equal to zero.

This assumption holds very well for all viscous liquids. The studies of den Otter (1971) on the melt fracture and flow mechanism of polymer melts show that the no-slip assumption is valid for slow flow of the most viscoelastic materials. At higher flow rates and at a critical value of the wall shear stress, the melt no longer adheres to the wall and the no-slip condition will not be valid.

Kraynik and Schowalter (1981) have studied the wall slip of viscoelastic fluids through cylindrical tubes and surface character of the extrudate by using aqueous solutions of polyvinyl alcohol and sodium borate. Their experiments with rough and smooth tubes of plexiglass (polymethylmetacrylate) and aluminum show that the nature of the flow is highly dependent on the characteristics of the tube surface and that the microscopic nature of the wall can promote or inhibit macroscopic slip.

Ramamurthy (1986), by using a capillary rheometer, studied the wall slip and influence of materials of construction on the observed extrudate irregularities for high viscosity molten polyethylenes. His results indicate that the assumption of "no-slip at the rigid boundary" is generally not valid for polyethylenes above a critical shear stress of approximately 0.1 - 0.14 MPa, when either surface or gross irregularities are present in the extrudate.

The work of Kalika and Denn (1987) on wall slip and extrudate distortion in linear low-density polyethylene shows that there is a failure of adhesion at the melt-metal interface for stresses around 0.43 Mpa.

Yilmazer and Kalyon (1989) have reported the rheological behavior of highly filled suspensions employing capillary and parallel disk torsional flows with emphasis

on the wall slip phenomena. However, more studies can be find in the literature about the wall slip effects in capillary flows of polymer solutions and polymer melts (e.g., Kozicki et al. 1970, Cohen and Metzner 1985, Jiang et al. 1986, Yoshimura and Prud'homme 1988a, 1988b).

#### 4.6 Determination of the Slip Velocity

As discussed earlier, for flow in capillaries with a slip velocity  $v_s$  at the wall, the volumetric flow rate (equation (4-9)) may be written as

$$Q = \pi R^2 v_s + \frac{\pi R^3}{3 \tau_w^3} \int_0^{\tau_w} \dot{\gamma} d(\tau_w^3) \quad (4-36)$$

or

$$\frac{Q}{\pi R^3} = \frac{v_s}{R} + \frac{1}{3 \tau_w^3} \int_0^{\tau_w} \dot{\gamma} d(\tau_w^3) \quad (4-37)$$

The slip velocity at the wall of the capillary can be determined by differentiating equation (4-37) with respect to  $1/R$  at constant shear stress at the wall, therefore,

$$v_s = \frac{\partial \left( \frac{Q}{\pi R^3} \right)}{\partial \left( \frac{1}{R} \right)} \Big|_{\tau_w = \text{constant}} \quad (4-38)$$

or

$$v_s = \frac{\partial(\frac{\bar{v}}{R})}{\partial(\frac{1}{R})} \Big|_{\tau_w = \text{constant}} \quad (4-39)$$

where  $\bar{v}$  is the average velocity through the capillary. Thus, a plot of  $Q/(\pi R^3)$  versus  $1/R$  at constant  $\tau_w$  should give a straight line with a slope of  $v_s$ .

When the data from two capillaries with different diameter are available, one can determine the significance of the slip velocity by performing a log-log plot of  $\tau_w$  versus  $Q/(\pi R^3)$  for two capillaries. If the plots superimposed, then at a specific  $\tau_w$   $Q/(\pi R^3)$  is the same for both capillaries and the slope of  $Q/(\pi R^3)$  versus  $1/R$  will be equal to zero or the slip velocity is insignificant. However, if the plots are not unique,  $v_s$  can not be ignored and the equations involving velocity has to be modified by replacing  $v$  by  $(v - v_s)$  (Dealy and Wissbrun 1990).

For a non-Newtonian fluid, with slip velocity  $v_s$  at the wall of the capillary, equations (4-9) and (4-15) may be written as

$$Q = \pi R^2 v_s - \int_0^{\tau_w} \frac{\pi R^3}{\tau^3} \left( \frac{dv_s}{dr} \right) \tau^2 d\tau \quad (4-40)$$

$$\dot{\gamma}_w = \frac{Q}{\pi R^3} \left( \frac{\frac{dQ}{d\tau_w}}{\frac{Q}{\tau_w}} - \pi R^2 \frac{\tau_w}{Q} \frac{dv_s}{d\tau_w} + 3 \right) \quad (4-41)$$

or

$$\dot{\gamma}_w = \frac{Q}{\pi R^3} \left( \frac{3n' + 1}{n'} - \frac{\pi R^2}{Q} \frac{1}{n''} \right) \quad (4-42)$$

where  $n'' = (d \log_e \tau_w) / (d \log_e \dot{\gamma}_s)$

For a non-Newtonian fluid that obeys the power-law model, equation (4-23) can be written as

$$Q = \frac{\pi R^3}{3 + \frac{1}{n}} \left( \frac{\tau_w}{k} \right)^{\frac{1}{n}} + \pi R^2 v_s \quad (4-43)$$

This can be solved for slip velocity to give

$$v_s = \frac{Q}{\pi R^2} - \frac{Rn}{(3n+1)} \left( \frac{\tau_w}{k} \right)^{\frac{1}{n}} \quad (4-44)$$

If the power-law constant,  $n$ , is available from previous experiments, it can be used to calculate the slip velocity as a function of shear stress for any values of the volumetric flow rate ( $Q$ ). Kalika and Denn (1987) have reported the values of the slip velocity for low-density Polyethylene by using the above procedure.

#### 4.7 Experimental Setup and Data Analysis

An Instron Capillary Rheometer (model 3211) was used to determine the viscosity of black liquors at high solids concentrations. The Instron model 3211 is a self-contained instrument and consists of four basic parts. These are: extrusion barrel assembly, the drive assembly, the temperature control and distribution assembly and the load measurement and readout assembly.

The extrusion barrel consists of a hardened steel barrel enclosed in an aluminum jacket to which four cylindrical heating elements are clamped. A capillary is inserted into the bottom of the barrel and is held by a clamping nut as shown in Figure 4-16.

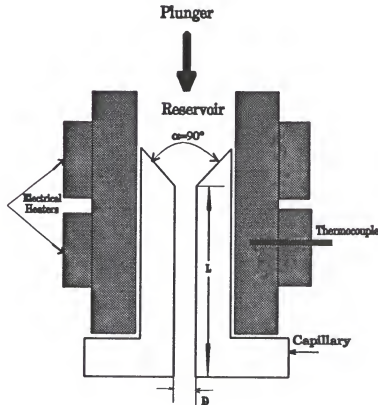


Figure 4-16. Schematic of the Extrusion Barrel Assembly

The drive assembly consists of a synchronous motor driving a translating lead screw through a mechanical drive that allows selection of six speeds. This speed range can be changed by using different gear-to-gear ratios.

The heating rate in the barrel is controlled by the temperature control and distribution system and the temperature stability at the capillary is limited to  $\pm 0.5$

\*C. The forces on the plunger are measured by a load cell and indicated on the panel meter or a strip chart recorder.

The black liquor was loaded into the extrusion barrel and allowed to come to the desired temperature (usually 5-10 minutes), then the sample was forced through the capillary at constant speed. The plunger forces (the force that is required to drive the liquor through the capillary) corresponding to different speeds, which were indicated on the panel meter or a strip-chart recorder, were noted. These forces can be used to calculate the pressure drop through the capillary.

#### 4.8 Data Analysis

The forces and corresponding plunger speeds can be converted to shear stress and shear rate by using the procedure which was given earlier in this chapter. The pressure through the capillary and the volumetric flow rate can be calculated from

$$\Delta P = \frac{F}{A_p} \quad (4-45)$$

$$Q = 2 \pi R_b^2 v_p \quad (4-46)$$

where

$F$  = the force which is required to drive the liquor through the capillary at a specific speed of plunger and is equal to  $F_p - F_f$ , where  $F_p$  is the force measured by the load cell when the barrel is loaded with liquor and  $F_f$  is frictional force, measured by the load cell when the barrel is empty,

$A_p$  = cross-sectional area of the plunger,  $m^2$ ,

$R_b$  = radius of the barrel, m,

$v_p$  = plunger speed, (m/sec).

When the data for pressure drop are available as a function of flow rate for different capillaries with the same diameter,  $\Delta P$  can be plotted versus  $L/D$  for each flow rate and the corresponding intercept with the  $L/D$  axis can be calculated. Figures (4-4) through (4-15) are representatives of  $\Delta P$  as a function of  $L/D$  for different black liquors. As can be observed, these plots are linear as was reported by several other investigators (e.g., Bagley 1957, Philippoff and Gaskins 1956, Grant and Dieckmann 1965, La Nieve and Bogue 1968, Kim *et al.* 1981, Laun 1983, Cohen and Metzner 1985, Jiang *et al.* 1986, and Laun and Schuch 1989) in the literature for polymer melts and polymer solutions. If the plots are linear, a two capillary method can be used to determine the viscosity of the samples. Linear regression analysis can be used to obtain the best fit straight lines and the intercept of these lines can be calculated. The illustrations show that the extrapolated lines give negative intercepts as expected. The shear stress,  $\tau_w$ , at the wall of the capillary corresponding to each flow rate can be calculated from equation (4-35).

A number of investigators (e.g., McLuckie and Rogers 1969, Kamal and Nyun 1973, and Hyun 1974) have observed non-linear plots of  $\Delta P$  versus  $L/D$  for some polymers. In these cases, using linear regression to obtain the best straight line will result in negative values for pressure drop. Therefore, it is suggested to consider the linear part of the plot (Hyun 1974) or higher order polynomials to fit  $\Delta P$  as a function of  $L/D$  and determine the intercept (Kamal and Nyun 1973).



Shear rate at the wall of the capillary can be calculated using equation (4-16) for no-slip condition and equation (4-42) for cases with slip at the wall of the capillary. For a Newtonian fluid  $n' = 1$ , therefore,

$$\dot{\gamma}_w = \frac{4Q}{\pi R^3} \quad (4-47)$$

For a non-Newtonian fluid,  $n'$  can be determined from the plots of  $\log(\tau_w)$  against  $\log(Q/(\pi R^3))$  as it is shown in Figures (4-17) through (4-28) for some of the black liquors. At any flow rate,  $n'$  is equal to the slope of the curve at this point. Linear regression methods can be used to obtain the best fit for  $\log(\tau_w)$  as a function of  $\log(Q/(\pi R^3))$ . In this work it was found that, a polynomial of degree (4) will fit the experimental data for all black liquors satisfactorily with  $R^2 \geq 0.999$ , therefore,

$$\begin{aligned} \log_e \tau_w = & a + b \log_e \left( \frac{Q}{\pi R^3} \right) + c \left( \log_e \left( \frac{Q}{\pi R^3} \right) \right)^2 + d \left( \log_e \left( \frac{Q}{\pi R^3} \right) \right)^3 \\ & + e \left( \log_e \left( \frac{Q}{\pi R^3} \right) \right)^4 \end{aligned} \quad (4-48)$$

and  $n'$  will be equal to

$$\begin{aligned} n' = \frac{d \log_e \tau_w}{d \log_e \left( \frac{Q}{\pi R^3} \right)} = & b + 2c \log_e \left( \frac{Q}{\pi R^3} \right) + 3d \left( \log_e \left( \frac{Q}{\pi R^3} \right) \right)^2 \\ & + 4e \left( \log_e \left( \frac{Q}{\pi R^3} \right) \right)^3 \end{aligned} \quad (4-49)$$

In cases where the slip velocity is significant,  $v_s$  can be determined as a function of  $\tau_w$  using the procedure that was given earlier. A plot of  $\log(\tau_w)$  as a

function of  $v_s$  can be performed and the slope of this curve at any flow rate will be equal to  $n''$ .

Figures (4-17) through (4-28) are plots of  $\log(\tau_w)$  as a function of  $\log(Q/(\pi R^3))$  with two capillaries (different diameters) for some of the liquors. These Figures show that the slip velocity is insignificant for these liquors.

Once the wall shear stress,  $\tau_w$ , and the wall shear rate,  $\dot{\gamma}_w$ , are available, the apparent viscosity ( $\eta_{app}$ ) can be determined as a function of shear rate from

$$\eta_{app} = \frac{\tau_w}{\dot{\gamma}_w} \quad (4-50)$$

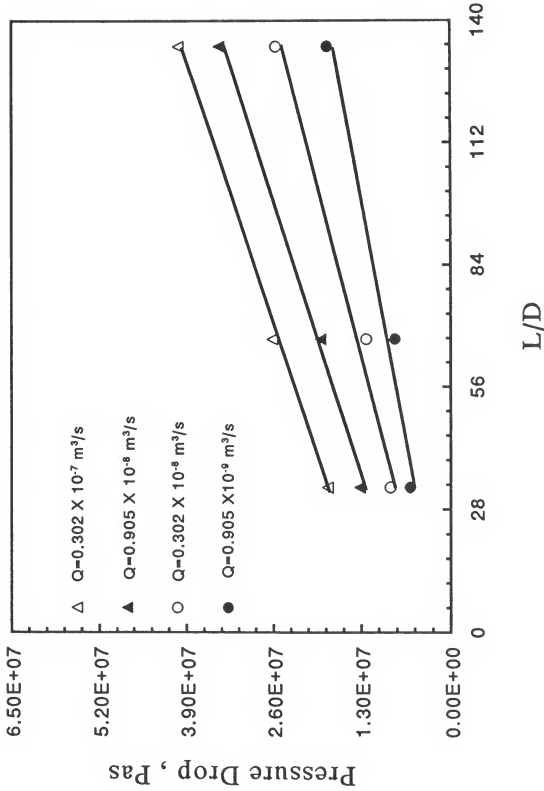


Figure (4-4): Pressure Drop as a Function of L/D for Black Liquor ABAFX013,14 at 55 °C.

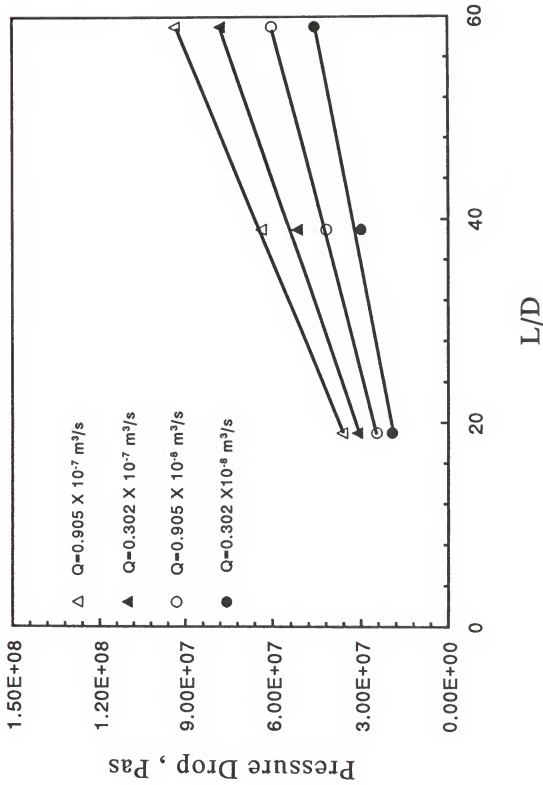


Figure (4-5): Pressure Drop as a Function of L/D for Black Liquor ABAPX013,14 at 75.05 % Solids at 40 °C.

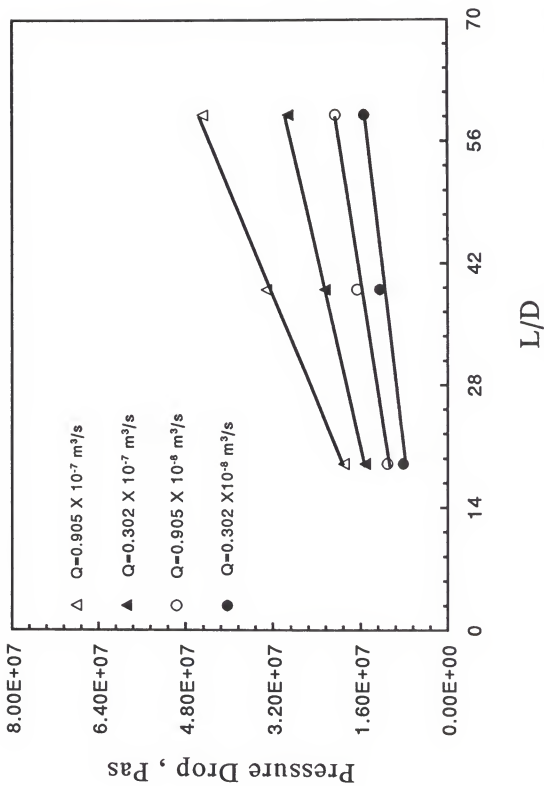


Figure (4-6): Pressure Drop as a Function of L/D for Black Liquor ABAFX013,14 at 75.05 % Solids at 55 °C.

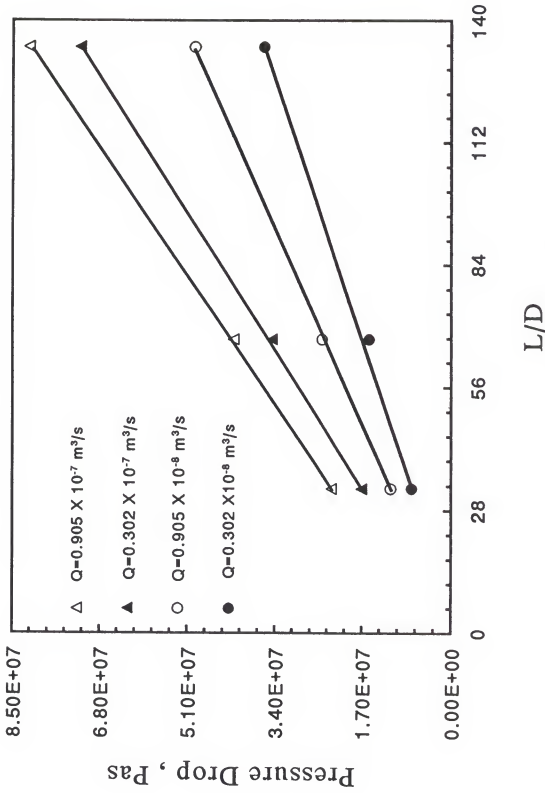


Figure (4-7): Pressure Drop as a Function of  $L/D$  for Black Liquor ABAFX013,14 at 75.05 %Solids at 70 °C.

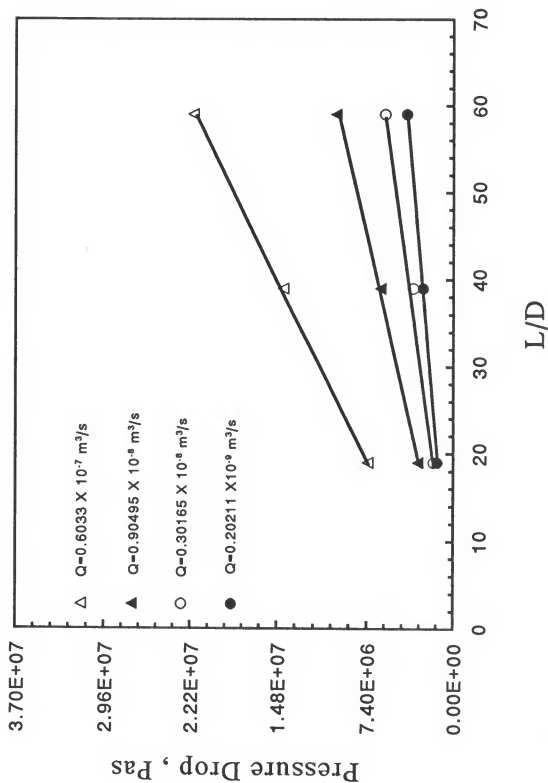


Figure (4-8): Pressure Drop as a Function of  $L/D$  for Black Liquor ABAFX025,26 at 75.7 % Solids at 40 °C.

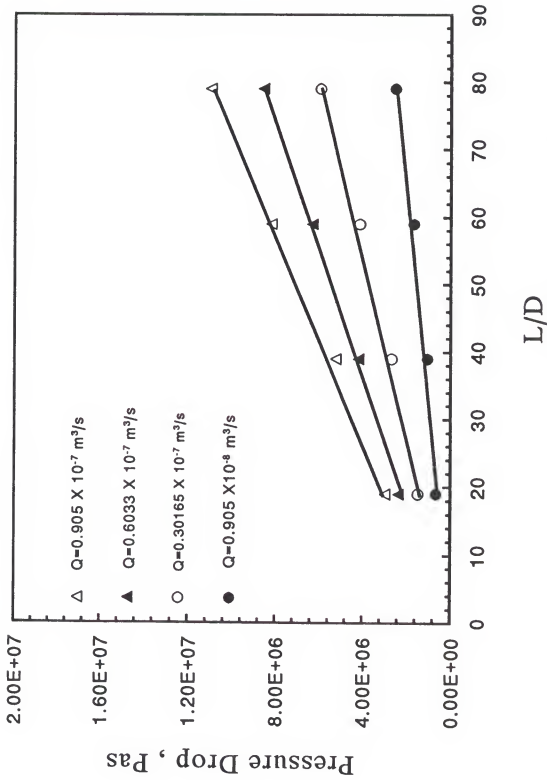


Figure (4-9): Pressure Drop as a Function of L/D for Black Liquor ABAFX025,26 at 75.7 % Solids at 55 °C.



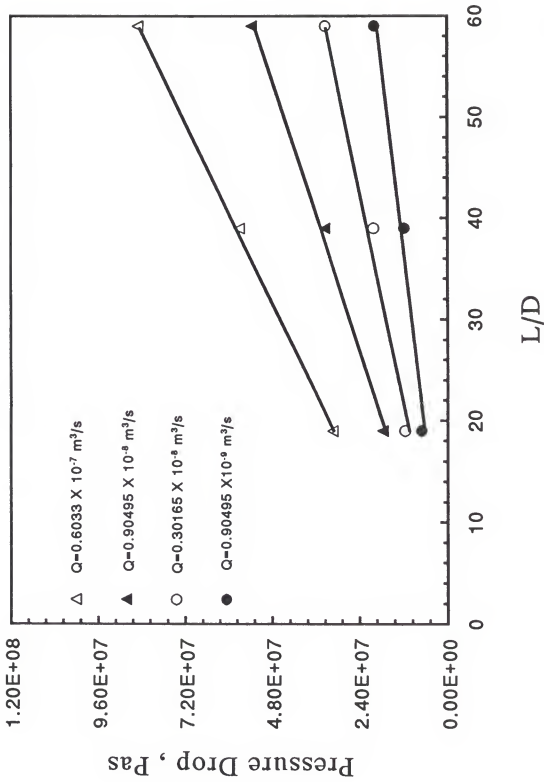


Figure (4-10): Pressure Drop as a Function of L/D for Black Liquor ABAFX025,26 at 81.05 % Solids at 40 °C.

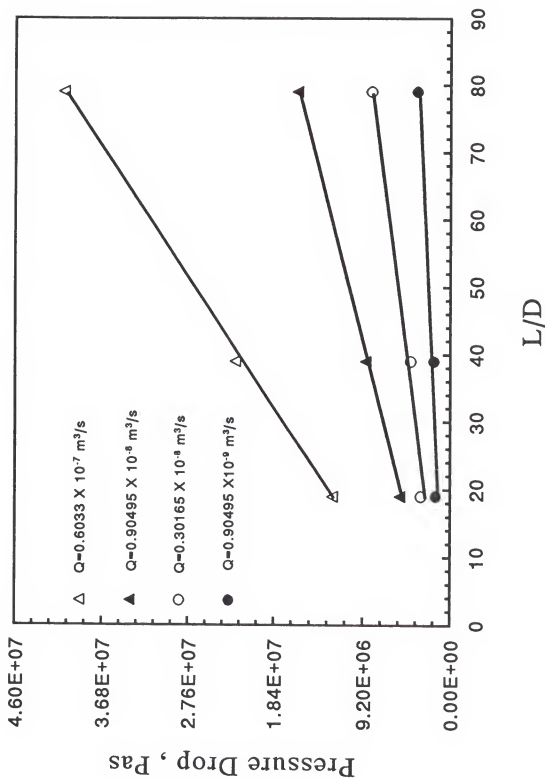


Figure (4-11): Pressure Drop as a Function of L/D for Black Liquor ABAFX025,26 at 81.05 % Solids at 55 °C.

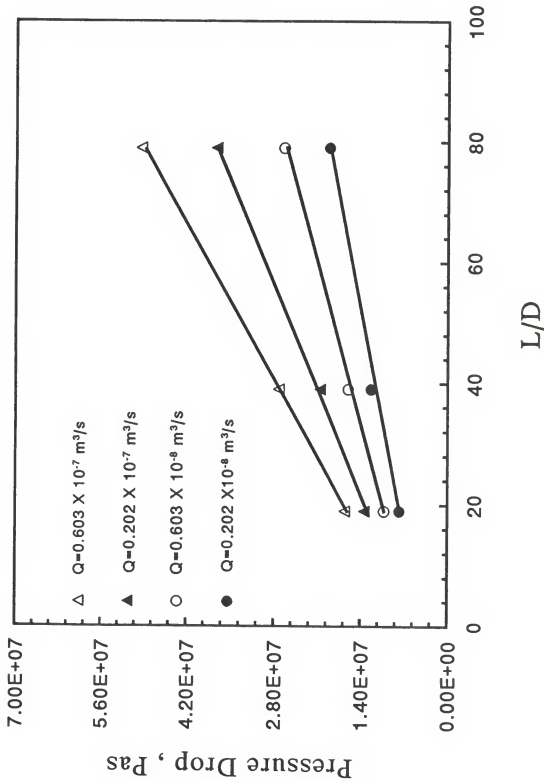


Figure (4-12): Pressure Drop as a Function of L/D for Black Liquor ABAFX043,44 at 72.89 % Solids at 40 °C.

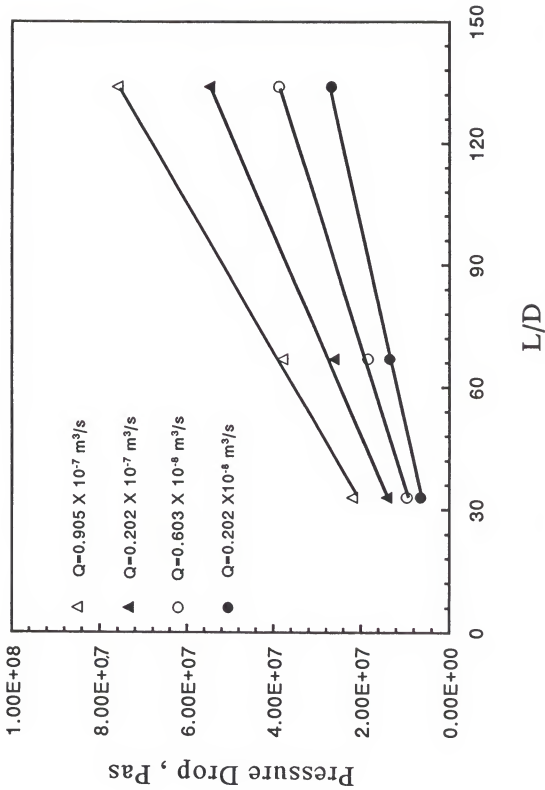


Figure (4-13): Pressure Drop as a Function of L/D for Black Liquor ABAFX043,44 at 72.89 % Solids at 55 °C.

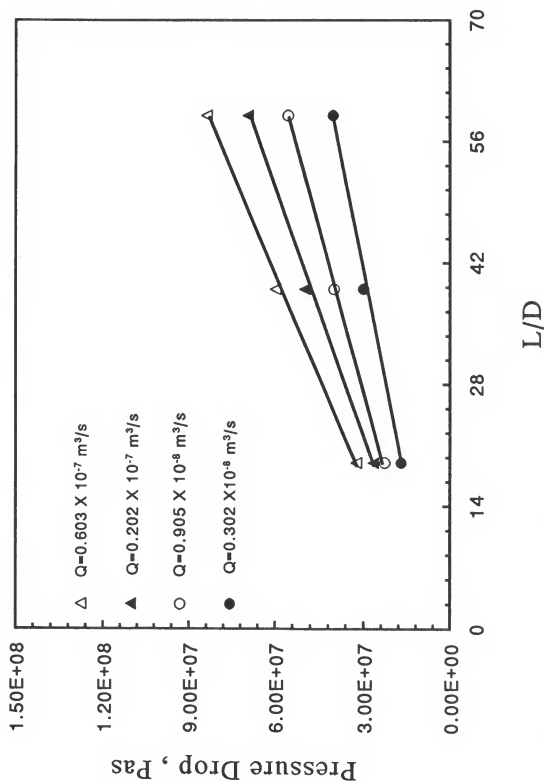


Figure (4-14): Pressure Drop as a Function of L/D for Black Liquor ABAFX043,44 at 76.28 % Solids at 40 °C.

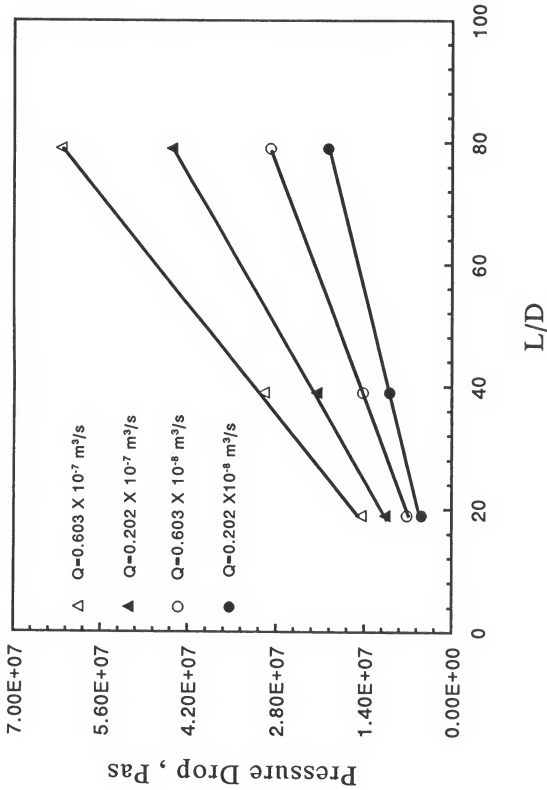


Figure (4-15): Pressure Drop as a Function of L/D for Black Liquor ABAFX043,44 at 76.28 % Solids at 55 °C.

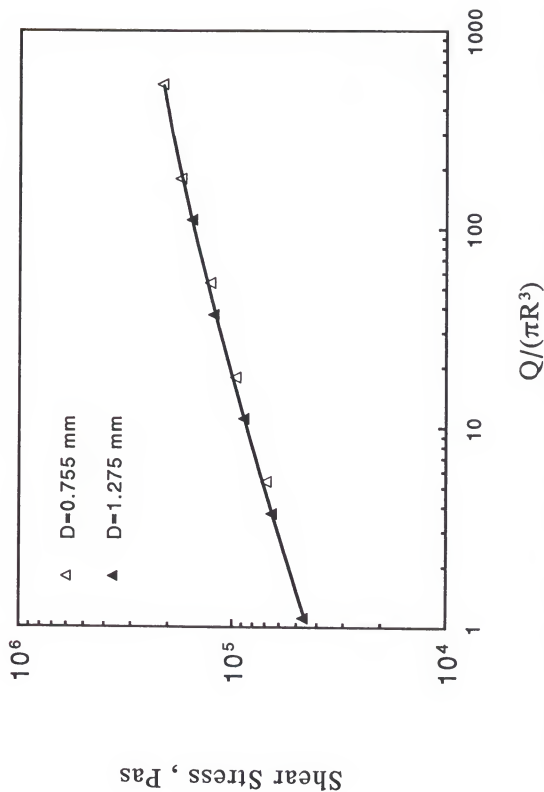


Figure (4-17): Shear Stress as a Function of  $Q/(\pi R^3)$  for Black Liquor ABAFX013,14 at 70.05 % Solids at 40 °C.

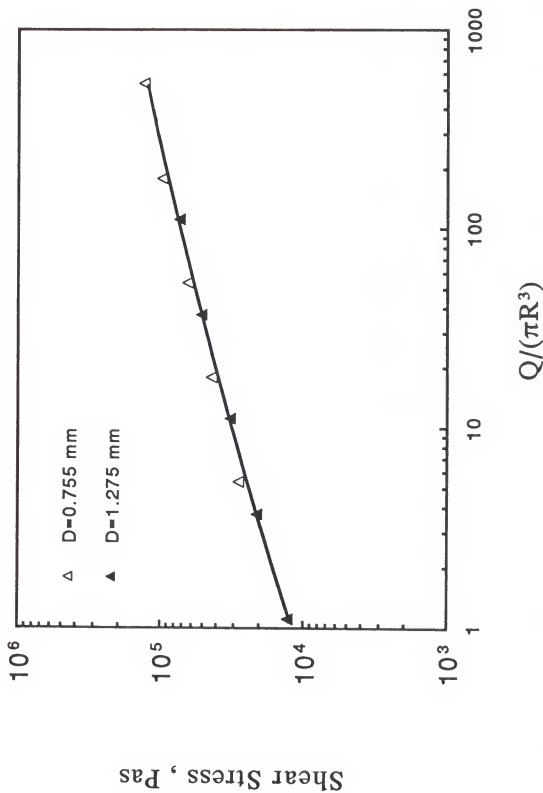


Figure (4-18): Shear Stress as a Function of  $Q/(\pi R^3)$  for Black Liquor ABAFX013,14 at 70.05 % Solids at 55 °C.



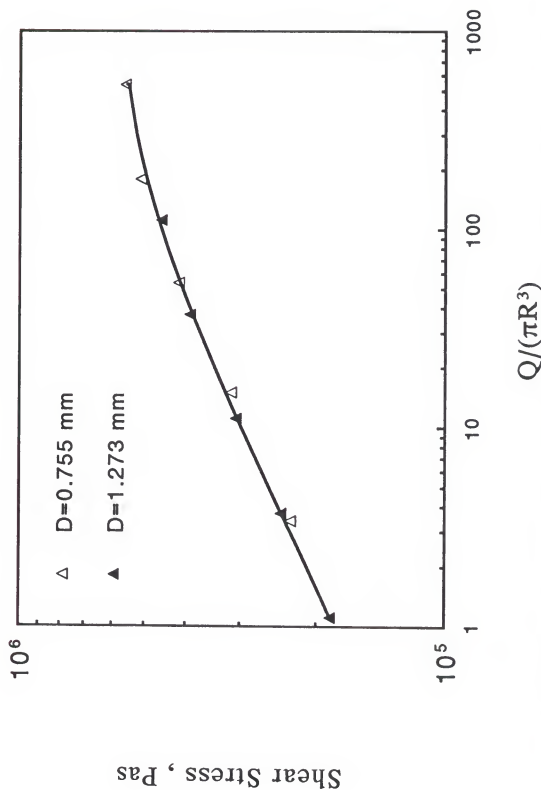


Figure (4-19): Shear Stress as a Function of  $Q/(\pi R^3)$  for Black Liquor ABAFX013,14 at 75.05 % Solids at 40 °C.

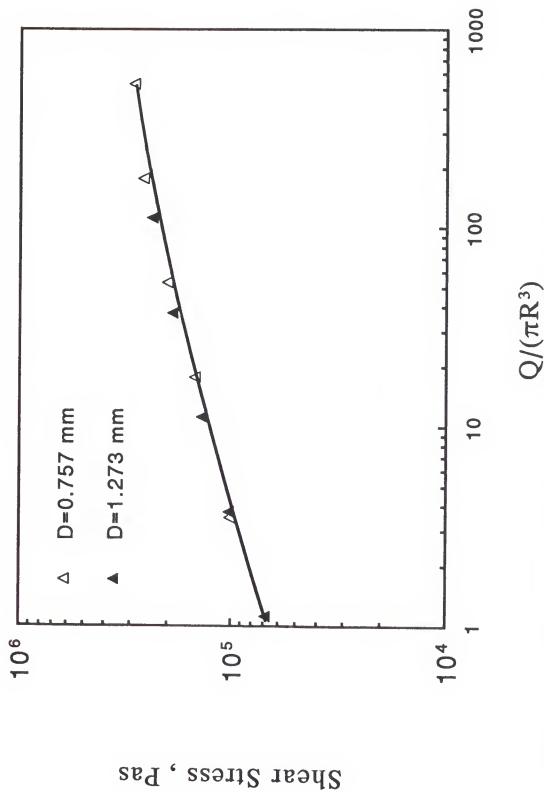


Figure (4-20): Shear Stress as a Function of  $Q/(\pi R^3)$  for Black Liquor ABAFX013,14 at 75.05 %Solids at 55 °C.

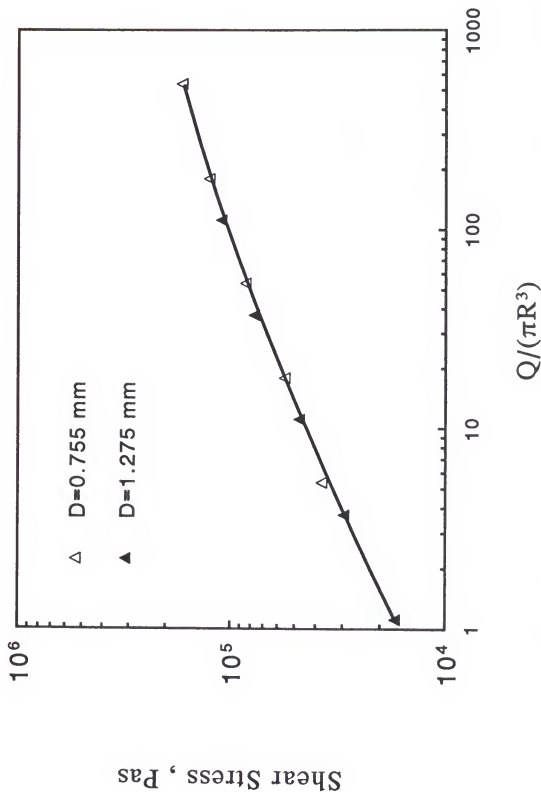


Figure (4-21): Shear Stress as a Function of  $Q/(\pi R^3)$  for Black Liquor ABAFX013,14 at 75.05 % Solids at 70 °C.

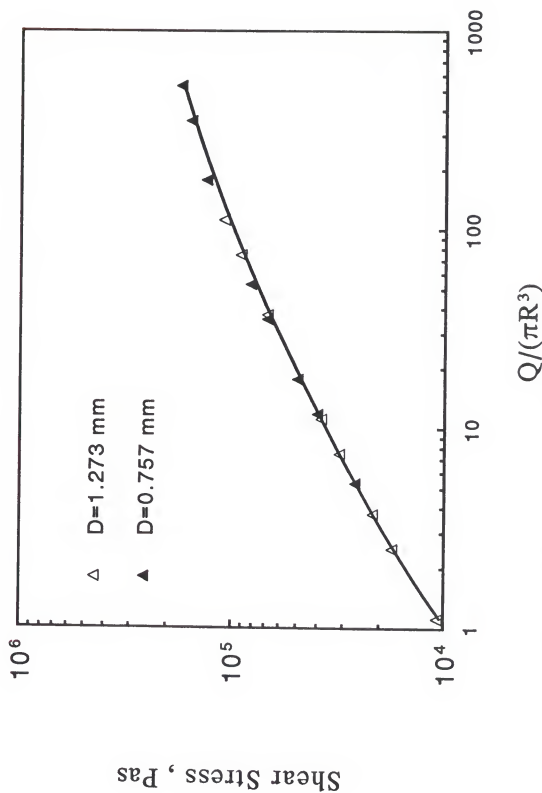


Figure (4-22): Shear Stress as a Function of  $Q/(\pi R^3)$  for Black Liquor ABAFX025,26 at 75.7 % Solids at 40 °C.

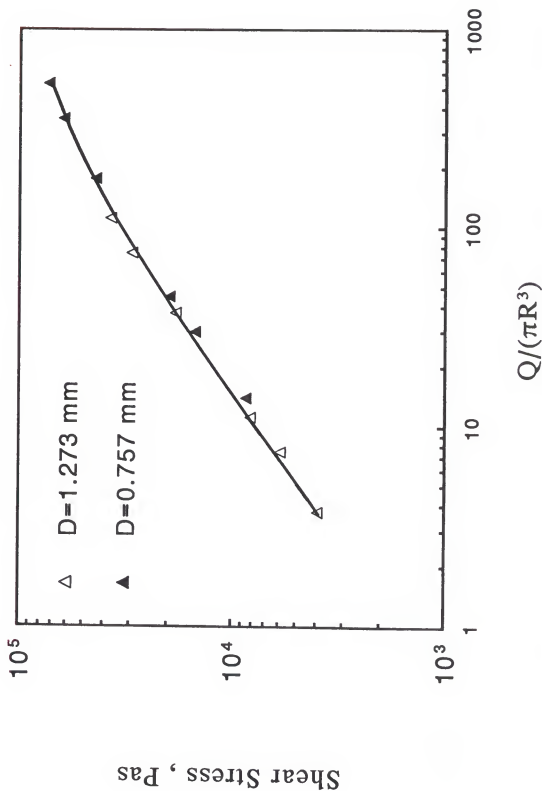


Figure (4-23): Shear Stress as a Function of  $Q/(\pi R^3)$  for Black Liquor ABAPX025,26 at 75.7 °C.

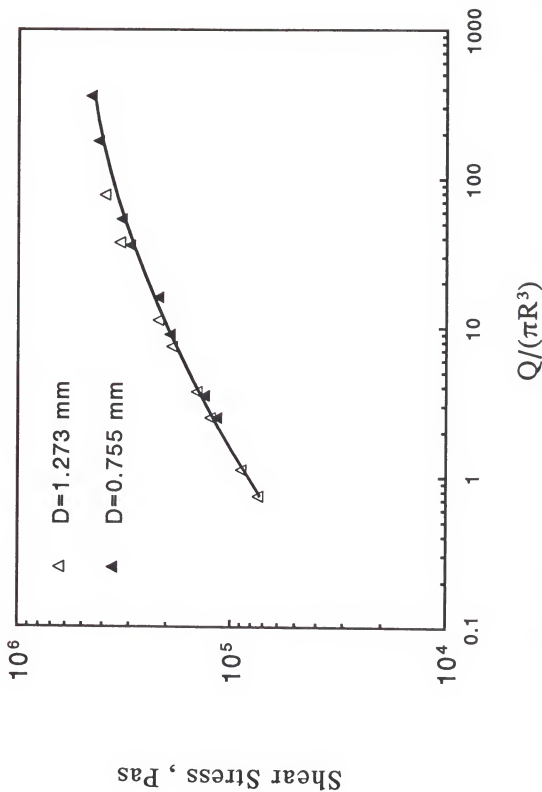


Figure (4-24): Shear Stress as a Function of  $Q/(\pi R^3)$  for Black Liquor ABAFX025,26 at 81.05 % Solids at 40 °C.

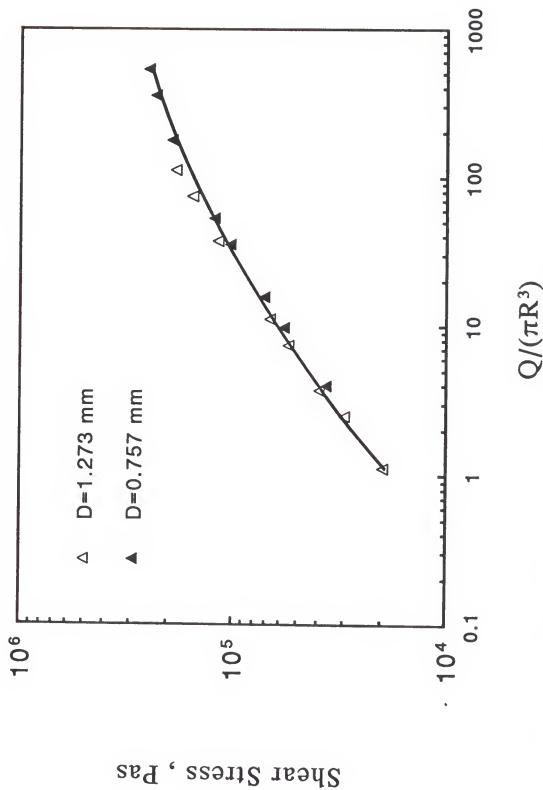


Figure (4-25): Shear Stress as a Function of  $Q/(\pi R^3)$  for Black Liquor ABAFX025,26 at 81.05 % Solids at 55 °C.

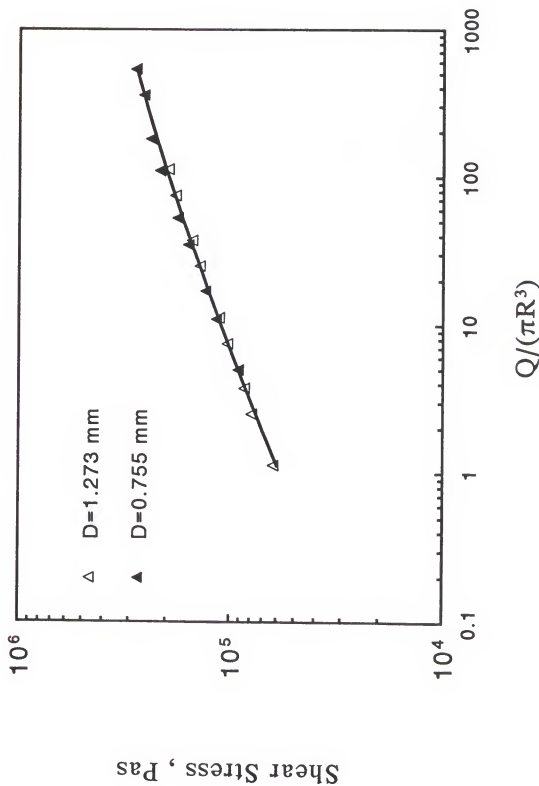


Figure (4-26): Shear Stress as a Function of  $Q/(\pi R^3)$  for Black Liquor ABAFX043,44 at 72.89 % Solids at 40 °C.



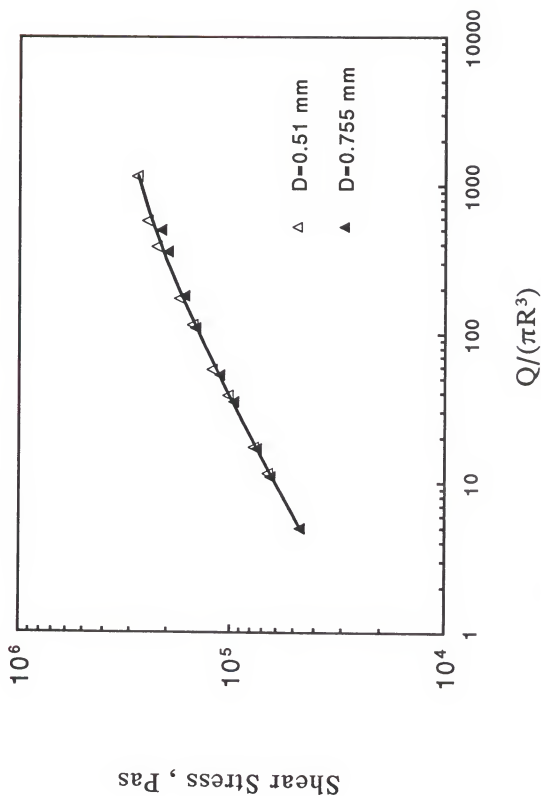


Figure (4-27): Shear Stress as a Function of  $Q/(\pi R^3)$  for Black Liquor ABAFX043,44 at 72.89 % Solids at 55 °C.

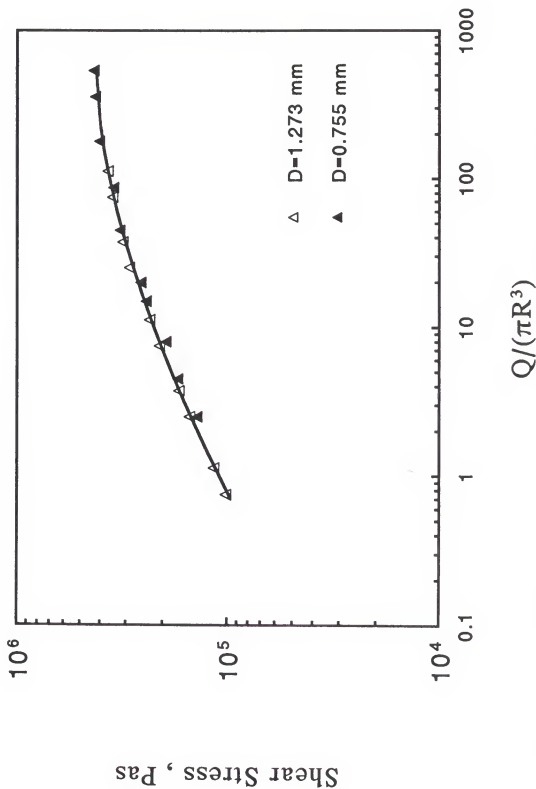


Figure (4-28): Shear Stress as a Function of  $Q/(\pi R^3)$  for Black Liquor ABAFX043,44 at 76.28 % Solids at 40 °C.

## CHAPTER 5 LOW SOLIDS VISCOSITY

### 5.1 Introduction

The kinematic viscosities of several kraft black liquors from a two level, four variable factorial designed pulping experiment were determined for solids concentrations up to 50% and temperatures up to 80 °C by glass capillary methods using Ostwald capillary viscometers. The experimental setup and the operating procedure are described. Relationships between temperature and kinematic viscosity have been developed by using free volume and absolute rate theories. The results from these two methods have been compared and discussed. A reduced variables method for dilute polymer solutions was used to correlate the viscosity with the combined effect of temperature and solids concentrations.

### 5.2 Glass Capillary Viscometer

At low solids concentrations and temperatures up to 100 °C, it is possible to measure the viscosity of black liquors using of glass capillary viscometer, in which the solution flows through the capillary under its own head. Flow (efflux) times,  $t$ , are related to the viscosity of the solution by an equation of the form:

$$\frac{\eta}{\rho} = \nu = at + \frac{b}{t} \quad (5-1)$$

where  $a$  and  $b$  are instrument constants,  $\rho$  is the fluid density, and  $\nu$  is the kinematic viscosity. The last term is related to the kinetic energy correction and it is negligible for flow times of over a minute.

### 5.3 Experimental Setup

Ostwald capillary viscometers of sizes 50, 100, 200, 300, and 400 were used to determine the kinematic viscosity of black liquors. The calibration constants were checked with standard mineral oils and found to be accurate within  $\pm 5\%$ .

After choosing an appropriate size viscometer for the temperature and solids concentrations of the black liquor to be investigated, the viscometer was filled with about 10 cm<sup>3</sup> of black liquor and placed into the temperature controlled water bath. The viscometers were loaded with the same volume of sample so that approximately the same head of the fluid was obtained in each viscometer. A time of 25 - 30 minutes was allowed for temperature equilibrium. The time which is required for the level of black liquor to fall between the two timing lines (efflux time), was measured. This procedure was repeated at least three times for each sample. The kinematic viscosity can be calculated by multiplying the calibration constant of the viscometer by the efflux time. Experimental setup for the system is shown in Figure 5-1.

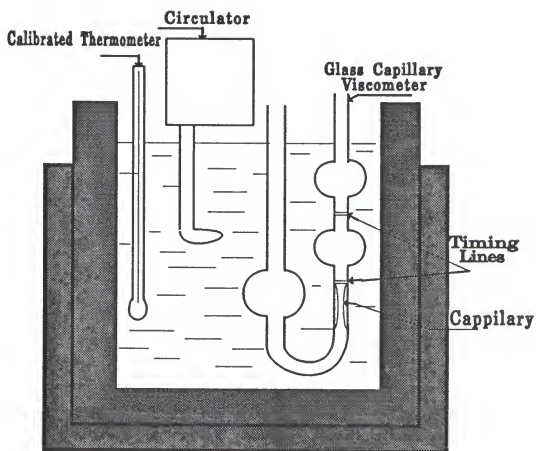


Figure 5-1: Experimental Setup of Glass Capillary Viscometer

### 5.4 Viscosity-Temperature Relationships

Two different approaches have been used to derive expressions for the temperature dependence of viscosity. One is associated with the theory of absolute reaction rates and the other with free volume theory. Because of two different mechanisms, the final expressions for the temperature dependence of viscosity are different in these approaches.

Probably, the most successful theories of liquid viscosity have been based on the assumption of a quasicrystalline liquid structure (Macedo and Litovitz 1965). A molecule is considered to vibrate about an equilibrium position, and transition from this state is possible when it possesses sufficient energy and a free space is available into which the molecule can jump to attain a new equilibrium position.

If the probability of accumulation of the energy required to overcome the potential energy barrier is  $P_E$  and the probability of free volume existing near the initial equilibrium position is  $P_v$ , then the total probability of a transition, or jump, from one site to another is (Macedo and Litovitz 1965)

$$P = P_E \times P_v \quad (5-2)$$

Eyring (1935, 1936, 1937,) developed the theory of absolute reaction rates and made extensive use of the concepts of free volume in the flow of liquids. However instead of using  $P$  as in equation (5-2) to express the total probability of a transition, he used  $P_E$ ; therefore, the temperature dependence of viscosity reduces to the

determination of the number of possible jumps of molecular units over the potential barrier at different temperatures in his approach.

Application of the general methods of absolute rate theory lead to the following relationship for the viscosity of liquids (Vinogradov and Malkin 1980):

$$\eta = \left[ \frac{hN}{v} \exp\left(-\frac{\Delta S^*}{R}\right) \right] \exp\left(\frac{\Delta H^*}{RT}\right) \quad (5-3)$$

where

$\eta$  = viscosity,

$h$  = Plank's constant,

$N$  = The Avogadro number,

$v$  = molar volume,

$\Delta S^*$  = entropy,

$\Delta H^*$  = heat of activation,

$R$  = gas constant,

$T$  = absolute temperature,

With the assumption that the dependence of the molar volume on temperature is negligible and  $\Delta S^*$  is independent of temperature, equation (5-3) can be written as

$$\eta = A \exp\left(\frac{E}{RT}\right) \quad (5-4)$$

where  $A$  is a constant and  $E$  is the activation energy for flow. Equation (5-4) has been derived empirically by De Gusman (1913) and other investigators (i.e., Arrhenius 1916). It was derived theoretically by Andrade (1930) and other workers

(i.e., Frenkle 1925). Equation (5-3) is usually successful for simple nonassociated liquids, but fails to account for the temperature dependence of the viscosity of associated liquids and polymeric liquids (i.e., Macedo and Litovitz 1965). For this reason, the free volume approach has been considered by many investigators for liquids and polymer solutions. The free volume theory is based on the observations by Doolittle (1951a, 1951b) who studied the viscosity of n-alkanes. Doolittle and Ferry et al. (1955) have shown that the dependence of viscosity on free volume can be expressed as

$$\eta = A \exp\left(\frac{BV_o}{V_f}\right) \quad (5-5)$$

where

A and B = constant,

$V_o$  = specific volume occupied by the molecules of the substance,

$V_f = (V - V_o)$  = free volume,

V = specific volume of the liquid,

Cohen and Turnbull (1959, 1961, 1970) showed that equation (5-5) can be derived by associating a local free volume with each molecule and assuming a distribution of local free volumes. They considered a liquid consisting of hard spheres and repulsive forces only. Another empirical viscosity equation using the free volume concept was given by Batschinski (1913), which correlates the fluidity with the free volume of the liquid:



$$\frac{1}{\eta} = A(V - V_o) \quad (5-6)$$

The limiting volume,  $V_o$ , has a value between solid and liquid volume at the melting point. Hildebrand (1971, 1975) and Hildebrand and Lamoreaux (1972, 1973) have discussed this correlation in detail and verified its validity for different substances. Eicher and Zwolinski (1972) and Ertl and Dullien (1973a, 1973b) have discussed the limitations of equation (5-6) by comparison with experimental data.

Many workers (i.e., Macedo and Litovitz 1965), have reported that equations (5-5) and (5-6) fail to account for the temperature dependence of the shear viscosity of many liquids when they are over 373.2 K above the glass transition temperature and also below it. Also, these equations predict that  $[\partial(\log_e \eta)/\partial(T)]_v = 0$ , which is not true for most of the liquids. Barlow et al. (1965), Matheson (1966), Miller (1963), Van Velzen et al. (1972), Chhabra and Hunter (1981), Przedziecki and Sridhar (1985), and Luckas and Lucas (1986), have modified these equations in various ways in order to increase the region of validity. Barlow considered the effect of temperature on density and Matheson has taken into account the pressure dependence of free volume.

Macedo and Litovitz (1965), by reconsidering the Eyring rate and free volume theories and combining these two effects have proposed the following equation:

$$\eta = A \exp\left(\frac{E_v}{RT} + \frac{\gamma V_o}{V_f}\right) \quad (5-7)$$

where  $E_v$  is the activation energy for flow at constant volume and  $\gamma$  is a constant.

They applied this equation to many liquids and obtained consistent fits to both temperature and pressure dependence of viscosity. They followed Doolittle's assumption that the free volume is the total thermal expansion at constant pressure and that  $V_o$  is independent of temperature to develop the following equation:

$$\eta = A \exp\left(\frac{E_v}{RT} + \frac{\alpha T_o}{T - T_o}\right) \quad (5-8)$$

where  $T_o$  is the apparent temperature where the free volume becomes zero and  $\alpha$  is a constant.

Also, Dienes (1953) considered a temperature dependent activation energy for non-Arrhenius behavior of the viscosity and obtained an equation which is similar to equation (5-8).

The coefficient  $A$  in equation (5-8) is temperature dependent, and various investigators (i.e., Gubbins and Tham 1969) have predicted that  $A$  varies with  $T^{0.5}$ . Such a temperature dependence is assumed in this work. Equation (5-7) will reduce to equation (5-4) if the liquid has a very small thermal expansion coefficient and if  $V_f$  is independent of temperature. It will reduce to equation (5-5) if the activation energy for flow is negligible.

Figures (5-2) through (5-6) are representatives of  $\log \nu$  (kinematic viscosity) versus  $1/T$  for some of liquors at solids concentrations below 50%. At lower solids contents, the plots are close to being straight lines, but the nonlinear behavior is more significant at higher concentrations. The effect of free volume on viscosity probably becomes more important at higher concentrations. In order to be able to

obtain the best correlations for viscosity as a function of temperature for different black liquors at low solids concentrations and to find the best model for extrapolation at higher temperatures at a fixed concentration, both free volume and absolute rate theories have been examined in this work and the results have been compared. Equations (5-4) and (5-5) can be written as

$$\eta = A_1 T^{0.5} \exp\left(-\frac{B_1}{T}\right) \quad (5-9)$$

$$\eta = A_2 T^{0.5} \exp\left(\frac{B_2 T_o}{T - T_o}\right) \quad (5-10)$$

where  $A_1$ ,  $A_2$ ,  $B_1$ , and  $B_2$  are constants and  $T_o$  is the temperature where free volume equals zero. Masse (1984) has studied the phase diagram for three black liquors. His results show that the freezing point of black liquors is a strong function of solids concentrations and varies from 273.2 K to 183 K.

In this work, equations (5-9) and (5-10) have been used to fit the experimental data for viscosity of 23 different black liquors. The cooking conditions for these liquors are summarized in Table (2-2). At first, we chose the approximate values for  $T_o$  over the whole range of solids concentrations for each liquor by considering Masse's work, then we tried to choose an average value for  $T_o$  over the whole range of solids concentrations (close to 220 K); the difference between the results are insignificant. A fixed value of  $T_o = 220$  K for all the liquors will give very good results with  $R^2 \geq 0.99$  for all liquors at different solids concentrations.  $R^2$  for equation (5-9) is also greater than 0.99. At lower concentrations, the results using

equation (5-9) are better than equation (5-10) (smaller errors), but it seems that, above 40% solids both theories yield equally accurate correlations. Coefficients  $A_1$ ,  $B_1$ ,  $A_2$ , and  $B_2$  have been summarized in Tables (5-1) and (5-2) for some of the liquors. As can be observed, the constants for each black liquor are concentration dependent and attempts were made to determine consistent relationships for constants as a function of concentration. The results will be discussed later.

### 5.5 Reduced Correlation for Low Solids Viscosity

The concepts of reduced variables methods for dilute polymer solutions as suggested by several investigators (e.g., Ferry 1980, Billmeyer 1971, Vinogradov and Malkin 1980) can be used to reduce the viscosity data for black liquors at low solids concentration as reported earlier (Fricke 1985 and 1987, Wight 1985, Adams 1965).

Using the relative kinematic viscosity with respect to water (the solvent),  $\nu_R = \nu/\nu_w$  and defining the combined concentration-temperature variable as

$$X = \frac{S}{T} \quad (5-11)$$

where  $S$  is the solids mass fraction and  $T$  is absolute temperature.

On the assumption that the lignin polymer concentration is proportional to the solids concentration, one can express the reduced viscosity as

$$\log(\nu_R) = \sum_{i=1}^n a_i \left(\frac{S}{T}\right)^i \quad (5-12)$$

Figures (5-7) through (5-11) represent the reduced form of the data for different

black liquors. A polynomial of degree (2) will fit the experimental data with  $R^2 \geq 0.997$ . The constants  $a_1$ ,  $a_2$  and  $R^2$  for some of the liquors are

<u>Black Liquor</u>	<u><math>a_1 \times 10^{-2}</math></u>	<u><math>a_2 \times 10^{-4}</math></u>	<u><math>R^2</math></u>
ABAFX015,16	4.76	168.04	0.998
ABAFX025,26	3.51	135.76	0.999
ABAFX035,36	5.3	144.44	0.998
ABAFX043,44	6.10	160.00	0.999
ABAFX053,54	5.23	174.73	0.999

### 5.6 Results and Discussion

The model based on the absolute rate theory (equation (5-9)) is a two constant model,  $A_1$  and  $B_1$ , with  $B_1$  related to the activation energy for flow. Equation (5-10), which is based on free volume theory, is a three constant model, but one constant ( $T_o$ ) can be a set value for all liquors. These give highly accurate results and can be used for extrapolation of temperature effects on viscosity at a fixed concentration. The corresponding states model (equation (5-12)) is not quite as good for extrapolation to high temperatures at a fixed concentration; however, it includes the effect of concentration. Equation (5-9) could not be used to give  $A_1$  and  $B_1$  as correlatable functions of concentration. Since the constants in the equation are not universal, these must be evaluated for each liquor and thus have no predictive value. Equation (5-10) could be arranged such that

$$A_2 = f(\text{concentration}) = A'_2 + A''_2 S \quad (5-13)$$

for all liquors of one species. For the liquors used in this study  $A_2$  will be equal to

$$A_2 = 2.75 \times 10^{-3} + 3.18 \times 10^{-4} S \quad (5-14)$$

The values of  $A_2$  can be replaced in equation (5-10) and the values of  $B_2$  can be recalculated for each liquor at different solids concentration. The new values of  $B_2$  and  $R^2$  for each liquor have been summarized in Tables (5-12) through (5-16). With this approach, the accuracy of the fits will be increased since  $R^2 \approx 1$  for all liquors. Figure (5-12) represents  $B_2$  as a function of solids concentration for each liquor. As can be observed,  $B_2$  for a single liquor may be written as

$$B_2 = B'_2 + B''_2 S + B'''_2 S^2 \quad (5-15)$$

The values of  $B'_2$ ,  $B''_2$ , and  $B'''_2$  can be calculated for each liquor and replaced in equation (5-10) which then can be used to calculate the viscosity of the corresponding liquor at any temperature or concentration. However, in this approach, the final model for viscosity involves five constants in addition to  $T_0$  and  $B'_2$ ,  $B''_2$  and  $B'''_2$  are functions of solids composition. The accuracy of this model is higher than the corresponding states involving two constants  $a_1$ , and  $a_2$  which are functions of solids composition.

### 5.7 Conclusions

At low solids ( $\leq 50\%$ ), black liquor can be treated as a polymer solution and the theories developed for dilute polymer solutions can be used to correlate viscosity

data with temperature and solids concentrations. The relationship between viscosity and temperature can be expressed by using either free volume theory and an average value for the freezing point of the liquors or absolute rate theory. However, it seems that the constant  $A_2$  in equation (5-10) can be universal for all liquors of one species and the constant  $B_2$ , which depends on the solids composition, can be written as a function of solids concentrations for a single liquor. Therefore, a model based on free volume theory is probably the best for 1: defining the viscosity of a liquor as a function of temperature and solids contents and 2: extrapolation to higher temperatures at a fixed concentration. The corresponding states method can be used to correlate the relative viscosity with respect to water (solvent) as a function of  $S/T$  as the correlating variable. This is less time consuming and easier to use, but one cannot expect to have higher precision than equation (5-10). The constants  $a_1$  and  $a_2$  can be correlated empirically with non-volatiles composition and pulping conditions for single species in future work. In general, the viscosity is not only affected by temperature and solids concentration of the liquors, but it is also a function of cooking conditions that lead to variations in solids composition and lignin molecular weight. However, more statistical work has to be performed to determine the effects of cooking time, cooking temperature, effective alkali and sulfidity on the viscosity of black liquor.

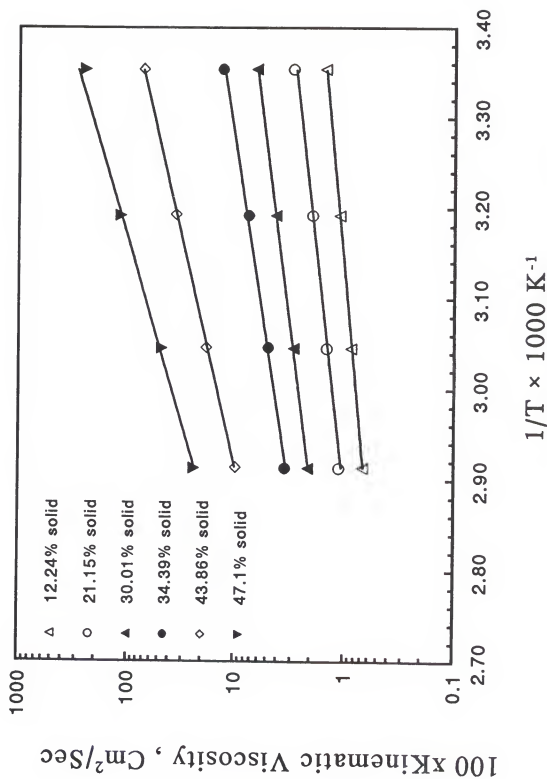


Figure (5-2): Kinematic Viscosity as a Function of Temperature for Black Liquor ABAFX015,16.



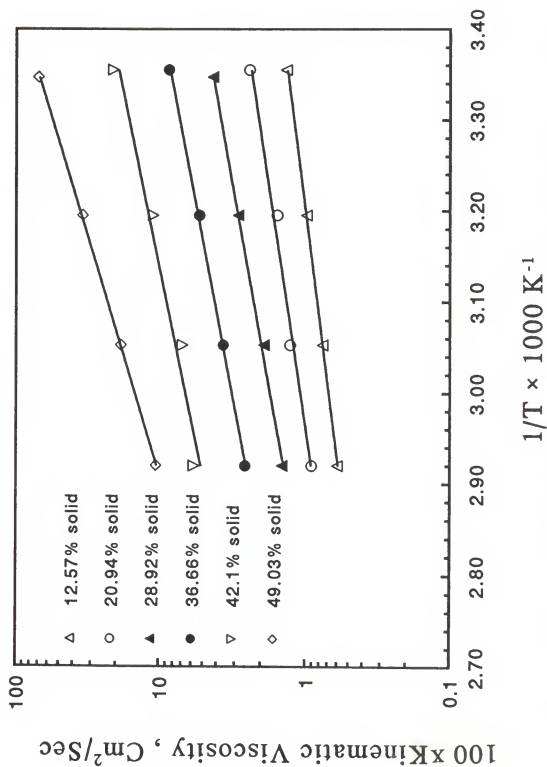


Figure (5-3): Kinematic Viscosity as a Function of Temperature for Black Liquor ABAFX025,26.

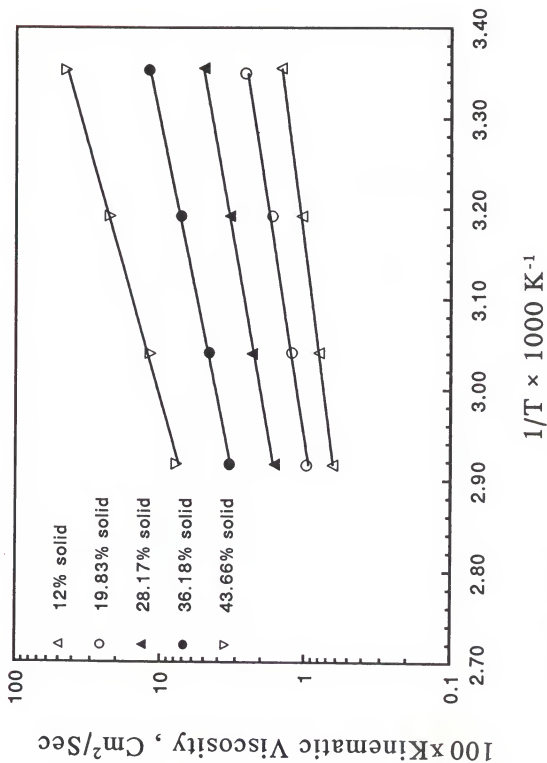


Figure (5-4): Kinematic Viscosity as a Function of Temperature for Black Liquor ABAFX035,36.

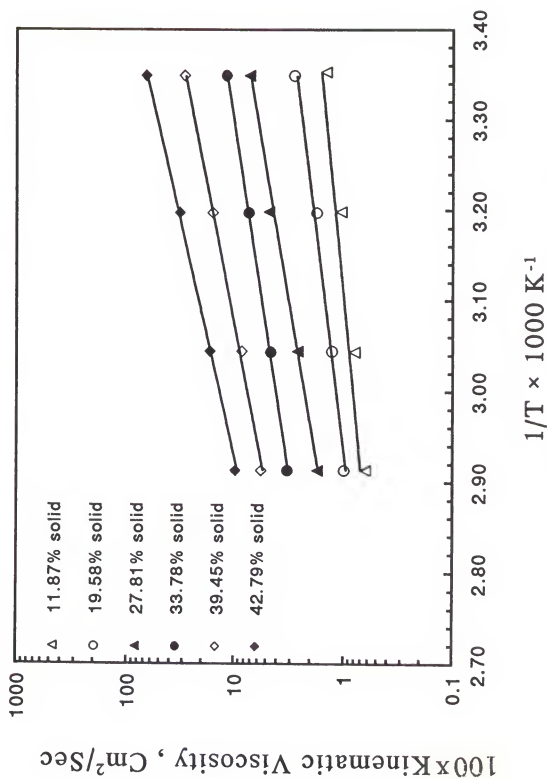


Figure (5-5): Kinematic Viscosity as a Function of Temperature for Black Liquor ABAFX043,44.

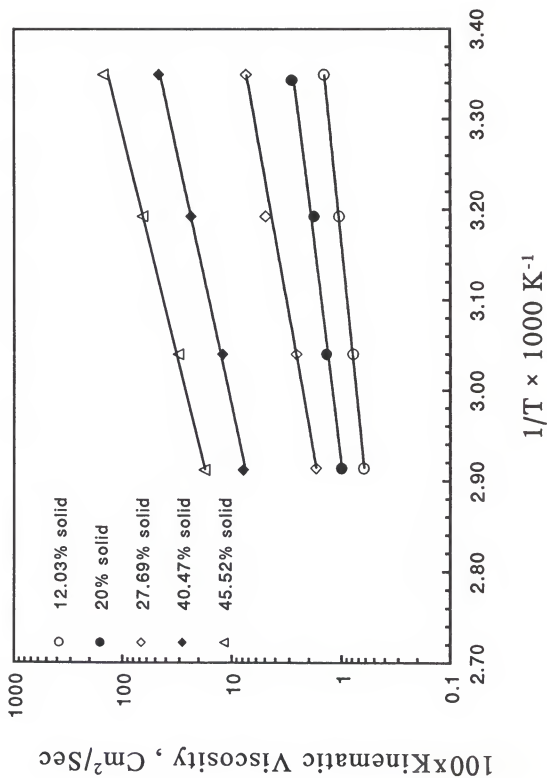


Figure (5-6): Kinematic Viscosity as a Function of Temperature for Black Liquor ABAFX053,54.

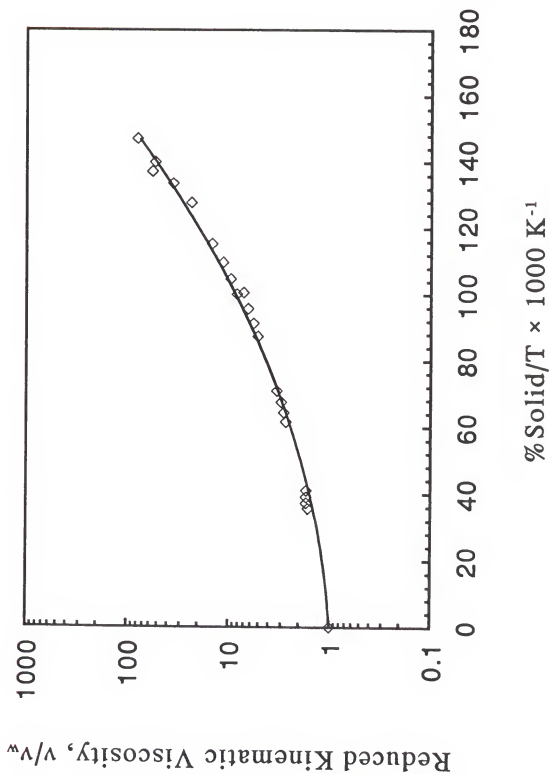


Figure (5-7): Reduced Kinematic Viscosity for Black Liquor ABAPX015,16.

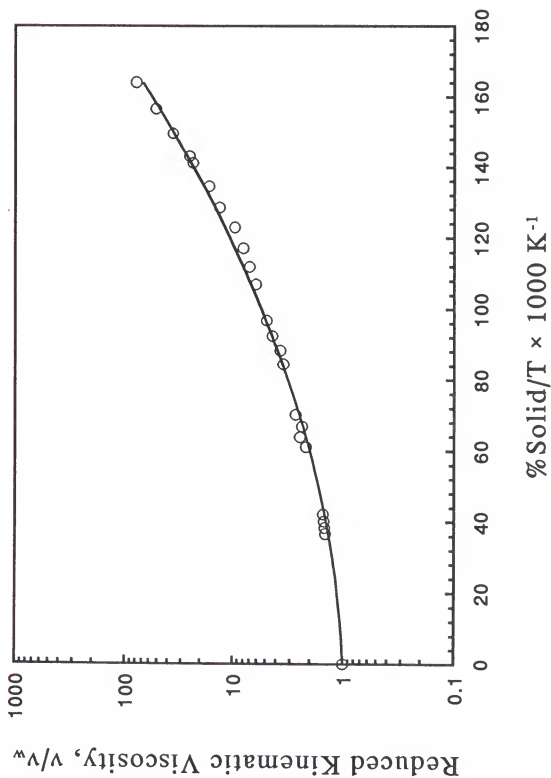


Figure (5-8): Reduced Kinematic Viscosity for Black Liquor ABAPX025, 26.

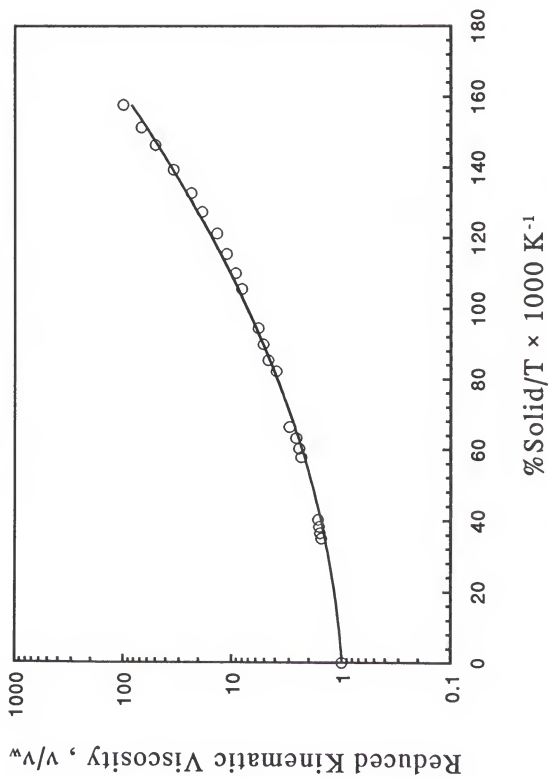


Figure (5-9): Reduced Kinematic Viscosity for Black Liquor ABAFX035,36.

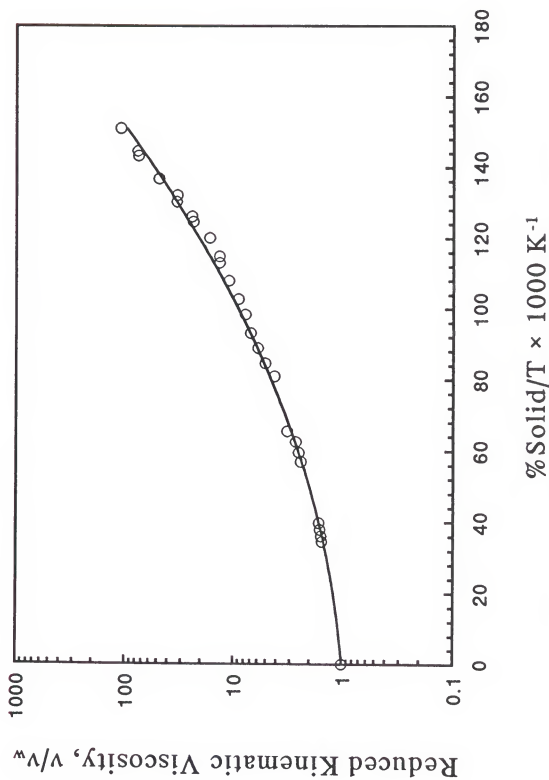


Figure (5-10): Reduced Kinematic Viscosity for Black Liquor ABAFX043,44.



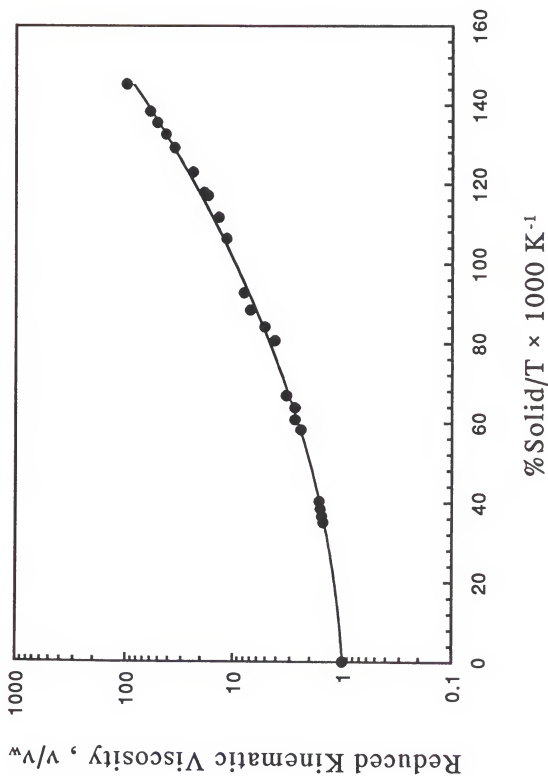


Figure (5-11): Reduced Kinematic Viscosity for Black Liquor ABAPX053,54.

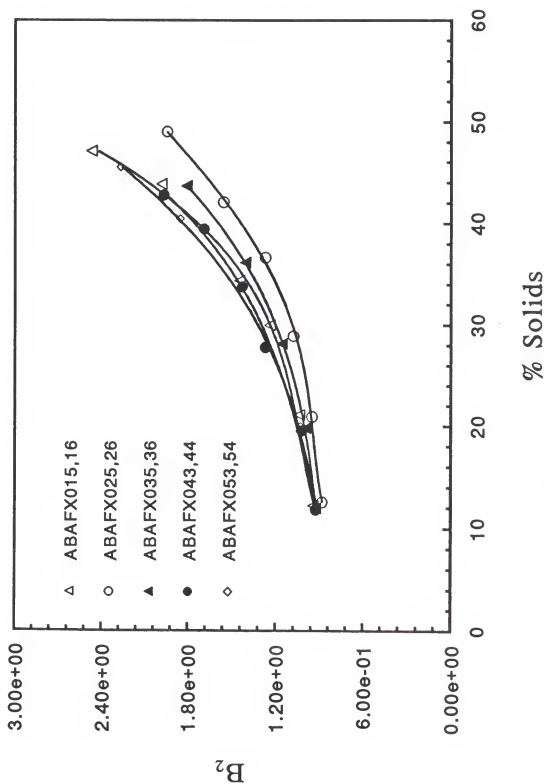


Figure (5-12):  $B_2$  as a Function of Solids Concentrations for Different Black Liquors.

Table (5-1): Coefficients of Equation (5-9) for Different Black liquors.

Black Liquor	% Solids	$A_i$	$B_i$	$R^2$
ABAFX015,16	12.24	$1.12 \times 10^{-4}$	1985.41	1.0
ABAFX015,16	21.15	$5.55 \times 10^{-5}$	2383.47	0.997
ABAFX015,16	30.01	$4.87 \times 10^{-5}$	2664.64	1.0
ABAFX015,16	34.39	$1.59 \times 10^{-5}$	3206.03	0.997
ABAFX015,16	43.89	$6.22 \times 10^{-7}$	4689.54	1.0
ABAFX015,16	47.10	$4.14 \times 10^{-8}$	5915.7	0.998
ABAFX025,26	12.57	$8.87 \times 10^{-5}$	2019.37	1.0
ABAFX025,26	20.94	$5.49 \times 10^{-5}$	2330.05	0.99
ABAFX025,26	28.92	$2.42 \times 10^{-5}$	2759.56	0.997
ABAFX025,26	36.66	$2.593 \times 10^{-5}$	2936.61	1.0
ABAFX025,26	42.10	$2.57 \times 10^{-5}$	3185.44	0.99
ABAFX025,26	49.03	$9.01 \times 10^{-7}$	4572.09	1.0
ABAFX035,36	12.00	$8.36 \times 10^{-5}$	2064.18	1.0
ABAFX035,36	19.83	$3.95 \times 10^{-5}$	2456.10	0.99
ABAFX035,36	28.17	$2.92 \times 10^{-5}$	2752.31	0.999
ABAFX035,36	36.18	$1.98 \times 10^{-5}$	3120.54	0.999
ABAFX035,36	43.66	$1.73 \times 10^{-6}$	4238.26	0.998
ABAFX043,44	11.87	$9.44 \times 10^{-5}$	2058.0	1.0
ABAFX043,44	19.58	$3.17 \times 10^{-5}$	2539.55	0.99
ABAFX043,44	27.81	$4.0 \times 10^{-6}$	3448.79	1.0
ABAFX043,44	33.78	$1.63 \times 10^{-5}$	3177.51	1.0
ABAFX043,44	39.45	$2.60 \times 10^{-6}$	3992.02	0.999
ABAFX043,44	42.79	$6.78 \times 10^{-7}$	4640.82	1.0
ABAFX053,54	12.03	$7.41 \times 10^{-5}$	2099.56	0.995
ABAFX053,54	20.0	$3.36 \times 10^{-5}$	2530.74	0.99
ABAFX053,54	27.69	$3.55 \times 10^{-6}$	3491.0	1.0
ABAFX053,54	40.47	$1.67 \times 10^{-6}$	4255.14	0.999
ABAFX053,54	45.52	$7.30 \times 10^{-7}$	4832.29	0.998

Table (5-2): Coefficients of Equation (5-10) for Different Black liquors.

Black Liquor	% Solids	$A_1$	$B_1$	$R^2$
ABAFX015,16	12.24	$8.42 \times 10^{-3}$	0.8424	0.992
ABAFX015,16	21.15	$1.0 \times 10^{-2}$	1.016	0.996
ABAFX015,16	30.01	$1.58 \times 10^{-2}$	1.132	0.994
ABAFX015,16	34.39	$1.66 \times 10^{-2}$	1.367	0.999
ABAFX015,16	43.89	$1.67 \times 10^{-2}$	1.985	0.99
ABAFX015,16	47.10	$7.7 \times 10^{-3}$	2.87	1.0
ABAFX025,26	12.57	$7.19 \times 10^{-3}$	0.8552	0.996
ABAFX025,26	20.94	$8.70 \times 10^{-3}$	0.987	0.987
ABAFX025,26	28.92	$9.54 \times 10^{-3}$	1.18	0.996
ABAFX025,26	36.66	$1.54 \times 10^{-2}$	1.244	0.997
ABAFX025,26	42.10	$2.52 \times 10^{-2}$	1.37	0.99
ABAFX025,26	49.03	$1.83 \times 10^{-2}$	1.95	0.995
ABAFX035,36	12.00	$7.41 \times 10^{-3}$	0.875	0.995
ABAFX035,36	19.83	$8.04 \times 10^{-3}$	1.05	1.0
ABAFX035,36	28.17	$1.17 \times 10^{-2}$	1.16	0.99
ABAFX035,36	36.18	$1.73 \times 10^{-2}$	1.33	0.997
ABAFX035,36	43.66	$1.70 \times 10^{-2}$	1.80	0.997
ABAFX043,44	11.87	$7.30 \times 10^{-3}$	0.877	0.996
ABAFX043,44	19.58	$7.64 \times 10^{-3}$	1.09	1.0
ABAFX043,44	27.81	$7.1 \times 10^{-3}$	1.475	0.996
ABAFX043,44	33.78	$1.59 \times 10^{-2}$	1.360	0.997
ABAFX043,44	39.45	$1.47 \times 10^{-2}$	1.71	0.996
ABAFX043,44	42.79	$1.58 \times 10^{-2}$	1.98	0.994
ABAFX053,54	12.03	$6.99 \times 10^{-3}$	0.896	0.996
ABAFX053,54	20.0	$7.97 \times 10^{-3}$	1.09	0.993
ABAFX053,54	27.69	$6.82 \times 10^{-3}$	1.49	0.995
ABAFX053,54	40.47	$1.69 \times 10^{-2}$	1.82	0.997
ABAFX053,54	45.52	$1.48 \times 10^{-2}$	2.34	1.0

Table (5-3):  $B_2$  as in Equation (5-10) for Different Black liquors.

Black Liquor	% Solids	$B_2$	$R^2$
ABAFX015,16	12.24	0.9545	1.0
ABAFX015,16	21.15	1.04	1.0
ABAFX015,16	30.01	1.242	1.0
ABAFX015,16	34.39	1.451	1.0
ABAFX015,16	43.89	1.986	1.0
ABAFX015,16	47.10	2.469	1.0
ABAFX025,26	12.57	0.883	1.0
ABAFX025,26	20.94	0.954	1.0
ABAFX025,26	28.92	1.11	1.0
ABAFX025,26	36.66	1.273	1.0
ABAFX025,26	42.10	1.559	0.999
ABAFX025,26	49.03	1.95	1.0
ABAFX035,36	12.00	0.927	1.0
ABAFX035,36	19.83	1.00	1.0
ABAFX035,36	28.17	1.16	1.0
ABAFX035,36	36.18	1.41	1.0
ABAFX035,36	43.66	1.8114	1.0
ABAFX043,44	11.87	0.927	1.0
ABAFX043,44	19.58	1.024	1.0
ABAFX043,44	27.81	1.271	0.998
ABAFX043,44	33.78	1.431	1.0
ABAFX043,44	39.45	1.693	1.0
ABAFX043,44	42.79	1.971	1.0
ABAFX053,54	12.03	0.9232	1.0
ABAFX053,54	20.0	1.032	1.0
ABAFX053,54	27.69	1.261	0.999
ABAFX053,54	40.47	1.855	1.0
ABAFX053,54	45.52	2.268	1.0

## CHAPTER 6 SHEAR VISCOSITY OF BLACK LIQUORS

### 6.1 Introduction

Interest in the rheological properties of black liquors comes from the fact that, in the pulp and paper industry, liquors are concentrated and burned to recover the inorganic chemicals as well as energy from the combustion of the organic compounds. Therefore, the knowledge of black liquor viscosity over a wide range of temperature, concentration and shear rate is essential in design and operation of kraft recovery systems, particularly for high solids concentrations. Not only does viscosity affect evaporator and concentrator operation and power requirements for fluid transport, but it affects the droplet formation, drying and swelling characteristics in the furnace. There is a trend towards higher black liquor solids content in kraft pulp mills. If the solids contents for firing were increased from 65% to 80% at a steam economy of 4/1, the energy saving would be about  $760 \times 10^9$  J/day for a typical 1000 ton/day mill (Fricke 1987).

As was mentioned in chapter 2, many studies have reported viscosity data for black liquors, but relatively few studies have been performed on liquors at high solids concentrations. The most extensive data are reported by Wight (1985), Fricke (1987)

and Zaman and Fricke (1991), who have also shown that black liquors behave as Newtonian fluids at concentrations up to 50% solids.

Much of the past work is suspect as black liquors at high solids concentrations behave generally as non-Newtonian fluids, but data have not always been taken to account for this. The viscosity of most black liquors is known to decrease with time when the black liquor is held at high temperatures (above 110 °C) at high solids concentrations (about 65%), as has been shown by Small (1985) and Söderhjelm (1986, 1988). This decrease occurs most probably as a result of degradation of the lignin contained in the black liquor (Small 1985). The lignin concentration and its molecular weight is believed to have the largest effect on the viscosity of black liquor. It has been reported that, when the high molecular weight portion of lignin was removed by ultrafiltration from several black liquors at the same solids concentrations, the viscosities decreased considerably (Söderhjelm 1986). Also, it is known that the viscosity of black liquors varies with the degree of delignification of the wood species (Wight 1985, Fricke 1987). This is due to the fact that the molecular weight distribution of the lignin is affected by the liquor composition, which will be determined by the wood species and cooking condition (Milanova and Dorris 1989, Fricke 1987).

In this study, data have been taken for four different kraft black liquors made during a two level-four variable factorial designed pulping experiment at liquor solids concentrations from 50% to 84%, at temperatures up to 140 °C, and at shear rates up to 10000 sec<sup>-1</sup>. The cooking conditions for these liquors are summarized in Table

(2-2). The rheological equipment was especially designed to maintain very precise temperature control. Also techniques were developed to insure that measurements are made within a time period that is short compared to the time required for degradation of the lignin within the liquor.

The theoretical basis and experimental setup for the instruments that were used in this study and the methods of data analysis are described in chapters 3 and 4. In this chapter, the results are discussed, viscosity-shear rate relations and methods of data reduction to rationalize the data are described. The reduced correlations can be used to estimate the viscosity of the liquors at high temperatures and high solids concentrations at which measurements are very difficult to make.

## 6.2 High Solids Viscosity

Most of the past work on the shear viscosity of black liquor have been made on a narrow range of solids concentrations (i.e, 55-70%) and temperatures below 100 °C. Even so, black liquors can exhibit non-Newtonian behavior at high solids concentration; the onset of the non-Newtonian behavior is determined by solids concentrations, solids composition and temperature.

In this work, viscosities of four different experimental softwood kraft black liquors with solids concentrations ranging from 50% to 85% were determined using a variety of viscometers modified to permit precise temperature control ( $\pm 0.2$  °C or better) and using techniques that insure that the time for measurements is short compared to the time required for lignin degradation.



Figures (6-1) through (6-20) represent the viscosity as a function of shear rate for these liquors at different temperatures and solids concentrations. Figures (6-1) through (6-5) show viscosities as a function of shear rate for liquor ABAFX011,12 at temperatures from 40 °C to 130 °C and concentrations from 55.84 to 84.14% solids. Figures (6-6) through (6-10) show viscosities as a function of shear rate for liquor ABAFX013,14 at temperatures from 40 °C to 140 °C and concentrations from 50.82 to 75.05% solids. Figures (6-11) through (6-15) represent viscosities as a function of shear rate for liquor ABAFX025,26 at temperatures from 40 °C to 140 °C and concentrations from 53.08 to 81.05% solids. Figures (6-16) through (6-20) show viscosities as a function of shear rate for liquor ABAFX043,44 at temperatures from 40 °C to 140 °C and concentrations from 53.12 to 76.28% solids. The viscosity shows changes with temperature, solids concentrations and solids composition. At lower temperatures and higher solids concentrations, the viscosity falls monotonically with increasing shear rate as shown in some of the curves in these Figures. At lower concentrations and higher temperatures, the liquors exhibit Newtonian behavior. However, the behavior of a specific liquor depends upon the solids concentration, temperature and shear rate. It can be observed that the degree of shear thinning will be decreased by increasing the temperature or decreasing the solids concentrations. For conditions where the liquors exhibit non-Newtonian behavior, the zero shear rate viscosity,  $\eta_0$ , can be determined directly by measurement at very low shear rates or by extrapolation of data taken at higher shear rates. These methods are described in chapter 7.

The shear viscosity of black liquors ABAFX013,14 and ABAFX043,44 are close together but higher than those of liquors ABAFX011,12 and ABAFX025,26, as is shown in Figure (6-21), which is a composite plot of viscosity as a function of shear rate for these liquors at  $T=70^{\circ}\text{C}$ . It can be observed that the viscosity of liquors ABAFX011,12 and ABAFX025,26 are also close to each other. These two liquors are the extremes of the design for pulping experiments. The weight average molecular weight for liquor ABAFX043,44 is higher than those for liquors ABAFX013,14, ABAFX011,12 and ABAFX025,26 (Schmidl 1992 by GPC). The lignin concentration in liquor ABAFX013,14 is higher than in liquors ABAFX043,44, ABAFX025,26 and ABAFX011,12. The results indicate that the shear viscosity is affected by both lignin concentration and lignin molecular weight in the liquor. Figure (6-22) represents the zero shear rate viscosities as a function of solids content for these liquors at  $T=70^{\circ}\text{C}$ . It is evident from this Figure that the liquors with intermediate kappa number are the most viscous at any solids content. The kappa number indicates how much lignin was left in the pulp after the pulping operations, and the maximum in viscosity at intermediate kappa number can be related to the presence of lignin with highest weight average molecular weight in the liquor. Similar relationships have been reported for black liquors by other workers (e.g, Wight 1985 and Söderhjelm 1986).

### 6.3 Dependence of Viscosity on Shear Rate

From the plots of  $\log \eta$  as a function of  $\log \dot{\gamma}$ , it appears that the behavior of black liquors at different temperatures depends upon the solids concentrations and

the solids composition. At lower temperatures and higher solids concentrations, there are two distinguishable regions of viscosity behavior a shear rate independent and a shear thinning region. In general, it can be said that black liquor exhibits pseudo-plastic behavior and its viscosity decreases as shear rate is increased. The transition from a shear independent region to shear rate dependent region occurs at lower shear rates as the solids concentration is increased or temperature is decreased. The degree of shear thinning is decreased by increasing temperature. At lower solids concentrations and higher temperatures, viscosity is independent of shear rate and the liquors exhibit Newtonian behavior. Over the shear rate dependent region, some of the plots of viscosity as a function of shear rate are linear (i.e, liquor ABAFX013,14 at 70.05 and 75.05% solids and liquor ABAFX043,44 at 72.89 and 76.28% for  $T = 40\text{ }^{\circ}\text{C}$  and  $55\text{ }^{\circ}\text{C}$ ). Therefore, the flow behavior of black liquors depend upon the solids concentration, solids composition and temperature. The linear region of the plots of  $\log \eta$  as a function of  $\log \dot{\gamma}$  can be described by the power-law model of Ostwald-de Waele (1923, 1925). Various empirical equations have been proposed to express viscosity-shear rate relationship over the entire range of shear rate. The flow behavior of black liquors can be described accurately with the following models:

1. The power-law (Ostwald-de Waele) model:

When the logarithmic plots of viscosity and shear rate are linear over the shear rate dependent region, the relation can be described by a simple power-law expression:

$$\eta = m \dot{\gamma}^{(n-1)} \quad (6-1)$$

where

$m$  = a measure of the consistency of the fluid, pas-sec<sup>n</sup>

$n$  = a measure of the degree of non-Newtonian behavior,

This empirical model was proposed by Ostwald (1925) and de Waele (1923) and it contains two parameters,  $m$  and  $n$ . The dimensions of  $m$  depend upon the constant index,  $n$ . It is generally stated that, the higher the value of  $m$ , the more viscous the fluid, and the greater the deviation of  $n$  from unity, the more significant the non-Newtonian behavior.

## 2. Cross model:

A number of generalized power-law equations have been proposed to predict the shape of the viscosity-shear rate curves over the entire range of shear rate. One of them is the Cross (1965) equation given by

$$\frac{\eta - \eta_{\infty}}{\eta_0 - \eta_{\infty}} = \frac{1}{(1 + (\lambda \dot{\gamma})^m)} \quad (6-2)$$

where  $\eta_0$  and  $\eta_{\infty}$  refer to the asymptotic values of viscosity at very low and very high shear rates respectively,  $\lambda$  is a constant parameter with the dimension of time and  $m$  is a dimensionless constant. If we assume that  $\eta_{\infty}$  is negligible, then equation (6-2) can be written as

$$\frac{\eta}{\eta_0} = \frac{1}{(1 + (\lambda \dot{\gamma})^m)} \quad (6-3)$$

At very low shear rates, the viscosity approaches  $\eta_0$ , while at higher shear rates ( $|\lambda \dot{\gamma}| \gg 1$ ), power-law behavior is predicted as

$$\frac{\eta}{\eta_0} = \frac{1}{(\lambda \dot{\gamma})^m} \quad (6-4)$$

In this form,  $m$  can be related to the power-law index,  $n$ , as follows:

$$m = 1 - n \quad (6-5)$$

### 3. The Carreau-Yasuda model:

Another generalized power-law equation which was proposed by Carreau (1972) and was modified by Yasuda (1979) has the form

$$\frac{\eta - \eta_\infty}{\eta_0 - \eta_\infty} = [1 + (\lambda \dot{\gamma})^a]^{\frac{n-1}{a}} \quad (6-6)$$

with the assumption that  $\eta_\infty$  is negligible, equation (6-6) can be written as

$$\frac{\eta}{\eta_0} = [1 + (\lambda \dot{\gamma})^a]^{\frac{n-1}{a}} \quad (6-7)$$

If the zero shear rate viscosities are available, then equation (6-7) will be a three parameter model that can be used to fit the experimental data.  $\lambda$  is a characteristic time for the fluid and  $1/\lambda$  is equal to a critical shear rate at which  $\eta$  begins to decrease with shear rate (Yasuda *et al.*, 1981). The power-law slope is  $(n-1)$ , and the parameter  $a$ , which was taken to be 2 by Carreau, adjusts the breadth of the transition region between the zero shear rate viscosity and the power-law region.

The above mentioned three models were used to fit the experimental data for black liquors. The results have been summarized in Tables (6-1) through (6-6). It seems that both Cross and Carreau-Yasuda models will fit the experimental data with very good accuracy. The Cross model, because of its simplicity and fewer parameters, is easier to use. The power-law model must be limited to cases where the plots of  $\log \eta$  versus  $\log \dot{\gamma}$  are linear over the shear rate dependent region. Values of the power-law exponent listed in Tables (6-1) through (6-4) indicate that the degree of shear thinning (non-Newtonian) behavior is decreased by increasing temperature and the parameter,  $n$ , approaches unity as the temperature is increased.

#### 6.4 Reduced Correlations for Shear Viscosity of Black Liquors

For concentrated polymer solutions with low to moderate molecular weights, the data for shear viscosity can be normalized by superposition principles (Ferry, 1980 Vinogradov and Malkin 1980 and Akonis 1983). From the plots of  $\log \eta$  versus  $\log \dot{\gamma}$ , it can be observed that the shape of the shear viscosity functions at various temperatures are similar to one another and can be brought together on a single master curve. Molecular theory predicts that, for polymer melts and concentrated polymer solutions, the following equation applies (Ferry 1980)

$$\frac{\eta}{\eta_0} = f(a_T \dot{\gamma}) \quad (6-8)$$

where  $a_T$  is the temperature shift factor that is given by

$$a_T = \frac{\eta_o T_o \rho_o}{\eta_o^o T \rho} \quad (6-9)$$

where

$\eta$  = shear viscosity, pas-sec

$\eta_o$  = zero shear rate viscosity at T, pas-sec

$\eta_o^o$  = zero shear rate viscosity at  $T_o$ , pas-sec

$\rho$  = density at T, kg/m<sup>3</sup>

$\rho_o$  = density at  $T_o$ , kg/m<sup>3</sup>

T = absolute temperature, K

$T_o$  = absolute reference temperature (here is equal to 313.16 K).

Over the temperature range studied, it may be assumed that  $\rho \approx \rho_o$ , so that

$$a_T = \frac{\eta_o T_o}{\eta_o^o T} \quad (6-10)$$

In order to obtain a master curve for shear viscosity at an arbitrary reference temperature  $T_o$  from the plots of  $\log \eta$  versus  $\log \dot{\gamma}$  at different temperatures at a particular solids concentrations a two step procedure has been followed: 1- the curve at temperature T is first shifted vertically upward by an amount of  $\log(1/\eta_o)$  and 2- the resulting curve is then shifted horizontally in such a way that any overlapping regions of the  $T_o$ -curve and shifted T curve superimpose. The amount by which  $\eta$  must be shifted to the right in order to achieve superposition is defined as  $\log a_T$  (Bird et al. 1987).

Once the zero shear rate viscosities are available, the temperature shift factor can be calculated as a function of temperature at each solids concentration and then a reduced plot of  $\log(\eta/\eta_0)$  as a function of  $\log(a_T \dot{\gamma})$  can be obtained. In our earlier work (Zaman and Fricke 1991), we showed that black liquor can be treated as a polymer solution and by applying the superposition principles, we were able to normalize our data and obtain the reduced plots for shear viscosity of black liquors. In order to investigate the validity of this method for other black liquors, the reduced variables method were applied to obtain the master curves at each solids concentrations. Examples of typical reduced viscosity data are shown in Figures (6-23) through (6-28). The shift factor  $a_T$ , is a function of temperature and solids and in general, for any liquor at constant solids concentrations is expressible as (Zaman and Fricke 1991)

$$\log_e(a_T) = A + \frac{B}{T} + \frac{C}{T^2} \quad (6-11)$$

where A, B, and C are constants.

Two models that were applied to obtain the reduced correlations for shear viscosity of black liquors are the modified form of equations (6-3) and (6-7), which can be expressed as

$$\frac{\eta}{\eta_0} = \frac{1}{(1 + (\lambda \dot{\gamma}_r)^a)} \quad (6-12)$$

$$\frac{\eta}{\eta_0} = [1 + (\lambda \dot{\gamma}_r)^a]^{\frac{(n-1)}{n}} \quad (6-13)$$

where  $\dot{\gamma}_r = a_T \dot{\gamma}$ .



Equation (6-12) has two parameters; therefore, it is easier to use than equation (6-13), which has three parameters. Also, it is possible to use polynomials to fit the experimental data as it was given in our earlier work (Zaman and Fricke 1991). The model parameters for reduced viscosity as a function of reduced shear rate, as in equations (6-12) and (6-13), are summarized in Tables (6-7) and (6-8).

The reduced curves at different solids concentrations can be superimposed by defining a solids shift factor as (Zaman and Fricke 1991)

$$a_r = \left( \frac{\eta_o S_o}{\eta_o S} \right) \quad (6-14)$$

where

$S$  = solids mass fraction,

$S_o$  = reference solids mass fraction,

$\eta_o^\circ$  = zero shear rate viscosity at  $S_o$ .

Figures (6-29), (6-30) and (6-31) are plots of reduced viscosity as a function of reduced shear rate ( $a_r a_s \dot{\gamma}$ ) for these liquors. Equations (6-12) and (6-13) were applied (with  $\dot{\gamma}_r = a_r a_s \dot{\gamma}$ ) to obtain the reduced correlations for viscosity of these liquors over the whole range of temperature, concentration and shear rate. The model parameters as in these equations are summarized in Tables (6-9) and (6-10). As it can be observed,  $R^2 \geq 0.98$  for all liquors.

The above mentioned method is a two step shifting procedure which takes into account the effects of temperature and solids concentrations on shear viscosity as a function of shear rate. The method seems to be generally applicable, although

cumbersome. Attempts were made to find simpler methods of data reduction combining the effects of temperature, concentration, and shear rate at one step. For polymer solutions Williams *et al.* (1955) have shown that, if a reference temperature  $T_s (=T_o)$  is suitably chosen, the data can be shifted in one step. Using this approach, a shift factor  $a_{ST}$  can be defined as

$$a_{ST} = \frac{\eta_o T_s \rho_s}{\eta_s^\circ T \rho} \approx \frac{\eta_o T_s}{\eta_s^\circ T} \quad (6-15)$$

where  $\eta_s^\circ$  and  $\rho_s$  are viscosity and density at a reference temperature  $T_s$ .

For polymers,  $T_s$  lies about 50° above the glass transition temperature  $T_g$  (Williams *et al.* 1955). Values of  $a_{ST}$  were determined for these liquors at  $T_s$  values of 50-90° above their glass transition temperature. At a specific value of  $T_s$  (for each liquor) the data for a single liquor can be shifted in one step over the whole range of temperature, solids content and shear rate. The reduced viscosity data are shown in Figures (6-32) through (6-35) and the model parameters as in equation (6-13) are summarized in Table (6-11) for these liquors.

### 6.5 Relation Between $T_s$ and $T_g$

The appropriate values of  $T_s$  and the glass transition temperature of the liquors at different solids concentrations are summarized in Table (6-12) (the glass transition temperature is discussed in chapter 7).  $T_s$  evidently lies 75-85° above  $T_g$  for different black liquors and  $1.3T_g \leq T_s \leq 1.4T_g$ . In principle,  $T_g$  would be a better reference temperature than  $T_s$ , since it can be specified by physical measurement,

while  $T_s$  values are based on arbitrary choice. In practice, measurement of zero shear rate viscosity of black liquors is almost impossible near  $T_g$ , but can be measured or estimated approximately from viscosity-temperature relations near  $T_g$ . Therefore, we prefer to use  $T_s$  as a reference temperature.

### 6.6 Analytical Expression for $a_{ST}$

Figures (6-36) through (6-39) illustrate  $-1/\log_e a_{ST}$  as a function of  $1/(T-T_s)$  for several black liquors used in this study. Two types of exponential functions can be found in the literature that have been used for describing the temperature dependence of  $a_{ST}$  for polymers. An Arrhenius type relationship is often found to fit the experimental data for low molecular weight fluids and polymers, which can be expressed as (Bird et al. 1987)

$$a_{ST} = \exp\left[\frac{\Delta H}{R}\left(\frac{1}{T} - \frac{1}{T_s}\right)\right] \quad (6-16)$$

where  $\Delta H$  is the activation energy for flow.

Another equation that has been found to hold for a wide variety of polymers is the WLF, or Williams-Landel-Ferry, equation that can be expressed as

$$\log_e a_{ST} = \frac{-C_1(T-T_s)}{(C_2+T-T_s)} \quad (6-17)$$

Equation (6-17) were used to fit the data for black liquors, and the results are

Black Liquor	$C_1$	$C_2, K$	$R^2$
ABAFX011,12	27.71	113.65	0.990
ABAFX013,14	35.07	132.66	0.996
ABAFX025,26	19.363	71.53	0.994
ABAFX043,44	32.52	137.4	0.998

From several published papers, the values of  $C_1$  and  $C_2$  are found to be 8.86 and 101.6, respectively, for polymers. The value of  $C_1$  for black liquors is about four times larger than the value reported for polymers while the value of  $C_2$  for black liquors and polymers are in closer agreement. The constant  $C_1$  is affected by the specific volume and free volume of the fluid at the glass transition temperature (i.e., Vinogradov and Malkin 1980). This depends upon the lignin molecular weight and its concentration in the liquor. The constant  $C_2$  depends on the thermal expansion of free volume,  $\alpha_o$  ( $C_2 = \alpha_o^{-1}$ ), which is a function of solids concentration and solids composition.

Figure (6-40) is a composite plot of  $-1/\log a_{ST}$  versus  $1/(T-T_s)$  for all the liquors. It seems that all the data points form a single line, which leads to a generalized WLF equation for black liquors. This plot represents the shift factor as

$$\log_e a_{ST} = \frac{-26.77(T - T_s)}{(104.16 + T - T_s)} \quad (6-18)$$

with  $R^2 \geq 0.99$ .

Equation (6-18) predicts a monotonic increase of  $\log_e a_{ST}$  with decreasing temperature.  $\log_e a_{ST}$  would become infinite at  $T = T_2 - C_2$ . This very simple equation

can be used to predict the temperature and solids dependence of viscosity of black liquors. From the values of  $C_1$  and  $C_2$  for each black liquor, it is evident that there is variation from one liquor to another and the use of  $C_1=26.77$  and  $C_2=104.16$  K as universal constants must be in conjunction with a reference temperature  $T_s$  as an adjustable parameter that can be chosen to obtain a best fit of the data.

### 6.7 Conclusions

At high solids (>50%), black liquors can exhibit non-Newtonian behavior. In general, liquors behave as pseudoplastic (shear thinning) fluids. The degree of shear thinning increases with decreasing temperature or increasing concentration. The exact level of viscosity at any given concentration, temperature and shear rate is dependent upon the solids composition, that is, it will vary from liquor to liquor. The flow behavior (viscosity-shear rate or shear stress-shear rate relations) of black liquors can be described very well by Cross and Carreau-Yasuda models over the entire range of experimental shear rate.

Superposition principles developed for polymer melts and concentrated polymer solutions have been shown to apply, in general, to black liquors at high concentrations. Methods have been developed for general data reduction that can be used for calculation of viscosity at a specific condition. By choosing a suitable reference temperature,  $T_s$ , related to the glass transition temperature of black liquors, the data can be normalized to obtain a reduced plot of viscosity as a function of temperature, solids concentrations and shear rate. A generalized WLF

equation has been obtained for the liquors used in this study and it probably can be used as a universal shift factor for other black liquors, with  $T_g$  as a parameter. The calculated viscosity values should be accurate to within about  $\pm 25\%$  or better for a range of viscosity of more than seven orders of magnitude. In this work, the effect of density on shift factor was ignored, because the density data are not available for these liquors. However, for precise reduction of viscosity data, the effect of density will be considered in future work. In present mill operations at high solids, temperatures are high enough that the liquors behave as Newtonian fluids. At these conditions, a correlation of zero shear rate viscosity versus temperature and solids concentrations as presented in chapter 7, is sufficient to define viscosity.

The methods developed and the demonstration of general applicability significantly reduce the quantity of data necessary to describe the viscosity behavior of a new liquor. Thus, the work necessary to determine the effects of solids composition on liquor viscosity at specific conditions has been greatly reduced.

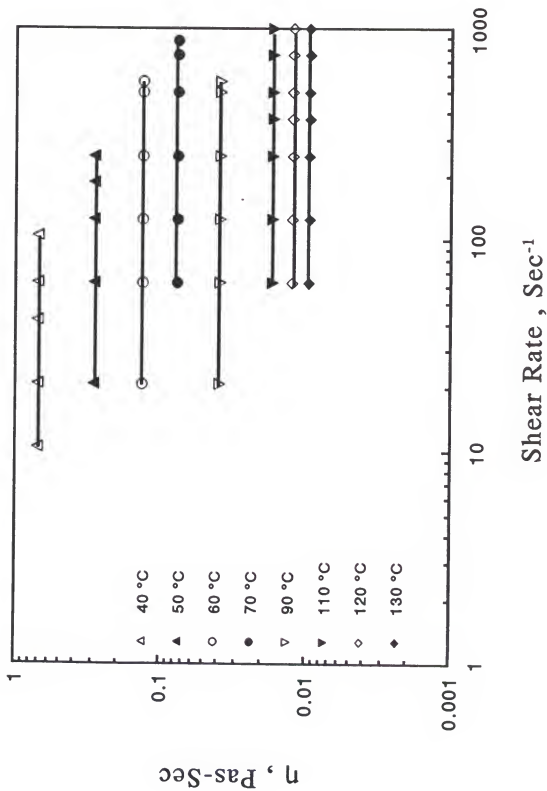


Figure (6-1): Viscosity as a Function of Shear Rate for Black Liquor ABAFX011,12 at 55.84% Solids.

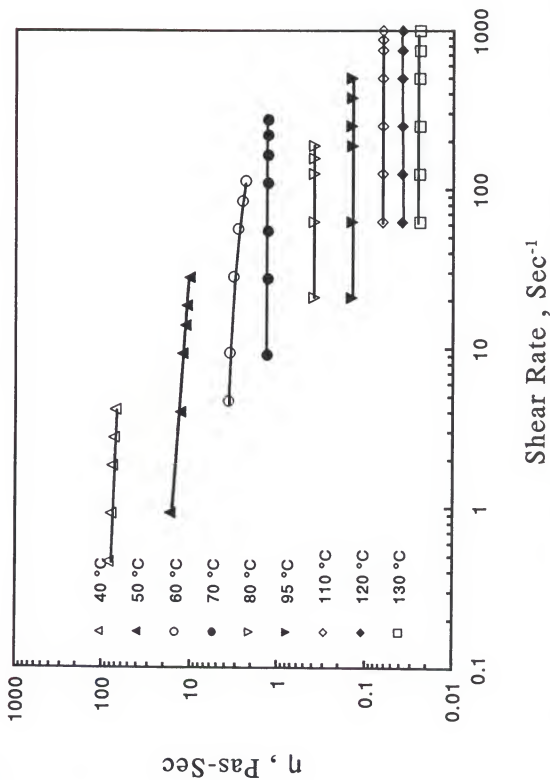


Figure (6-2): Viscosity as a Function of Shear Rate for Black Liquor ABAPX011,12 at 63.49% Solids.



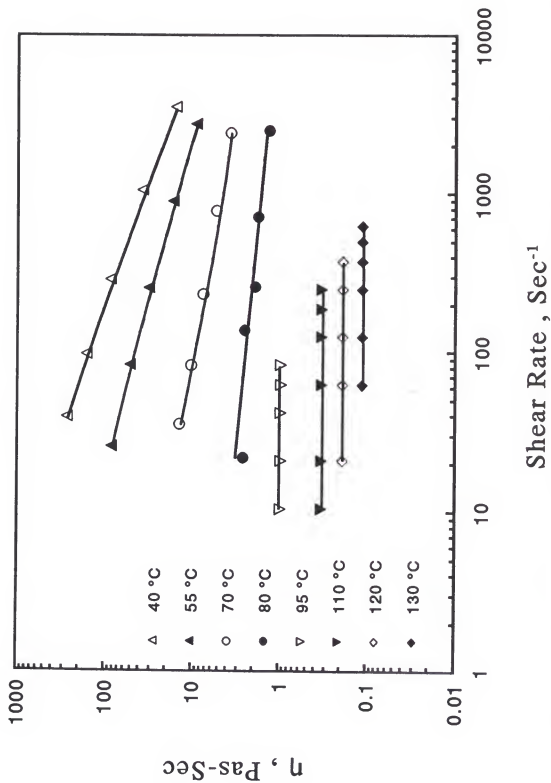


Figure (6-3): Viscosity as a Function of Shear Rate for Black Liquor ABAFX011,12 at 72.67% Solids.

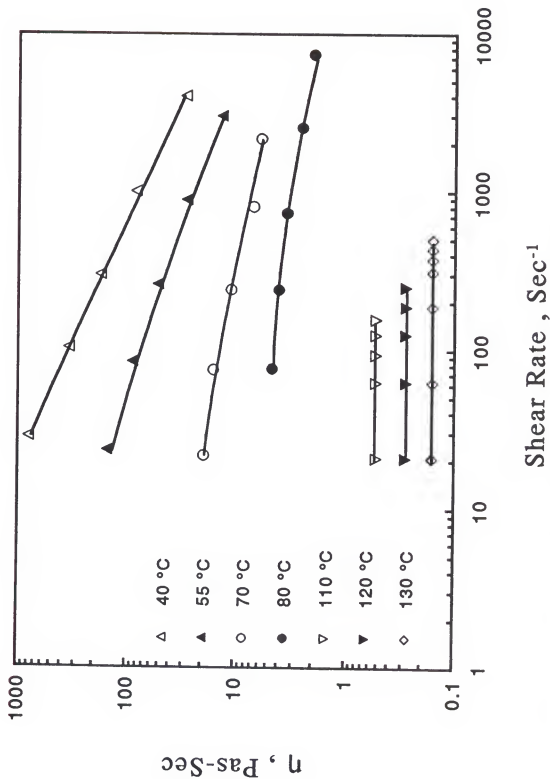


Figure (6-4): Viscosity as a Function of Shear Rate for Black Liquor ABAFX011,12 at 75.36% Solids.

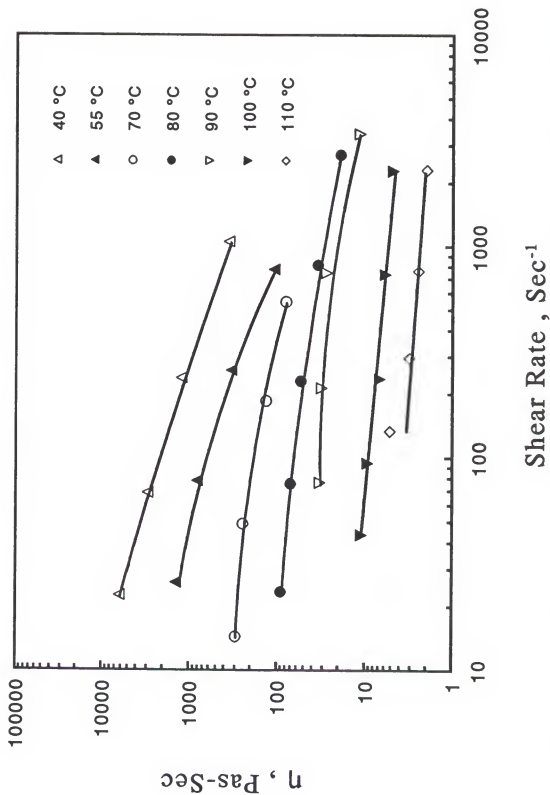


Figure (6-5): Viscosity as a Function of Shear Rate for Black Liquor ABAFX011,12 at 84.14% Solids.

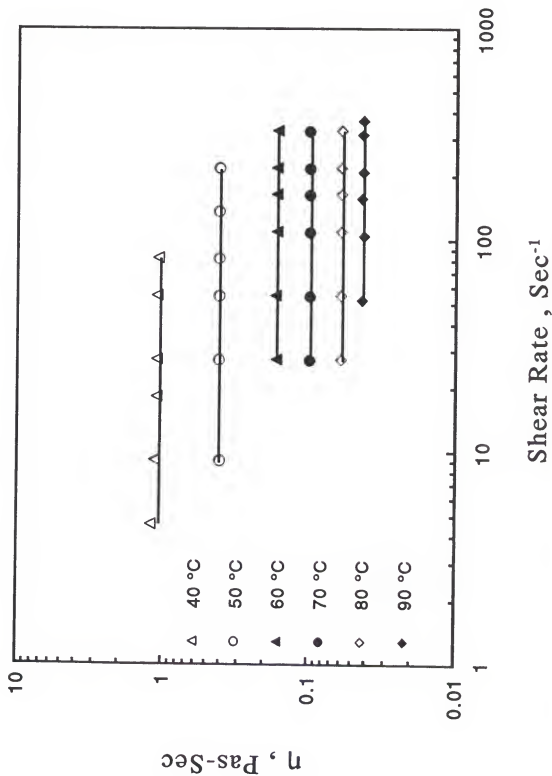


Figure (6-6): Viscosity as a Function of Shear Rate for Black Liquor ABAFX013,14 at 50.82% Solids.

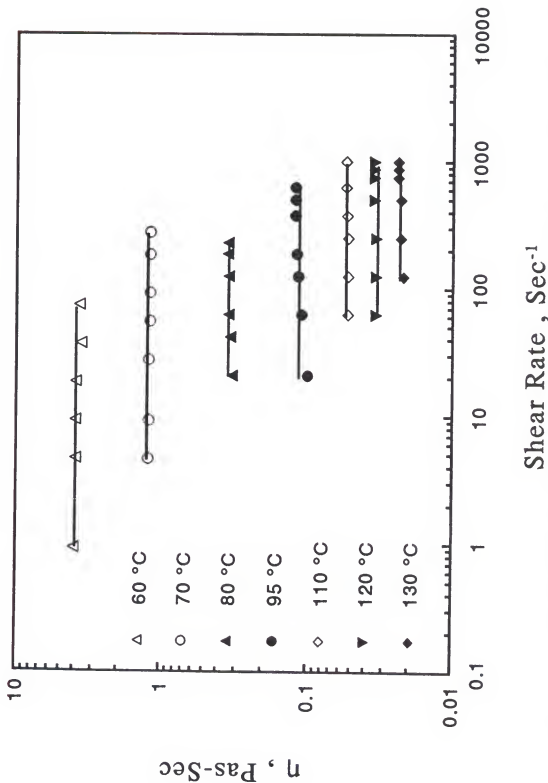


Figure (6-7): Viscosity as a Function of Shear Rate for Black Liquor ABAFX013,14 at 59.08% Solids.

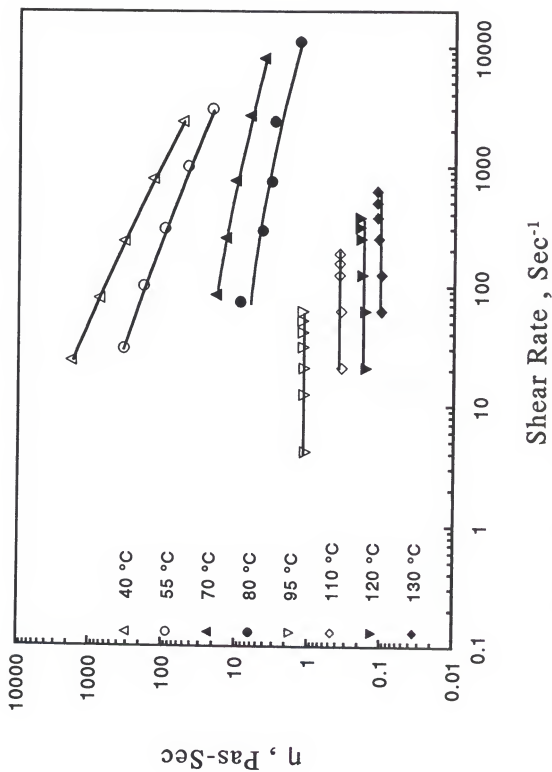


Figure (6-8): Viscosity as a Function of Shear Rate for Black Liquor ABAPX013,14 at 67.20% Solids.

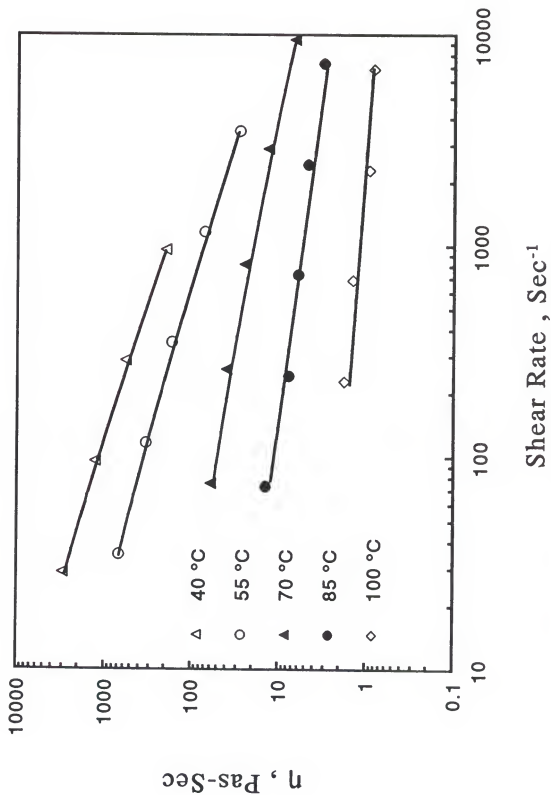


Figure (6-9): Viscosity as a Function of Shear Rate for Black Liquor ABAPX013,14 at 70.05% Solids.

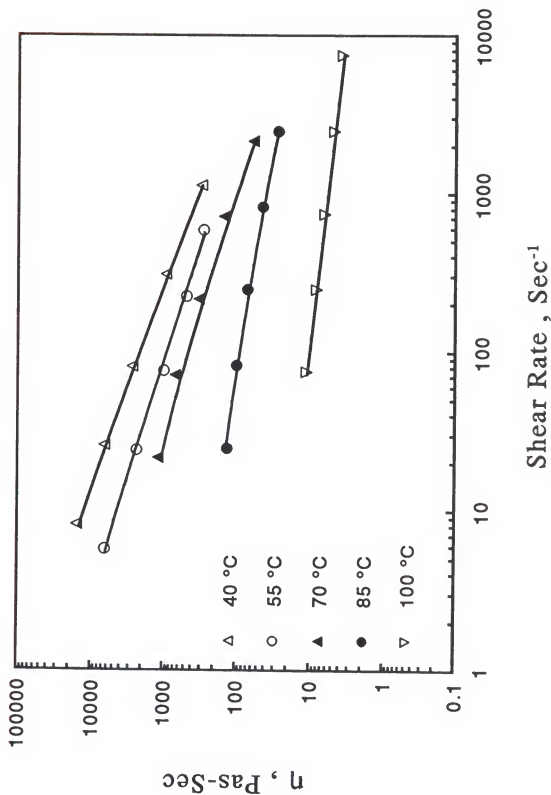


Figure (6-10): Viscosity as a Function of Shear Rate for Black Liquor ABAFX013,14 at 75.05% Solids.



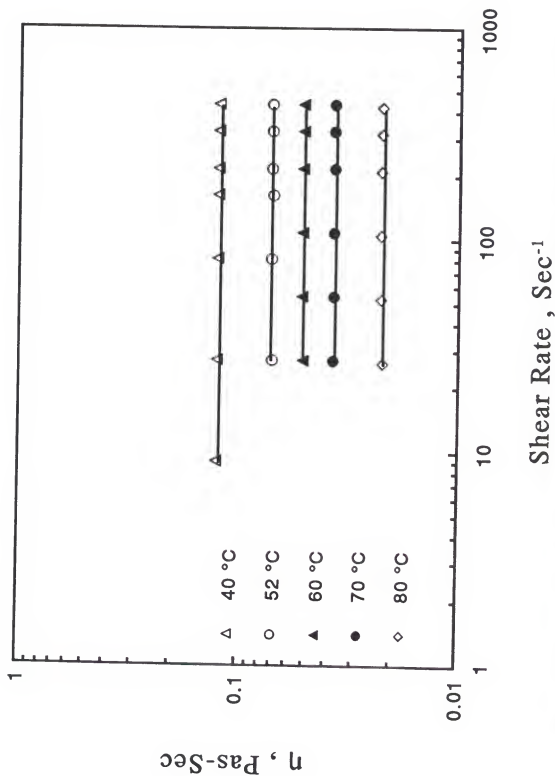


Figure (6-11): Viscosity as a Function of Shear Rate for Black Liquor ABAFX025,26 at 53.08% Solids.

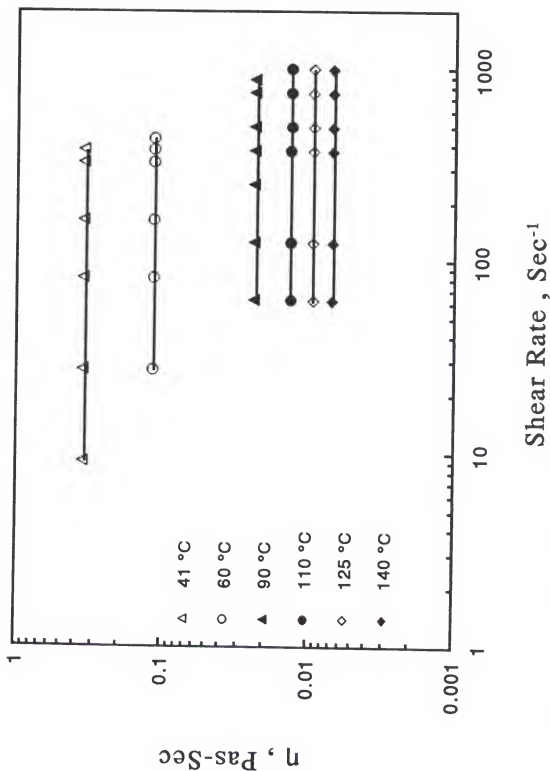


Figure (6-12): Viscosity as a Function of Shear Rate for Black Liquor ABAFX025,26 at 57.68% Solids.

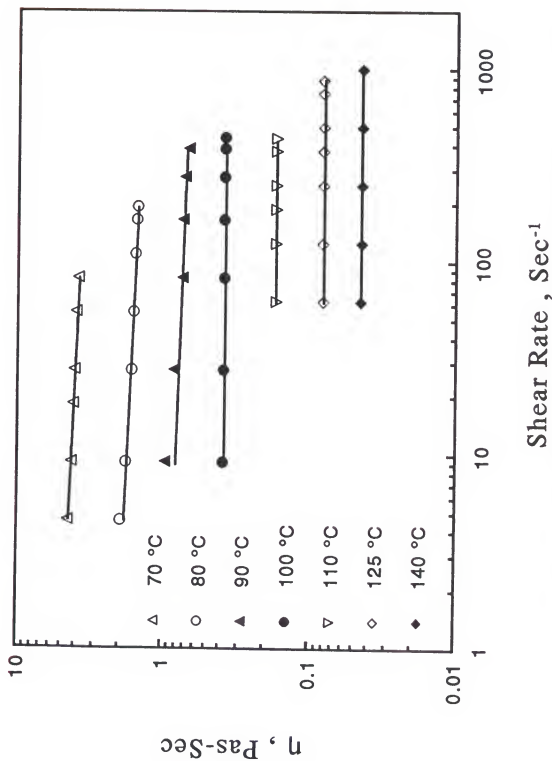


Figure (6-13): Viscosity as a Function of Shear Rate for Black Liquor ABAFX025,26 at 71.98% Solids.

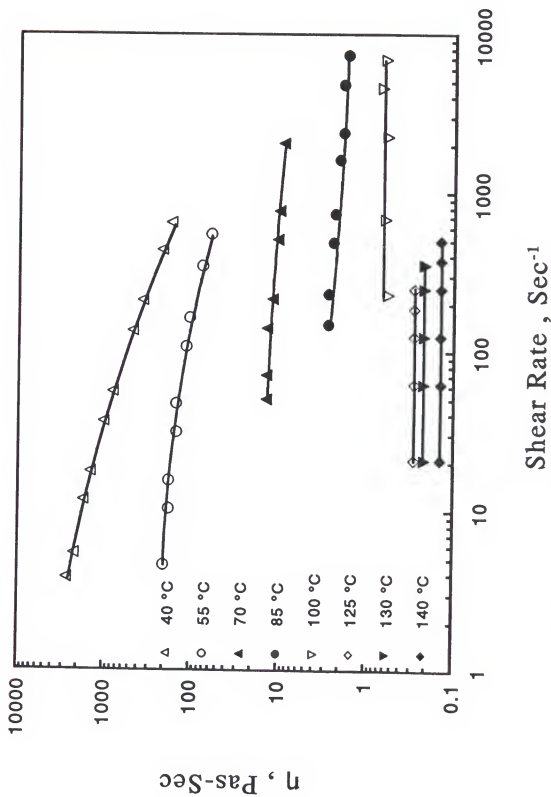


Figure (6-14): Viscosity as a Function of Shear Rate for Black Liquor ABAFX025,26 at 75.70% Solids.

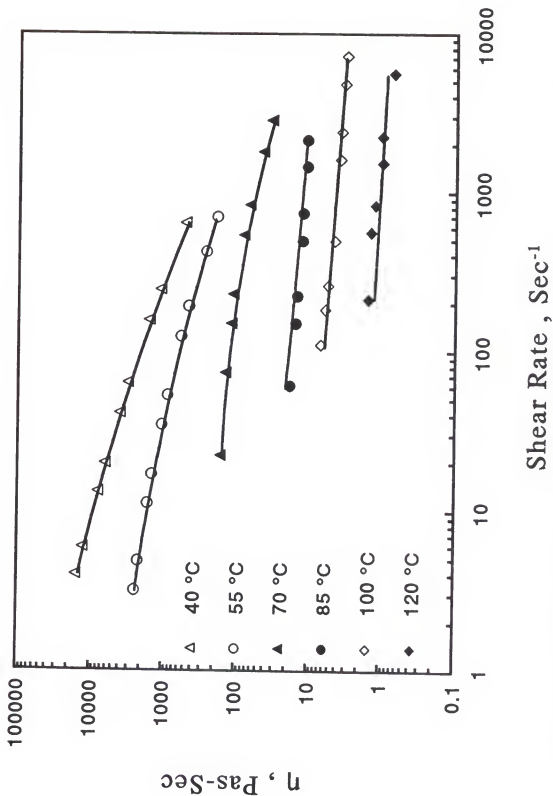


Figure (6-15): Viscosity as a Function of Shear Rate for Black Liquor ABAFX025,26 at 8.05% Solids.

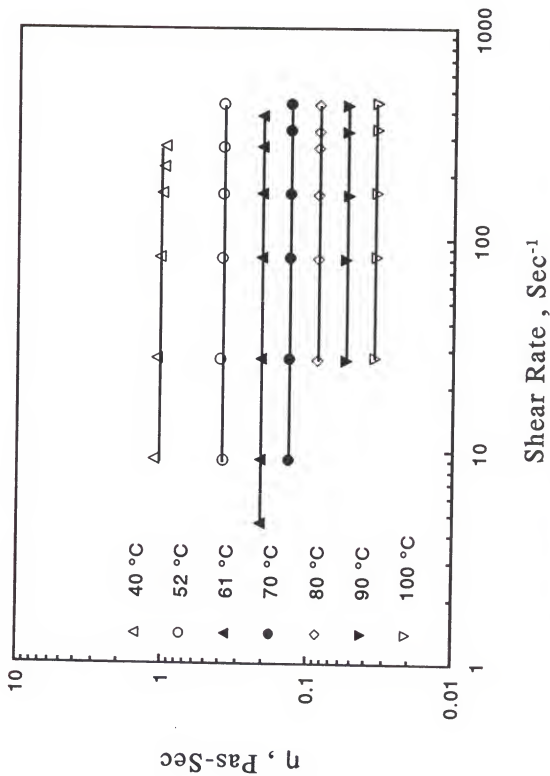


Figure (6-16): Viscosity as a Function of Shear Rate for Black Liquor ABAFX043,44 at 53.12% Solids.

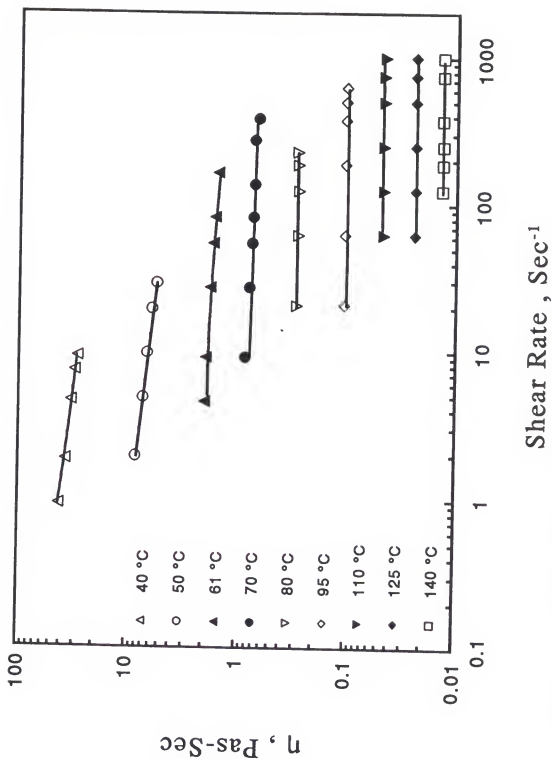


Figure (6-17): Viscosity as a Function of Shear Rate for Black Liquor ABAFX043,44 at 58.33% Solids.

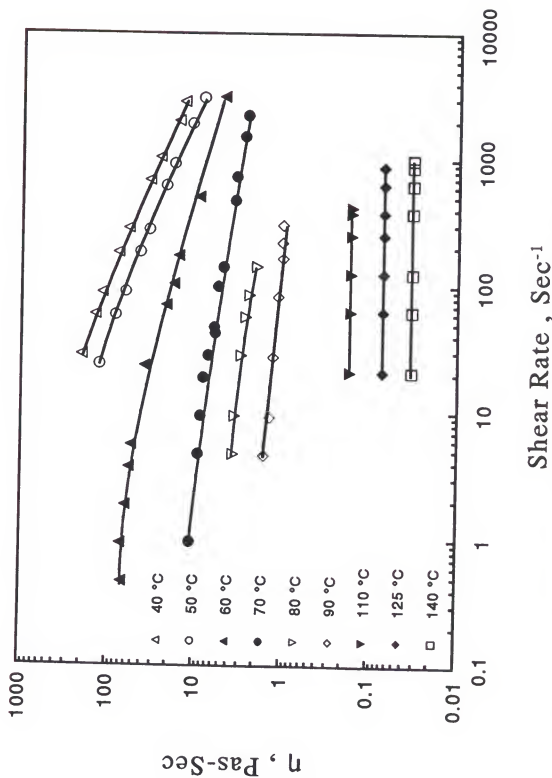


Figure (6-18): Viscosity as a Function of Shear Rate for Black Liquor ABAPX043,44 at 64.17% Solids.



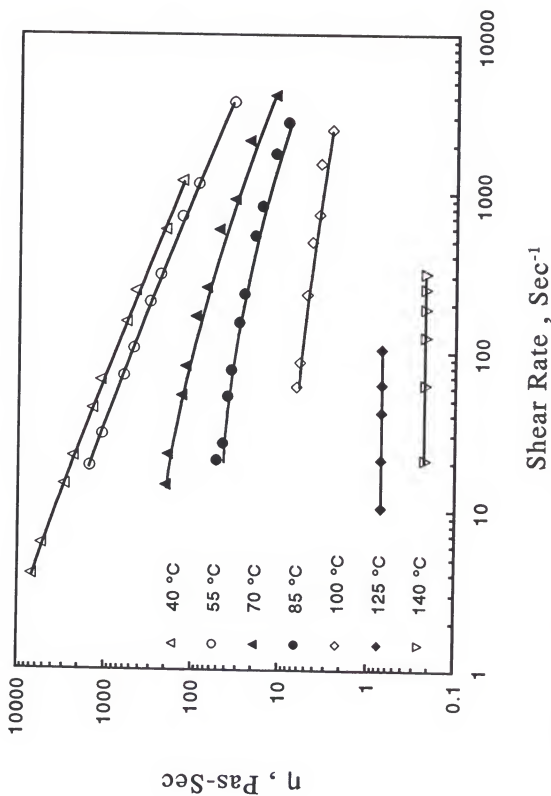


Figure (6-19): Viscosity as a Function of Shear Rate for Black Liquor ABAFX043,44 at 72.89% Solids.

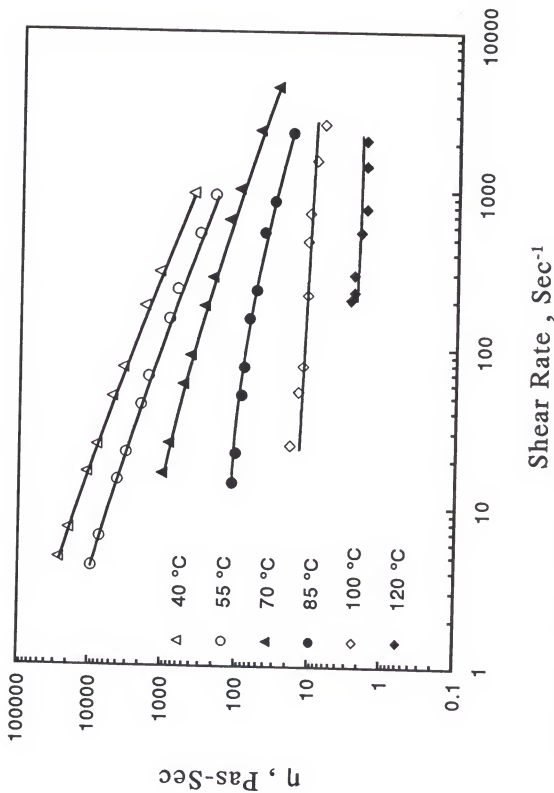


Figure (6-20): Viscosity as a Function of Shear Rate for Black Liquor ABAFX043,44 at 76.28% Solids.

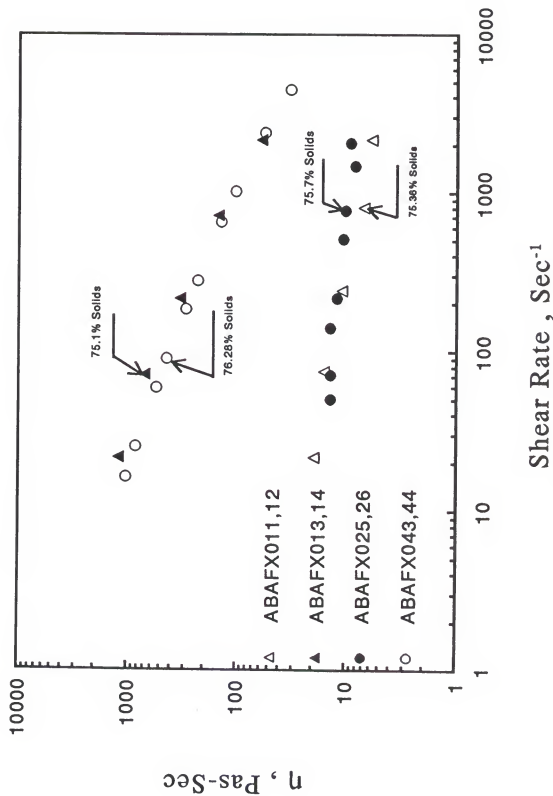


Figure (6-21): Viscosity as a Function of Shear Rate for Different Black Liquors at  $T=70^\circ\text{C}$ .

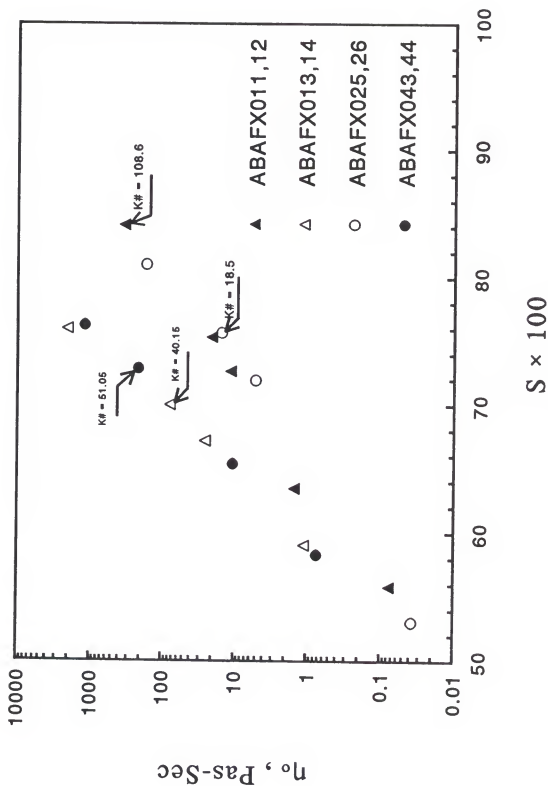


Figure (6-22): Viscosity as a Function of Solids Concentrations for Different Black Liquors at  $T=70^\circ\text{C}$ .

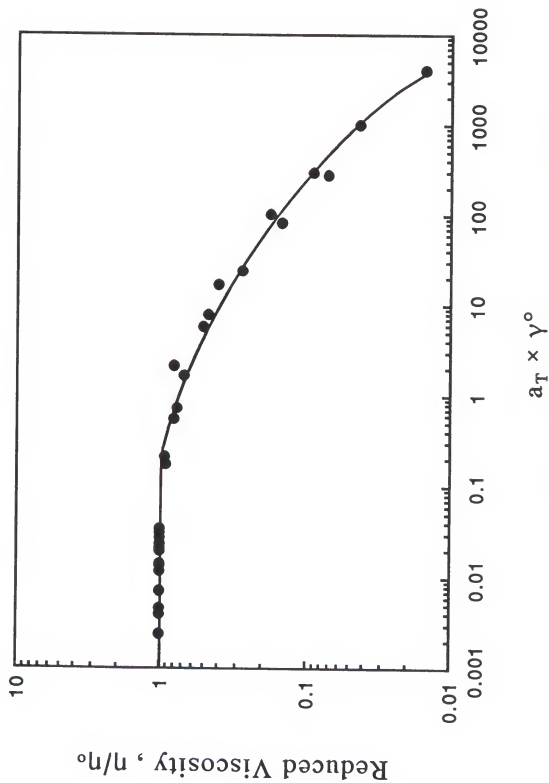


Figure (6-23): Reduced Plot for Viscosity of Black Liquor ABAFX011,12 at 75.36% Solids, (Ref. T=40°C)

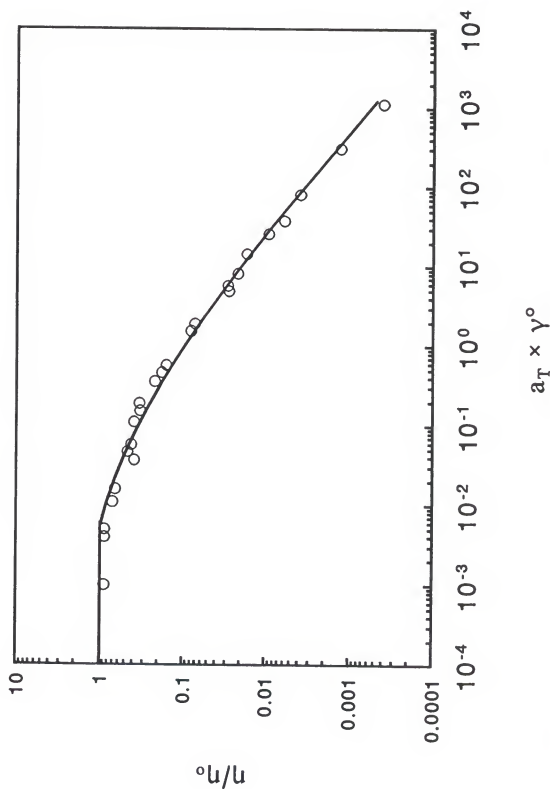


Figure (6-24): Reduced Plot for Viscosity of Black Liquor ABAPX013,14 at 75.05% Solids. (Ref. T=40 °C)

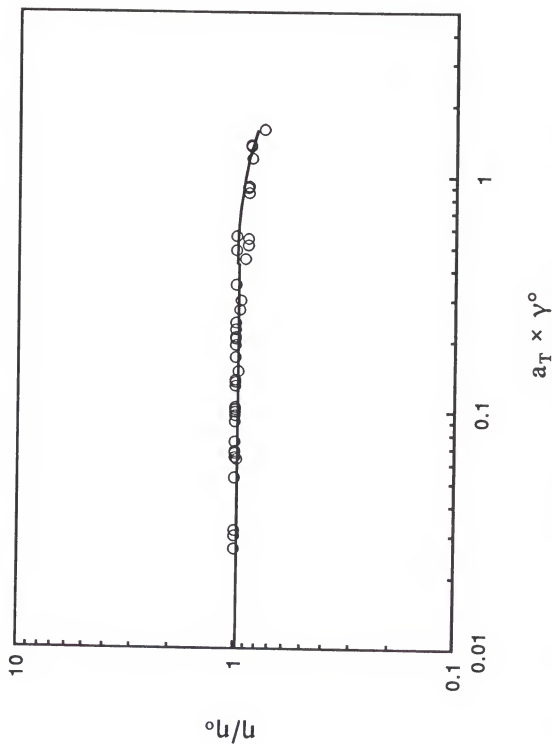


Figure (6-25): Reduced Plot for Viscosity of Black Liquor ABAFX025,26 at 71.98% Solids. (Ref.  $T=40\text{ }^{\circ}\text{C}$ )

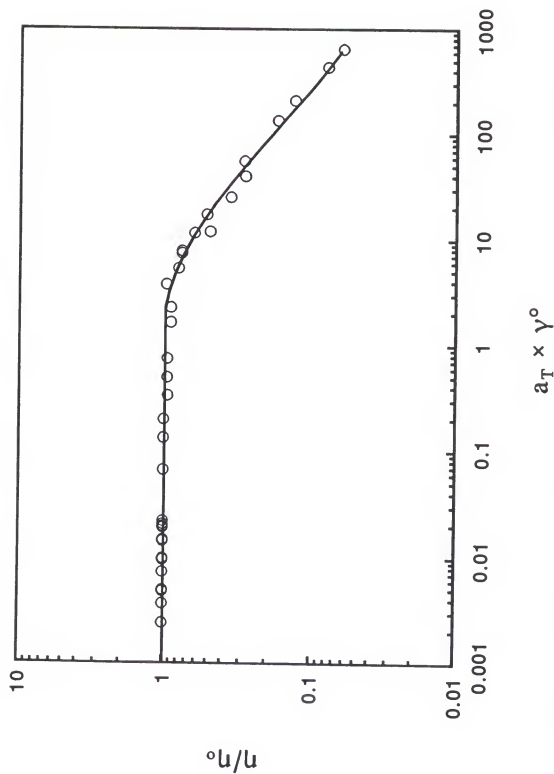


Figure (6-26): Reduced Plot for Viscosity of Black Liquor ABAFX025,26 at 75.7% Solids. (Ref. T=40 °C)



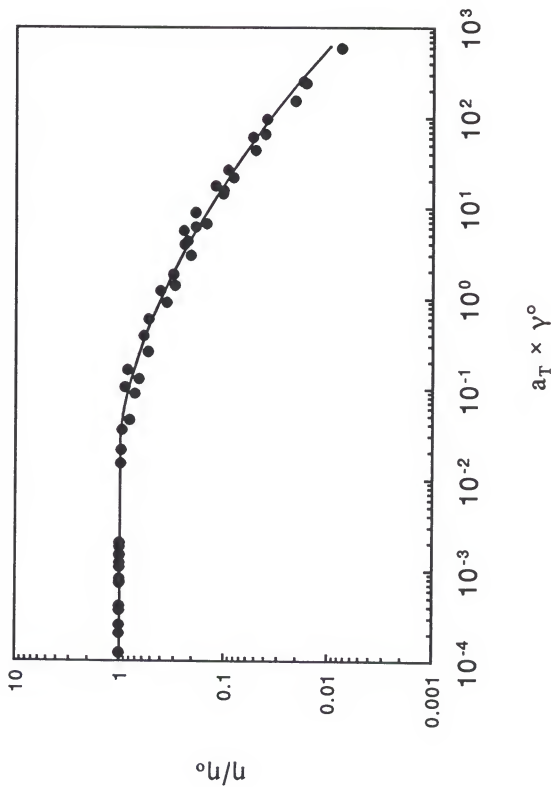


Figure (6-27): Reduced Plot for Viscosity of Black Liquor ABAPX043,44 at 72.89% Solids. (Ref. T=40 °C)

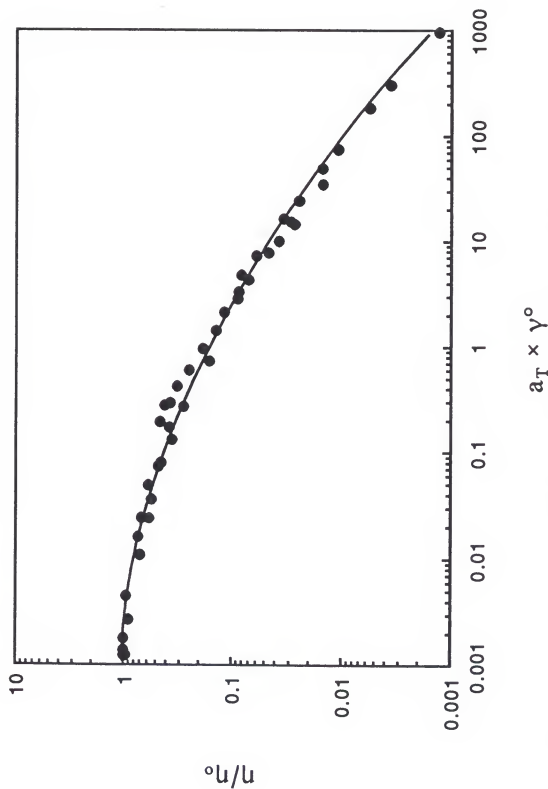


Figure (6-28): Reduced Plot for Viscosity of Black Liquor ABAFX043,44 at 76.28% Solids. (Ref T=40 °C)

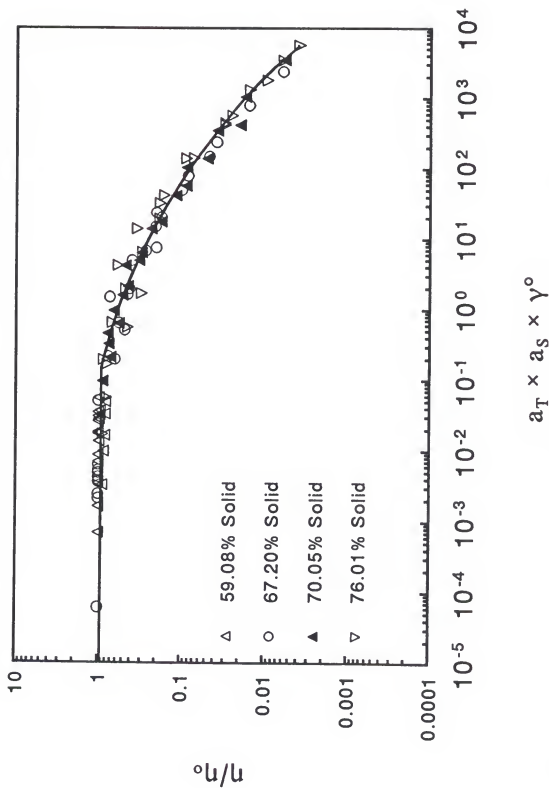


Figure (6-29): Reduced Plot for Viscosity of Black Liquor ABAFX013,14. (Ref. T=40 °C, Ref. Solids=67.2%)

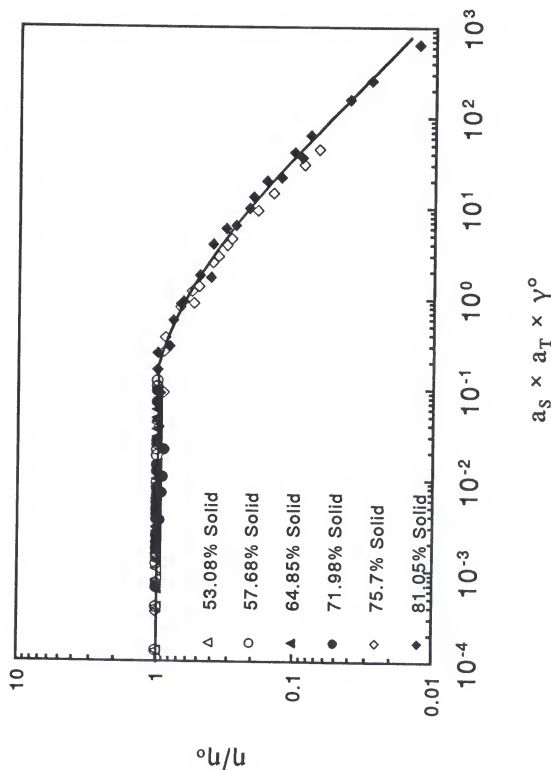


Figure (6-30): Reduced Plot for Viscosity of Black Liquor ABAFX025,26. (Ref. T=40 °C, Ref. Solids=81.05%)

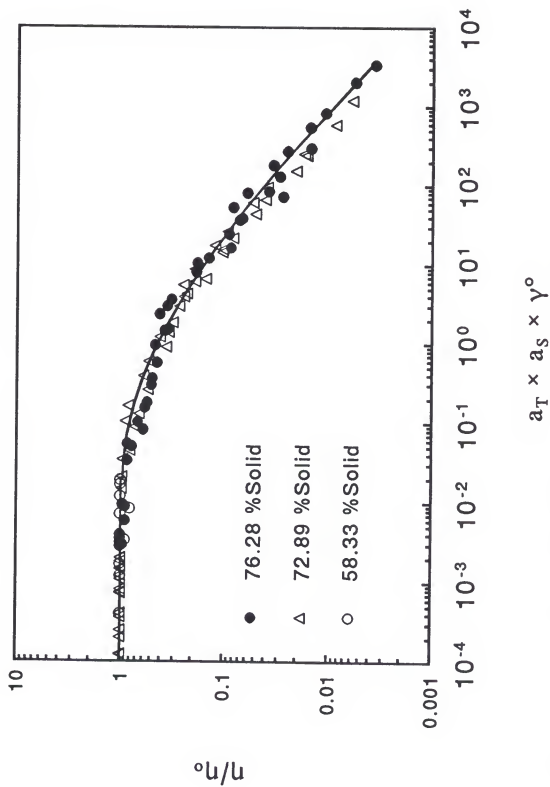


Figure (6-31): Reduced Plot for Viscosity of Black Liquor ABAFX043,44. (Ref. T=40 °C, Ref. Solids=72.89%)

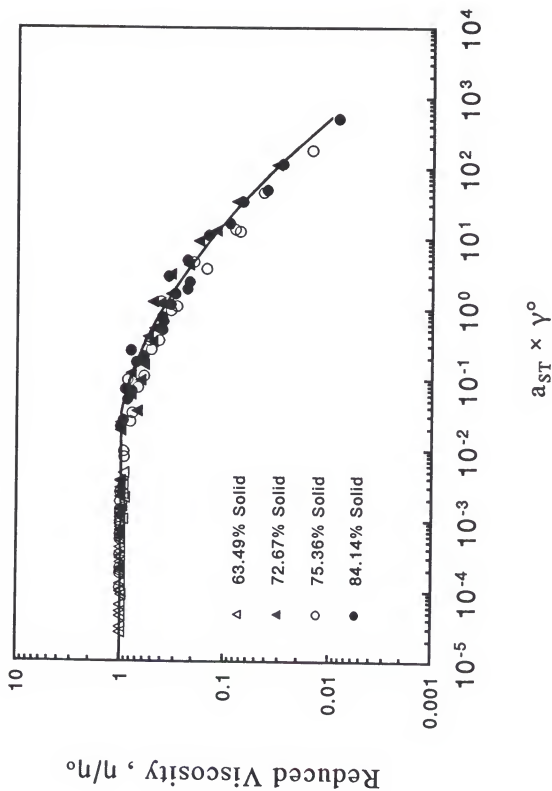


Figure (6-32): Reduced Plot for Viscosity of Black Liquor ABAFX011,12. ( $T_s = T_g + 74.5$ )

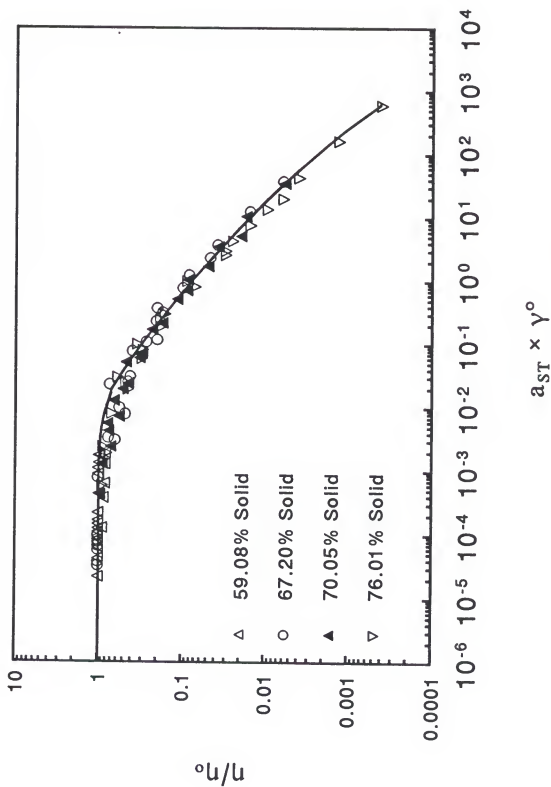


Figure (6-33): Reduced Plot for Viscosity of Black Liquor ABAFX013,14. ( $T = T_s + 82.6$ )

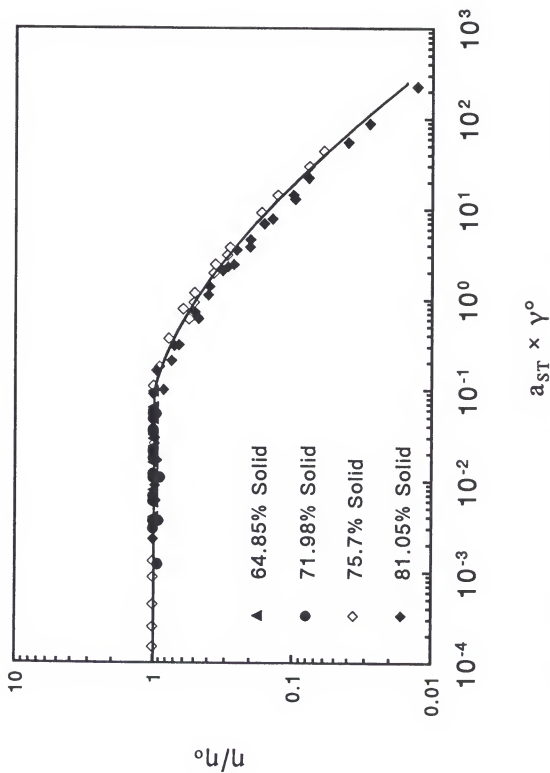


Figure (6-34): Reduced Plot for Viscosity of Black Liquor ABAFX025,26. ( $T_s = T + 78.6$ )



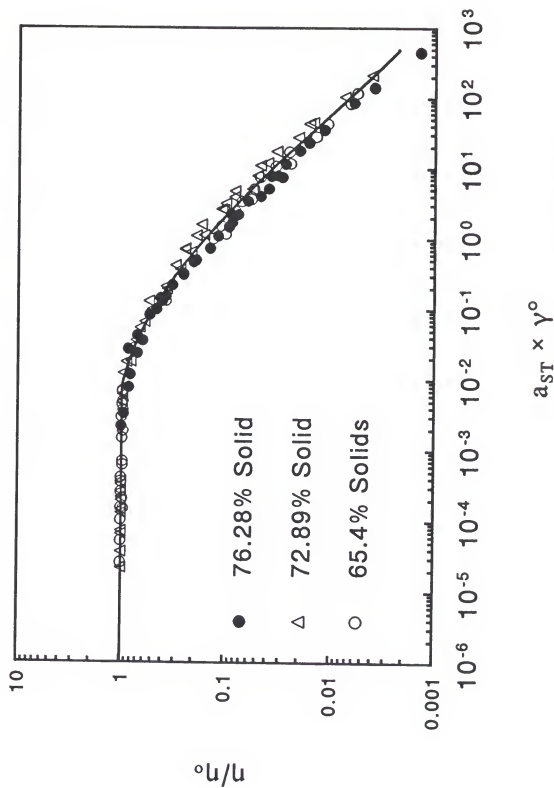


Figure (6-35): Reduced Plot for Viscosity of Black Liquor ABAFX043,44. ( $T_s = T + 84.3$ )

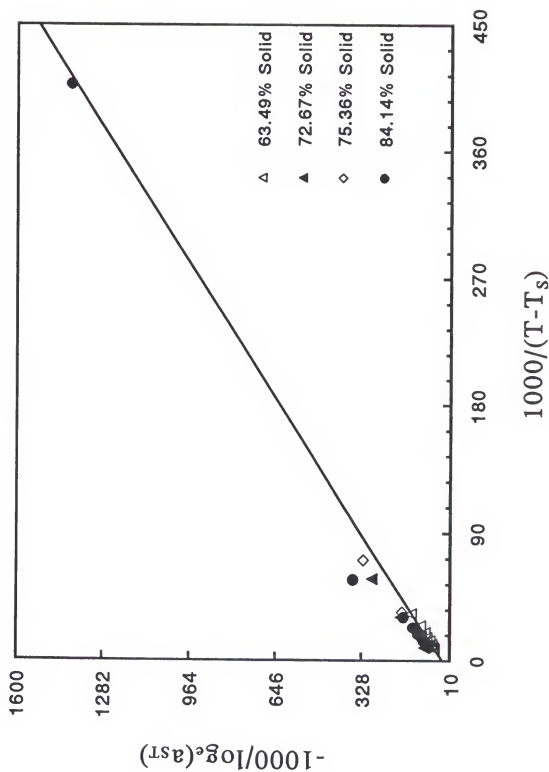


Figure (6-36): Shift Factor for Black Liquor ABAFX011,12 at Different Solids Concentrations.

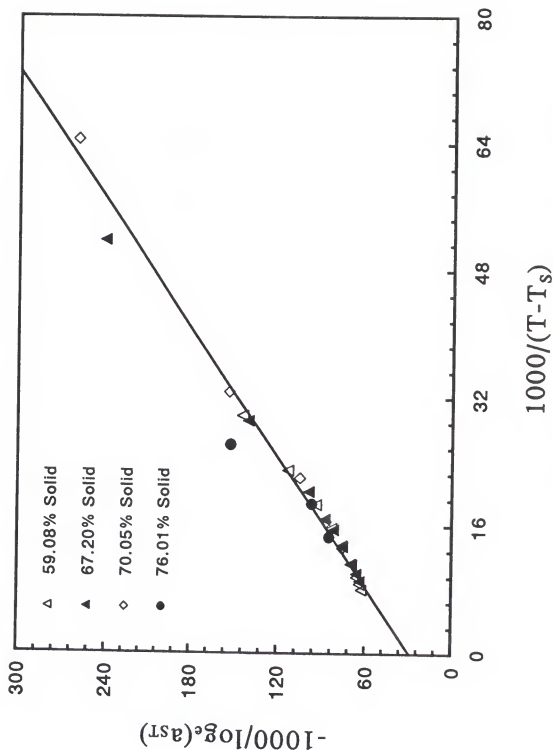


Figure (6-37): Shift Factor for Black Liquor ABAFX013,14 at Different Solids Concentrations.

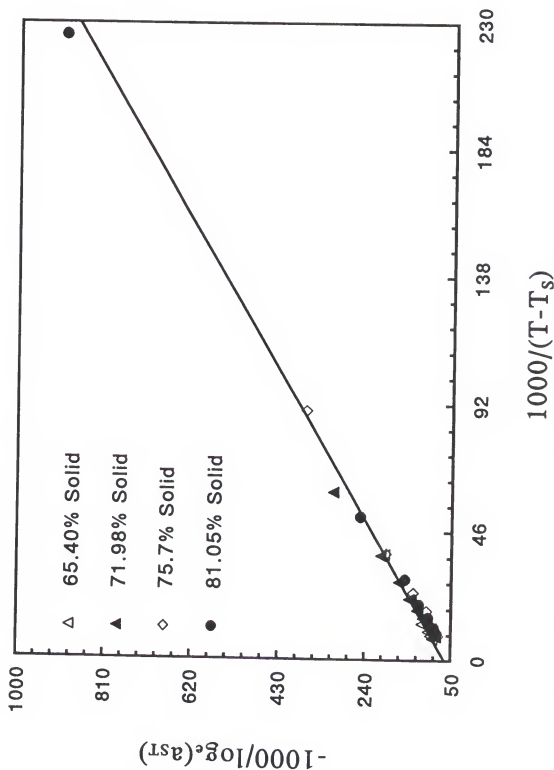


Figure (6-38): Shift Factor for Black Liquor ABAFX025,26 at Different Solids Concentrations.

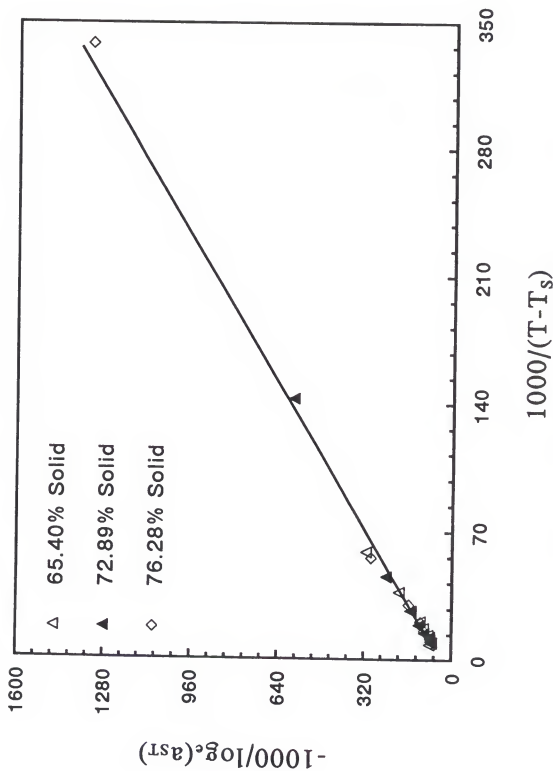


Figure (6-39): Shift Factor for Black Liquor ABAFX043,44 at Different Solids Concentrations.

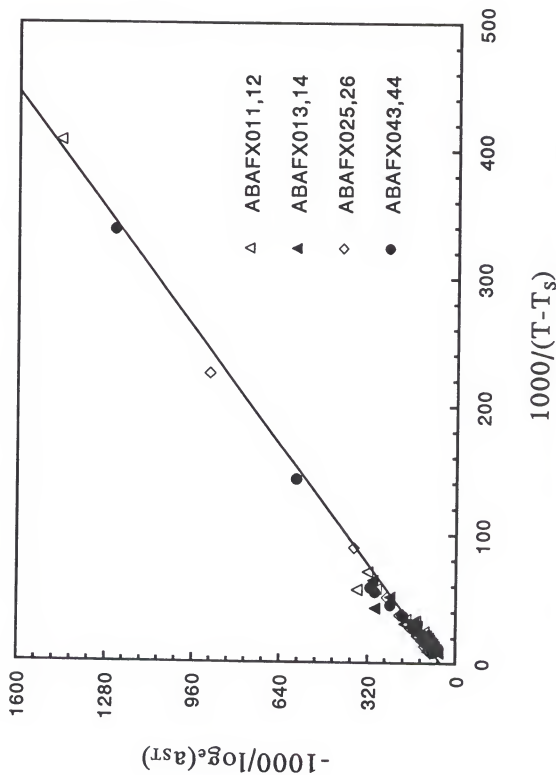


Figure (6-40): Composite Plot for Shift Factor of Different Black Liquors.

Table (6-1): The Power-Law Model Parameters for Black Liquor ABAFX011,12.

% Solids	T, °C	m	n	R <sup>2</sup>
72.67	40	2912.880	0.369	0.997
72.67	55	410.713	0.527	0.997
72.67	70	40.804	0.694	0.999
72.67	80	6.326	0.802	0.935
72.67	95	1.039	0.981	0.914
75.36	40	6722.96	0.355	0.997
75.36	55	771.50	0.50	0.995
75.36	70	48.14	0.733	0.980
75.36	80	10.675	0.818	0.977
84.14	40	57094.9	0.285	0.998
84.14	55	9884.27	0.366	0.960
84.14	70	892.73	0.629	0.960
84.14	80	271.17	0.683	0.97
84.14	100	32.24	0.744	0.93

Table (6-2): The Power-Law Model Parameters for Black Liquor ABAFX013,14.

% Solids	T, °C	m	n	R <sup>2</sup>
67.2	40	20413.14	0.249	0.999
67.2	55	2826.40	0.4015	0.998
67.2	70	85.10	0.677	0.992
67.2	80	35.32	0.66	0.96
70.05	40	41071.1	0.2335	0.997
70.05	55	8349.44	0.32	0.995
70.05	70	462.63	0.551	0.99
70.05	85	32.74	0.743	0.98
70.05	100	6.484	0.78	0.962
75.05	40	86612.723	0.206	0.999
75.05	55	20303.123	0.3214	0.998
75.05	70	10301.47	0.346	0.99
75.05	85	429.112	0.658	0.99
75.05	100	30.58	0.77	1.0

Table (6-3): The Power-Law Model Parameters for Black Liquor ABAFX025,26.

% Solids	T, °C	m	n	R <sup>2</sup>
75.7	40	6567.74	0.453	0.99
75.7	55	315.6	0.761	0.942
75.7	70	31.86	0.832	0.983
75.7	85	5.354	0.873	0.974
81.05	40	43230.65	0.34	0.994
81.05	55	4805.72	0.534	0.982
81.05	85	31.66	0.857	0.98
81.05	100	15.29	0.9	0.97



Table (6-4): The Power-Law Model Parameters for Black Liquor ABAFX043,44.

% Solids	T, °C	m	n	R <sup>2</sup>
65.4	40	1621.7	0.41	0.997
65.4	50	794.31	0.444	0.998
65.4	70	12.16	0.83	0.943
65.4	80	4.93	0.86	0.944
65.4	90	1.81	0.895	0.97
72.89	40	20228.3	0.293	0.996
72.89	55	12491.25	0.301	0.997
72.89	85	157.0654	0.655	0.98
72.89	100	19.05	0.76	0.97
76.28	40	97025	0.228	0.998
76.28	55	27344.46	0.307	0.998
76.28	70	6369.46	0.395	0.992
76.28	100	30.15	0.83	0.911
76.28	120	2.76	0.942	0.57

Table (6-5): The Cross Model Parameters Different Liquors.  $\eta = f(\dot{\gamma})$ 

Black Liquor	% Solids	T, °C	$\lambda$	m	R <sup>2</sup>
ABAFX025,26	75.70	40	0.0375	0.952	0.996
ABAFX025,26	75.7	55	0.00647	0.702	1
ABAFX025,26	81.05	40	0.441	0.755	1
ABAFX025,26	81.05	55	0.0262	0.991	0.99
ABAFX025,26	81.05	70	0.002	0.823	1
ABAFX043,44	65.4	60	0.338	0.759	0.998
ABAFX043,44	65.4	70	0.0128	0.448	0.994
ABAFX043,44	72.89	70	0.0091	0.849	0.996
ABAFX043,44	76.28	85	0.0043	0.747	0.998

Table (6-6): The Carreau-Yasuda Model Parameters for Different Liquors.  $\eta = f(\dot{\gamma})$ 

Black Liquor	% Solids	T, °C	$\lambda$	a	n	R <sup>2</sup>
ABAFX025,26	75.70	40	0.136	1.914	0.426	1
ABAFX025,26	75.7	55	0.0343	0.912	0.614	1
ABAFX025,26	81.05	40	0.7475	0.987	0.338	1
ABAFX025,26	81.05	70	0.003684	0.932	0.346	1
ABAFX043,44	65.4	60	0.1257	1.012	0.517	0.999
ABAFX043,44	65.4	70	0.4574	1.495	0.786	0.998
ABAFX043,44	72.89	70	0.0396	1.592	0.499	0.998
ABAFX043,44	72.89	85	0.0068	0.815	0.362	0.998

Table (6-7): The Cross Model Parameters for Different Black Liquors.  $\eta_r = f(a_T \dot{\gamma})$ 

Black Liquor	% Solids	$\lambda$	a	$R^2$
ABAFX013,14	67.2	0.699	0.611	0.994
ABAFX013,14	75.05	23.492	0.62	0.99
ABAFX025,26	75.7	0.0744	0.6	0.997
ABAFX025,26	81.05	0.45	0.8454	0.991
ABAFX043,44	72.89	1.933	0.614	0.991
ABAFX043,44	76.28	9.35	0.633	0.981

Table (6-8): The Carreau-Yasuda Model Parameters for Different Black Liquors.  
 $\eta_r = f(a_T \dot{\gamma})$ 

Black Liquor	% Solids	$\lambda$	a	n	$R^2$
ABAFX013,14	67.2	5.68	0.929	0.658	0.994
ABAFX013,14	75.05	8.414	0.489	0.214	0.975
ABAFX025,26	75.70	0.1803	0.725	0.485	0.997
ABAFX025,26	81.05	1.415	1.25	0.437	0.991
ABAFX043,44	72.89	1.35	0.592	0.315	0.991
ABAFX043,44	76.28	6.304	0.593	0.302	0.981

Table (6-9): The Cross Model Parameters for Different Black Liquors.  $\eta_r = f(a_S a_T \dot{\gamma})$ 

Black Liquor	$\lambda$	a	$R^2$
ABAFX013,14	0.777	0.557	0.985
ABAFX025,26	0.4378	0.7273	0.98
ABAFX043,44	0.786	0.521	0.986

Table (6-10): The Carreau-Yasuda Model Parameters for Different Black Liquors.  
 $\eta_r = f(a_S a_T \dot{\gamma})$ 

Black Liquor	$\lambda$	a	n	$R^2$
ABAFX011,12	0.162	1.295	0.546	0.999
ABAFX013,14	0.282	0.501	0.284	0.984
ABAFX025,26	0.563	0.742	0.344	0.98
ABAFX043,44	0.824	0.5384	0.29	0.986

Table (6-11): The Carreau-Yasuda Model Parameters for Different Black Liquors.  
 $\eta_r = f(a_{ST} \dot{\gamma})$ 

Black Liquor	$\lambda$	a	n	$R^2$
ABAFX011,12	8.187	1.077	0.515	0.975
ABAFX013,14	25.744	0.565	0.255	0.984
ABAFX025,26	2.726	1.047	0.428	0.982
ABAFX043,44	5.463	0.549	0.218	0.97

Table (6-12):  $T_g$  and  $T_s$  for Different Black Liquors.

Black Liquor	% Solids	$T_g$ , K	$T_s$ , K	$T_s - T_g$	$T_s/T_g$
ABAFX011,12	63.49	208.90	283.10	74.2	1.355
ABAFX011,12	72.67	221.70	295.90	74.2	1.335
ABAFX011,12	75.36	224.90	299.10	74.2	1.330
ABAFX011,12	84.14	236.50	310.70	74.2	1.314
ABAFX013,14	67.20	211.24	293.84	82.6	1.390
ABAFX013,14	70.05	215.10	297.66	82.6	1.384
ABAFX013,14	76.01	222.28	304.88	82.6	1.372
ABAFX025,26	71.98	218.96	297.56	78.6	1.360
ABAFX025,26	75.7	223.40	302.00	78.6	1.352
ABAFX025,26	81.05	232.12	310.72	78.6	1.340
ABAFX043,44	65.40	211.90	296.19	84.26	1.398
ABAFX043,44	72.89	221.90	306.16	84.26	1.380
ABAFX043,44	76.28	225.94	310.20	84.26	1.373

## CHAPTER 7

### CORRELATIONS FOR NEWTONIAN VISCOSITY OF BLACK LIQUORS

#### 7.1 Introduction

The Newtonian (zero shear rate) viscosities of four different kraft black liquors from a two level, four variable factorial designed pulping experiments were determined for solids concentrations up to 84% and temperatures up to 140 °C (413.16 K). Methods of measurement and estimation of zero shear rate viscosities from viscosity-shear rate data have been described and compared. The combination of the absolute reaction rates and free volume concepts were used to express the relationship between the Newtonian viscosity and temperature. Attempts were made to obtain a generalized correlation for viscosity as a function of temperature and solids concentrations. The results of this model and our previous empirical correlation have been compared and discussed.

#### 7.2 Background

Knowledge of the Newtonian viscosity of black liquors at high temperatures and solids concentrations is essential since, at a firing temperature of 130 °C - 140 °C and concentrations up to 80-83%, it can be expected that liquors show Newtonian behavior (Zaman and Fricke 1991). Therefore, knowledge of the Newtonian (zero

shear rate) viscosity is important for the design and control of process equipment. Yet, to date, very little work has been done to develop appropriate correlations for Newtonian viscosity of black liquors. The purpose of work described here is 1) to study methods of measurement and estimation of the Newtonian viscosity of concentrated ( $> 50\%$ ) black liquors and 2) to evaluate the utility of a fundamentally based model for correlating the zero shear rate viscosity of different black liquors as a function of temperature and concentration of non-volatile components. These correlations can be used to estimate the Newtonian viscosity of the mill black liquors made at the same pulping conditions at different temperatures and concentrations.

### 7.3 Determination of the Newtonian (zero shear rate) Viscosity

Zero shear rate viscosities are of particular importance in normalizing data and applying superposition principles. For non-Newtonian fluids at sufficiently low shear rates, we can expect that the variation in structure will become insignificant, so that the dependency of viscosity on shear rate will disappear, unless the material has a yield stress (Dealy 1982). The value of viscosity in this range is called the zero shear rate viscosity, which is equal to the shear rate independent viscosity for Newtonian fluids. In this study, the Newtonian viscosities were determined through the use of a parallel plate viscometer (for  $40\text{ }^{\circ}\text{C} \leq T \leq 85\text{ }^{\circ}\text{C}$  and  $\% \text{ solids} \geq 65$ ), an open cup coaxial cylinder viscometer (for  $40\text{ }^{\circ}\text{C} \leq T \leq 90\text{ }^{\circ}\text{C}$  and  $\% \text{ solids} \leq 65$ ) and a pressure cell coaxial cylinder viscometer (for  $T \geq 100\text{ }^{\circ}\text{C}$  and  $\% \text{ solids} < 75$ ). In experimental work, however, it is not always possible to reach the very low shear

rate regions of Newtonian flow of highly concentrated black liquors. In some cases, experimental data on viscosity versus shear rate must be extrapolated to zero shear rates (or shear stresses) in order to determine the zero shear rate viscosities. The parallel plate and coaxial cylinder viscometers have been discussed in chapters 8 and (3) respectively. The methods of extrapolation will be discussed in this chapter.

#### 7.4 Estimation of Zero Shear Rate Viscosities

In order to estimate the zero shear rate viscosities, experimental data on viscosity versus shear rate must be extrapolated to zero shear rates. Kataoka and Ueda (1968) have summarized several methods that can be used to estimate the zero shear rate viscosities, these are

1. Use of plots of  $1/\eta$  as a function of  $\tau_w$  which is based on Ferry's equation:

$$\frac{\eta}{\eta_0} = 1 + \frac{\tau_w}{G_i} \quad (7-1)$$

where  $\eta$ (pas-sec) is the shear viscosity,  $G_i$ (pas) is the internal shear modulus of rigidity and  $\tau_w$ (pas) is the shear stress at the wall of the rotor (in coaxial cylinder viscometer) or capillary (in a capillary viscometer).

2. Use of plots of  $\log(1/\eta)$  as a function of  $\tau_w$  which is based on the Spencer and Dillon's equation:

$$\frac{\eta_0}{\eta} = A \exp(B \tau) \quad (7-2)$$

3. Use of Plots of  $1/\eta$  as a function of  $\dot{\gamma}^{2/3}$  which is based on the equation derived



by Cross:

$$\eta = \eta_{\infty} + \frac{\eta_0 - \eta_{\infty}}{1 + \alpha \dot{\gamma}^{\frac{2}{3}}} \quad (7-3)$$

where  $\eta_{\infty}$ (pas-sec) is the viscosity at infinite shear rate,  $\dot{\gamma}$ (sec<sup>-1</sup>) is the shear rate and  $\alpha$  is a constant.

Also, when the data from a capillary viscometer are available, a plot of  $\log(Q/(\pi R^3 \tau_w))$  versus  $\tau_w$ , where  $Q$ (m<sup>3</sup>/sec) = flow rate,  $R$  = capillary radius (m) will be a straight line at low shear rates. For this range we can assume (Spencer and Dillon 1948, 1949)

$$\frac{1}{4\eta_0} = \frac{Q}{\pi R^3 \tau_w} \quad (7-4)$$

Therefore, by plotting  $\log(Q/(\pi R^3 \tau_w))$  as a function of  $\tau_w$ , and extrapolating to zero  $\tau_w$  (equivalent to very low shear rates), the value of  $(Q/(\pi R^3 \tau_w))$  appropriate for equation (7-4) can be determined and  $\eta_0$  estimated. In this work, the above mentioned procedure and method 3 (assuming that  $\eta_{\infty}$  is negligible) were used to estimate the zero shear rate viscosities of different black liquors. The results using the two methods do agree with together, however method 3 gives straight lines over the wide range of shear rate and this method appears to be better. Some of the results have been summarized in Table (7-1). Comparison of estimates of  $\eta_0$  agree with direct measurement within 8% for these liquors.

### 7.5 Glass Transition Temperature of Kraft Black Liquors

Because of the particular importance of glass transition temperature in modeling the zero shear viscosity data, it is worthwhile to discuss this. The freezing point and glass transition phenomena in kraft black liquors was studied by Masse (1984, 1986) and Fricke (1985) using Differential Scanning Calorimetry (DSC). They were able to illustrate that black liquor behaves qualitatively in a manner similar to Polystyrene-Benzene and Polyvinylpyrrolidone-water systems, i.e., it behaves as a polymer-solvent system with water as the principle solvent (Fricke 1987). They observed that there exist a particular concentration ( $\sim 50\%$ ) at which the phenomenon occurring changes from freezing to glass transition. At lower solids, the black liquor solutions exhibit freezing of the liquor, while at high solids concentrations, the liquor undergoes a glass transition and there is no evidence of freezing. In this work we were interested in the glass transition temperature of black liquors at solids concentrations higher than 50% to model our Newtonian viscosity data. The measurements of  $T_g$  for four different black liquors were made using a differential scanning calorimeter. Figure (7-1) shows a composite plot of  $T_g$  as a function of solids concentrations for all liquors. As could be expected, the glass transition temperature is a function of solids concentrations. There is a small variation in  $T_g$  from liquor to liquor which is due to the lignin molecular weight and the amounts of the inorganics in the liquor. However at higher solids concentrations, the differences are more significant. Comparison of the results of this work with those for polymer-solvent systems show that black liquor can be treated as a binary

system of water and a compositionally complex solute with lignin as a main constituent. This was also mentioned earlier by Fricke (1985) and Masse (1984, 1986).

### 7.6 Influence of Temperature on Zero Shear Rate Viscosity

The Newtonian viscosity of four different kraft black liquors were determined at different solids concentrations using methods which were discussed earlier. The results are presented in Figures (7-2) through (7-5).

Several viscosity-temperature relationships can be found in the literature for black liquors at high solids concentrations. Wennberg (1985) used the free volume theory to model the viscosity data for black liquors. As it was discussed in chapter 5, the free volume approach takes into account the probability that there is an adjacent empty site into which a properly oriented unit can move. Using this theory, the Newtonian viscosity of liquids and polymer solutions can be described with equation(5-10):

$$\eta_o = A \exp\left(\frac{BT_o}{T - T_o}\right) \quad (7-5)$$

where T is the absolute temperature and  $T_o$  is the temperature at which the extrapolated conformational entropy and free volume of the liquid becomes zero. Parameter A is a constant and parameter B is related to the internal barriers to rotation of the main chain bonds in the polymer molecule (Miller 1963).

Wight *et al.* (1981) and Fricke (1985, 1987) have expressed the viscosity data for black liquors using the theory of absolute reaction rates or Arrhenius relationship. This equation was derived theoretically by the application of the absolute rate processes to viscous flow as it was mentioned in chapter 5 and can be written as

$$\eta_o = A \exp\left(\frac{E}{RT}\right) \quad (7-6)$$

where R is the gas constant and E is the activation energy for flow and can be defined as

$$E = R \frac{d \log_e \eta_o}{d\left(\frac{1}{T}\right)} \quad (7-7)$$

Equation (7-6) predicts that a plot of  $\log_e \eta_o$  as a function of  $1/T$  should yield a straight line of slope  $E/R$ .

Some investigators (e.g., Wennberg 1985 and Söderhjelm 1986) have used empirical correlations to express viscosity-temperature relationships for concentrated black liquors. Most of them have used  $T^x$  instead of  $T$  in equation (7-6) which however do not have a theoretical basis.

From the plots of  $\log \eta_o$  versus  $1/T$  it can be observed that over the narrow ranges of temperature, the plots are linear and it seems that either equation (7-5) or (7-6) can be used to fit the experimental data. However, over wide ranges of temperature, the plots are nonlinear and both equations fail to express the viscosity-temperature relationship. For this reason, many workers have used the combination of the absolute reaction rates and free volume concepts to express the Newtonian

viscosity of liquids and polymer solutions. However from chapter 5, the final combined expression is

$$\eta_o = A T^{0.5} \exp\left(\frac{B}{T} + \frac{CT_o}{T-T_o}\right) \quad (7-8)$$

where  $B=E_v/R$ ,  $E_v$  is the activation energy for flow at constant volume and  $A$  and  $C$  are constants.

The temperature at which the free volume becomes zero is  $T_o$  and is related to the glass transition temperature,  $T_g$ , of the material. Free volume theory predicts that, for polymers  $T_o$  appears to be about 50 °C below their glass transition temperature (Ferry 1980). With this approach, we fitted our data with equation (7-8) using SAS statistics nonlinear data fitting. We observed that the correlation coefficient for all the liquors is above 0.999, but that the values of  $B$ , which are related to the activation energy for flow, were negative at several concentrations. Two important factors must be considered regarding  $B$ : 1)  $B$  must be a positive number as can be observed from the slopes of  $\log \eta_o$  as a function of  $1/T$  plots and 2)  $B$  should increase as the solids concentration of a particular black liquor increases. Considering these two factors, we varied  $T_o$  as a function of  $T_g$  for each liquor at different solids concentrations. The best fits were obtained at  $T_o \approx 1.3 T_g$ . The resulting values of  $A$ ,  $B$ , and  $C$  have been summarized in Table (7-2). As it can be observed,  $R^2 \geq 0.998$  for all the liquors and the values of  $B$  which are related to the activation energy for flow are positive and are an increasing function of the solids concentrations. The constants for each liquor are concentration dependent and we

tried to determine consistent relationships for constants as a function of solids concentrations. The results will be discussed later.

### 7.7 Results and Discussion

The model based on the combination of the absolute reaction rate and free volume theories is a four constant model,  $A$ ,  $B$ ,  $C$  and  $T_0$  with  $B$  related to the activation energy for flow and  $T_0$  related to the glass transition temperature. The model yields highly accurate results and can be used to correlate the Newtonian viscosity of the concentrated black liquors at different temperatures at a fixed concentration. This equation could be arranged such that

$$A = \exp(a_1 + b_1 S) \quad (7-9)$$

for all liquors of one species. For the liquors used in this study  $A$  may be written as

$$A = \exp(11.824 - 52.456 S) \quad (7-10)$$

The value of  $A$  can be replaced in equation (5-8) and the values of  $B$  and  $C$  can be redetermined for each liquor at different solids concentration. The new values of  $B$ ,  $C$ , and  $R^2$  for each liquor have been summarized in Table (7-3). Figures (7-6) and (7-7) represent  $B$  and  $C$  as a function of solids concentration for each liquor. As can be observed,  $B$  for each liquor may be written as

$$B = a_2 + b_2 S \quad (7-11)$$

and the constant  $C$  for a single liquor can be fitted with polynomials.

However,  $a_2$  and  $b_2$  can be determined for each liquor and  $C$  can be fitted with polynomials and replaced in equation (7-8) which then can be used to calculate the Newtonian viscosity of the corresponding liquor at any temperature or concentration. However in this approach, the final model for viscosity involves at least seven parameters in addition to  $T_0$ . Figure (7-8) shows that the constant  $B$  at a specific solids concentration for all the liquors are very close together and one may assume that the dependency of  $B$  on the solids composition is negligible. However, in order to have more accurate results, we recommend that the constants  $a_2$  and  $b_2$  be calculated for every single liquor. Figure (7-9) shows that the constant  $C$  is a strong function of the solids concentration and solids composition.

### 7.8 Comparison with Previous Work

An empirical correlation was suggested in our earlier work (Zaman and Fricke 1991) to correlate the zero shear rate viscosities to temperature and solids concentrations, which was

$$\log_e \eta_0 = \sum_{i=0}^n g_i \left[ \left( \frac{S}{S+1} \right) \frac{1}{T} \right]^i \quad (7-12)$$

where

$S$  = mass fraction solids,

$T$  = temperature (K),

$g_i$  = empirical constants.

In order to investigate the validity of this correlation for other black liquors, in this

work, the zero shear rate viscosities for three different black liquors were fitted by

$$\log_e \eta_o = g_o + g_1 \left[ \left( \frac{S}{S+1} \right) \frac{1}{T} \right] + g_2 \left[ \left( \frac{S}{S+1} \right) \frac{1}{T} \right]^2 \quad (7-13)$$

The values of  $g_o$ ,  $g_1$ ,  $g_2$ , and  $R^2$  for each liquor are (these values for liquor ABAFX011,12 are from our earlier work)

Black Liquor	$-g_o-$	$-g_1-$	$-g_2-$	$R^2$
ABAFX011,12	6.313	$-3.6679 \times 10^4$	$2.726 \times 10^7$	0.998
ABAFX013,14	22.125	$-7.4027 \times 10^4$	$4.961 \times 10^7$	0.998
ABAFX025,26	12.802	$-5.0235 \times 10^4$	$3.795 \times 10^7$	0.997
ABAFX043,44	9.572	$-4.8376 \times 10^4$	$3.477 \times 10^7$	0.998

Figures (7-8) through (7-11) represent the zero shear rate viscosities of these liquors as a function of the reduction variable  $[(S/(S+1))/T]$ . The liquors used in this study are from a  $2^4$  factorial designed pulping experiment. The liquors ABAFX011,12 and ABAFX025,26 are extremes and the liquor ABAFX043,44 is the center point of the design. However it can be expected that equation (7-13) will fit the experimental data for other liquors.

Figure (7-12) is a composite plot of zero shear rate viscosities as a function of the reduction variable  $[(S/(S+1))/T]$ . The zero shear rate viscosity of liquors ABAFX013,14 and ABAFX043,44 are considerably higher than liquors ABAFX011,12 and ABAFX025,26. The liquors can be categorized in two groups A, and B. Group A consist of liquors ABAFX011,12 and ABAFX025,26 and group B



consist of liquors ABAFX013,14 and ABAFX043,44. For each group, there is a region where the zero shear rate viscosities are very close together. Below this region, liquor ABAFX043,44 is more viscous than liquors ABAFX013,14, ABAFX011,12 and ABAFX025,26. These region corresponds to lower solids concentrations and higher temperatures. Probably in this range, the viscosity is dominated by the lignin molecular weight. The weight average molecular weight of lignin in liquor ABAFX043,44 is higher than liquors ABAFX013,14, ABAFX011,12 and ABAFX025,26 respectively (Schmidl 1992 by GPC). Above this region, liquor ABAFX013,14 is more viscous than liquors ABAFX043,44, ABAFX025,26 and ABAFX011,12 respectively. The lignin concentration in liquor ABAFX013,14 is higher than liquors ABAFX043,44, ABAFX025,26 and ABAFX011,12 respectively. In this range, the zero shear rate viscosities are probably dominated by the lignin concentration in the liquors. However, the zero shear rate viscosities for a single liquor are not only affected by the lignin molecular weight and lignin concentration, but also by other organic and inorganic components.

In order to compare the results of equation (7-8) and equation (7-13), B and C for liquors ABAFX013,14 and ABAFX025,26 were fitted with polynomials and replaced in equation (7-8). Then the zero shear rate viscosities were calculated at different temperatures and solids concentrations using equations (7-8) and (7-12) for these two liquors. The results are summarized in Tables (7-4) and (7-5).

Comparison of the results show that both methods can be used to estimate the Newtonian viscosity of the liquors within  $\pm 20\%$  range, however, equation (7-13) is

easier to use and the degree of its accuracy can be increased by using higher order polynomials. Equation (7-8) gives highly accurate results ( $\pm 5\%$  error) for a single liquor at a specific concentration over a wide range of temperature without using the generalized approach.

### 7.9 Conclusions

At high solids concentrations ( $> 50\%$ ), black liquor can be treated as a polymer continuous material and theories for polymer melts can be applied to concentrated liquors. The relationship between the Newtonian viscosity and temperature can be expressed by using the combination of the absolute reaction rates and free volume concepts. This model can be used to extrapolate over wide ranges of temperature at a fixed concentration and the results are highly accurate. Equation (7-8) can be used to obtain a general correlation for viscosity of a single liquor as a function of temperature and solids concentrations, but the method is difficult and time consuming. Further application of our previous model has been investigated and it appears that this model can be used to express the Newtonian viscosity of all liquors as a function of solids concentration and temperature. The zero shear rate viscosities can be estimated by using this model over wide ranges of temperature and concentration with very good accuracy. This is more practical, less time consuming, and easier to use, although it does not have a theoretical basis. The constants  $g_0, g_1, g_2, \dots, g_n$  can be correlated empirically with solids composition and pulping conditions which require the determination (measurement) of the Newtonian viscosity for all the

liquors of single species. As it can be observed, the viscosity is not only a function of temperature and solids concentration, but will vary from liquor to liquor which is due to the solids composition and lignin molecular weight in every liquor.

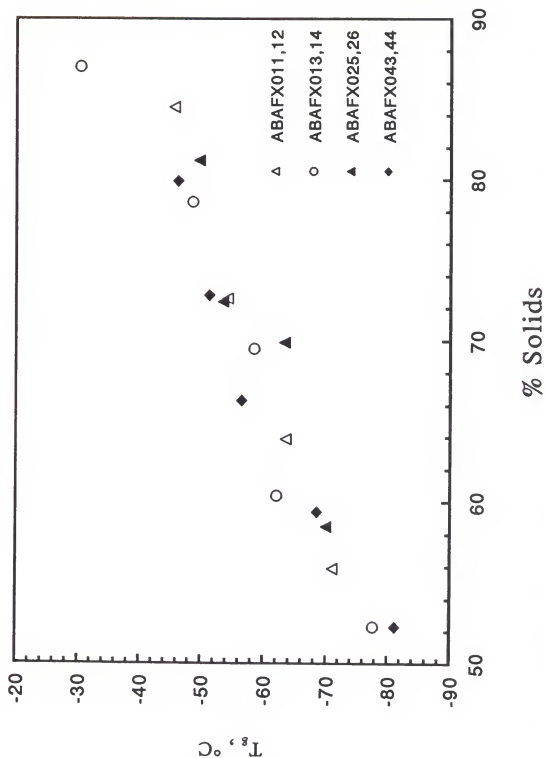


Figure (7-1): Glass Transition Temperature as a Function of Solids Concentration for Different Black Liquors.

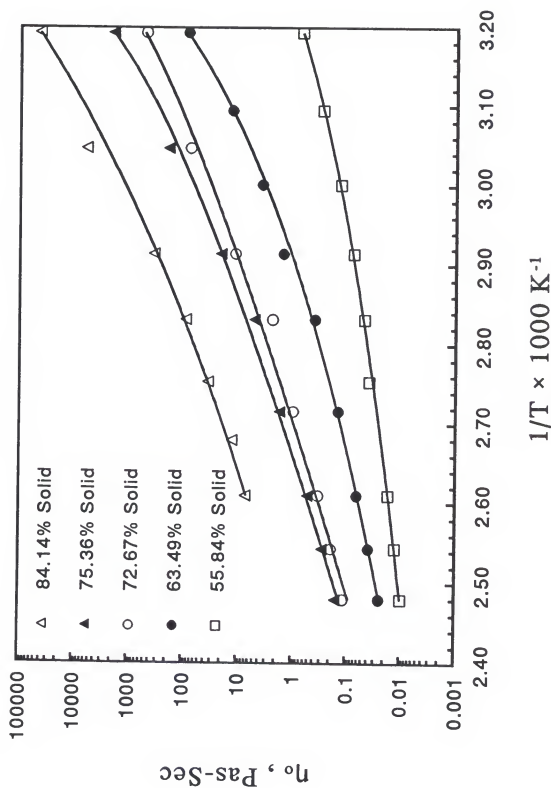


Figure (7-2): Effect of Temperature on Zero Shear Rate Viscosity of Black Liquor ABAPX011,12.

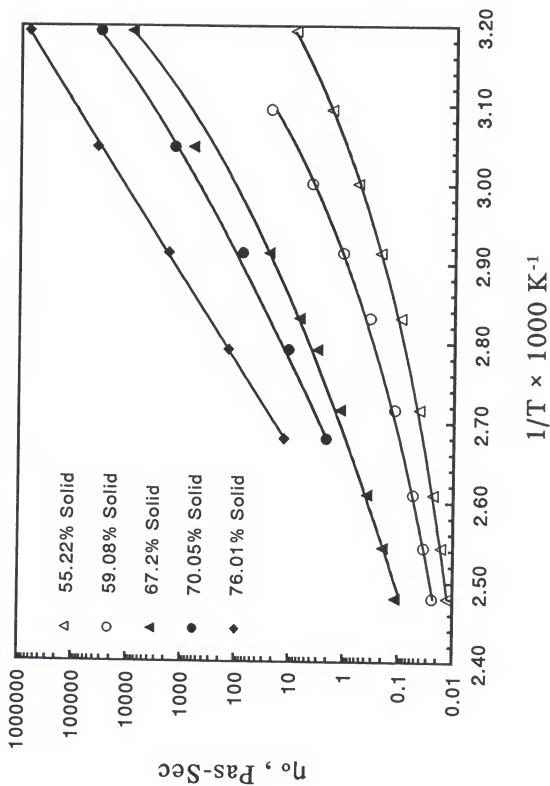


Figure (7-3): Effect of Temperature on Zero Shear Rate Viscosity of Black Liquor ABAFX013,14.

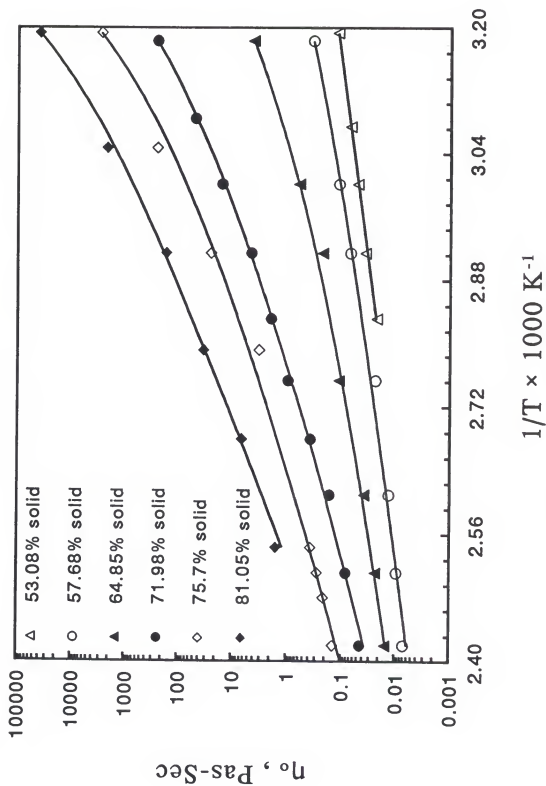


Figure (7-4): Effect of Temperature on Zero Shear Rate Viscosity of Black Liquor ABAFX025,26.

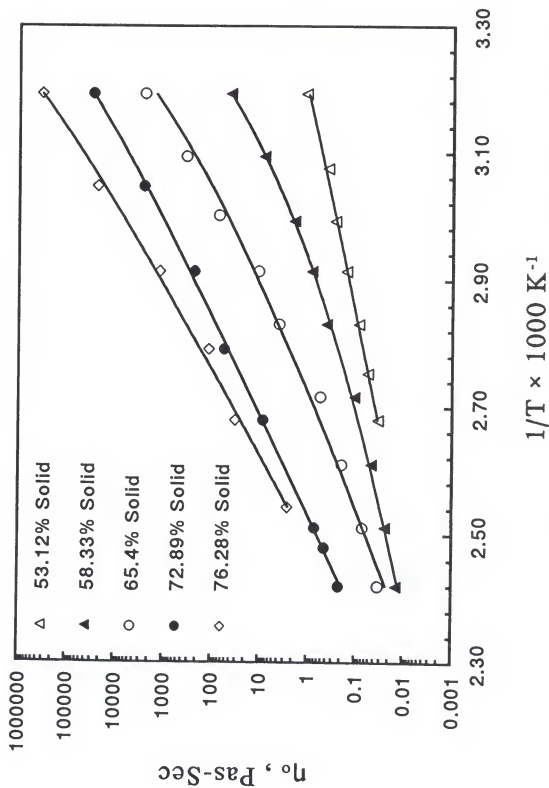


Figure (7-5): Effect of Temperature on Zero Shear Rate Viscosity of Black Liquor ABAFX043,44.



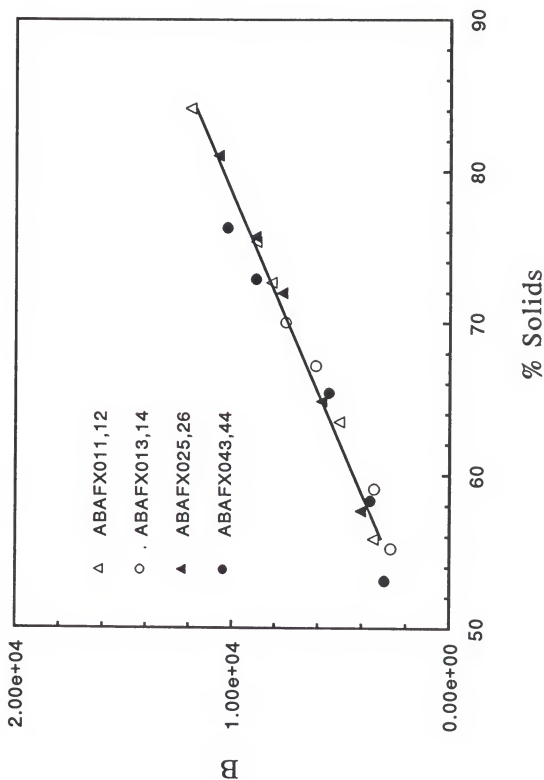


Figure (7-6): B as in Equation (7-8) for Different Black Liquors with A Considered as a Universal Constant.

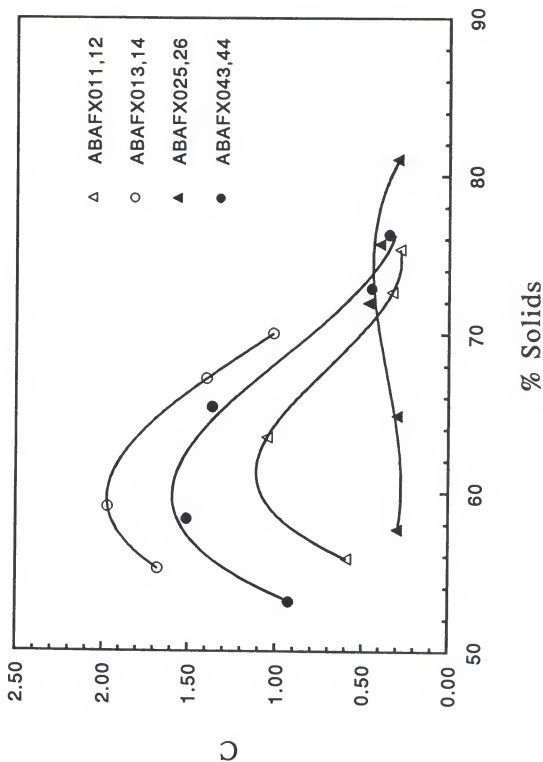


Figure (7-7):  $C$  as in Equation (7-8) for Different Black Liquors with  $A$  Considered as a Universal Constant.

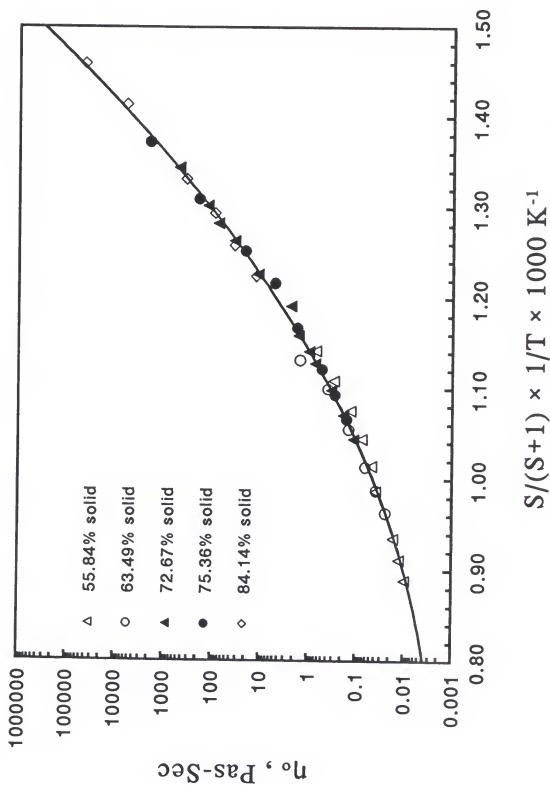


Figure (7-8): Reduced Plot of Zero Shear Rate Viscosity for Black Liquor ABAFX011,12.

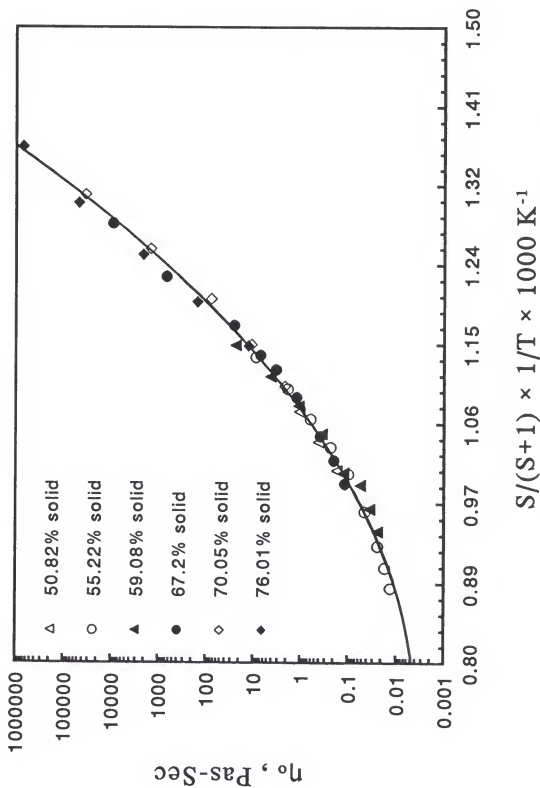


Figure (7-9): Reduced Plot of Zero Shear Rate Viscosity for Black Liquor ABAFX013,14.

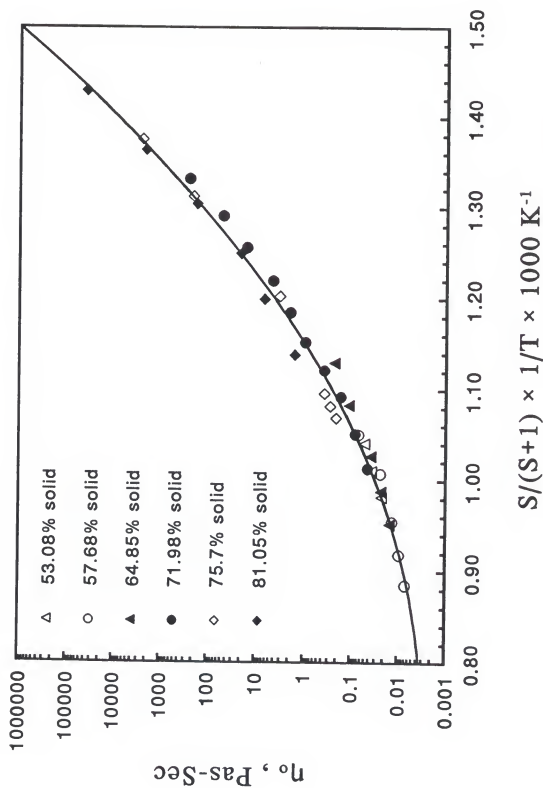


Figure (7-10): Reduced Plot of Zero Shear Rate Viscosity for Black Liquor ABAFX025,26.

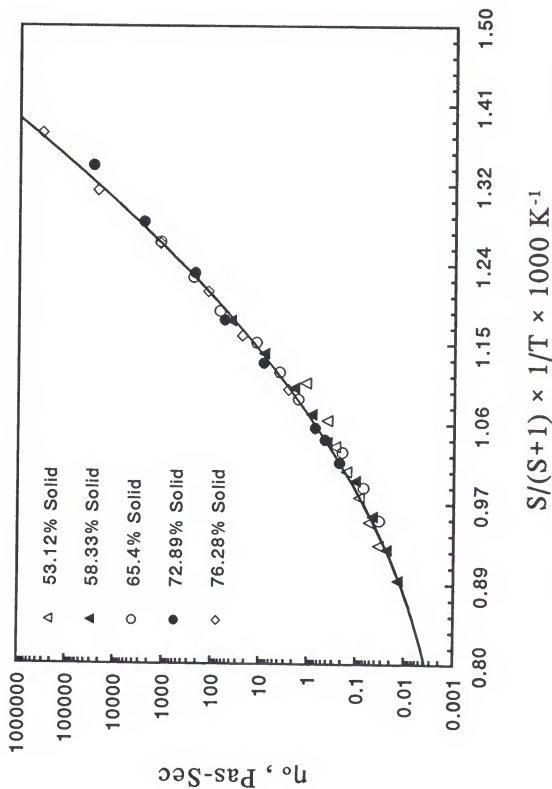


Figure (7-11): Reduced Plot of Zero Shear Rate Viscosity for Black Liquor ABAFX043,44.

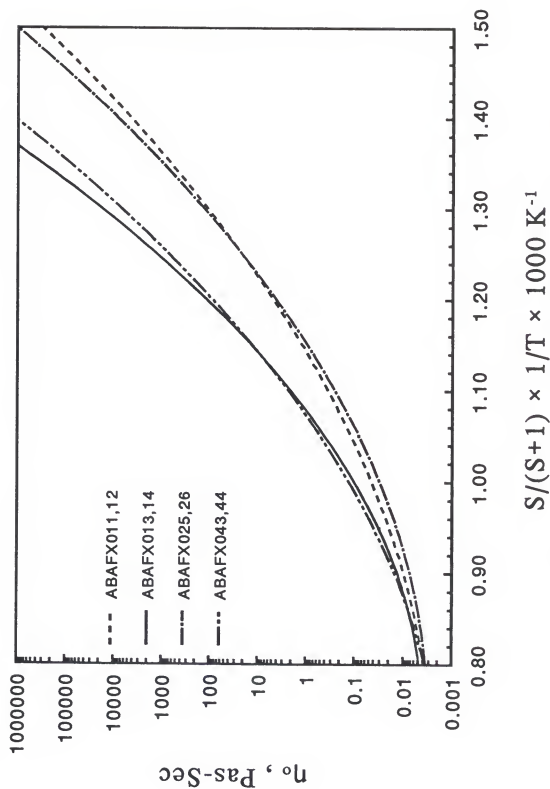


Figure (7-12): Reduced Plot of Zero Shear Rate Viscosity for Different Black Liquors.

Table (7-1): Comparison Between the Calculated and Measured Newtonian Viscosity of Different Black Liquors at Different Temperatures.

Liquor	% Solids	Temperature , K	Calculated $\eta_{\infty}$ Pas-Sec	Measured $\eta_{\infty}$ Pas-Sec	% Error
ABAFX013,14	76.01	313.16	709664	700060	-1.4
ABAFX013,14	76.01	328.16	47883.77	49774.0	-3.8
ABAFX013,14	76.01	343.16	2073.12	2068.9	0.2
ABAFX013,14	76.01	358.16	152.07	150.43	1.1
ABAFX025,26	81.05	313.16	39134.51	40033	-2.25
ABAFX025,26	81.05	328.16	2104.74	2219	-5.2
ABAFX025,26	81.05	343.16	172.38	168.74	2.2
ABAFX043,44	76.28	313.16	323481.4	308060	5
ABAFX043,44	76.28	328.16	22879.35	22990	-0.5
ABAFX043,44	76.28	343.16	1191.44	1200	-0.71
ABAFX043,44	76.28	358.16	121.63	114.68	6.0



Table (7-2): Constants A, B, and C as given in Equation (7-8) for Different Black Liquors at Different Solids Concentrations.

Liquor	% Solids	A	B	C	R <sup>2</sup>
ABAFX011,12	55.84	$2.526 \times 10^{-7}$	2436.19	0.825	0.998
ABAFX011,12	63.49	$2.810 \times 10^{-9}$	4233.92	1.188	0.999
ABAFX011,12	72.67	$4.101 \times 10^{-14}$	10057.0	0.1931	0.999
ABAFX011,12	75.36	$4.380 \times 10^{-14}$	10154.0	0.220	1.0
ABAFX011,12	84.14	$1.840 \times 10^{-15}$	12549.0	0.0102	1.0
ABAFX013,14	55.22	$3.188 \times 10^{-6}$	560.29	2.202	1.0
ABAFX013,14	59.10	$4.158 \times 10^{-7}$	1375.1	2.40	1.0
ABAFX013,14	67.20	$9.311 \times 10^{-13}$	8001.56	1.161	1.0
ABAFX013,14	70.05	$7.70 \times 10^{-13}$	8788.95	0.896	0.999
ABAFX025,26	57.68	$6.70 \times 10^{-9}$	4210.123	0.2782	1.0
ABAFX025,26	64.85	$8.70 \times 10^{-9}$	4246.69	0.530	1.0
ABAFX025,26	71.98	$4.98 \times 10^{-12}$	7732.1	0.465	1.0
ABAFX025,26	75.70	$8.265 \times 10^{-12}$	7973.1	0.484	0.999
ABAFX025,26	81.05	$2.152 \times 10^{-15}$	11891.0	0.2475	1.0
ABAFX043,44	58.33	$1.877 \times 10^{-9}$	4256.41	1.369	0.999
ABAFX043,44	65.40	$1.10 \times 10^{-15}$	11044.0	0.446	1.0
ABAFX043,44	72.89	$5.44 \times 10^{-18}$	14425.0	0.0879	1.0
ABAFX043,44	76.28	$3.45 \times 10^{-20}$	16701.0	0.0882	1.0

Table (7-3): Constants B and C, as in Equation (7-8) for Different Black Liquors with A Considered as a Universal Constant.

Liquor	% Solids	B	C	R <sup>2</sup>
ABAFX011,12	55.84	3492.654	0.5931	1.0
ABAFX011,12	63.49	5054.503	1.053	1.0
ABAFX011,12	72.67	8192.80	0.3312	1.0
ABAFX011,12	75.36	8913.41	0.2862	1.0
ABAFX011,12	84.14	11966.0	0.0117	1.0
ABAFX013,14	55.22	2688.134	1.676	1.0
ABAFX013,14	59.10	3444.96	1.970	1.0
ABAFX013,14	67.20	6131.19	1.396	1.0
ABAFX013,14	70.05	7522.10	1.017	1.0
ABAFX025,26	57.68	4056.74	0.298	1.0
ABAFX025,26	64.85	5868.20	0.30	1.0
ABAFX025,26	71.98	7699.20	0.468	1.0
ABAFX025,26	75.70	8950.34	0.404	1.0
ABAFX025,26	81.05	10680.0	0.3023	1.0
ABAFX043,44	58.33	3627.04	1.51	1.0
ABAFX043,44	65.40	5526.45	1.364	1.0
ABAFX043,44	72.89	8908.83	0.451	1.0
ABAFX043,44	76.28	10250.0	0.3495	1.0

Table (7-4): Comparison Between the Calculated and Measured Zero Shear Rate Viscosity of Black Liquor ABAFX013,14.

% Solids	T , K	$\eta_{\infty}$ calculated by (7-8)	$\eta_{\infty}$ calculated by (7-12)	$\eta_{\infty}$ measured pas-sec
0.5908	323.16	19.281	21.117	23.81
0.5908	333.16	4.133	3.9	4.212
0.5908	343.16	1.23	1.124	1.1
0.5908	353.16	0.38	0.39	0.35
0.5908	368.16	0.138	0.127	0.122
0.5908	383.16	0.053	0.049	0.055
0.5908	393.16	0.031	0.029	0.035
0.5908	403.16	0.019	0.019	0.024
0.7005	313.16	32718.53	35821.0	33470.0
0.7005	343.16	77.272	95.0	86.55
0.7005	358.16	13.44	13.0	13.8
0.7005	373.16	2.80	2.37	2.133

Table (7-5): Comparison Between the Calculated and Measured Zero Shear Rate Viscosity of Black Liquor ABAFX025,26.

% Solids	T , K	$\eta_{00}$ calculated by (7-8)	$\eta_{00}$ calculated by (7-12)	$\eta_{00}$ measured pas-sec
0.757	313.16	3478.0	3060.68	3478.1
0.757	328.16	179.70	200.3	179.665
0.757	343.16	25.312	25.914	25.312
0.757	358.16	5.485	5.1	5.5
0.757	393.16	0.353	0.28	0.353
0.757	403.16	0.184	0.15	0.184
0.8105	313.16	35358.93	32096.25	30647.79
0.8105	343.16	155.02	156.487	172.38
0.8105	358.16	29.111	28.303	33.10
0.8105	373.16	7.02	6.08	6.6
0.8105	393.16	1.36	1.26	1.56

## CHAPTER 8 VISCOELASTIC PROPERTIES OF HIGH SOLIDS KRAFT BLACK LIQUORS

### 8.1 Introduction

Within the extremes of purely viscous and purely elastic behavior we encounter viscoelastic materials. The idea of elasticity was developed by Hooke in 1678 and the idea of viscosity (viscous response) was introduced by Isaac Newton in 1687. The governing equations for a Newtonian viscous liquid were developed by Navier and Stokes in the nineteenth century. The work of many investigators show that, in all materials, both viscous and elastic properties coexist. The particular response of a typical sample in any experiment depends on the time-scale of the experiment in relation to a natural time of the material (e.g, Ferry 1980 and Bird *et al.* 1987). If the experiment is relatively slow, the sample will appear to be viscous rather than elastic; if the experiment is relatively fast, it will appear to be elastic rather than viscous. At moderate time scales, viscoelastic response will be observed. Depending on the externally applied deformations or stresses, the viscoelastic material may exhibit properties which are either solely functions of time or of time and the magnitude of the externally applied stresses (or deformations). The first type of behavior is called linear viscoelasticity, while the latter falls within the domain of nonlinear viscoelasticity.

For a purely viscous material all internal stresses are only a function of the rate of strain (shear rate). Conversely, a purely elastic material develops stresses that are only a function of the instantaneous strain. For a viscoelastic material, internal stresses are not only a function of strain and strain rate, but also depend upon the entire past history of deformation. The most recent past history is more important than more distant history, so a viscoelastic material can be described as having a fading memory. The differences in the mechanical behavior of the material are more evident in unsteady, or time dependent, situations.

The determination of the linear viscoelastic response of the material is necessary for quality control of industrial products, and to determine the effects of molecular structure of the material on their viscoelastic response. Also, several attempts have been made to find an analogy between the shear viscosity and the corresponding dynamic viscosity under linear viscoelastic conditions. Measuring the shear viscosity is difficult at high shear rates due to viscous heating, while the dynamic viscosity is easier to measure (Dyson 1970 and Barnes *et al.* 1989).

### 8.2 Small Amplitude Oscillatory Shear Flow

A common method of studying the mechanical properties of viscoelastic material is to determine their response to an oscillatory stress or strain input. The simplest type of viscoelastic behavior is linear viscoelasticity, which can be observed if the amplitude of the oscillation is sufficiently small so that the molecules of the material are disturbed from their equilibrium configuration to a negligible extent.

The theoretical and experimental aspects of linear viscoelasticity have been studied by many investigators (e.g, Gross 1965, Carreau et al. 1968, Ferry 1980, Vinogradove and Malkin 1980, Pearson and Rochefort 1982, Lynn 1983, Bird et al. 1987, Greener and Connelly 1986, and Berger and Meissner 1992) and the basic equations for linear viscoelasticity can be found in most of the viscoelastic textbooks.

Suppose that the material is subjected to a sinusoidal shearing strain between two parallel plates of area  $A$  and a gap height  $H$  as shown in Figure 8-1. The area of the plates is large compared to the gap height  $H$  and the bottom plate oscillates with frequency  $\omega$  in its own plane in the  $x$  direction.

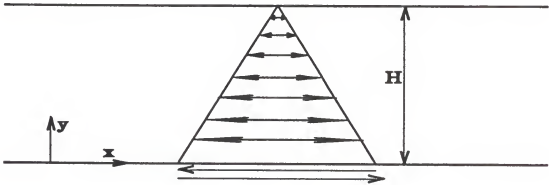


Figure 8-1. Small Amplitude Oscillatory Shear Flow Between Two Parallel Plates

The velocity profile will be nearly linear in  $y$  if  $\omega \rho H / 2\eta_0 \ll 1$  (Bird et al. 1987),  $\rho$  and  $\eta_0$  are density and zero shear rate viscosity of the fluid, respectively. The shear strain varies sinusoidally with time and can be defined as

$$\gamma_{yx}(\omega) = \gamma_{yx}^0 \sin(\omega t) \quad (8-1)$$

and the rate of strain is

$$\dot{\gamma}_{yx}(\omega) = \gamma_{yx}^0 \omega \cos(\omega t) = \dot{\gamma}_{yx}^0 \cos(\omega t) \quad (8-2)$$

For a linear elastic material (i.e., Hookean), the shear stress will be in phase with the shear strain (Bird et al., 1987), therefore,

$$\tau_{yx}(\omega) = G \gamma_{yx}(\omega) = G \gamma_{yx}^0 \sin(\omega t) \quad (8-3)$$

where  $G$  is the relaxation modulus.

For a Newtonian (linearly viscous) fluid, the stress is proportional to the rate of strain (shear rate) and

$$\tau_{yx}(\omega) = \mu \dot{\gamma}_{yx}(\omega) = \mu \dot{\gamma}_{yx}^0 \cos(\omega t) = \mu \dot{\gamma}_{yx}^0 \sin(\omega t + \alpha) \quad (8-4)$$

where  $\alpha = \pi/2$ . The phase shift,  $\alpha$ , between the shear stress and shear strain for viscoelastic material is expected to be between  $0^\circ$  and  $90^\circ$  (Lodge 1964).

A convenient means of manipulating oscillatory quantities is in terms of their complex equivalents; hence, oscillatory strain and stress can be written as (Darby 1976)

$$\gamma_{yx}(\omega) = \gamma_{yx}^0 \exp(i\omega t) = \gamma_{yx}^0 [\cos(\omega t) + i\sin(\omega t)] = \gamma'(\omega) + i\gamma''(\omega) \quad (8-5)$$

$$\tau_{yx}(\omega) = \tau_{yx}^0 \exp[i(\omega t + \alpha)] = \tau_{yx}^0 [\cos(\omega t + \alpha) + i\sin(\omega t + \alpha)] = \tau'_{yx}(\omega) + i\tau''_{yx}(\omega) \quad (8-6)$$

where  $\tau'_{yx}$  and  $\gamma'_{yx}$  are the amplitude of stress and strain and  $\alpha$  is the phase angle between them. The material functions, complex shear modulus and complex viscosity, can be defined in terms of oscillatory stress, strain and the rate of strain (shear rate).



The complex shear modulus,  $G^*$ , can be defined as the ratio of stress to strain:

$$G^* = \frac{\tau_{yx}(\omega)}{\gamma_{yx}(\omega)} = \frac{\tau_{yx}^0}{\gamma_{yx}^0} \exp(i\alpha) = \frac{\tau_{yx}^0}{\gamma_{yx}^0} (\cos \alpha + i \sin \alpha) = G' + iG'' \quad (8-7)$$

where

$$G' = \frac{\tau_{yx}^0}{\gamma_{yx}^0} \cos \alpha \quad (8-8)$$

$$G'' = \frac{\tau_{yx}^0}{\gamma_{yx}^0} \sin \alpha \quad (8-9)$$

The tangent of the phase angle,  $\alpha$ , is called the loss tangent, and is equal to

$$\tan \alpha = G''/G' = \tau''/\tau'$$

The magnitude of the complex modulus gives an indication of the total energy required to deform a material, and can be defined as

$$|G^*| = [(G')^2 + (G'')^2]^{0.5} \quad (8-10)$$

The "in-phase" component,  $G'$ , is called the storage modulus, and it is a measure of the energy stored and recovered per cycle, when different systems are compared at the same strain amplitude (Ferry 1980). The "out-of-phase" component,  $G''$ , represents the viscous character of the material, and is called the loss modulus. It is a measure of the energy dissipated, or lost, as heat per cycle of sinusoidal deformation, when different systems are compared at the same strain amplitude (Ferry 1980).

From equations (8-2) and (8-4) it can be seen that, for a Newtonian fluid,

$$G^* = \frac{\tau_{yx}(\omega)}{\gamma_{yx}(\omega)} = \mu \frac{\dot{\gamma}_{yx}(\omega)}{\gamma_{yx}(\omega)} = i\mu\omega \quad (8-11)$$

or  $G' = 0$ ,  $G'' = \mu\omega$  and  $\alpha = 90^\circ$ . For a linear elastic solid, equations (8-1) and (8-3) give

$$G^* = \frac{\tau_{yx}(\omega)}{\gamma_{yx}(\omega)} = \frac{G\gamma_{yx}(\omega)}{\gamma_{yx}(\omega)} = G \quad (8-12)$$

or  $G' = G$ ,  $G'' = 0$  and  $\alpha = 0^\circ$ . For viscoelastic materials, both  $G'$  and  $G''$  will be nonzero, and, in general, are functions of frequency.

The complex viscosity,  $\eta^*$ , which is more appropriate for fluids, is defined in terms of stress and the rate of strain (shear rate):

$$\eta^*(\omega) = \frac{\tau_{yx}(\omega)}{\dot{\gamma}_{yx}(\omega)} = \frac{\tau_{yx}(\omega)}{i\omega\gamma_{yx}(\omega)} = \eta'(\omega) - i\eta''(\omega) \quad (8-13)$$

where  $\eta'$  represents the in-phase or viscous component between stress and strain rate. It is associated with energy dissipation in the fluid, and it is called the dynamic viscosity. The imaginary part of the complex viscosity,  $\eta''$ , represents the elastic or "out of phase" component, and it is associated with energy storage in the fluid. From equation (8-4) it can be seen that, for a Newtonian fluid,  $\eta' = \mu$  and  $\eta'' = 0$ . The two material functions,  $\eta'$  and  $\eta''$ , are often called linear viscoelastic functions. These components can be related to those of complex modulus by combining equations (8-12) and (8-13)

$$\eta^* = \frac{G^*}{i\omega} \quad (8-14)$$

$$\eta' - i\eta'' = \frac{G' + iG''}{i\omega} = \frac{G''}{\omega} - i\frac{G'}{\omega} \quad (8-15)$$

or  $\eta' = G''/\omega$  and  $\eta'' = G'/\omega$

Small amplitude oscillatory shear experiments can be performed using a cone-and-plate or parallel plate rheometer. High solids black liquors have the potential for salt precipitation, and the presence of salt crystals in the liquor would cause erroneous results if the diameter of the particles are near the gap height of the selected geometry (Wight 1985). For this reason, the parallel plate geometry was used with gap heights of 0.15-0.05 cm instead of the cone-and-plate geometry, which has a minimum gap height of 50  $\mu\text{m}$ .

### 8.3 The Parallel-plate Geometry in Oscillatory Shear Flow

The parallel-plate system, sketched schematically in Figure 8-2, is used for measuring rheological properties of fluids( e.g, Walters 1975, Keentok and Tanner 1982, Connelly and Greener 1985). The sample is placed between two parallel plates of radius R separated by a gap size H, one of which is oscillating in the  $\theta$  direction sinusoidally with a frequency  $\omega$  and angular amplitude  $\theta^\circ$ , while the other one is stationary. The time-dependent torque which is required to maintain the stationary position of the plate is measured. The motion of the oscillating plate can be given by the angular displacement,  $\theta$ , as a function of the time,  $t$  (Bird et al. 1987).

$$\theta = \theta^0 \sin \omega t$$

(8-16)

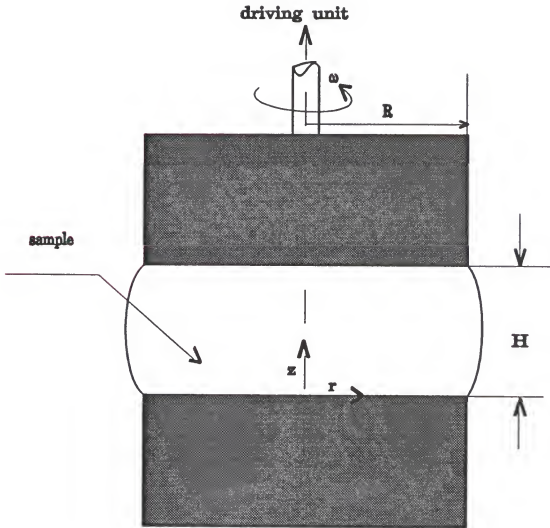


Figure 8-2. The Parallel-Plate System

As previously mentioned, the velocity profile in the gap between plates will be very nearly linear if  $\omega \rho H / 2\eta_0 < 1$  (Bird et al. 1987). The total torque,  $T$ , required to hold the other plate stationary also varies sinusoidally at the same frequency,  $\omega$ , but with a phase shift,  $\alpha$ , as

$$T(\omega) = T^0 \sin(\omega t + \alpha) \quad (8-17)$$

The rate of strain (shear rate) is proportional to  $\theta$ , and can be written as

$$\dot{\gamma}(\omega) = \frac{\theta^0 r \sin \omega t}{H} \quad (8-18)$$

and

$$\eta^*(\omega) = \eta' - i\eta'' = \frac{\tau(\omega)}{\dot{\gamma}(\omega)} \quad (8-19)$$

The real and imaginary parts of the complex viscosity for the parallel plate geometry can be calculated from (Wight 1985, Fricke 1987)

$$\eta'(\omega) = \frac{T^0 H \sin \alpha}{(2\pi R^4 \theta^0 \omega)} \left[ 3 + \frac{d \log_e \left( \frac{T^0 \sin \alpha}{2\pi R^3} \right)}{d \log_e \left( \frac{R \theta^0 \omega}{H} \right)} \right] \quad (8-20)$$

$$\eta''(\omega) = \frac{T^0 H \cos \alpha}{(2\pi R^4 \theta^0 \omega)} \left[ 3 + \frac{d \log_e \left( \frac{T^0 \sin \alpha}{2\pi R^3} \right)}{d \log_e \left( \frac{R \theta^0 \omega}{H} \right)} \right] \quad (8-21)$$

If  $\theta^0 \ll 1$ , equations (8-20) and (8-21) can be written as (Bird et al. 1987)

$$\eta'(\omega) = \frac{2HT^0 \sin \alpha}{\pi R^4 \omega \theta^0} \quad (8-22)$$

$$\eta''(\omega) = \frac{2HT^0 \cos \alpha}{\pi R^4 \omega \theta^0} \quad (8-23)$$

The assumptions used to drive the equations for a parallel-plate system are (Walter 1975)

1. the liquid inertia is neglected,
2. the free surface is cylindrical with radius  $R$ ,
3. edge effects and surface tension are neglected.

The derivative on the right hand side of equation (8-20) or (8-21) is the non-Newtonian correction to the stress (Bird *et al.* 1987). It originates from the inhomogeneity of the shear field in torsional flows (Connelly and Greener 1985). The surface tension of the liquid and the general shape of the interface at  $r=R$  are expected to have considerable effect on the apparent torque. Indeed, the two main failures in rotational rheometers, radial migration and surface fracture are associated with the dynamics of the interface at the rim. Radial migration will occur, if the centrifugal stress exceeds the surface tension stress,  $\sigma$  (Walter 1975, Connelly and Greener 1985):

$$\frac{3}{20} \rho \Omega^2 R^2 > \frac{\sigma}{H} \quad (8-24)$$

In terms of a critical shear rate, equation (8-24) can be written as (Connelly and Greener 1985)

$$\dot{\gamma}_c = \frac{1}{H} \sqrt{\frac{20\sigma}{3\rho H}} \quad (8-25)$$

This equation suggests that radial migration can be eliminated by using a small gap size and low speeds.

A viscoelastic material will develop a curved surface between the plates that would tend to stabilize the system with regard to the radial migration problem (Connelly and Greener 1985). Some of investigators (e.g. Hutton 1965 and 1969, Walters 1975, Tanner and Keentok 1983), observed that, above some critical speed, fracture at the interface of the rim occurs which is accompanied by a large drop in torque and normal stress. Tanner and Keentok (1983) have shown that the condition for fracture is

$$|N_2| > \frac{2\sigma}{3\beta} \quad (8-26)$$

where

$N_2$  = second normal stress difference,

$\beta$  = the size of the fracture (normally  $\alpha = O(H)$ ).

As pointed out by Connelly and Greener, the radial migration and fracture can be decreased if the gap size between the plates is reduced.

#### 8.4 Slip at the Wall of a Parallel-Plate Rheometer

The "no-slip" assumption at the wall of the system is not always valid for most of the fluids above a critical shear stress (Dealy and Wissbrun 1990). Wall slip for polymer solutions and polymer melts has been studied in detail and suitable methods for wall slip corrections has been suggested by several investigators (e.g. Yoshimura and Prud'homme 1988a and 1988b, Wein and Tovchigrechko 1992). At steady state operation the apparent viscosity can be significantly lower than the actual viscosity,

if slip occurs at the wall of the system. The more recent work on the calculation of wall slip velocities and fluid velocities in a parallel plate viscometer has been done by Yoshimura and Prud'homme (1988a, 1988b), for both steady state and dynamic oscillatory measurements. At steady state conditions, with a "no-slip" assumption, the apparent viscosity in a parallel plate system can be calculated from (Bird *et al.* 1987)

$$\eta(\dot{\gamma}_R) = \frac{\frac{T}{2\pi R^3}}{\dot{\gamma}_R} \left[ 3 + \frac{d \log_e \left( \frac{T}{2\pi R^3} \right)}{d \log_e (\dot{\gamma}_R)} \right] \quad (8-27)$$

where  $\tau_R$  and  $\dot{\gamma}_R$  are the stress and the rate of strain at the edge of the disk, respectively. Yoshimura and Prud'homme, by considering two different gap sizes, H1 and H2, presented the following equation for cases that the slip velocity,  $U_s$  is not negligible:

$$\eta(\dot{\gamma}_R) = \frac{\tau_R(H1 - H2)}{H1 \dot{\gamma}_{aR1}(\tau_R) - H2 \dot{\gamma}_{aR2}(\tau_R)} \quad (8-28)$$

where

$$\dot{\gamma}_{aR1}(\tau_R) = \dot{\gamma}_R(\tau_R) + \frac{2U_s(\tau_R)}{H1} \quad (8-29)$$

$$\dot{\gamma}_{aR2}(\tau_R) = \dot{\gamma}_R(\tau_R) + \frac{2U_s(\tau_R)}{H2} \quad (8-30)$$

From equations (8-29) and (8-30) it can be seen that



$$\dot{\gamma}_R(\tau_R) = \frac{H1 \dot{\gamma}_{aR1}(\tau_R) - H2 \dot{\gamma}_{aR2}(\tau_R)}{H1 - H2} \quad (8-31)$$

and

$$U_s(\tau_R) = \frac{\dot{\gamma}_{aR1}(\tau_R) - \dot{\gamma}_{aR2}(\tau_R)}{2\left(\frac{1}{H1} - \frac{1}{H2}\right)} \quad (8-32)$$

The shear stress at the edge of the disk for a gap size,  $H$ , can be calculated from

$$\tau_R = \frac{T}{2\pi R^3} \left[ 3 + \frac{d \log_e \left( \frac{T}{2\pi R^3} \right)}{d \log_e \dot{\gamma}_{aR}} \right] \quad (8-33)$$

where  $\dot{\gamma}_{Ar} = \Omega R/H$ . When  $\tau_R$  and  $\dot{\gamma}_{Ar}$  are available for gap sizes  $H1$  and  $H2$ ,  $\tau_R$  can be taken to be the independent variable and, therefore, have  $\dot{\gamma}_{aR1} = \dot{\gamma}_{aR1}(\tau_R)$  for gap height  $H1$  and  $\dot{\gamma}_{aR2} = \dot{\gamma}_{aR2}(\tau_R)$  for gap height  $H2$ .

Effects of wall slip on dynamic oscillatory shear measurements are less well understood. To date no general method can be found in the literature to account for the slip velocity for a parallel-plate system in oscillatory shear flows. The more recent work in this area has been done by Yoshimura and Prud'homme (1988a, 1988b). They considered a linear viscoelastic (Kelvin-Voight) material and derived the governing equations for three special cases: 1) the fluidity of the slip layer is constant; 2) the fluidity depends on stress; and 3) the fluidity is time dependent. The fluidity is defined as the ratio of the slip velocity to stress at the wall. Their goal was to see whether it was possible to determine from the shape of the waveform stress whether or not slip was occurring. For an oil-in-water emulsion with known dynamic

viscosity ( $\eta'$ ) and storage modulus ( $G'$ ), they found that 1) when the fluidity of the slip layer is constant, the presence of slip makes the fluid appear to be less elastic than it really is; 2) when the fluidity is stress dependent, the resulting stress waveforms are nonlinear (nonsinusoidal) and symmetric; and 3) for a time dependent fluidity, stress waveforms will be nonlinear and nonsymmetric, but the same type of stress response can result from nonlinear properties of the fluid at this condition, so we can not easily distinguish between the effects of slip and of fluid rheology. In another work, Yoshimura and Prud'homme (1987) have investigated the effect of yield stresses on dynamic oscillatory measurements in the absence of slip. They observed that the materials that show tendency to slip also will have tendency to display yield behavior. Therefore, nonlinear nonsymmetric wave forms of similar shape can result from slip or yielding, even for materials with linear rheological properties, and the shape of the stress waveform may not be an indication of the presence or absence of slip. They suggested that two different gap sizes be used at the same frequency and strain. If stress waveforms from both measurements are identical, then slip is not occurring and nonlinearities or phase shifts are due to the rheological properties of the fluid. If the waveforms are different, then slip is occurring. However, because of the stress and time dependency of slip, it is not possible to measure the viscoelastic properties of the material by using two different gap sizes, as can be done for steady shear in a parallel-plate system.

### 8.5 Dynamic Mechanical Testing

Small amplitude oscillatory shear experiments were carried out on a Rheometrics Mechanical Spectrometer (RMS-800), using a parallel-plate geometry for black liquors above 60% solids at a temperature range of 40 °C - 85 °C. The RMS has a torque motor which rotates the lower plate at a constant speed during the steady shear flow experiments. Also, the lower plate can oscillate during dynamic testing. The top disk is mounted on the bottom of a transducer which measures the torque and normal force. An IBM PC computer, connected to the system, is used to analyze the data. The gap height was generally in a range of 0.15 - 0.05 cm, depending upon the solids concentration of the sample and the temperature. Also, the plate diameters were varied, depending upon the solids concentration of the sample and the operating temperature. The ranges were

$$T \geq 70 \text{ }^{\circ}\text{C and solids} \leq 70\% \quad r=2.5 \text{ cm}$$

$$T < 70 \text{ }^{\circ}\text{C and all solid ranges} \quad r=1.25 \text{ cm}$$

$$\text{all temperature ranges and solids} > 75\% \quad r=1.25 \text{ cm}$$

In many cases, at high frequencies (i.e.,  $\geq 300$  rad/sec) we observed that, even though the torque values were well within the normal limits of the instrument, there was a sudden drop in torque values, which is probably due to slip at the wall of the plates. It is therefore, in many cases, worthwhile repeating the experiments with a smaller diameter geometry to assure that slip does not occur.

Sample temperature in the RMS was maintained through the use of the fluids bath, using water as the heat transfer fluid. With this setup a temperature stability

better than 0.1 °C (Rheometrics operation manual) can be obtained. This is preferred for black liquors, because of the evaporation problems. The heat transfer between the fluid media and the plates (+ sample) will be by conduction which causes less evaporation problems than would be caused by forced convection. The temperature of the sample is measured with a type J thermocouple connected to the bottom of the lower plate.

Before loading the system, a calibration check was done on the torque and normal force transducer. A portion of the black liquor to be investigated was heated in a constant temperature bath. Meanwhile, the gap height of the parallel-plate system was zeroed, and a sufficient amount of black liquor was loaded into the rheometer. The top disk was lowered to obtain the desired gap height and the excess liquor was scraped off completely. A small amount of silicon oil was placed around the rim of the plate to retard evaporation of water from the liquor. A time of 10 minutes was allowed for temperature equilibrium. Data were collected for up to 10 - 12 different frequencies at a fixed strain amplitude. After the first run, the experiment was repeated to check how much the sample had changed during the running time. If the results were close enough (about 1% difference), the system was stopped, the top and bottom plates were removed from the system, cleaned, and prepared for another run; otherwise, the same sample was loaded again and the experiment was repeated until good results were obtained. In most cases, this procedure was repeated at least five times for each sample, because of the operational difficulties, such as evaporation problems. The rheometer used in this

study operates as an open system and it is not equipped with a humidity control device; therefore, reliable data could not be obtained without minimizing the evaporation of water from the liquor. It seems that methods, such as using silicon oil around the rim of the plate and limiting data collection to a short period of time will do the job; however, finding the proper conditions and obtaining reliable data can be very time consuming.

A crucial requirement for small amplitude oscillatory shear flow is that the experiments are carried out within the linear viscoelastic range, i.e., that the material functions such as  $G'$  and  $\eta'$  must be independent of the applied strain levels. In this work, frequency sweeps at different strain levels were used to determine if this is the case. If the data are equivalent at each strain level, we may assume that data are in linear viscoelastic range over the entire range of frequencies. If this was not the case, the strain was reduced until the frequency sweeps of the two smallest strain levels were commensurate.

## 8.6 Results

The linear viscoelastic characteristics of three different experimental softwood kraft black liquors with solids concentrations ranging from 67% to 81% were investigated in small-amplitude oscillatory shear flow for a temperature range from 40 °C (313.16 K) to 85 °C (358.16 K). Figures (8-3) through (8-11) show dynamic viscosities ( $\eta'$ ) as a function of frequency and Figures (8-12) through (8-20) are

representatives of storage modulus ( $G'$ ) as a function of frequency at different solids concentrations and temperatures for these liquors.

The dynamic viscosity shows changes with temperature and solids content, and it also varies from liquor to liquor. At lower temperatures and higher concentrations, dynamic viscosity falls monotonically, with increasing frequency as shown in these Figures. This indicates that black liquors behave like uncross-linked polymer solutions. The plots show that, at sufficiently low frequencies,  $\eta'$  will approach a finite limiting value, which is expected to be close to the zero shear rate viscosity. The effect of temperature on dynamic viscosity is more significant at lower frequencies (e.g., Figures (8-5), (8-8) and (8-10)).

The magnitude of  $\eta'$  is higher for liquor ABAFX013,14 than for liquors ABAFX043,44 and ABAFX025,26. The transition from a frequency independent region to a frequency dependent region occurred at lower frequencies for liquor ABAFX043,44 than for liquors ABAFX013,14 and ABAFX025,26, which indicates that the lignin molecular weight for liquor ABAFX043,44 is higher than for the other two liquors, as mentioned in chapter 6. The lignin concentration and organic-to-inorganic ratio are higher for liquor ABAFX013,14 than for liquors ABAFX043,44 and ABAFX025,26. These differences indicate that the dynamic viscosity is not only affected by the lignin molecular weight, but it is also a function of lignin concentration and other organic and inorganic components in black liquor.

The storage modulus,  $G'$ , also shows changes with temperature, solids concentrations and frequency. Its magnitude is higher for liquor ABAFX013,14 than

for liquors ABAFX043,44 and ABAFX025,26. Like dynamic viscosity,  $G'$  is also a function of lignin molecular weight, lignin concentration and other constituents of black liquor. The results indicate that  $G'$  approaches zero with decreasing frequency, which means that the phase angle between the stress and strain approaches  $90^\circ$  as the stored energy per cycle of deformation becomes negligible compared with that dissipated as heat (Ferry 1980). At high solids concentrations and low temperatures, the liquors showed an indication of a plateau region at higher frequencies. The plateau is representative of the maximum amount of energy that can be stored in the fluid structure during one cycle of oscillation. The level of the plateau for liquor ABAFX013,14 is higher than for liquors ABAFX043,44 and ABAFX025,26, which indicates that the maximum energy storage for black liquors depends upon the lignin molecular weight, lignin concentration and the amount of organic and inorganics in the liquor.

### 8.7 Correlations for Dynamic Viscosity and Storage Modulus

From the plots of  $\log(\eta')$  as a function of  $\log(\omega)$ , it appears that the behavior of the liquors at different temperatures depends upon the solids concentration and the solids composition. At lower temperatures and higher solids, there are two distinguishable regions of dynamic viscosity behavior, frequency independent and shear thinning regions. The degree of shear thinning is decreased by increasing temperature or decreasing the solids concentrations. Also, it appears that, over the frequency dependent region, the plots for some of the liquors are linear (e.g, liquor

ABAFX013,14 at 67.2 and 70.02% solids) and for some are nonlinear. In other words, black liquors can exhibit power-law behavior depending upon solids concentrations and cooking conditions, but they can deviate from the power-law model. Therefore, the dynamic viscosity- frequency relationship can be described with different models depending upon the behavior of the liquors. When the plots are linear, the power-law model of Ostwald-de Waele (1923, 1925) can be used to describe the viscosity-frequency relationship. However, among the various empirical equations that have been proposed, the behavior of black liquors can be described very accurately with models that we discussed for shear viscosity in chapter 6. For dynamic viscosity as a function of frequency, these models can be described as

1. The power-law (Ostwald-de Waele) model:

$$\eta' = m \omega^{(n-1)} \quad (8-34)$$

2. Cross model:

$$\frac{\eta'}{\eta_0} = \frac{1}{1 + (\lambda \omega)^m} \quad (8-35)$$

At very low frequencies, the dynamic viscosity approaches  $\eta_0$ , while at high frequencies ( $|\lambda \omega| \gg 1$ ), power-law behavior is predicted:

$$\frac{\eta'}{\eta_0} = [(\lambda \omega)^m]^{-1} \quad (8-36)$$

where  $m$  can be related to the power-law index,  $n$  as follows:



$$m = 1 - n \quad (8-37)$$

### 3. The Carreau-Yasuda model:

$$\frac{\eta'}{\eta_0} = [1 + (\lambda \omega)^a]^{\frac{(n-1)}{a}} \quad (8-38)$$

If the zero shear rate viscosities are available, then equation (8-38) will be a three parameter model that can be used to fit the experimental data. The characteristic time for the fluid is  $\lambda$  and  $1/\lambda$  is equal to a critical frequency (or shear rate) at which  $\eta'$  begins to decrease with frequency (Yasuda *et al.* 1980). The power-law slope is  $(n-1)$ , and the parameter,  $a$ , that was taken to be 2 by Carreau, adjusts the breadth of the transition region between the zero shear rate viscosity and the power-law region.

The above mentioned three models were used to fit the experimental data for black liquors. The results are summarized in Tables (8-1) through (8-3). Both Cross and Carreau-Yasuda models will fit the experimental data with very good accuracy. However, the Cross model, because of its simplicity and fewer parameters, will be easier to use. The power-law model must be limited to cases where the plots of  $\log(\eta')$  as a function of  $\log(\omega)$  are linear.

The storage modulus of black liquors at different solids concentrations and temperatures are frequency dependent, as can be seen from plots of  $\log(G')$  as a function of  $\log(\omega)$ . In some cases, linear behavior (e.g. for liquor ABAFX025,26 at 71.98% solids) and, in other cases, nonlinear behavior (e.g. for liquor ABAFX013,14

at 76.01% solids and temperatures equal to 40 °C and 55 °C) can be observed. When the plots are linear, a power-law type relationship can be used to fit the experimental data. This equation can be written as

$$G' = m \omega^{(n-1)} \quad (8-39)$$

When the liquors exhibit nonlinear behavior, a Cross or Carreau-Yasuda type relation can be used to fit the experimental data. A Cross type relationship can be defined as

$$\frac{G'}{G'_\infty} = (1 + (\lambda \omega)^n)^{-1} \quad (8-40)$$

where  $G'_\infty$  is the storage modulus at very high frequencies. In this investigation, equations (8-39) and (8-40) were used to model the storage modulus data. Usually the measurements are extremely difficult to make at very high frequencies. Therefore, in this work,  $G'_\infty$  was treated as a parameter. The model parameters for storage modulus as a function of frequency from these equations are summarized in Tables (8-4) and (8-5). It seems that the calculated values of  $G'_\infty$  are close to the limiting values for  $G'$  at high frequencies.

### 8.8 Time-Temperature Superposition

For uncross-linked polymers and concentrated polymer solutions with low to moderate molecular weights, the data for linear viscoelastic functions can be normalized by superposition principles (Ferry 1980, Vinogradov and Malkin 1980 and Akonis 1983). It is often found that the shape of the dynamic functions at various

temperatures are similar to one another and can be brought together on a single master curve. For polymer solutions, molecular theory predicts that the reduced functions can be written as (Ferry 1980)

$$\frac{\eta'}{\eta_0} = f(a_T \omega) \quad (8-41)$$

$$G' \frac{T_0 \rho_0}{T \rho} = g(a_T \omega) \quad (8-42)$$

Over the temperature range studied, it may be assumed that  $\rho \approx \rho_0$ , so that

$$G' \frac{T_0}{T} = g(a_T \omega) \quad (8-43)$$

the temperature shift factor is given by

$$a_T = \frac{\eta_0 T_0 \rho_0}{\eta_0 T \rho} \approx \frac{\eta_0 T_0}{\eta_0 T} \quad (8-44)$$

where  $\eta_0^\circ$  is the zero shear rate viscosity at reference temperature  $T_0^\circ$ .

In order to obtain a master curve for dynamic viscosity or storage modulus at an arbitrary reference temperature,  $T_0^\circ$ , from plots of  $\log(\eta')$  and  $\log(G')$  as a function of  $\log(\omega)$  at different temperatures, a two step procedure has been followed:

1. the curve at temperature  $T$  is first shifted vertically upward by an amount of  $\log(1/\eta_0)$  for dynamic viscosity and  $\log(T_0/T)$  for storage modulus, and 2. The resulting curve is then shifted horizontally in such a way that any overlapping regions of the  $T_0^\circ$  curve and shifted  $T$  curve superimpose. The amount by which  $\eta'$  or  $G'$

must be shifted to the right in order to achieve superposition is defined as  $\log(a_T)$  (Bird *et al.* 1987).

Once the zero shear rate viscosities are available, the temperature shift factor can be calculated as a function of temperature from equation (8-44), and then equations (8-41) and (8-43) can be used to obtain reduced plots of dynamic viscosity and storage modulus as a function of reduced frequency ( $a_T\omega$ ) at different solids concentrations. In chapter 6, it was shown that black liquor can be treated as a polymer solution and by applying the superposition principles, we were able to normalize our data and obtain the reduced plots for shear viscosity of black liquors. In this chapter, the reduced variables method was applied to obtain the reduced plots of dynamic viscosity and storage modulus as a function of reduced frequency for three black liquors. The results are shown in Figures (8-21) through (8-38).

Two models that can be applied to obtain the reduced correlations for dynamic viscosity of black liquors are equations (8-35) and (8-39), which in this case may be written as

$$\frac{\eta'}{\eta_0} = \frac{1}{(1 + (\lambda \omega_r)^a)} \quad (8-45)$$

$$\frac{\eta'}{\eta_0} = [1 + (\lambda \omega_r)^a]^{\frac{(n-1)}{a}} \quad (8-46)$$

where  $\omega_r$  is the reduced frequency and equal to  $a_T\omega$ .

Equation (8-45) has two parameters; therefore, it is easier to use than equation (8-46), which has three parameters. Also, it is possible to use polynomials to fit the experimental data. The model parameters for reduced dynamic viscosity as a function of reduced frequency from equations (8-45) and (8-46) are summarized in Tables (8-6) and (8-7).

The model that was applied to express the reduced storage modulus as a function of reduced frequency is

$$\log_e \left( G' \frac{T}{T_0} \right) = a + b(\log_e(a_T \omega)) + c(\log_e(a_T \omega))^2 \quad (8-47)$$

The model parameters for reduced storage modulus as a function of reduced frequency are shown in Table (8-8). Equation (8-47) accurately fits the experimental data and the level of accuracy can be increased by increasing the order of polynomial.

The reduced curves at different solids concentrations for dynamic viscosity can be superimposed by defining a solids shift factor as was described in chapter 6:

$$a_s = \frac{\eta_0 S^0}{\eta_0^0 S} \quad (8-48)$$

Figures (8-39), (8-40) and (8-41) are plots of reduced dynamic viscosity ( $\eta'/\eta_0$ ) as a function of reduced frequency ( $a_T a_s \omega$ ) for these liquors. The reduced variables method seems to be generally applicable to dynamic viscosity of black liquors, although cumbersome. Attempts were made to use a one step procedure as it was used for shear viscosity; however, it did not work. This is due to the fact that

the shear viscosity is affected more by the molecular weight of the lignin than dynamic viscosity.

The data for reduced storage modulus at different solids concentrations were treated in the same manner, but the reduced curves at different solids concentrations for reduced storage modulus can not be superimposed in a single curve.

Two models were applied to express the reduced dynamic viscosity as a function of reduced frequency ( $a_1 a_5 \omega$ ), these are

$$\frac{\eta}{\eta_0} = [1 + (\lambda a_s a_T \omega)^a]^{-1} \quad (8-49)$$

$$\frac{\eta}{\eta_0} = [1 + (\lambda a_s a_T \omega)^a]^{\frac{(n-1)}{a}} \quad (8-50)$$

The model parameters for these equations are summarized in Tables (8-9) and (8-10). Equation (8-50) did not converge for liquor ABAFX025,26. Using a polynomial of degree (2) will also fit the experimental data, as was mentioned before. As an example, the reduced dynamic viscosity of black liquor ABAFX013,14 can be expressed as

$$\log_e \left( \frac{\eta'}{\eta_0} \right) = -1.0711 - 0.3635 \log_e (a_T a_s \omega) - 0.03117 [\log_e (a_T a_s \omega)]^2 \quad (8-51)$$

with  $R^2 \geq 0.98$ .

### 8-9 Relations Between Shear Viscosity ( $\eta$ ) and the Magnitude of the Complex Viscosity $|\eta^*|$

Attempts have been made to find an analogy between the viscometric functions and linear viscoelastic functions by some investigators. The empirical method suggested by Cox and Merz (1958) for relating steady shear viscosity,  $\eta$ , with the magnitude value of the complex viscosity,  $\eta^*$ , is of particular importance. This empirical equation predicts that the magnitude of the complex viscosity is equal to the shear viscosity at the corresponding values of frequency and shear rate.

$$\eta(\dot{\gamma}) = |\eta^*(\omega)| \quad \text{at} \quad \dot{\gamma} = \omega \quad (8-52)$$

In order to test the above method of correlation for black liquors, plots of shear viscosity versus shear rate were superimposed on the plots of complex viscosity as a function of frequency. The resulting plots are shown in Figures (8-42) through (8-46). This shows the excellent agreement between the shear viscosity and the complex viscosity for black liquors ABAFX013,14 and ABAFX025,26 within the experimental range of shear rate and frequency. Both  $\eta(\dot{\gamma})$  and  $\eta^*(\omega)$  approach  $\eta_0$  at low values of  $\dot{\gamma}$  and  $\omega$ . For liquor ABAFX043,44, there is agreement between  $\eta(\dot{\gamma})$  and  $\eta^*(\omega)$  at temperatures 70 °C and 80 °C. At 40 °C and 55 °C, it can be observed that  $\eta^*(\omega)$  decreases more rapidly with  $\omega$  than  $\eta$  does with  $\dot{\gamma}$ , but still both of them approach  $\eta_0$  at low  $\dot{\gamma}$  or  $\omega$ . A similar deviation was found by Harris for a narrow distribution of polystyrene solution (high weight average molecular weight and low concentration) in PCB (Yasuda *et al.* 1981). From the shear viscosity and dynamic viscosity data presented in this section, it is evident that, at low shear rates and

frequencies,  $\eta(\dot{\gamma})$  and  $\eta^*(\omega)$  agree within experimental error and zero shear rate viscosity of black liquors can be estimated from the complex viscosity data.

#### 8-10 The Effect of Black Liquor Viscoelasticity on Droplet Formation

Droplet size and size distribution are the most important parameters in controlling black liquor droplet combustion in a pulp and paper mill recovery boiler (Adams 1988). The droplets should be small enough to dry before reaching the char bed but large enough to avoid being entrained in the furnace gas flow. The work of many investigators show that, in addition to other physical parameters, the dynamic viscosity has an important effect on the size of droplets (Adams 1988).

The range of shear rates that black liquor is subjected to in flow through the nozzles to form droplets will depend upon the nozzle diameter (11/16 to 17/16 inch) and can vary from 1000 - 4000  $\text{sec}^{-1}$  for mass flow rates of 6000 - 22000 lbs/hr. (Wight 1985, Fricke 1987). The results of this work show that high solid black liquors (>50%) should be treated as viscoelastic fluids for temperatures up to 85 °C. This is in agreement with results of previous workers (Co and Wight 1982, Wight 1985 and Fricke 1987). For a viscoelastic fluid, the relative importance of energy storage to viscous dissipation can be estimated from the ratio of  $(G'/\omega)/\eta'$  or  $\eta''/\eta'$ . This ratio can be estimated for the nominal operating temperature in a recovery furnace (about 120 °C) from equation (8-45) and (8-47) at any concentration. The value of  $\eta''/\eta'$  for these three black liquors at  $T=120$  °C and frequencies equal to 1 rad/sec and 4000 rad/sec for the highest concentrations are



<u>Liquor</u>	<u>%solids</u>	<u><math>\eta''/\eta'</math> at <math>\omega=1</math> rad/sec</u>	<u><math>\eta''/\eta'</math> at <math>\omega=4000</math> rad/sec</u>
ABFX013,14	76.01	0.0395	0.633
ABAFX025,26	81.05	0.000	0.051
ABAFX043,44	76.28	0.0617	0.443

Wight (1985) determined the storage modulus and dynamic viscosity for a 1% solution of Separan AP 30, which was reported to have difficulties in jet break up and droplet formation by Goldin et al. (1968). The ratio of  $\eta''/\eta'$  at  $\omega = 1$  rad/sec was reported to be equal to 1 at three different temperatures for this solution. For black liquors, the value of  $\eta''/\eta'$  at  $\omega = 1$  rad/sec is much smaller than 1 and can be neglected. At higher frequencies, the data is not available for Separan solution, but it can be expected that  $\eta''/\eta'$  would be much higher than unity. The ratio of  $\eta''/\eta'$  for black liquors at  $\omega = 4000$  rad/sec is still less than 1. Therefore, it can be said that black liquors, even at very high solids concentrations, will not have problems in droplet formation due to the viscoelasticity of the fluid at temperatures above 120 °C. The ratio of energy storage to viscous dissipation is not the same for different black liquors and depends upon the general condition of the liquor. There will be an increase in energy storage compared to viscous dissipation at higher frequencies.

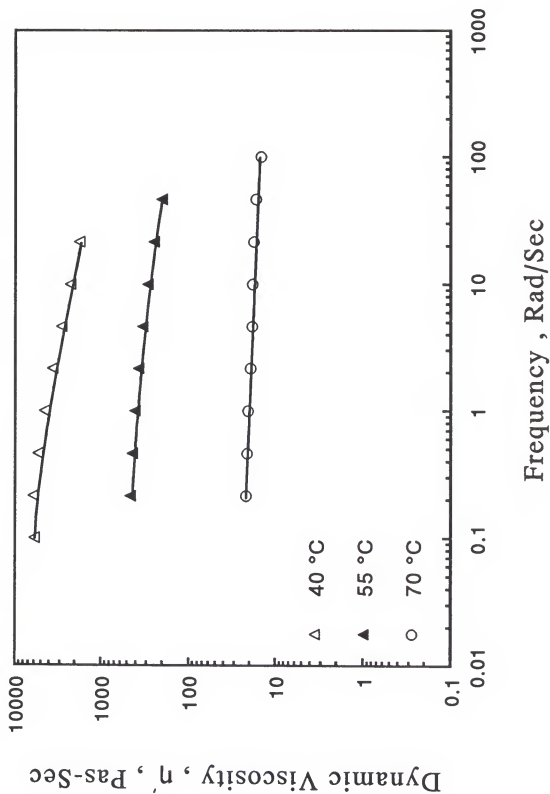


Figure (8-3): Dynamic Viscosity as a Function of Frequency for Black Liquor ABAFX013,14 at 67.2% Solids.

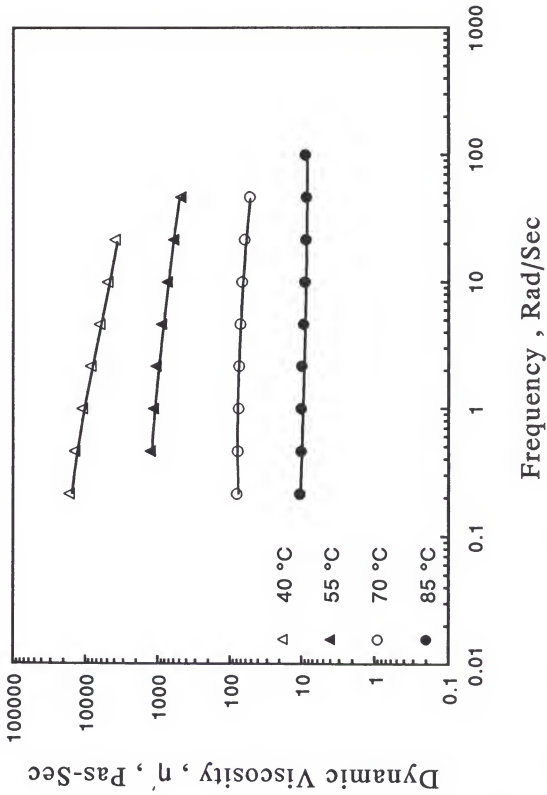


Figure (8-4): Dynamic Viscosity as a Function of Frequency for Black Liquor ABAFX013,14 at 70.05% Solids.

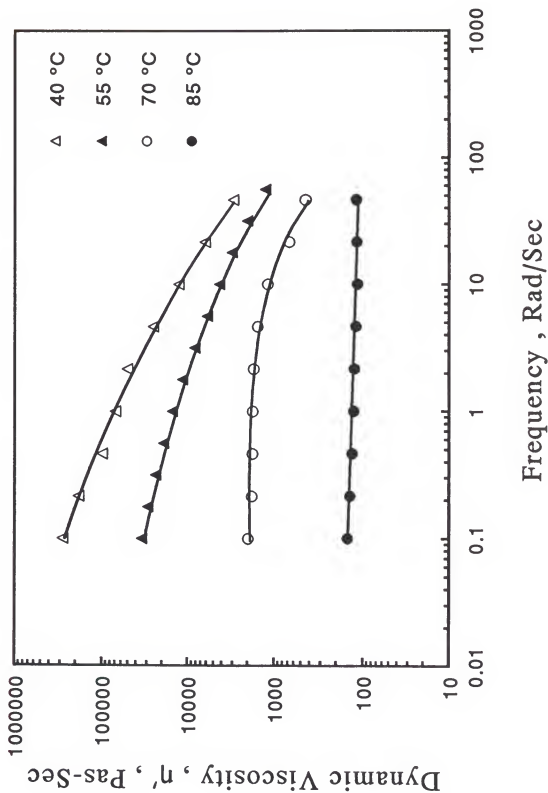


Figure (8-5): Dynamic Viscosity as a Function of Frequency for Black Liquor ABAFX013,14 at 75.05% Solids.

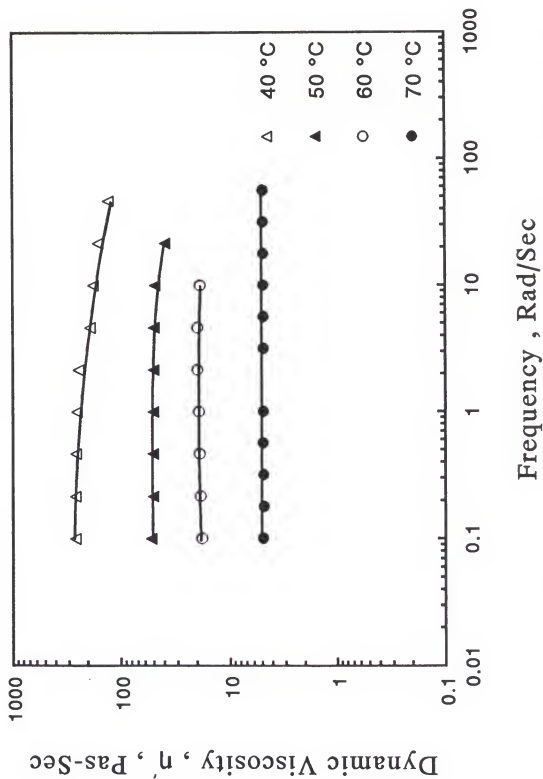


Figure (8-6): Dynamic Viscosity as a Function of Frequency for Black Liquor ABAFX025,26 at 71.98% Solids.

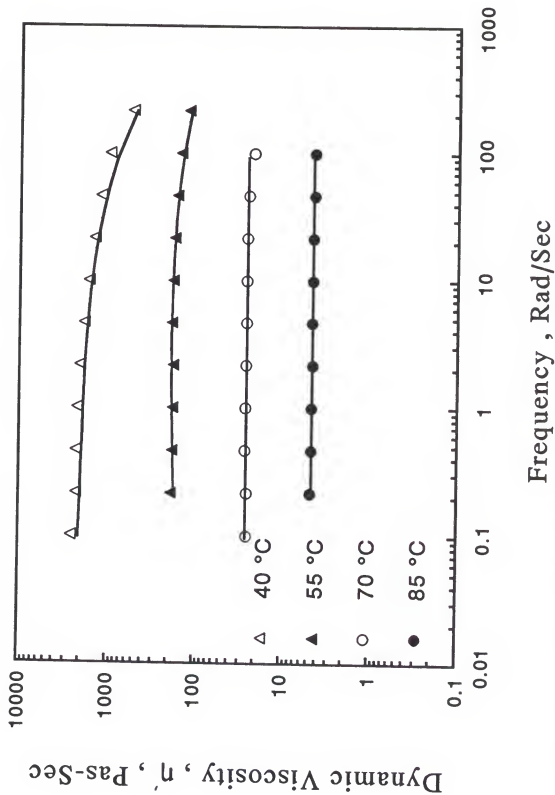


Figure (8-7): Dynamic Viscosity as a Function of Frequency for Black Liquor ABAFX025,26 at 75.70% Solids.

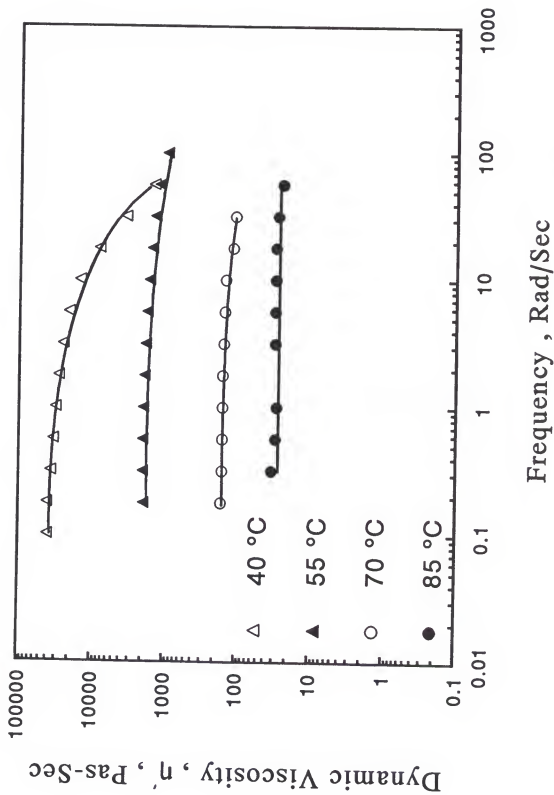


Figure (8-8): Dynamic Viscosity as a Function of Frequency for Black Liquor ABAFX025,26 at 81.05% Solids.

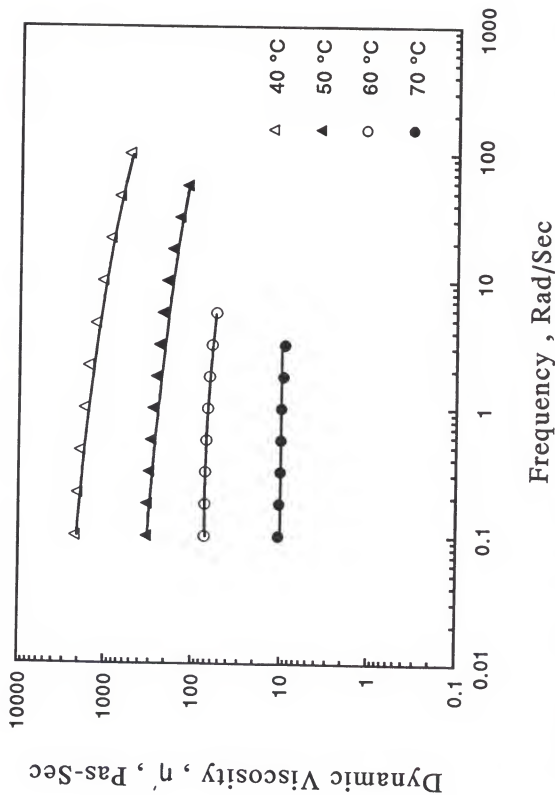


Figure (8-9): Dynamic Viscosity as a Function of Frequency for Black Liquor ABAFX043,44 at 65.40% Solids.



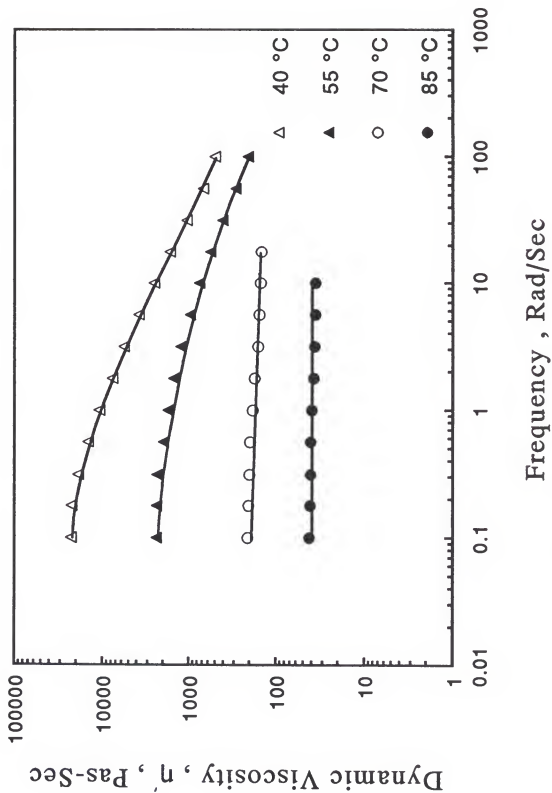


Figure (8-10): Dynamic Viscosity as a Function of Frequency for Black Liquor ABAFX043,44 at 72.89% Solids.

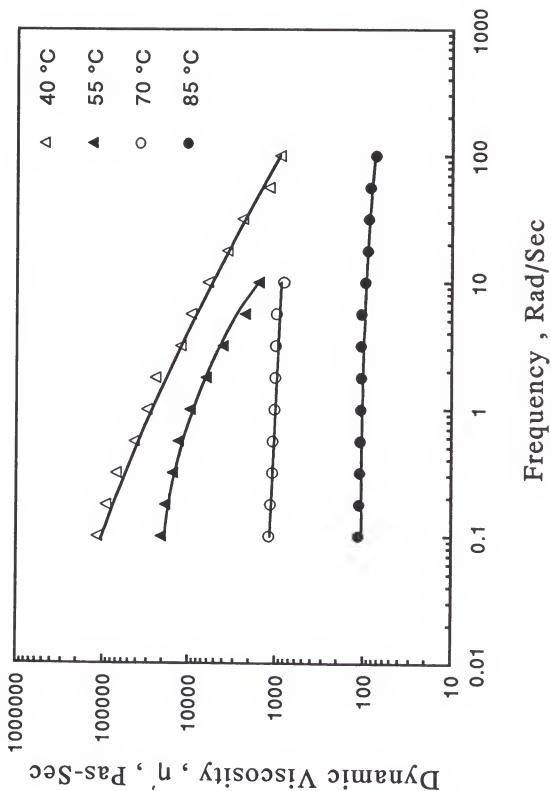


Figure (8-11): Dynamic Viscosity as a Function of Frequency for Black Liquor ABAFX043,44 at 76.28% Solids.

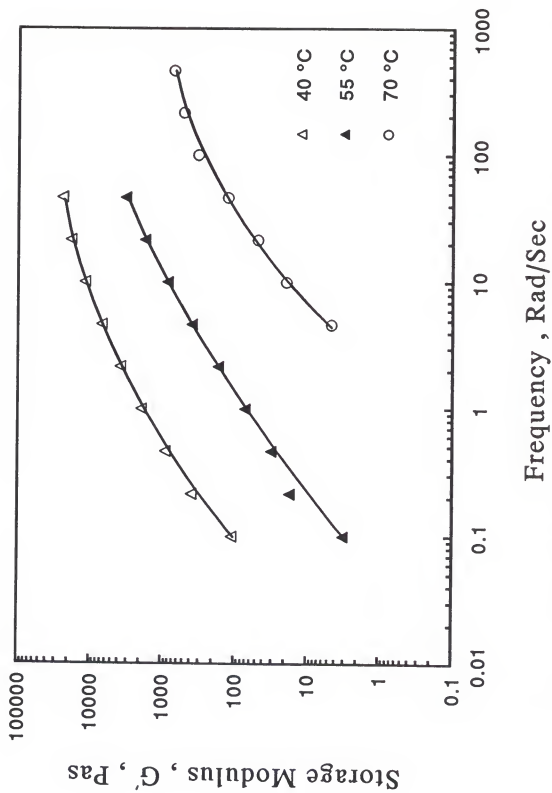


Figure (8-12): Storage Modulus as a Function of Frequency for Black Liquor ABAFX013,14 at 67.20% Solids.

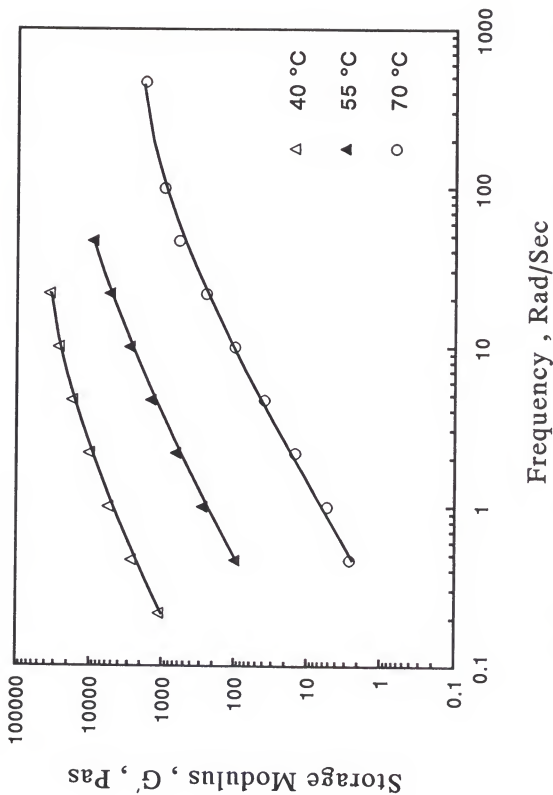


Figure (8-13): Storage Modulus as a Function of Frequency for Black Liquor ABAFX013,14 at 70.05% Solids.

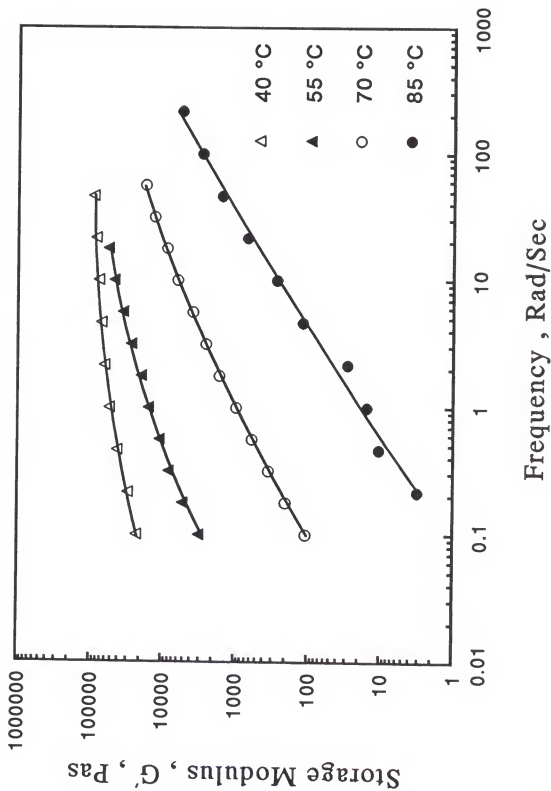


Figure (8-14): Storage Modulus as a Function of Frequency for Black Liquor ABAFX013,14 at 76.05% Solids.

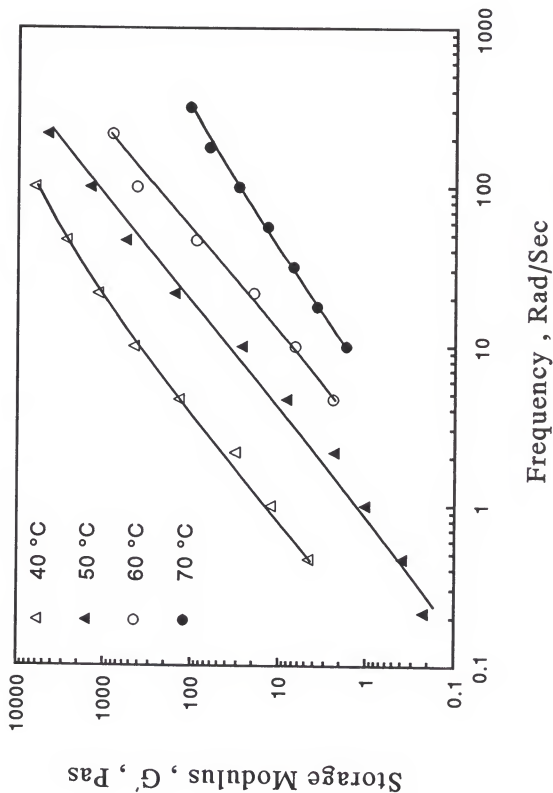


Figure (8-15): Storage Modulus as a Function of Frequency for Black Liquor ABAFX025,26 at 71.98% Solids.

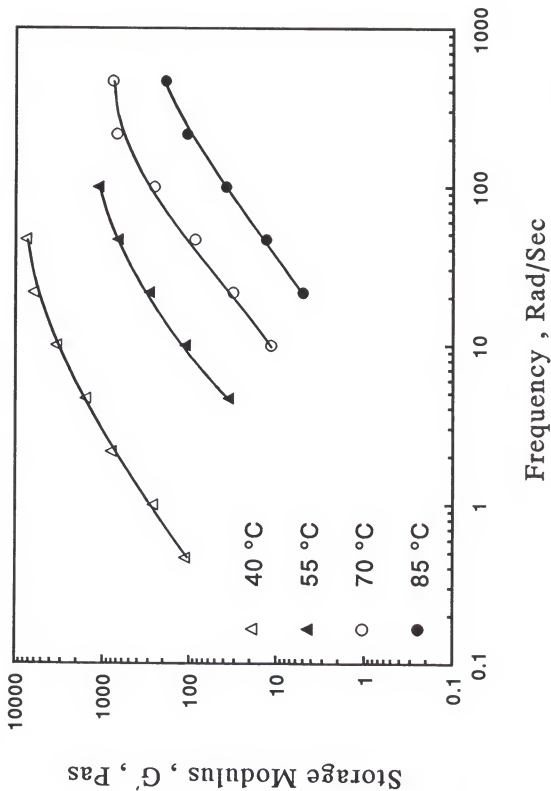


Figure (8-16): Storage Modulus as a Function of Frequency for Black Liquor ABAFX025,26 at 75.70% Solids.

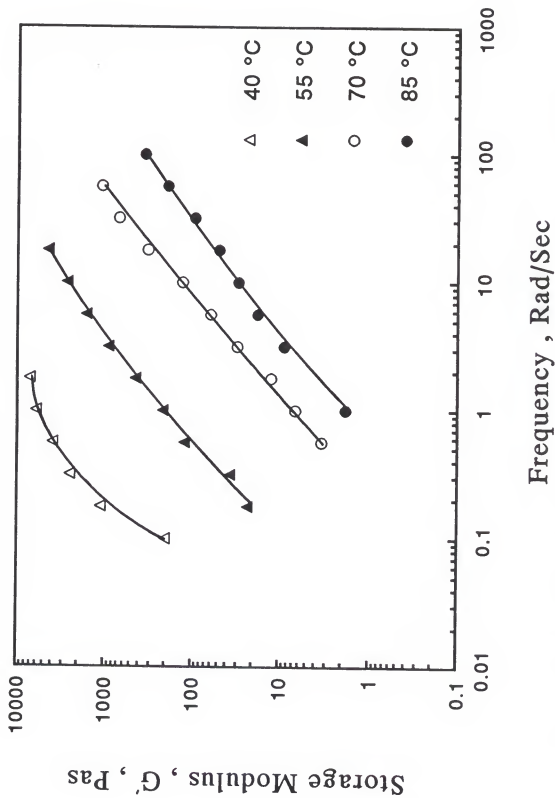


Figure (8-17): Storage Modulus as a Function of Frequency for Black Liquor ABAFX025,26 at 81.05% Solids.



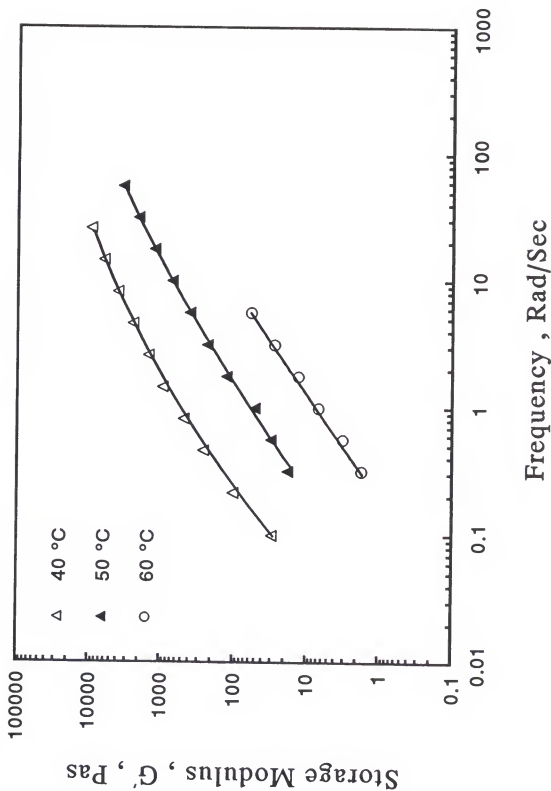


Figure (8-18): Storage Modulus as a Function of Frequency for Black Liquor ABAFX043,44 at 65.40% Solids.

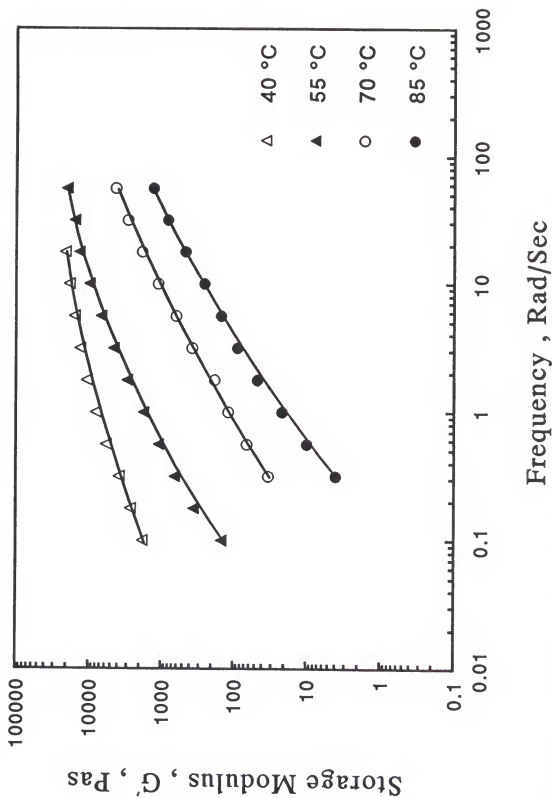


Figure (8-19): Storage Modulus as a Function of Frequency for Black Liquor ABAFX043,44 at 72.89% Solids.

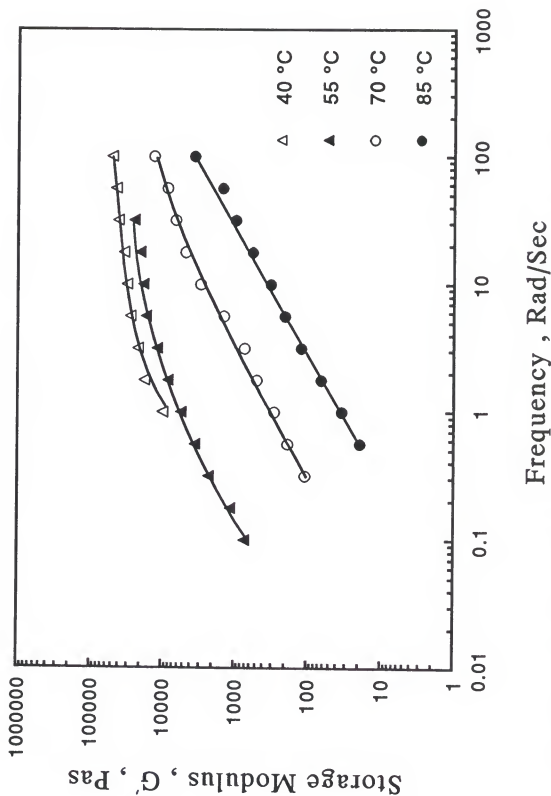


Figure (8-20): Storage Modulus as a Function of Frequency for Black Liquor ABAFX043,44 at 76.28 % Solids.

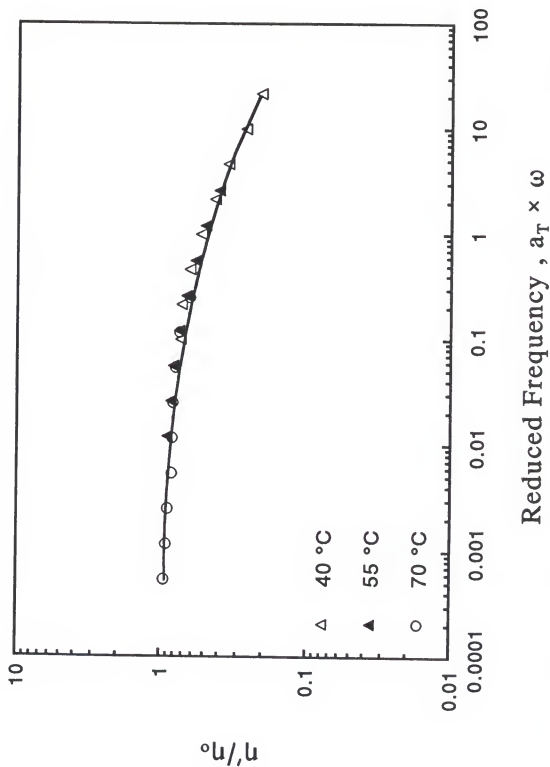
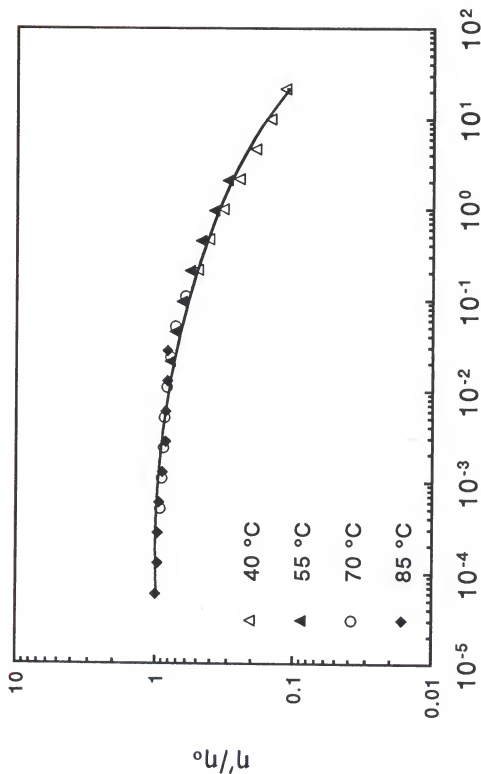
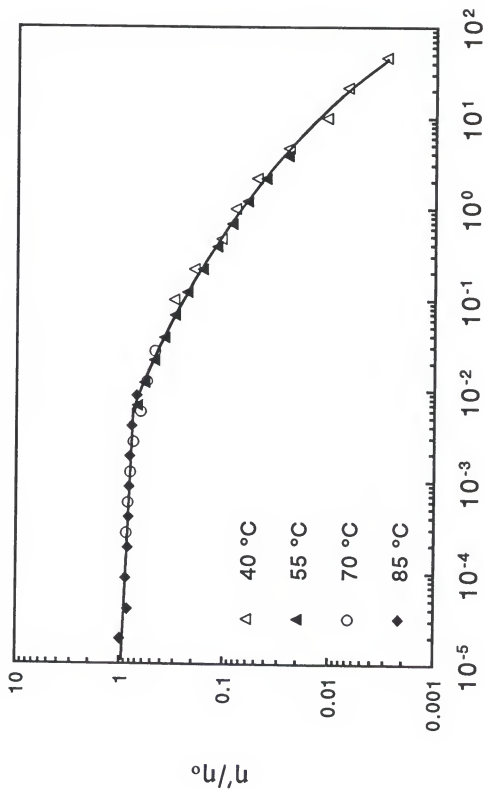


Figure (8-21): Reduced Dynamic Viscosity for Black Liquor ABAFX013,14 at 67.20% Solids. (Ref. T=40 °C)



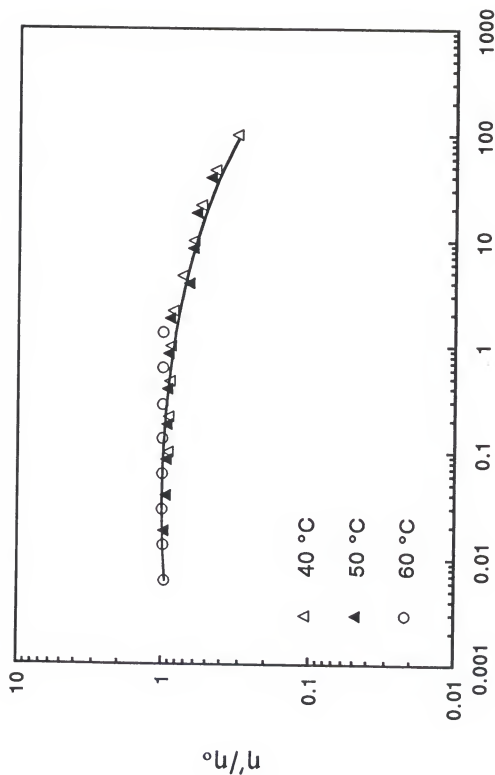
### Reduced Frequency, $a_T \times \omega$

Figure (8-22): Reduced Dynamic Viscosity for Black Liquor ABAPX013,14 at 70.05% Solids. (Ref. T=40 °C)



### Reduced Frequency, $a_T \times \omega$

Figure (8-23): Reduced Dynamic Viscosity for Black Liquor ABAFX013,14 at 76.05% Solids. (Ref. T=40 °C)



### Reduced Frequency, $a_T \times \omega$

Figure (8-24): Reduced Dynamic Viscosity for Black Liquor ABAFX025,26 at 71.98% Solids. (Ref.  $T=40$  °C)

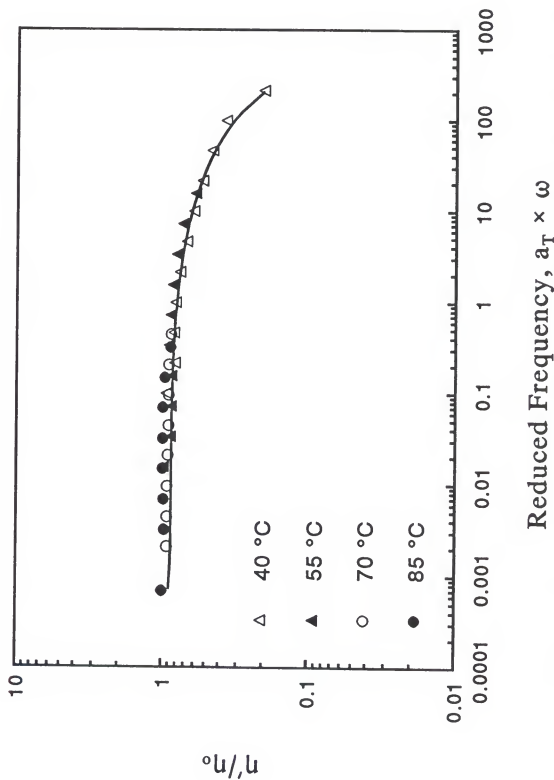


Figure (8-25): Reduced Dynamic Viscosity for Black Liquor ABAFX025,26 at 75.7% Solids. (Ref.  $T=40$  °C)



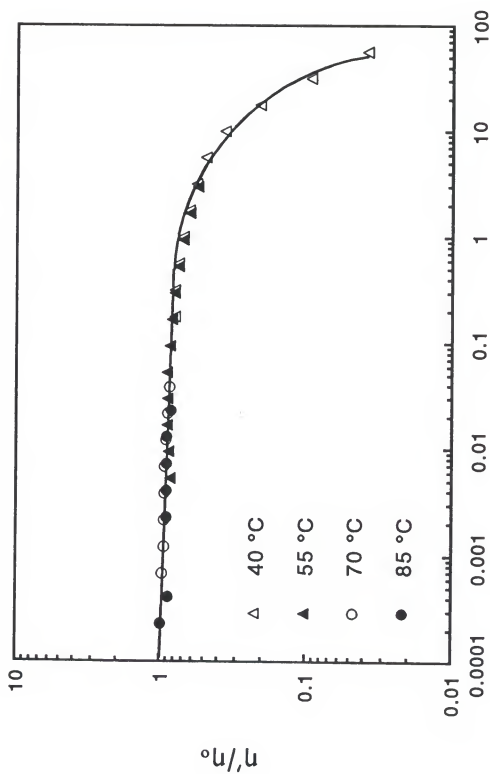


Figure (8-26): Reduced Dynamic Viscosity for Black Liquor ABAFX025,26 at 81.05% Solids. (Ref. T=40 °C)

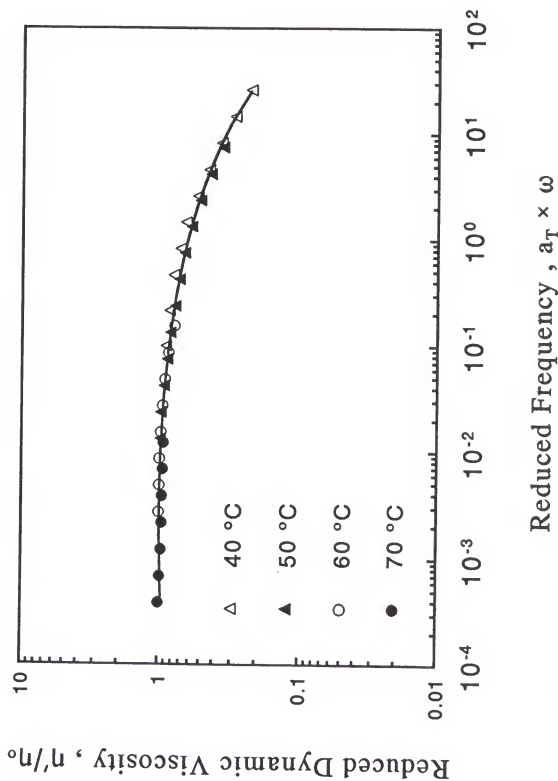


Figure (8-27): Reduced Dynamic Viscosity for Black Liquor ABAFX043,44 at 65.4 % Solids. (Ref. T=40 °C)

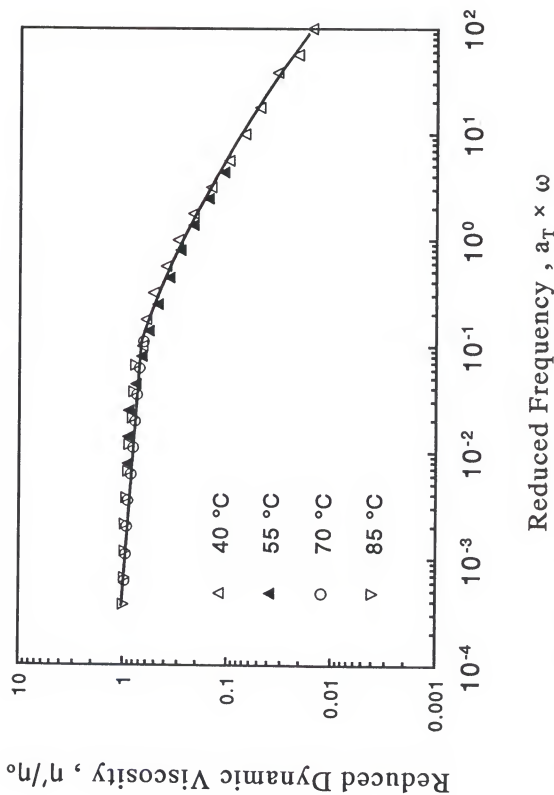


Figure (8-28): Reduced Dynamic Viscosity for Black Liquor ABAFX043,44 at 72.89% Solids. (Ref. T=40 °C)

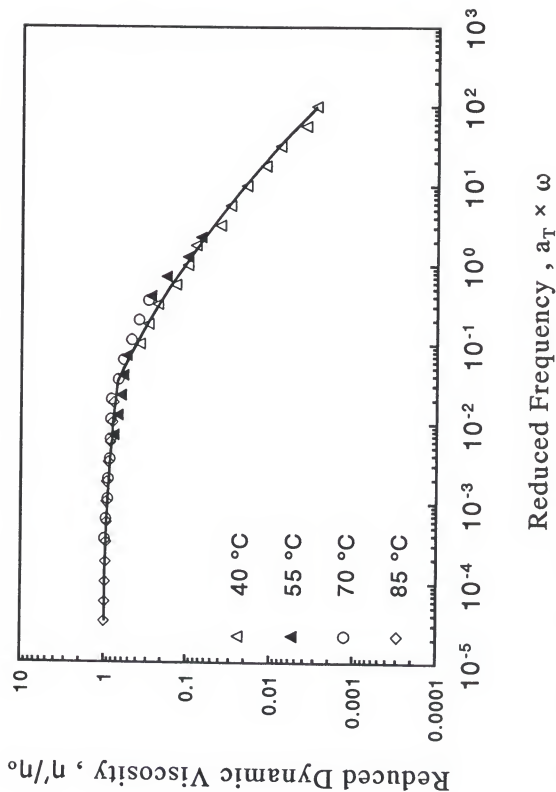


Figure (8-29): Reduced Dynamic Viscosity for Black Liquor ABAFX043,44 at 76.28% Solids. (Ref. T=40 °C)

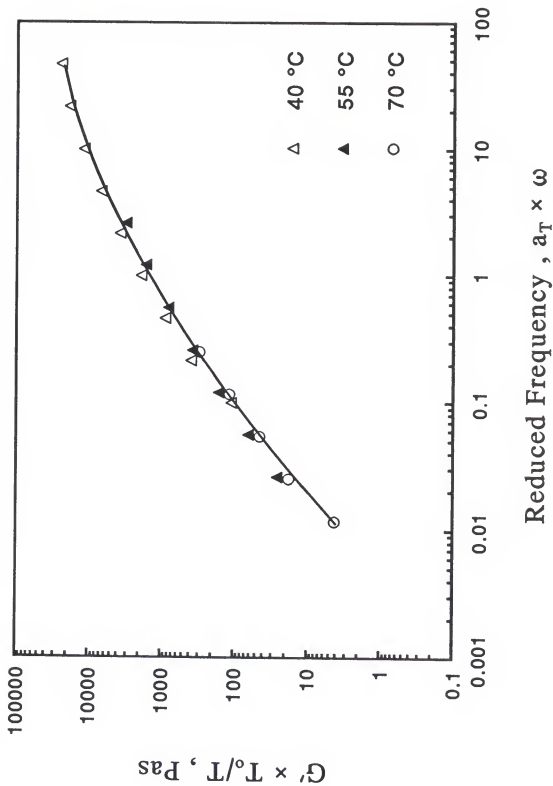


Figure (8-30): Reduced Storage Modulus for Black Liquor ABAFX013,14 at 67.2% Solids. (Ref.  $T=40\text{ }^{\circ}\text{C}$ )

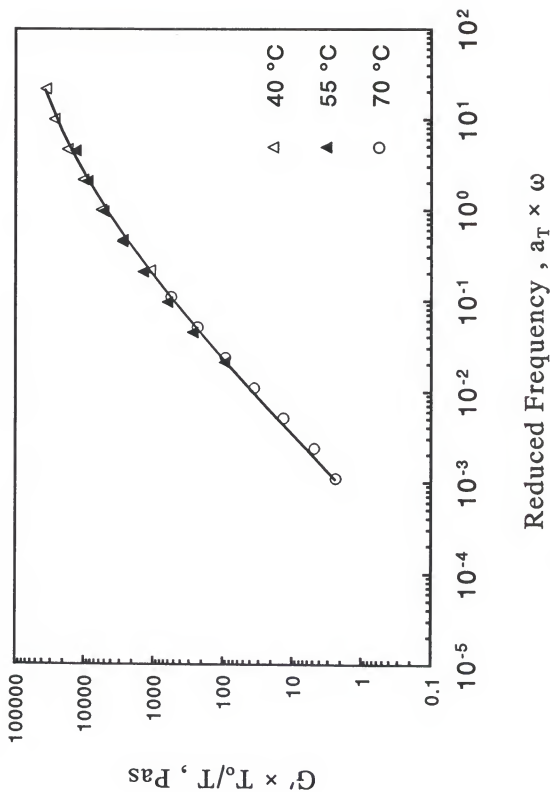
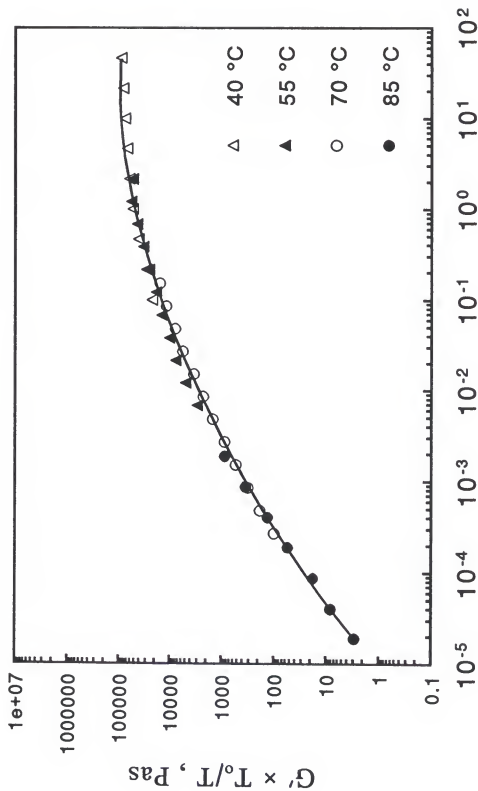


Figure (8-31): Reduced Storage Modulus for Black Liquor ABAFX013,14 at 70.05% Solids. (Ref. T=40 °C)



Reduced Frequency,  $a_T \times \omega$

Figure (8-32): Reduced Storage Modulus for Black Liquor ABAFX013,14 at 76.05% Solids. (Ref. T=40 °C)

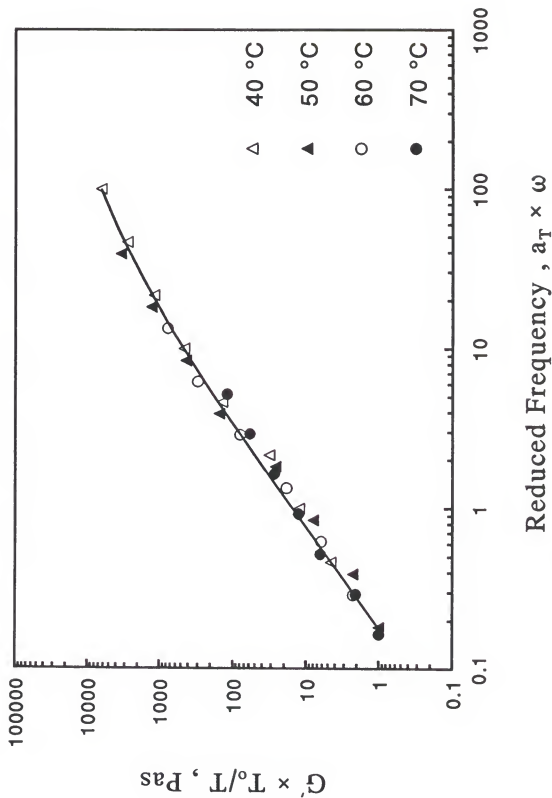


Figure (8-33): Reduced Storage Modulus for Black Liquor ABAFX025,26 at 71.98% Solids. (Ref.  $T=40$  °C)



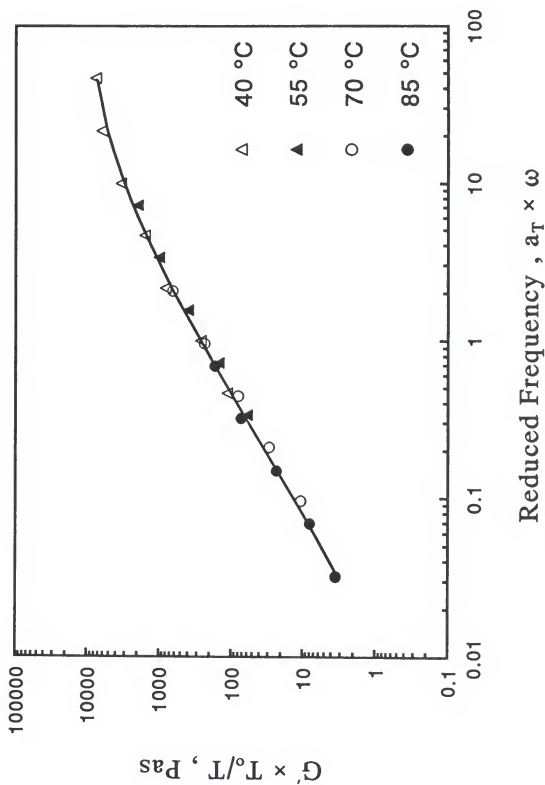
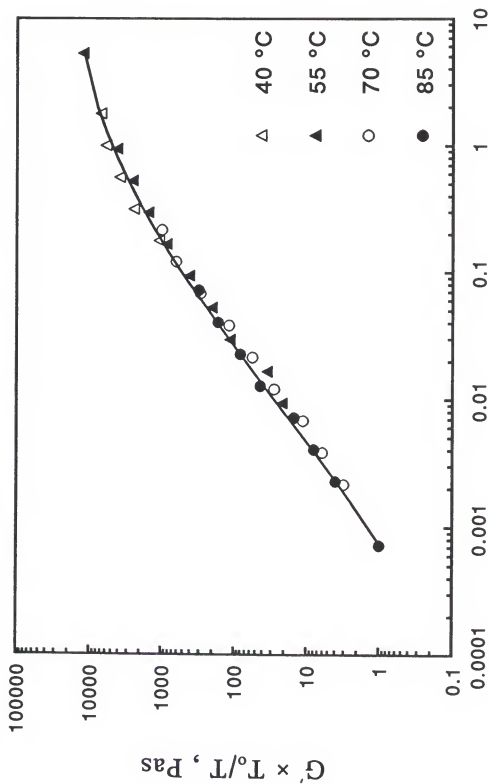


Figure (8-34): Reduced Storage Modulus for Black Liquor ABAFX025,26 at 75.70% Solids. (Ref.  $T=40\text{ }^{\circ}\text{C}$ )



Reduced Frequency,  $a_T \times \omega$

Figure (8-35): Reduced Storage Modulus for Black Liquor ABAFX025,26 at 81.05% Solids. (Ref. T=40 °C)

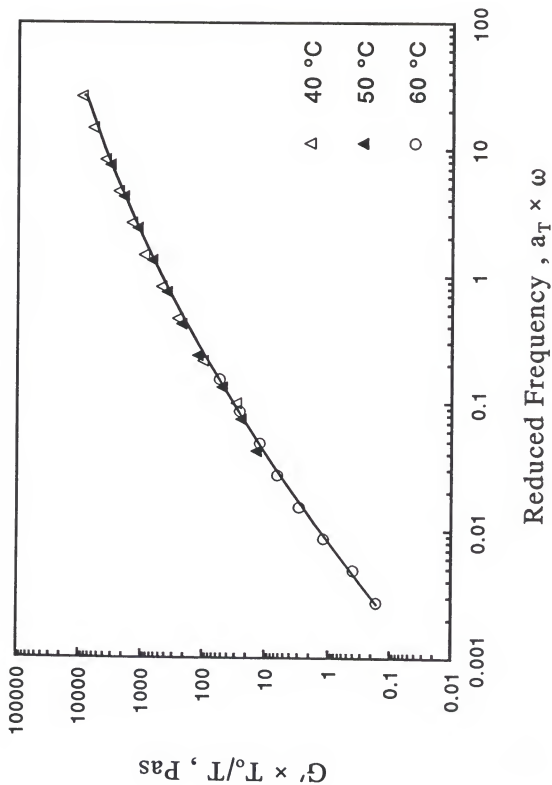
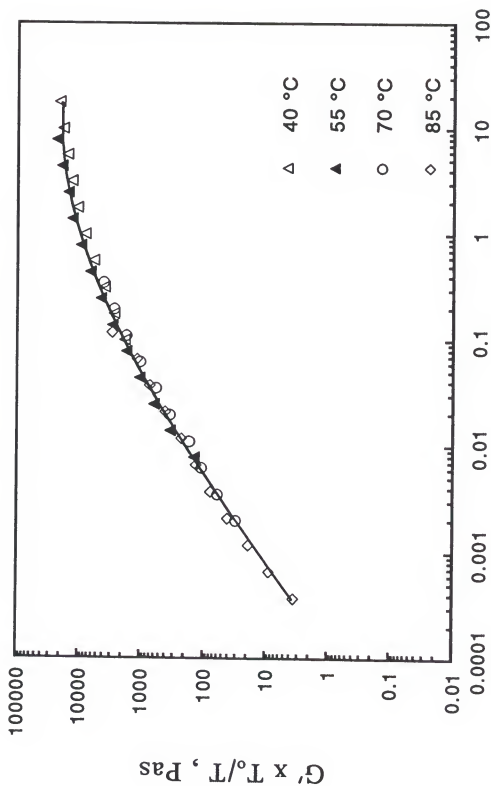
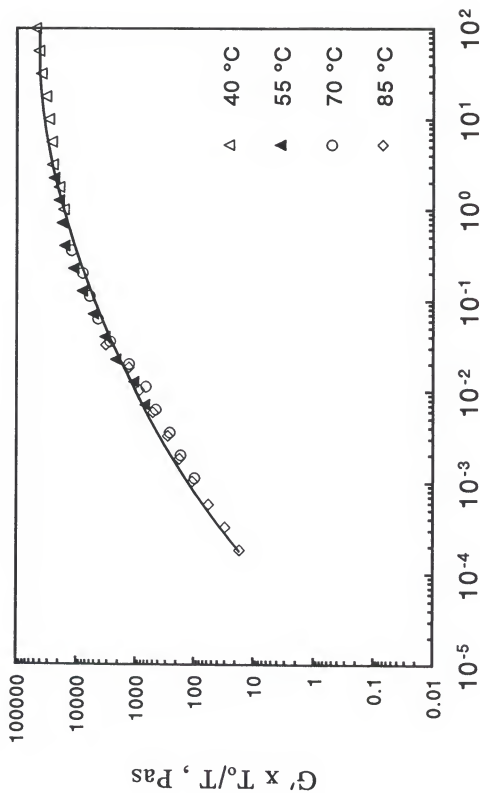


Figure (8-36): Reduced Storage Modulus for Black Liquor ABAFX043,44 at 65.4% Solids. (Ref.  $T=40$  °C)



Reduced Frequency,  $a_T \times \omega$

Figure (8-37): Reduced Storage Modulus for Black Liquor ABAFX043,44 at 72.89% Solids. (Ref. T=40 °C)



Reduced Frequency,  $a_T \times \omega$

Figure (8-38): Reduced Storage Modulus for Black Liquor ABAFX043,44 at 76.28% Solids. (Ref.  $T=40$  °C)

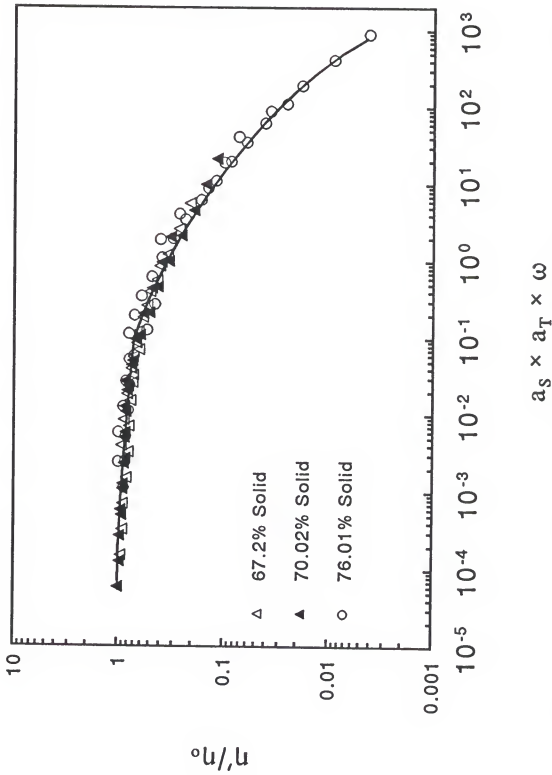


Figure (8-39): Reduced Dynamic Viscosity for Liquor ABAFX013,14. (Ref. T=40 °C Ref. Solids=70.05%)

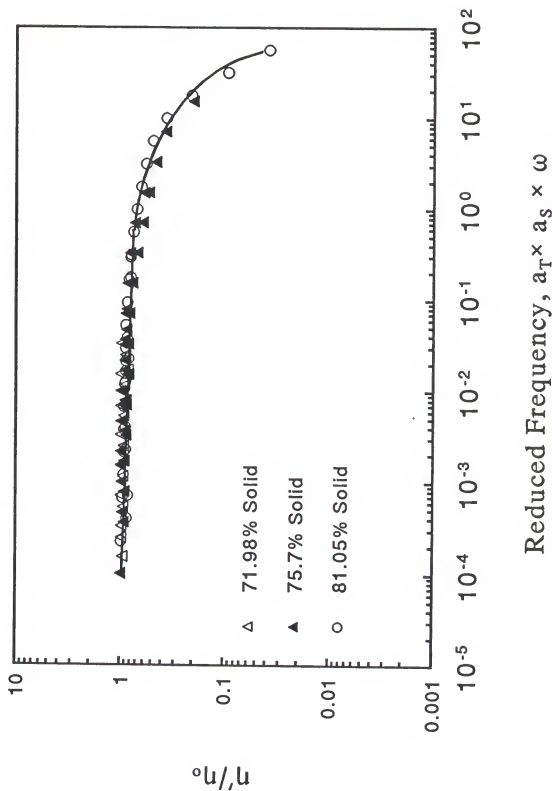
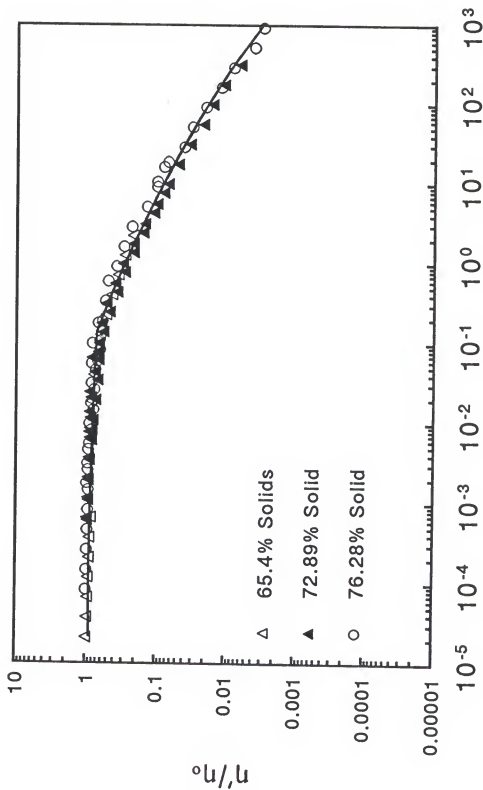


Figure (8-40): Reduced Dynamic Viscosity for Liquor ABAFX025,26. (Ref. T=40 °C Ref. Solids=81.05%)



### Reduced Frequency, $a_s \times a_T \times \omega$

Figure (8-41): Reduced Dynamic Viscosity for Liquor ABAFX043,44. (Ref. T=40 °C Ref. Solids=72.89%)



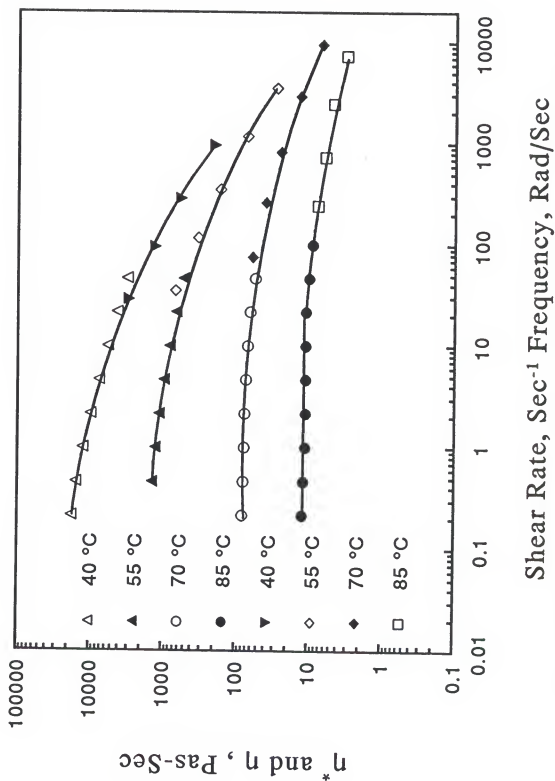


Figure (8-42): Complex and Shear Viscosity of Black Liquor ABAFX013,14 at 70.05% Solids.

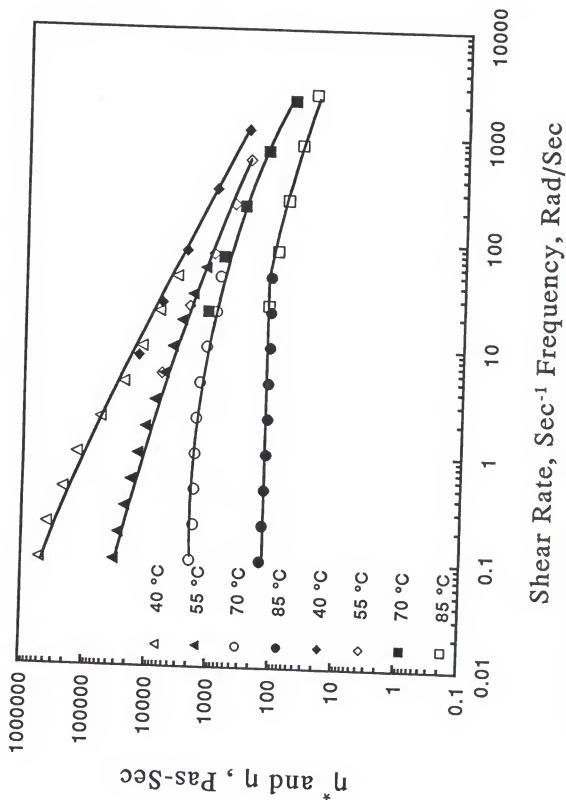
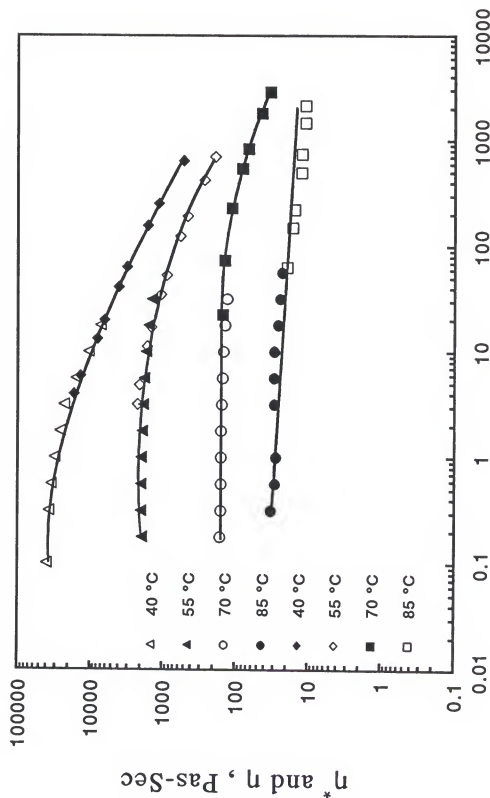
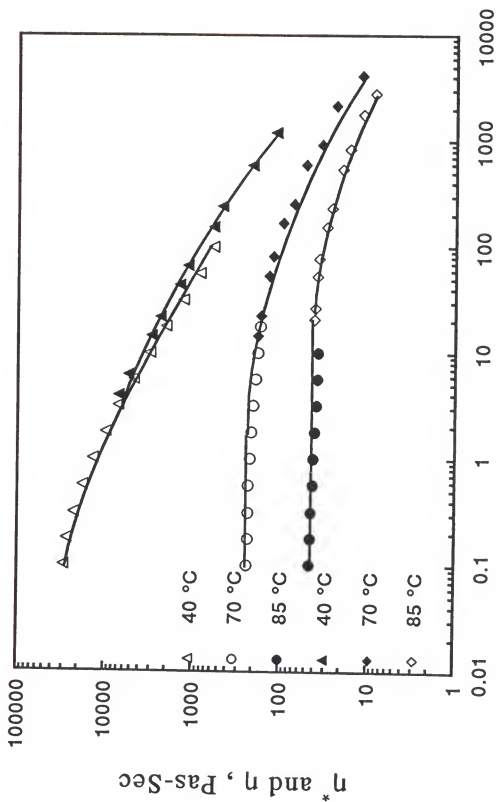


Figure (8-43): Complex and Shear Viscosity of Black Liquor ABAFX013,14 at 76.05% Solids.



### Shear Rate, $\text{Sec}^{-1}$ Frequency, Rad/Ses

Figure (8-44): Complex and Shear Viscosity of Black Liquor ABAPX025,26 at 81.05% Solids.



Shear Rate,  $\text{Sec}^{-1}$  Frequency, Rad/Sec

Figure (8-45): Complex and Shear Viscosity of Black Liquor ABAFX043,44 at 72.89% Solids.

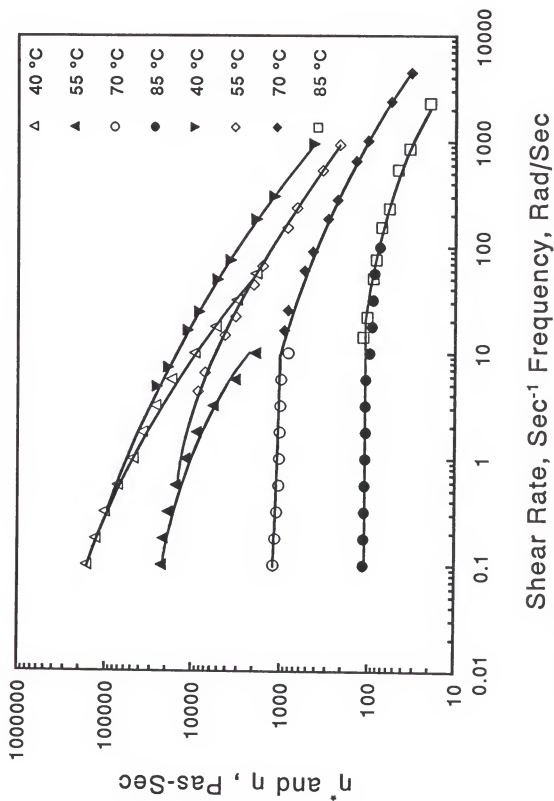


Figure (8-46): Complex and Shear Viscosity of Black Liquor ABAFX043,44 at 76.28% Solids.

Table (8-1): The Power-Law Model Parameters for Dynamic Viscosity as a Function of Frequency for Black Liquor ABAFX013,14.

% Solid	Temperature, °C	m	n	R <sup>2</sup>
67.2	40	4109.27	0.757	0.962
67.2	55	397.03	0.848	0.96
67.2	70	20.59	0.943	0.94
70.02	40	10765.8	0.675	0.997
70.02	55	1180.15	0.787	0.974
70.02	70	76.10	0.951	0.93
70.02	85	10.08	0.970	0.9
76.01	40	64925.78	0.320	0.99
76.01	55	13253.28	0.481	0.983
76.01	70	1230.65	0.690	0.9414
76.01	85	128.38	0.970	0.74

Table (8-2): Cross Model Parameters for Dynamic Viscosity as a Function of Frequency for Different Black Liquors.

Black Liquor	% Solids	T, °C	$\lambda$	m	R <sup>2</sup>
ABAFX013,14	76.05	40	17.2	0.7873	0.997
ABAFX013,14	76.05	55	3.324	0.6891	1.00
ABAFX013,14	76.05	70	0.3047	0.74	0.999
ABAFX025,26	75.7	40	0.0322	0.4203	0.999
ABAFX025,26	75.7	55	0.00052	0.3041	0.999
ABAFX025,26	81.05	40	0.2115	0.51	0.999
ABAFX025,26	81.05	55	0.00035	0.376	1.00
ABAFX043,44	65.4	40	0.283	0.662	0.999
ABAFX043,44	65.4	50	0.0585	0.572	0.999
ABAFX043,44	72.89	40	2.206	0.786	0.998
ABAFX043,44	72.89	55	0.331	0.757	0.999
ABAFX043,44	76.28	40	18.587	0.733	0.998
ABAFX043,44	76.28	55	1.43	0.540	0.995

Table (8-3): Carreau-Yasuda Model Parameters for Dynamic Viscosity as a Function of Frequency for Different Black Liquors.

Black Liquor	% Solids	T, °C	$\lambda$	a	n	R <sup>2</sup>
ABAFX013,14	76.05	40	35.177	1.261	0.350	1.0
ABAFX013,14	76.05	55	5.996	0.806	0.412	1.0
ABAFX013,14	76.05	70	1.03	0.510	0.510	1.0
ABAFX025,26	75.7	40	0.0655	0.438	0.638	0.999
ABAFX025,26	75.7	55	0.0391	0.577	0.800	1.0
ABAFX025,26	81.05	40	0.139	0.511	0.395	0.999
ABAFX025,26	81.05	55	0.1586	0.421	0.845	1.0
ABAFX043,44	65.4	40	0.794	0.7891	0.524	0.999
ABAFX043,44	65.4	50	1.194	0.873	0.788	0.999
ABAFX043,44	72.89	40	2.661	0.834	0.251	0.999
ABAFX043,44	72.89	55	0.895	0.945	0.460	0.999
ABAFX043,44	76.28	40	15.36	0.692	0.231	0.999
ABAFX043,44	76.28	55	0.556	0.485	0.330	0.999



Table (8-4): The Power-Law Model Parameters for Storage Modulus as a Function of Frequency for Different Black Liquors.

Black Liquor	% Solids	T, °C	m	n	R <sup>2</sup>
ABAFX013,14	67.2	40	1449.54	1.863	0.970
ABAFX013,14	67.2	55	65.63	2.084	0.990
ABAFX013,14	70.05	40	4788.63	1.749	0.974
ABAFX013,14	70.05	55	287.87	1.9164	0.982
ABAFX013,14	70.05	70	7.31	2.026	0.971
ABAFX025,26	71.98	40	13.863	2.392	0.994
ABAFX025,26	71.98	55	1.397	2.494	0.990
ABAFX025,26	71.98	60	0.1635	2.70	0.960
ABAFX025,26	71.98	70	0.11	2.211	0.998
ABAFX025,26	81.05	85	2.171	0.027	0.994
ABAFX043,44	65.4	40	586.99	1.89	0.995
ABAFX043,44	65.4	50	69.10	1.97	0.992
ABAFX043,44	65.4	60	5.92	2.41	0.990
ABAFX043,44	72.89	70	113.92	1.95	0.997
ABAFX043,44	72.89	85	19.94	2.10	0.993
ABAFX043,44	76.28	70	308.64	1.87	0.992
ABAFX043,44	76.28	85	35.99	1.97	0.997

Table (8-5): Model Parameters as in Equation (8-40) for Storage Modulus as a Function of Frequency for Different Black Liquors.

Black Liquor	% Solids	T, °C	G'	$\lambda$	a	R <sup>2</sup>
ABAFX013,14	67.20	70	842.89	0.0068	-1.41	0.999
ABAFX013,14	70.05	40	53816.52	0.1015	-0.95	1.0
ABAFX013,14	70.05	55	23822.34	0.0142	-1.01	1.0
ABAFX013,14	70.05	70	2161.23	0.0089	-1.17	1.0
ABAFX013,14	76.05	40	100467.1	1.157	-0.56	1.0
ABAFX013,14	76.05	55	88303.95	0.1125	-0.73	0.999
ABAFX013,14	76.05	70	39915.0	0.0135	-0.86	0.999
ABAFX013,14	76.05	85	20827.54	0.00168	-1.02	0.999
ABAFX025,26	75.70	40	8970.0	0.076	-1.46	0.998
ABAFX025,26	75.70	55	1658.8	0.0173	-1.51	1.0
ABAFX025,26	81.05	40	8313.38	1.770	-1.67	0.998
ABAFX025,26	81.05	55	4611.24	0.136	-1.95	0.99
ABAFX025,26	81.05	70	1615.90	0.027	-1.82	0.99
ABAFX043,44	65.40	40	30815.13	0.01634	-0.95	1.0
ABAFX043,44	72.89	40	30481.95	0.208	-0.68	0.999
ABAFX043,44	72.89	55	27498.60	0.05	-0.87	0.999
ABAFX043,44	76.28	40	536040.7	0.2922	-0.67	0.997
ABAFX043,44	76.28	55	27878.5	0.2368	-0.94	0.998

Table (8-6): Model Parameters for Dynamic Viscosity as a Function of Reduced Frequency as in Equation (8-45) for Three Black Liquors.

Black Liquor	% Solids	$\lambda$	a	$R^2$
ABAFX013,14	67.2	0.77	0.394	0.998
ABAFX013,14	70.02	3.074	0.495	0.998
ABAFX013,14	76.01	52.99	0.519	0.990
ABAFX025,26	71.98	0.0343	0.65	0.998
ABAFX025,26	75.7	0.0258	0.386	0.997
ABAFX025,26	81.05	0.0906	0.318	0.998
ABAFX043,44	65.4	0.0422	0.48	0.999
ABAFX043,44	72.89	3.43	0.63	0.995
ABAFX043,44	76.28	15.61	0.689	0.996

Table (8-7): Model Parameters for Dynamic Viscosity as a Function of Reduced Frequency as in Equation (8-46) for Three Black Liquors.

Black Liquor	% Solids	$\lambda$	a	n	$R^2$
ABAFX013,14	67.2	0.591	0.39	0.582	0.998
ABAFX013,14	76.01	25.25	0.55	0.268	0.996
ABAFX025,26	75.7	0.112	0.4154	0.7391	0.998
ABAFX043,44	72.89	7.31	0.76	0.468	0.994
ABAFX043,44	76.28	7.28	0.625	0.135	0.995

Table (8-8): Model Parameters for Storage Modulus as a Function of Reduced Frequency as in Equation (8-47) for Different Black Liquors.

Black Liquor	% Solids	a	b	c	R <sup>2</sup>
ABAFX013,14	67.2	7.195	0.936	-0.048	0.98
ABAFX013,14	70.02	8.34	0.84	-0.045	0.99
ABAFX013,14	76.01	10.75	0.402	-0.0516	0.973
ABAFX025,26	71.98	2.712	1.424	0.00365	0.99
ABAFX025,26	75.7	5.503	1.037	-0.025	0.98
ABAFX025,26	81.05	8.45	0.945	-0.281	0.99
ABAFX043,44	65.4	6.302	1.05	-0.054	0.999
ABAFX043,44	72.89	9.022	0.526	-0.059	0.995
ABAFX043,44	76.28	10.87	0.724	-0.0295	0.97

Table (8-9): Model Parameters for Reduced Dynamic Viscosity as a Function of Reduced Frequency as in Equation (8-49) for Black Liquors.

Black Liquor	$\lambda$	a	R <sup>2</sup>
ABAFX013,14	2.91	0.4623	0.996
ABAFX025,26	0.1224	0.361	0.998
ABAFX043,44	2.835	0.5826	0.996

Table (8-10): Model Parameters for Reduced Dynamic Viscosity as a Function of Reduced Frequency as in Equation (8-50) for Different Black Liquors.

Black Liquor	$\lambda$	a	n	$R^2$
ABAFX013,14	0.435	0.412	0.268	0.995
ABAFX043,44	1.503	0.559	0.277	0.996

## CHAPTER 9

### SUMMARY, CONCLUSIONS AND RECOMMENDATIONS

The primary purpose of this investigation was to study the rheological properties of softwood kraft black liquors, especially at high solids concentration. The objectives of the work were described in chapter 1. To accomplish this, the kinematic viscosities, shear viscosities and linear viscoelastic functions, the dynamic viscosity and storage modulus, of a series of well-characterized liquors, pulped under carefully controlled conditions, were measured by using especially designed equipment to maintain very precise temperature control. Also techniques were developed to insure that measurements are made within a time period that is short compared to the time required for degradation of the lignin within the liquor.

The details of the mathematical analysis, experimental setup and data analysis for a concentric cylinder viscometer were described in chapter 3. The system could be used successfully to measure the shear viscosity of black liquors especially above their normal boiling point where evaporation is a major problem for shear rates up to  $1000 \text{ sec}^{-1}$ . Of the specific consideration is to minimize the end effects by using an equivalent length instead of the actual length of the rotor for this system. The equivalent length was found to be about 10-20 percent longer than the actual length of the rotor. Use of the equivalent length reduces the experimental error to about 3-4 percent. The shear rate can be increased by using a rotor of bigger diameter

(smaller gap size) and the shear stress can be reduced by using a rotor of longer length. This system is not appropriate for highly concentrated black liquors especially at temperatures lower than 90 °C.

An Instron capillary viscometer was used to study the flow properties of these liquors for shear rates ranging from  $0.1 \text{ sec}^{-1}$  -  $10^4 \text{ sec}^{-1}$ . The details of the mathematical analysis, entry flow corrections, wall slip in capillary flow, experimental setup and data analysis are described in chapter 4. It was shown that the plots of pressure drop through the capillary ( $\Delta P$ ) as a function of  $L/D$  are linear for all black liquors used in this work at different temperatures and concentrations. Therefore, a two capillary method can be used to determine the viscosity of the samples. Also, it was shown that the slip velocity at the wall of the capillary is insignificant for black liquors and need not to be considered in future work. At high temperatures, when the viscosity of the samples are low, the pressure drop along the capillary may not be in the normal range of the system. Use of capillaries of larger  $L/D$  values may result in pressure drops that are more reliable and well within the normal range of the system.

The kinematic viscosities of the liquors were determined for solids concentrations up to 50% and temperatures up to 80 °C by using glass capillary methods. It was shown that black liquor can be treated as a polymer solution and theories developed for dilute polymer solutions were used to correlate viscosity data with temperature and solids concentrations. The relationship between the viscosity and temperature can be expressed by using either free volume theory and an average

value for freezing point of the liquors or absolute rate theory. The model based on the absolute rate theory, equation (5-9), could not be used to give  $A_1$  and  $B_1$  as correlatable functions of concentrations. Thus, these constants have no predictive value and must be evaluated for each liquor. The model based on free volume theory, equation (5-10), could be arranged such that the constant  $A_2$  can be universal for all liquors of a single species and the constant  $B_2$ , which depends on the solids compositions, can be written as a function of solids concentrations for a single liquor. With this approach, the viscosity behavior of a single liquor at low solids content can be defined as a function of temperature and solids concentration by replacing  $A_2$  and  $B_2$  in equation (5-10). The values of  $B_2$ , as presented in Figure (5-12) for some of the liquors, are composition dependent and the differences are more significant at higher concentrations. In general, the higher the viscosity of the liquor, the higher the values of  $B_2$  for that liquor, as is to be expected. However, this Figure shows that, at concentrations above 42 and 44 percent, the values of  $B_2$  for liquor ABAFX015,16 lie above the values of  $B_2$  for liquors ABAFX043,44 and ABAFX053,54 respectively. The viscosities of these two liquors are higher than liquor ABAFX015,16. Probably, it can be said that the transition from a water continuous phase to a polymer continuous phase occurs at lower concentrations for this liquor due to the fact that the molecular weight of lignin in this liquor is higher than the molecular weight of lignin in the other liquors used in this work. Also, in another approach, it was shown that the viscosity data for a single liquor can be reduced to a single curve by the use of  $S/T$  as a reducing function (corresponding states). This curve can be defined for



a liquor by two or, at most, three constants that are dependent upon the solids composition. This greatly reduces the amount of the experimental data that is necessary to define the viscosity behavior of a specific liquor at low concentrations. When the data for all liquors are available, the constants can be correlated empirically with non-volatile composition and pulping conditions for liquors from one wood species in future work. This will enable one to predict the viscosity of black liquors at low solids concentrations at process conditions from a knowledge of black liquor composition and/or cooking conditions. More work has to be done to study the effects of lignin concentration, its molecular weight and other constituents of black liquor on viscosity to develop correlations for viscosity as a function of lignin concentration and lignin molecular weight. However, chemical analysis and lignin molecular weight for liquors of single species must be available before a general correlation can be developed.

The shear viscosity of the liquors were determined for concentrations from 50 to 85%, temperatures from 40 °C to 140 °C and shear rates up to 10000 sec<sup>-1</sup>. At higher solids (>50%), black liquor can exhibit non-Newtonian behavior dependent upon temperature, solids concentration, solids composition and shear rate. In general, liquors behave as pseudoplastic (shear thinning) fluids and the degree of shear thinning increases with decreasing temperature or increasing concentration. The transition from a shear rate independent region to a shear rate dependent region occurs at lower shear rates as the solids concentration is increased or temperature is decreased. For liquors with higher weight average lignin molecular weight, the

transition will happen at lower shear rates, as would be expected. The exact level of viscosity at any given concentration, temperature and shear rate is dependent upon the solids composition which varies from liquor to liquor. The results indicate that the shear viscosity is affected by both lignin concentration and lignin molecular weight in the liquor. The liquors with intermediate kappa number have the highest zero shear rate viscosity at any solids content. The maximum in viscosity at intermediate kappa number can be related to the presence of lignin with highest weight average molecular weight in the liquor. The flow behavior of black liquors can be described very well by Cross and Carreau-Yasuda models over the entire range of experimental shear rate. Superposition principles developed for polymer melts and concentrated polymer solutions have been shown to apply, in general, to black liquors at high concentrations. Methods have been developed for general data reduction that can be used for calculation of viscosity at a specific condition. By choosing a suitable reference temperature,  $T_s$ , related to the glass transition temperature of black liquors, the data can be normalized to obtain a reduced plot of viscosity as a function of temperature, solids concentration and shear rate. A generalized WLF type equation has been obtained for the liquors used in this study and it can be used as a universal shift factor for other black liquors, with  $T_s$  as a parameter. The methods developed and the demonstration of general applicability significantly reduce the quantity of data necessary to describe the viscosity behavior of a new liquor. Thus, the work necessary to determine the effects of solids composition on liquor viscosity at specific conditions has been greatly reduced. In this work, the effect of density on

shift factor was ignored, because the density data are not available for these liquors. However, for precise reduction of viscosity data, the effect of density should be considered in future work. Also, there is the possibility that one can correlate the Cross and Carreau-Yasuda model parameters as it was used to describe the reduced viscosity of the liquors as a function of reduced shear rate, with the liquor composition and the pulping conditions for liquors of single species.

Methods of measurements and estimation of the zero shear rate viscosity (Newtonian) of concentrated black liquors (>50%), the utility of a fundamentally based model for correlating the zero shear rate viscosity as a function of temperature and concentration of non-volatile components, and, also, an empirical correlation for defining the zero shear rate viscosities as a function of temperature and concentration are described in chapter 7. It was shown that the relationship between the zero shear rate viscosity and temperature can be expressed by using a combination of the absolute reaction rates and free volume concepts, and that the best fits were obtained at a value of  $T_0 = 1.3 T_g$ . This model can be used to extrapolate over wide ranges of temperature at a fixed concentration and the results are highly accurate. The model can be used to obtain a general correlation for Newtonian viscosity of a single liquor as a function of temperature and solids concentration, but the method is difficult and time consuming. Also, we were able to express the Newtonian viscosity data for black liquors as a function of solids concentration and temperature using  $(S/(S+1))(1/T)$  as a reducing function. The method is empirical, but it appears that it can be used to express the Newtonian

viscosity of softwood and hardwood black liquors as a function of solids concentration and temperature. The reduced zero shear rate viscosity curve for every liquor can be defined by three or, at most, four constants that are dependent upon the solids composition. Therefore, the amount of the experimental work required to describe the Newtonian viscosity of a new liquor is greatly reduced. When the zero shear rate viscosity data are available, these constants can be correlated empirically with non-volatile composition and pulping conditions for liquors from one wood species. These correlations can be used to estimate the Newtonian viscosity of concentrated black liquors from the knowledge of the liquors composition and pulping conditions. The effects of lignin concentration, its molecular weight and other constituents of black liquor on zero shear rate viscosities will be determined in future work to develop appropriate correlations for Newtonian viscosity as a function of lignin molecular weight and composition of black liquor. This probably will enable one to find a general shift factor that in addition to temperature and solids concentrations, can take into account the effects of the solids composition on the viscosity of black liquor.

The viscoelastic properties of three different experimental softwood kraft black liquors with solids concentrations ranging from 67% to 81% were investigated in small-amplitude oscillatory shear flow for a temperature range from 40 °C to 85 °C. The experiments were carried out on a Rheometric Mechanical Spectrometer, using a parallel-plate geometry. The dynamic viscosity shows changes with temperature, solids concentration and composition of the liquors. At lower

temperatures and higher concentrations, dynamic viscosity falls monotonically with increasing frequency, which indicates that black liquors behave like uncross-linked polymer solutions. The transition from a frequency independent region to a frequency dependent region occurred at lower frequencies for liquors with higher weight average lignin molecular weight. However, dynamic viscosity is not only affected by the lignin molecular weight, but it is also a function of lignin concentration and other organic and inorganic components in black liquor. The storage modulus also shows changes with temperature, solids concentration and frequency, and it is a function of lignin molecular weight, lignin concentration and other constituents of black liquor. The results indicate that the storage modulus approaches zero with decreasing frequency and there is an indication of a plateau region at higher frequencies. Superposition principles were applied to obtain reduced correlations for linear viscoelastic functions of black liquors as a function of temperature and frequency at different solids concentration. The reduced curves at different solids concentrations for dynamic viscosity can be superimposed in a single master curve by using a solids shift factor as was used for shear viscosity of black liquors. The data for reduced storage modulus were treated in the same manner, but the reduced curves at different solids concentrations for reduced storage modulus can not be superimposed in a single curve. It was shown that, at sufficiently low shear rates and frequencies, shear viscosity and the magnitude of the complex viscosity agree within experimental error; thus, the zero shear viscosity of black liquors can be estimated from the complex viscosity data. The elasticity of the liquors were estimated for a nominal

operating temperature (120 °C) in a recovery furnace, and it can be said that black liquors, even at very high solids content, will not have problems in droplet formation due to the viscoelasticity of the fluid at temperatures above 120 °C.

## REFERENCE LIST

- Adams, G. and Gibbs, J.H., "On the Temperature Dependence of Cooperative Relaxation Properties in Glass Forming Liquids," J. Chem. Phys., **43**, pp. 139 (1965).
- Adams, T.N. and Frederick, N.J., Kraft Recovery Boiler Physical and Chemical Processes, American Paper Institute, New York, NY (1988).
- Akonis, J.J. and McKnight, W.J., Introduction to Polymer Viscoelasticity, Wiley, New York, NY (1983).
- Alder, B.J. and Hildebrand, J.H., "Activation Energy: Not Involved in Transport Processes in Liquids," Ind. Eng. Chem. Fundam., **12**(3), pp. 387-388 (1973).
- Andrade, E.N. da C., "The Viscosity of Liquids," Nature, **125**, p. 309 (1930).
- Arai, T., "The Entrance Effect and the Barus Effect," Proceedings of the 5th International Congress on Rheology, S. Onogi, Ed., University of Tokyo Press, Tokyo, **4**, pp. 497-509 (1970).
- Attal, J.F., Characterization, Rheology and Stability of Coal Water Mixtures, M.S. Thesis, University of Illinois at Chicago, Chicago, Illinois (1989).
- Bagley, E.B., "End Corrections in the Capillary Flow of Polyethylene," Journal of Applied Physics, **28**(5), pp. 624-627 (1957).
- Barlow, J.A., Lamb, J. and Matheson, A.J., "Viscous Behavior of Supercooled Liquids," Pro. R. Soc. (London), **292A**, pp. 322-412 (1965).
- Barnes, H.A., Hutton, J.F. and Walters, K. An Introduction to Rheology, Elsevier Science Publishing Company Inc., New York, NY (1989).
- Batschinski, A.J., "Investigation of Internal Friction in Fluids. I," J. Phys. Chem., **84**, pp. 643-705 (1913).

- Berger, L. and Meissner, J., "Linear Viscoelasticity, Simple and Planar Melt Extension of Linear Polybutadienes with bimodal molar mass distributions," Rheol. Acta, **31**, pp. 63-74 (1992).
- Billmeyer, F.W., Jr., Textbook of Polymer Science, Wiley, New York, NY (1971).
- Bird, R.B., Armstrong, R.C. and Hassager O., Dynamics of Polymeric Liquids, Wiley-Interscience, New York, NY (1987).
- Bird, R.B., Stewart, W.E. and Lightfoot, E.N., Transport Phenomena, John Wiley and Sons, Inc., New York, NY (1960).
- Bodenheimer, B.V., "Viscosity Variations on High Solids Black Liquors," Southern Pulp and Paper Manufacturers, (June 10 1969).
- Broadbent, J.M. and Lodge, A.S., Rheol. Acta, **10**, 557 (1971).
- Calderbank, P.H. and Moo-Yang, M.B., Trans. Inst. Ch.E. (London), **37**, pp. 26-33 (1959).
- Carreau, P.J., "Rheological Equations from Molecular Network Theories," Trans. Soc. Rheol., **16**, pp. 99-127 (1972).
- Carreau, P.J., Macdonald, I.F. and Bird, R.B., "A Nonlinear Viscoelastic Model for Polymer Solutions and Melts-II," Chemical Engineering Science, **23**, pp. 901-911 (1968).
- Casey, J.P., Pulp and Paper Chemistry and Chemical Technology, Vol. 1, Wiley-Interscience, New York, NY (1980).
- Chhabra, R.P. and Hunter, R.J., "The Fluidity of Molten Salts," Rheol. Acta, **20**(2), pp. 203-206 (1981).
- Co, A., Kim, H.K., Wight, M.O. and Fricke, A.L., "Viscosity of Black Liquors at High Temperatures," TAPPI, **65**(8), pp. 111-113 (1982).
- Co, A. and Wight, M.O., "Rheological Properties of Black Liquors," Black Liquor Recovery Boiler Symposium, Helsinki, Finland (1982).
- Code, R.K. and Raal, J.D., "Rates of Shear in Coaxial Cylinder Viscometers," Rheol. Acta, **12**, pp. 578-587 (1973).
- Cohen, M.H. and Turnbull, D., "Molecular Transport in Liquids and Glasses," J. Chem. Phys., **31**(5), pp. 1164-1169 (1959).



- Cohen, Y. and Metzner, A.B., "Apparent Slip Flow of Polymer Solutions," Journal of Rheology, **29**(1), pp. 67-102 (1985).
- Collyer, A.A. and Clegg, P.W., Rheological Measurements, Elsevier Applied Science, New York, NY (1988).
- Connelly, R.W. and Greener, J., "High-Shear Viscometry with a Rotational Parallel-Disk Device," Journal of Rheology, **29**(2), pp. 209-226 (1985).
- Cox, W.P. and Merz, E.H., "Correlation of Dynamic and Steady Flow Viscosities," Journal of Polymer Science, **28**, pp. 619-622 (1958).
- Cross, M.M., "Rheology of Non-Newtonian Fluids: a New Flow Equation for Pseudo-Plastic Systems," Journal of Colloid Science, **20**, pp. 417-437 (1965).
- Darby, R., Viscoelastic Fluids, Marcel Dekker Inc., New York, NY (1976).
- De Guzman, J., An. Soc. Espan. Fis. Quim., **11**, p. 153 (1913).
- De Waele, A., Oil and Color Chem. Assoc. Journal, **6**, p. 33 (1923)
- Dealy, J.M. Rheometers for Molten Plastics, Van Nostrand Reinhold, New York, NY (1982).
- Dealy, J.M. and Wissbrun, K.F., Melt Rheology and its Role in Plastic Processing, Van Nostrand Reinhold, New York, NY (1990).
- Dienes, G.J., "Activation Energy for Viscous Flow and Short-Range Order," J. Appl. Physics, **24**(6), pp. 779-782 (1953).
- Doolittle, A.K., "Studies in Newtonian Flow. III. The Dependence of the Viscosity of Liquids on Molecular Volume and Free Space (in Homogeneous Series)," J. Appl. Phys., **23**(2), pp. 236-239 (1951a).
- Doolittle, A.K., "Studies in Newtonian Flow. II. The Development of the Viscosity of Liquids on Free Space," J. Appl. Phys., **22**(12), pp. 1471-1475 (1951b).
- Dyson, A., "Frictional Traction and Lubricant Rheology in Elastohydrodynamic Lubrication," Phil Trans. Roy. Soc., **A226**, pp. 1-33 (1970).
- Eicher, L.D., and Zwolinski, B.J., "Limitations of the Hildebrand-Batschinski Shear Viscosity Equation," Science, **77**, p. 369 (1972).

- Ertl, H. and Dullien, F.A.L., "Hildebrand's Equation for Viscosity and Diffusivity," J. Phys. Chem., **77**(25), pp. 3007-3011 (1973a).
- Ertl, H. and Dullien, F.A.L., "Self-Diffusion and Viscosity of Some Liquids as a Function of Temperature," AIChE, **19**(6), pp. 1215-1223 (1973b).
- Ewell, R.H. and Eyring, H., "Theory of the Viscosity of Liquids as a Function of Temperature and Pressure," J. Chem. Phys., **5**, pp. 726-736 (1937).
- Eyring, H., "The Activated Complex in Chemical Reactions," J. Chem. Phys., **3**, pp. 107-115 (1935).
- Eyring, H., "Viscosity, Plasticity and Diffusion as Examples of Absolute Reaction Rates," J. Chem. Phys., **4**, pp. 283-291 (1936).
- Ferry, J.D., Viscoelastic Properties of Polymers, Third Edition, John Wiley and Sons, Inc., New York, NY (1980).
- Frederickson, A.G., Principles and Applications of Rheology, Prentice Hall, Englewood Cliffs, N.J., pp. 196-200 (1964).
- Fricke, A.L., Physical Properties of Kraft Black Liquor: Interim Report-Phase II, DOE Report on Contract No. DG AC02-82CE40606, University of Maine, Orono and University of Florida, Gainesville (1985).
- Fricke, A.L., Physical Properties of Kraft Black Liquor: Summary Report-Phase I and II, DOE Report Nos. AC02-82CE40606 and FG02-85CE40740, University of Florida, Gainesville and University of Maine, Orono (1987).
- Fricke, A.L., A Comprehensive Program to Develop Correlations for the Physical Properties of Kraft Black Liquors, Interim Report No. 2, University of Florida, Gainesville (1990).
- Gahlke, S.N. and Veeramani, H., "Viscosity of Bamboo, Bagasse and Eucalyptus Black Liquors," TAPPI Non-Wood Plant Fiber Pulping Progress Report, **8**, pp. 33-40 (1977).
- Goldin, M. and Yerushalmi, J., Pfeffer, R. and Shinnar, R., "Break up of a Laminar Capillary Jet of a Viscoelastic Fluid," J. of Fluid Mech., **38**(4), pp. 689-711 (1969).
- Grant, D.E. and Dieckmann, S.E., "Some Melt Flow Properties of Polypropylene," Journal of Applied Polymer Science, **9**, pp. 3231-3243 (1965).

- Greener, J. and Connelly, R.W., "The Response of Viscoelastic Liquids to Complex Strain Histories: The Thixotropic Loop," Journal of Rheology, 30(2), pp. 285-300 (1986).
- Gross, M.M., "Rheology of Non-Newtonian Fluids: a New Flow Equation for Pseudo-Plastic Systems," Journal of Colloid Science, 20, pp. 417-437 (1965).
- Gubbins, K.E. and Tham, M.J., "Free Volume Theory for Viscosity of Simple Nonpolar Liquids," AIChE, 15(2), pp. 264-269 (1969).
- Han, C.D. and Charles, M., "Criterion for Fully-Developed Flow of Polymer Melts in Circular Tube," AIChE, 16(3), pp. 499-501 (1970).
- Han, S.T., "Physical Properties of Neutral Sulfide Spent Liquors," TAPPI, 40(11), pp. 921-925 (1957).
- Harvin, R.L., Study of the Thermal and Physical Properties and Heat Transfer Coefficients of Sulfate Paper Mill Black Liquors, Ph.D. Dissertation, University of Florida, Gainesville (1955).
- Herrick, F.W., Engen, R.J. and Goldschmid, O., "Spent Sulfite Liquor Viscosity and Lignin Sulfonate Molecular Weight: Effect of Heat Aging," TAPPI, 62(2), pp. 81-86 (1979).
- Highgate, D.J. and Whorlow, R.W., "End Effects and Particle Migration Effects in Concentric Cylinders Rheometry," Rheologica Acta, 8(2), pp. 142-151 (1969).
- Hildebrand, J.H., "Motions of Molecules in Liquids: Viscosity and Diffusivity," Science, 174, pp. 490-492 (1971).
- Hildebrand, J.H., "Kinetic Theory of Viscosity of Compressed Fluids," Proc. Nat. Acad. Sci., USA, 72(5), pp. 1970-1972 (1975).
- Hildebrand, J.H. and Lamoreaux, R.H., "Fluidity: A General Theory," Proc. Nat. Acad. Sci., USA, 69(11), pp. 3428-3431 (1972).
- Hildebrand, J.H. and Lamoreaux, R.H., "Fluidity and Liquid Structure," J. Phys. Chem., 77(11), pp. 1471-1473 (1973).
- Hunter, R.E., Tracy, J., Cutts, R., Young, R.E., Olin, J., and McCarty, J.L., "Density, Viscosity, Specific Heat, Thermal Conductivity, and Prandtl Number Versus Concentration and Temperature: Sulfite Waste Liquor," TAPPI, 36(11), pp. 493-497 (1953).

- Hutton, J.F., "The Fracture of Liquids in Shear: The Effects of Size and Shape," Proc. Roy. Soc., A287, pp. 222-239 (1965).
- Hutton, J.F., "Fracture and Secondary Flow of Elastic Liquids," Rheol. Acta, 8, pp. 54-59 (1969).
- Hyun, K.S., "End Correction in Capillary Flow of Polystyrene Melts," Polymer Engineering and Science, 14(9), pp. 666-673 (1974).
- Instron Capillary Rheometer, Model-3211, Manual No. 10-364-1(C), Instron Corporation, Canton, Massachusetts (1981).
- Janson, J. and Söderhjelm, L., "The Viscosity of Borate-Containing Black Liquor," Nord. Pulp Pap. Res. J., 3(2), pp. 107-110 (1988).
- Jiang, T.Q., Yang, A.C. and Metzner, A.B., "The Rheological Characterization of HPG Gels: Measurement of Slip Velocities in Capillary Tubes," Rheologica Acta, 25(4), pp. 397-404 (1986).
- Kalika, D.S. and Denn, M.M., "Wall Slip and Extrudate Distortion in Linear Low-Density Polyethylene," Journal of Rheology, 31(8), pp. 815-834 (1987).
- Kamal, M.R. and Nyun, H., "The Effect of Pressure on Shear Viscosity of Polymer Melts," Transactions of the Society of Rheology, 17(2), pp. 271-285 (1973).
- Kataoka, T. and Ueda, S., "Flow Properties of Polyethylene Melt," Journal of Applied Polymer Science, 12, pp. 939-953 (1968).
- Keentok, M. and Tanner, I., "Cone-Plate and Parallel-Plate Rheometry of Some Polymer Solutions," Journal of Rheology, 26(3), pp. 301-311 (1982).
- Kelly, J.E., The Effect of Particle Size and Concentration on the Capillary Rheometry of Calcium Carbonate/Polystyrene Composites, M.S. Thesis, University of Florida, Gainesville, Florida, (1989).
- Kim, H.K., "Viscosity of Black Liquors by Capillary Measurements," M.S. Thesis, University of Maine at Orono (1980).
- Kim, H.K., Co, A. and Fricke, A.L., "Viscosity of Black Liquor by Capillary Measurements," AIChE Symposium Series, 207(77), pp. 2-8, (1981).
- Kobe, K.A. and McCormack, E.J., "Viscosity of Pulping Waste Liquors," Industrial and Engineering Chemistry, 41(12), pp. 2847-2848 (1949).

- Kozicki, W., Pasari, S.N. and Rao, A.R.K., "Anomalous Effects in Laminar Capillary Flow of Polymer Solutions," Chemical Engineering Science, **25**, pp. 41-52 (1970).
- Kraynyk, A.M. and Schowalter, W.R., "Slip at the Wall and Extrudate Roughness with Aqueous Solutions of Polyvinyl Alcohol and Sodium Borate," Journal of Rheology, **25**(1), pp. 94-114 (1981).
- Krieger, I.M., "Shear rate in the Couette Viscometer," Transactions of the Society of Rheology, **12**(1), pp. 5-11 (1968).
- Krieger, I.M. and Elrod, H., "Direct Determination of the Flow Curves of Non-Newtonian Fluids. II. Shearing Rate in the Concentric Cylinder Viscometer," Journal of Applied Physics, **24**(2), pp. 134-136, February (1953).
- Krieger, I.M. and Maron, S.H., "Direct Determination of the Flow Curves of Non-Newtonian Fluids," Journal of Applied Physics, **23**(1), pp. 147-149 (1952).
- Krieger, I.M. and Maron, S.H., "Direct Determination of the Flow Curves of Non-Newtonian Fluids. III. Standardized Treatment of Viscometric Data," Journal of Applied Physics, **25**(1), pp. 72-75 (1954).
- La Nieve, H.L. and Bogue, D.C., "Correlation of Capillary Entrance Pressure Drops with Normal Stress Data," Journal of Applied Polymer Science, **12**, pp. 353-372 (1968).
- Lankenau, H.G. and Flores, A.R., "Multiple Effect Evaporation of Sulfate Liquors to 55-65% Solids," Pulp and Paper Magazine of Canada, pp. 63-66 (Jan. 17, 1969).
- Laun, H.M., "Polymer Melt Rheology with a Slit Die," Rheologica Acta, **22**(2), pp. 171-185 (1983).
- Laun, H.M. and Schuch, H., "Transient Elongational Viscosities and Drawability of Polymer Melts," Journal of Rheology, **33**(1), pp. 119-175 (1989).
- Lodge, A.S., Elastic Liquids, Academic Press, New York, NY (1964).
- Lucas, M. and Lucas, K., "Viscosity of Liquids: An Equation with Parameters Correlating with Structural Groups," AIChE, **32**(1), pp. 139-141 (1986).
- Lynn, R., "Operators and Fractional Derivatives for Viscoelastic Constitutive Equations," Journal of Rheology, **27**(4), pp. 351-372, (1983).

- Macedo, P.B. and Litovitz, T.A., "On the Relative Roles of Free Volume and Activation Energy in the Viscosity of Liquids," J. Chem. Phys., **42**(1), pp. 245-256 (1965).
- Malcolm, I.W., Robert, F.L. and Ferry, J.D., "The Temperature Dependence of Relaxation Mechanisms in Amorphous Polymers and Other Glass-Forming Liquids," J. Am. Chem. Soc., **77**, pp. 3701-3706 (1955).
- Marton, J., In Lignin, K.V. Sarkanen and C.H. Ludwig, Eds., Wiley Interscience, New York, NY (1971).
- Masse, M.A., Kiran, E. and Fricke, A.L., "Freezing and Glass Transition Phenomena in Polymer-Diluent Mixtures," Polymer, **27**, pp. 619-622 (1986).
- Masse, M.A., Thermal Analyses of Kraft Black Liquor, M.S. Thesis, University of Maine, Orono (1984).
- Matheson, A.J., "Role of Free Volume in the Pressure Dependence of the Viscosity of Liquids," J. Chem. Phys., **44**(2), pp. 695-699 (1966).
- McLuckie, C. and Rogers G.M., "Influence of Elastic Effects on Capillary Flow of Molten Polymers," Journal of Applied Polymer Science, **13**, pp. 1019-1063 (1969).
- Melcher, III, J., "Simplifying Experimentation by Factorial Design," TAPPI, **50**(11), pp. 548-552 (1961).
- Milanova, E. and Dorris, G.M., "Effects of Residual Alkali Content on the Viscosity of Kraft Black Liquors," JPPS, **16**(3), pp. 94-101 (1990).
- Miller, A.A., "Free Volume and Viscosity of Liquid: Effects of Temperature," J. Phys. Chem., **67**, pp. 1031-1035 (1963).
- Mooney, M., Journal of Rheology, **2**, pp. 210 (1931).
- Morre, H.K., "Multiple Effect Evaporation Separation," Transactions of American Institute of Chemical Engineers, **15**, pp. 244 (1923).
- Ostwald, W., Kolloid-Z., **36**, pp. 99-117 (1925).
- Otter, J.L. den, "Some Investigations of Melt Fracture," Rheol. Acta, **10**(2), pp. 200-207 (1971).

- Oye, R., Langford, N.G., Phillips, F.H. and Higgins, H.G., "The properties of Kraft Black Liquors from Various Eucalyptus and Mixed Tropical Hardwoods," APPITA, 31(1), pp. 33-40 (1977).
- Pearson, D.S. and Rochefort, W.E., "Behavior of Concentrated Polystyrene Solutions in Large-Amplitude Oscillating Shear Fields," Journal of Polymer Science, Polymer Physics Edition, 20, pp. 83-98 (1982).
- Philippoff, W. and Gaskins, F.H., "Viscosity Measurements on Molten Polyethylene," Journal of Polymer Science, 21, pp. 205-222 (1956).
- Polyakov, Yu. A., Smokvin, O.A. and Marshak, A.B., "Viscosity of Black Liquors," Tr. Leningrad. Tehnol. Inst. Tsely-Bum. Prom., 27, pp. 11-20 (1970).
- Przedzicki, J.W. and Sridhar, T., "Prediction of Liquid Viscosities," AIChE, 31(2), pp. 333-335 (1985).
- Rabinowitch, R., Z. Phys. Chem., A145, p. 1, (1929).
- Ramamurthy, A.V., "Wall Slip in Viscous Fluids and Influence of Materials of Construction," Journal of Rheology, 30(2), pp. 337-357 (1986).
- Rheometrics Technical Manual, Operating Instructions, Rheometrics Inc. Piscataway, NJ (1986).
- Rydholm, S.A., Pulping Processes, Interscience Publishers, New York, NY (1965).
- Sandquist, K., "Rheological Properties of Black Liquor," Svensk Papperstidn., 84(18), pp. R141-R145 (1982).
- Sandquist, K., "Rheological Properties and Evaporation of Black Liquor at High Dry-Solids Content," Pulp and Paper Canada, 84(2), pp. 30-34 (1983).
- Schmidl, W.G., Molecular Weight Characterization and Rheology of Lignins for Carbon Fibers, Ph.D. Dissertation, University of Florida, Gainesville (1992).
- Sjöström, E., Wood Chemistry. Fundamentals and Applications, Academic Press, New York, NY (1981).
- Small, J.D., Jr., The Thermal Stability of Kraft Black Liquor at Elevated Temperatures, M.S. Thesis, University of Maine, Orono (1984).
- Small, J.D., Jr., and Fricke, A.L. "Thermal Stability of Kraft Black Liquor Viscosity at Elevated Temperatures," I&EC Prod. Res. & Devel., 24, pp. 608-614 (1985).

- Söderhjelm, L., "Viscosity of Strong Black Liquor," Paperi Puu, **68**(9), pp. 642-652 (1986).
- Söderhjelm, L., "Viscosity of Strong Black Liquors from Birch Pulping," Paperi Puu, **70**(4), pp. 348-354 (1988).
- Söderhjelm, L. and Sågfor, P.-E., "Relationship Between the Viscosity and Composition of Black Liquor," International Chemical Recovery Conference, Book **2**, pp. 513-519 (1992).
- Spencer, R.S. and Dillon, R.E., "The Viscous Flow of Molten Polystyrene II," Journal of Colloid Science, **4**, pp.241-255 (1949).
- Spencer, R.S. and Dillon, R.E., "The Viscous Flow of Molten Polystyrene," Journal of Colloid Science, **3**, pp. 163-180, (1948).
- Sridhar, T., Chhabra, R.PI, Uhlherr, P.H.T. and Potter, O.E., "Application of Hildebrand's Fluidity Model to non-Newtonian Solutions," Rheol. Acta, **17**(5), pp. 519-524 (1978).
- Stenhof, T.J. and Agrawal, M.L., "Viscosity of Black Liquor," AIChE Symposium Series, **77**(207), pp. 13-17 (1981).
- Stevens, S., Rheology of Concentrated Kraft Black Liquors, M.S. Thesis, University of Florida, Gainesville (1987).
- Stoy, M., Zaman, A.A. and Fricke, A.L., "Vapor-Liquid Equilibria for Black Liquors," International Chemical Recovery Conference Proceedings, Book **2**, pp. 495-511 (1992).
- Tanner, R.C. and Keentok, M., "Shear Fracture in Cone-Plate Rheometry," Journal of Rheology, **27**(1), pp. 47-57 (1983).
- Toms, B.A., In Rheology, **2**, F.R. Eirich, Ed., Academic Press, New York, NY (1958).
- Turnbull, D. and Cohen, M.H., "Free-Volume Model of the Amorphous Phase: Glass Transition," J. Chem. Phys., **34**(1), pp. 120-124 (1961).
- Turnbull, D. and Cohen, M.H., "On the Free Volume Model of the Liquid-Glass Transition," J. Chem. Phys., **52**(6), pp. 3038-3041 (1970).



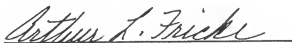
- Velzen, D.V., Cardozo, R.L. and Langenkamp, H., "A Liquid Viscosity-Temperature-Chemical Constitution Relation for Organic Compounds," Ind. Eng. Chem. Fundam., **11**(1), pp. 20-25 (1972).
- Vinogradov, G.V., and Malkin, A.Ya., Rheology of Polymers, Mir Publishers, Moscow (1980).
- Walters, K., Rheometry, Chapman and Hall, London (1975).
- Wein, O. and Tovchigrechko, V.V., "Rotational Viscometry Under Presence of Apparent Wall Slip," Journal of Rheology, **36**(5), pp. 821-844 (1992).
- Weissberg, H.L., "End Correction for Slow Viscous Flow Through Long Tubes," The Physics of Fluids, **5**(9), pp. 1033-1036 (1962).
- Wennberg, O., "Boiling Point Elevation and Viscosity of Black Liquor at High Solids Content and High Temperatures," International Chemical Recovery Proceedings, pp. 275-279 (1985).
- Wennberg, O., "Rheological Properties of Black Liquor," International Chemical Recovery Proceedings, pp. 89-93 (1989).
- White, J.L. and Kondo, A., "Flow Patterns in Polyethylene and Polystyrene Melts During Extrusion Through a Die Entry Region: Measurement and Interpretations," J. of Non-Newtonian Fluid Mechanics, **3**, pp. 41-64 (1977/1978).
- White, S.A. and Barid, D.G., "Flow Visualization and Birefringence Studies on Planar Entry Flow Behavior of Polymer Melts," J. of Non-Newtonian Fluid Mechanics, **29**, pp. 245-267 (1988).
- Wight, M.O., An Investigation of Black Liquor Rheology Versus Pulping Conditions, Ph.D. Thesis, University of Maine at Orono (1985).
- Wight, M.O., Co, A. and Fricke, A.L., "Viscosity of Black Liquor by Cone-and-Plate and Parallel-Disk Viscometry," AIChE Symposium Series, **77**(207), (1981).
- Wynne-Jones, W.K.F. and Eyring, H. "The Absolute Rate of Reactions in Condensed Phases," J. Chem. Phys., **4**, pp. 283-291 (1936).
- Yang, T.M.T. and Krieger, I.M., "Comparison of Methods for Calculating Shear Rates in Coaxial Viscometers," Journal of Rheology, **22**(4), pp. 413-421 (1978).

- Yasuda, K.Y., Investigation of the Analogies between Viscometric and Linear Viscoelastic Properties of Polystyrene Fluids, Ph.D. Thesis, Massachusetts Institute of Technology, Cambridge, MA (1979).
- Yasuda, K.Y., Armstrong, R.C. and Cohen, R.E., Rheological Acta, **20**, pp. 163-178 (1981).
- Yilmazer, U. and Kalyon, D.M., "Slip Effects in Capillary and Parallel Disk Torsional Flows of Highly Filled Suspensions," Journal of Rheology, **33**(8), pp. 1197-1212 (1989).
- Yoshimura, A.S. and Prud'homme, R.K., "Response of an Elastic Bingham Fluid to Oscillatory Shear," Rheol. Acta, **26**, pp. 428-436 (1987).
- Yoshimura, A.S. and Prud'homme, R.K., "Wall Slip Corrections for Couette and Parallel Disk Viscometers," Journal of Rheology, **32**(1), pp. 53-67 (1988a).
- Yoshimura, A.S. and Prud'homme, R.K., "Wall Slip Effects on Dynamic Oscillatory Measurements," Journal of Rheology, **32**(6), pp. 575-584 (1988b).
- Zaman, A.A. and Fricke, A.L., "Viscosity of Black Liquor up to 130 °C and 84% Solids," AIChE Forest Products Symposium Proceedings, pp. 59-77 (1991).
- Zaman, A.A., Dong, D.J. and Fricke, A.L., "Kraft Pulping of Slash Pine," AIChE Forest Products Symposium Proceedings, pp. 49-57 (1991).
- Zaman, A.A. and Fricke, A.L., "Correlations for Viscosity of Kraft Black Liquors at Low Solids Concentrations by Corresponding States," Accepted for Publication in AIChE (1993).

## BIOGRAPHICAL SKETCH

The author was born on May 26, 1957 in Semnan, Iran. He graduated from the University of Tehran with a master's degree in chemical engineering in 1988. He continued his education at the University of Florida and has served as a research assistant for the Chemical Engineering Department since April 1989. He is currently a candidate for the Doctor of Philosophy degree in chemical engineering from the University of Florida in August, 1993.

I certify that I have read this study and that in my opinion it conforms to acceptable standards of scholarly presentation and is fully adequate, in scope and quality, as a dissertation for the degree of Doctor of Philosophy.



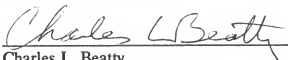
Arthur L. Fricke, Chairman  
Professor of Chemical Engineering

I certify that I have read this study and that in my opinion it conforms to acceptable standards of scholarly presentation and is fully adequate, in scope and quality, as a dissertation for the degree of Doctor of Philosophy.



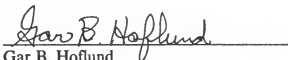
Reza Abbaschian  
Professor of Materials Science and  
Engineering

I certify that I have read this study and that in my opinion it conforms to acceptable standards of scholarly presentation and is fully adequate, in scope and quality, as a dissertation for the degree of Doctor of Philosophy.



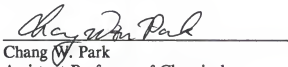
Charles L. Beatty  
Professor of Materials Science and  
Engineering

I certify that I have read this study and that in my opinion it conforms to acceptable standards of scholarly presentation and is fully adequate, in scope and quality, as a dissertation for the degree of Doctor of Philosophy.



Gar B. Hoflund  
Professor of Chemical Engineering


I certify that I have read this study and that in my opinion it conforms to acceptable standards of scholarly presentation and is fully adequate, in scope and quality, as a dissertation for the degree of Doctor of Philosophy.



Chang W. Park  
Assistant Professor of Chemical  
Engineering

This dissertation was submitted to the Graduate Faculty of the College of Engineering and to the Graduate School and was accepted as partial fulfillment of the requirements for the degree of Doctor of Philosophy.

August 1993



---

Winfred M. Phillips  
Dean, College of Engineering

---

Dean, Graduate School